A FIELD STUDY AND NUMERICAL SIMULATION OF NATURAL GROUND-WATER RECHARGE

by

Robert G. Knowlton, Jr.

Submitted in Partial Fulfillment of
the Requirements for the Degree of
Master of Science in Hydrology

New Mexico Institute of Mining and Technology
Socorro, New Mexico

December 1984

ACKNOWLEDGEMENTS

The author wishes to thank Dr. Dan Stephens for all the help and direction he has provided. The graduate students who provided assistance in manufacturing and installing instrumentation, and collecting field data, are given a special thanks, as these tasks were of a very time consuming, and often tedious, nature. Thanks to Chuck Spaulding, Richard Rabold, Mark Larson, Greg Lewis, Ward Herst, Stephen Heermann, Steve Conrad, Jim McCord, and Warren Cox.

Thanks are extended to the New Mexico Water Resources Research Institute for funding this project. The U.S. Fish and Wildlife Service is given a special thanks for their cooperation in helping to establish the research site at the Sevilleta National Wildlife Refuge. Ted Stans has been especially helpful in providing valuable assistance and information at the refuge.

I owe my parents a debt of gratitude for all the love and support that they have given me over all the years of my schooling.

The biggest thanks of all goes to my wife, Jan. Without her love, help, and confidence I would not have been able to complete this master's study.

ABSTRACT

An extensive amount of instrumentation and monitoring equipment was installed within a small drainage basin in a semi-arid lowland. This equipment is being used to measure and predict the hydrologic processes occurring at this site. The methods presented in this paper are specifically related to estimating the natural ground-water recharge flux and evapotranspiration rate at one monitoring site in this basin. A Darcy's Law approach yielded an estimated recharge flux between 0.90 and 4.73 cm/year, for the period of record between November 1982 and May 1984. This recharge flux corresponds to approximately 5.1% and 26.6% of the precipitation rate for the same period of record. The seepage velocity associated with this recharge flux was between 15.0 and 78.8 cm/year below the root zone. A temperature gradient method was used to calculate a recharge rate of 1.26 cm/year, or 7.1% of the precipitation rate. The seepage velocity for this method is calculated to be 21.0 cm/year. Averaging the estimated recharge rates from these methods yields a value of 2.30 cm/year. The average seepage velocity is about 38.3 cm/year. Assuming this seepage velocity is representative of the long term water particle velocity throughout the soil profile, and the depth to water at the site under investigation is 6 meters, then it takes approximately 15.7 years for water to travel from the land surface to the water table.

A water budget analysis resulted in an estimated evapotranspiration rate of between 13.1 and 16.9 cm/year, or 73.4% and 94.9% of the precipitation rate for the period of record. Estimates of actual evapotranspiration rate were also made from an approximation of the potential, or reference crop, evapotranspiration rate. The best estimates of input parameters were made and the resultant estimation of actual evapotranspiration was inadequate. A subsequent evaluation of the methods suggested that with minor modifications of estimating the input parameters to these models some adequate results could possibly be obtained.

A 'microlysimeter' technique was employed to measure the actual evaporation occurring within the upper 15cm of the soil profile. The resultant estimates of evaporation appeared to somewhat high.

Some bromide tracer experiments were carried out in the field with the intent of mapping out the wetting front advance after precipitation events. The results of this analysis suggested a need for further investigation into bromide tracer techniques. Dispersion and redistribution appeared to figure quite prominently in trying to evaluate the bromide tracer and

wetting front movement.

A numerical model was employed to simulate the unsaturated flow at the study site, and to make predictions about recharge behavior. A calibration of the transpiration uptake was done against observed data. A verification of the model results was also carried out against observed data for a specific precipitation event, and subsequent infiltration and redistribution. The calibrated model input data should be of suitable quality for predicting long term effects of precipitation and evapotranspiration for the site under investigation.

TABLE OF CONTENTS

LIST OF FIGURES

LIST OF FIGURES (CONTINUED)

LIST OF TABLES

1. INTRODUCTION:

Ground-water recharge is considered to be water that is added to the saturated zone of an aquifer across the water-table surface. Therefore, recharge may occur along bedrock surfaces near steep mountain slopes, through the infiltration of river waters, or by deep percolation of water derived from natural precipitation or irrigation. This study is concerned with that portion of ground-water recharge that is derived from the infiltration of natural precipitation. In particular, the research site under investigation is in a semi-arid lowland adjacent to an ephemeral river in central New Mexico.

The quantification of natural ground-water recharge can be very important. Planners and engineers need to know the amount of water available in aquifers for planning or design projects. Government agencies need this information for water-resource management purposes. If an aquifer has an appreciable amount of recharge it may be managed as a renewable resource. If the aquifer has a negligible recharge rate it has been accepted practice to 'mine' the ground water from the aquifer over a certain period of time, say 40 years. From that point on it is assumed that there will no longer be any water available from that aquifer.

Another reason to study ground-water recharge is to predict ground-water quality impacts. There have been proposals for storing hazardous wastes in desert environments, under the premise that recharge, and therefore seepage rates, are negligible (Winograd, 1981; Longmire et al., 1981; Hawley, 1983). If recharge is shown to be significant these hazardous wastes could eventually contaminate the underlying aquifer. From these few viewpoints there appears to be a need for further study on this subject.

To date there have been many recharge studies carried out in humid or agricultural irrigation areas. The study of natural ground-water recharge in arid or semi-arid regions has been done by only a few investigators. These investigators have found mixed results; some suggesting that recharge is negligible and others that it may be as much as a few percent of the annual precipitation. Preliminary data from this project suggested that areal recharge rates may be substantially more than just a few percent of the precipitation rate. The subsequent instrumentation of the research site used in this study is probably more extensive than any carried out to date in an arid or semi-arid environment.

The original intent of this project was to develop a good data base to better understand and explain the physical processes influencing recharge in a semi-arid lowland watershed. To this

end a great deal of instrumentation was installed throughout a small basin. This instrumentation was placed so that differences in vegetation cover, slopes, and soil type could be analyzed. The types of instrumentation being used are: tensiometers, for measuring pressure heads; neutron access tubes, for measuring water content profiles with a neutron probe; temperature thermistors, for measuring temperature-depth profiles; observation wells, for measuring water table elevations; a weather station, for measuring meteorological conditions; and an automated data acquisition system, employing a single pressure transducer, a scanning valve, and a microprocessor, for logging tensiometric data.

This report will be looking at only one phase of the overall project objectives. The data from one particular site will be analyzed; therefore the results will only apply to one soil type, vegetated cover, and slope. The types of analyses used in this report could later be used in evaluating the rest of the data from the research site so that comparisons could be made.

The aim of this report is to quantify the deep percolation recharge flux at this one site. The factors influencing the recharge rate are the amount and intensity of precipitation, evaporation from the soil surface, transpiration from plants, and the soil characteristics. Because of the relatively flat land surface and permeable soils at this site, it is assumed that

runoff and interflow are negligible. Probably the most difficult parameter to estimate in the hydrologic budget is the recharge flux. Therefore, a number of different methods are being employed to either estimate the recharge flux directly, or indirectly by estimating the other parameters in the hydrologic budget and solving for the recharge flux.

The recharge flux will be estimated directly through the Darcy's law approach, utilizing tensiometric and water content data as well as soil-water characteristics. The evaporation flux will be estimated with the use of a new micro-lysimeter technique. The evapotranspiration rate may be calculated with a water budget approach or any of a number of empirically or theoretically based equations utilizing meteorlological data with soil-moisture data. A temperature gradient method will also be used to approximate the seepage velocity of the recharge flux.

A computer flow model will be calibrated and verified against existing data to simulate infiltration, evapotranspiration, and the recharge flux. This model could be used at a later date to do some long term predictions of the ground-water recharge rate. It might also be used to estimate the lag time response between precipitation events and recharge.

2. RELATED RESEARCH:

This project will attempt to analyze and quantify the recharge phenomenon through a variety of methods. Some of these include estimations of hydraulic and temperature fluxes, tracer tests, and a numerical simulation. A number of previous studies have used one or more of these methods to estimate recharge. However, these studies are usually carried out in different climates or environments, and therefore may not be representative of the processes taking place under natural conditions in a semi-arid climate.

Enfield et al. (1973) evaluated the hydraulic and temperature gradient data from a site in the desert regions of Washington state and suggested that less than 1 cm/yr of water was recharging the underlying aquifer. Boyle and Saleem (1979) looked at temperature depth profiles in wells in northeast Illinois and concluded that the recharge rate was between 7.8 and 31.0 cm/yr. Klute et al. (1972) in an artificial recharge study in the high plains of Colorado calculated evaporation rates nearly equal to the precipitation rate. They found transpiration was not as pronounced as expected. Their conclusions suggested that natural ground-water recharge rates were very low. In this same general area Reddel (1967) estimated recharge rates from field methods and purported recharge rates on the order of 1 cm/yr. Reddel also says that low tension profiles in sandfill

areas suggest much larger recharge rates than the average stated previously.

Dincer et al. (1974) used stable isotopes and thermonuclear tritium to suggest that there is significant recharge through the sand dunes in arid Saudi Arabia. Meyboom (1966), through the use of water level hydrographs, estimated recharge to be approximately 7.5% of the annual precipitation on the Saskatchewan prairies in Canada.

Maxey and Eakin (1949) devised a method for use in the desert basins of Nevada to predict ground-water recharge. They assumed that ground-water discharge from a basin was essentially equal to the ground-water recharge coming into the basin. They then estimated that in areas where there was less than 20.3 cm/yr of precipitation the recharge rate was essentially zero. Watson et al. (1976) did a follow up study to the Maxey-Eakin technique. Using some multiple and linear regression models on the 1949 data, they estimated that as much as 3.4% of precipitation could become recharge in areas where precipitation was less than 20.3 cm/yr.

An interesting study by Sammis et al. (1982) compared three different techniques for estimating ground-water recharge on some irrigated agricultural land near Phoenix, Arizona. Their three methods were the hydraulic, temperature profile, and tritium analyses, which yielded rates of 18, 9, and 40 cm/yr

respectively. Averaging all three estimates yields a predicted recharge of 22 cm/yr.

Besides the physical or chemical means of estimating recharge, some researchers have utilized mathematical models to assist them in their predictions. Studies have been done from a completely theoretical viewpoint, where all data used in the model is hypothetical. There have been studies where the model is calibrated to the results of a laboratory column experiment and then the data is extrapolated to the field scale and predictions made. Still fewer studies have been done where the calibration and verification are carried out with field data.

Freeze's (1969) classical paper on the numerical simulation of natural ground-water recharge and discharge was done for various hypothetical application rates to look at the redistribution and recharge phenomena. No comparisons were made to field data. Hanks et al. (1969) simulated laboratory column data to make estimates of infiltration, redistribution, drainage and evaporation.

Krishnamurthi et al. (1977) simulated natural ground-water recharge on the high plains of Colorado with a mathematical model. They claimed good comparison of results to actual water level data, and presented a graph showing 5 years of simulated recharge rates, with values calculated monthly. These recharge rates were on the order of 1 cm/yr. Longenbaugh (1975) made

computer estimates of natural recharge in this same area of Colorado. He used field soil-moisture data for his simulations and concluded that recharge was approximately 6.1 cm/yr.

Gupta et al. (1978) developed a model for estimating soil-water movement, with their main emphasis being on evapotranspiration. The model calibrations and predictions from this study were for irrigated crops. Jensen (1983) presents an in-depth modeling study of unsaturated flow in two irrigated agricultural areas. He showed good correlation between model results and field data. Kirkham and Gee (1983) presented field and model results showing approximately 20% of the precipitation in the Washinton desert regions is recharge. They did state, however, that it was an unusually wet year.

Higuchi (1984) used numerical simulation results with field data for a humid region in Japan. He demonstrated that upward moisture fluxes occur above the 35cm depth following precipitation events, but that below this depth there is generally downward moisture flow. Thermal gradients are the cause of this upward moisture flux, while the general lack of diurnal temperature changes at depth yields a downward flux.

This is by no means a complete list of the studies done to date related to this project. However, it does show that there is a need for a larger data base in arid or semi-arid environments in order to predict more accurately the amount of

recharge that may be available. This project will hopefully supply some of that data, and this paper will utilize a portion of this data to give some initial results.

3. SITE SELECTION AND LOCATION:

The drainage basin under study is located approximately 24 kilometers north of Socorro, N. M. within the Sevilleta National Wildlife Refuge. More specifically, the drainage basin is approximately 4.8 kilometers west of Interstate 25 along the Rio Salado, an ephemeral river (see Figure 1). The basin is small, approximately 1.3 square kilometers in area.

There were several reasons for choosing this site to study natural ground-water recharge. First, a small portion of this area had been used for some previous research on borehole infiltration tests (Stephens et al, 1983). Much information had been obtained on soil characteristics in this one soil type through the use of in-situ and laboratory analyses. A soil-moisture station consisting of a set of tensiometers, set at various depths, a neutron access tube, and a set of subsurface temperature thermistors has been monitored at this site since November 1982. Analysis of this preliminary data seemed to suggest that relatively high recharge rates were taking place. Also contributing to this hypothesis was the fact that pressure heads within the soil profile were on the order of 0.1 to 0.3 bars, quite moist for a semi-arid environment. These low values of soil-moisture tension made possible the use of tensiometers for measuring pressure heads, rather than the more troublesome thermocouple psychrometers or degradable gypsum blocks.

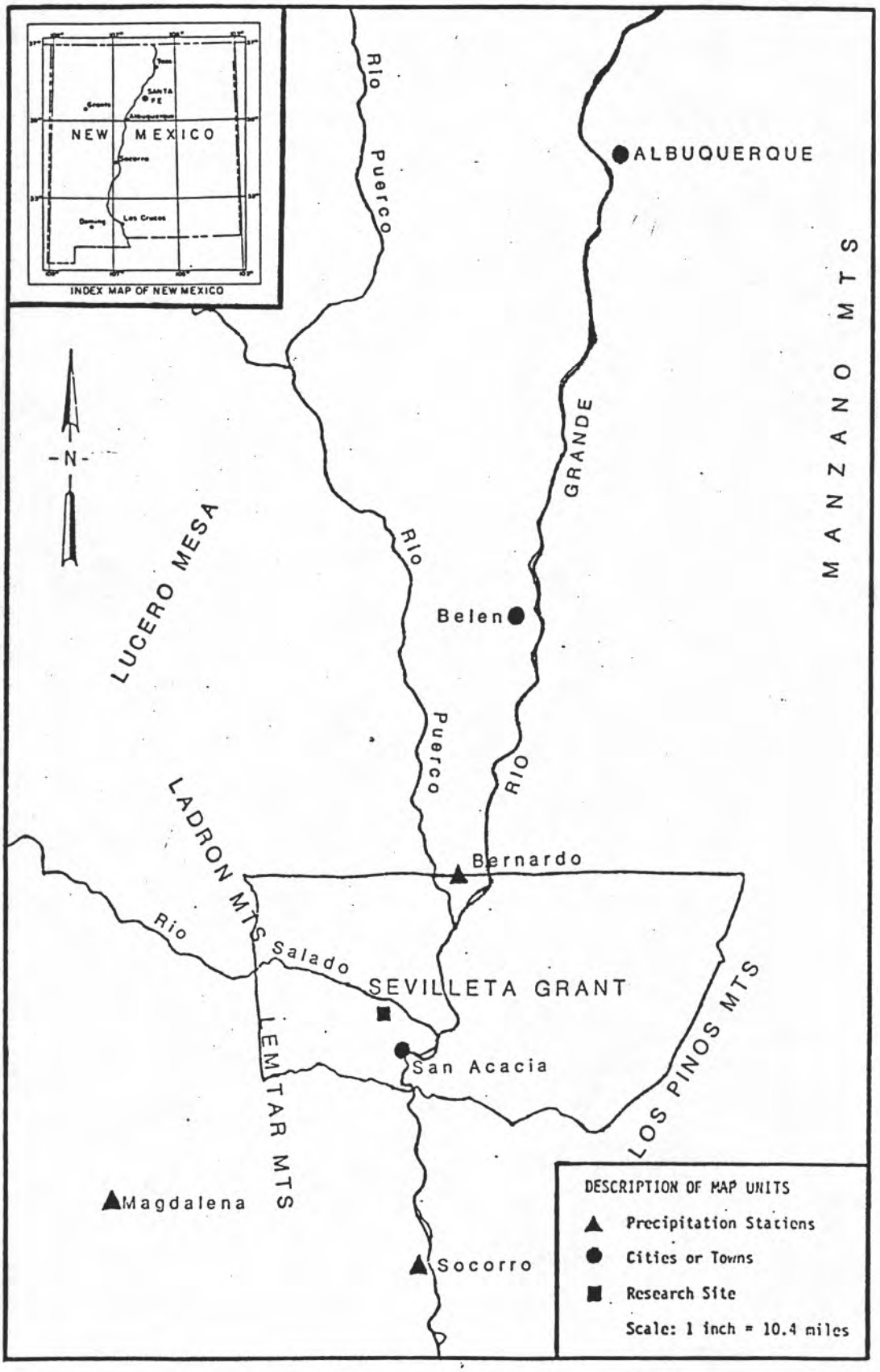

FIGURE 1 - Location Map of Site

Another reason for selecting this basin was its size. At approximately 1.3 square kilometers it was easy to install instrumentation throughout a good deal of the basin and still retain easy access. The basin also shows little or no signs of surface runoff. Most of the surface soils are quite permeable and therefore facilitate rapid infiltration of precipitation. Assuming the surface water runoff is negligible it becomes easier to estimate the water budget of the basin. This implies that almost all the precipitation that falls on this basin must either be evapotranspired or must be recharging the saturated zone.

Still another factor in choosing this basin was security. The Sevilleta National Wildlife Refuge is maintained by the U.S. Fish and Wildlife Service as a conservancy, and entrance to the area is only allowed by special permit. This permits the luxury of leaving delicate, and expensive, instrumentation out at the site without having to secure it in special enclosures.

This site will also give the opportunity to study recharge as a function of varying soil type, slope, location, and vegetation. Figure 2 shows a geologic map of soil type as mapped by Machette (1978). Machette has mapped four separate soil types within this basin. The topography of this basin is shown in Figure 2 also, along with the locations of the instrumentation sites.

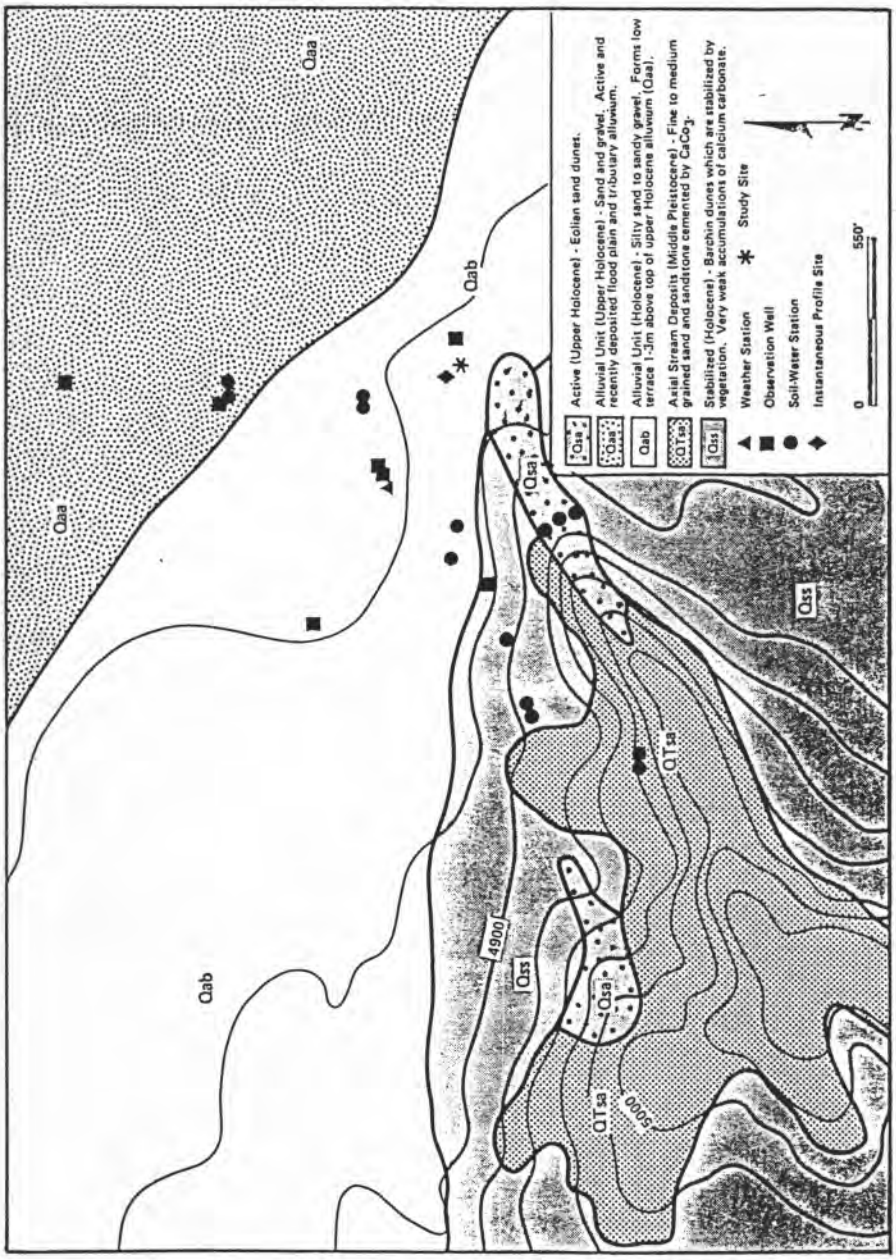

FIGURE 2 - Geologic Map Showing Instrumentation Sites

4. HYDROLOGIC PROCESSES:

The hydrologic processes occurring at the research site can be summed up briefly in terms of a hydrologic budget. Basically the concept of the hydrologic budget is inflow minus outflow equals the change in storage of water. This can be represented as follows:

$$P - ET - RU - I - R = \int(d\theta/dt)dZ \qquad (4.1)$$

where :

P = precipitation rate, [L/T]

ET = evapotranspiration rate, [L/T]

RU = surface water runoff rate, [L/T]

I = interflow rate, [L/T]

R = recharge rate from areal deep percolation, [L/T]

$\int(d\theta/dt)dZ$ = the change in water content per unit time over some increment of depth, [L/T]

The basin under study is quite small, as pointed out previously. There is little or no signs of surface water runoff within the basin. The small amounts of runoff observed to date have discharged into the Rio Salado river channel. Therefore the term RU in equation 4.1 is assumed to be negligible at the research site.

It is realized that the Rio Salado, when flowing, is a losing stream and probably contributes a significant amount of recharge to the underlying aquifer. The shallow water table

along the floodplain suggests that there is a fair amount of recharge. This study did not employ the equipment necessary for estimating this recharge from the Rio Salado. Gauging of the river channel flow into and out of the basin boundaries, along with soil-moisture instrumentation, would probably be required to accurately estimate stream loses. Techniques using the stable isotopes of oxygen and hydrogen may also be useful in quantifying the amount of recharge from the river to the underlying water-table aquifer. This study is involved in estimating the recharge phenomenon occurring through the unsaturated zone due to infiltration of precipitation. This is represented by the term R in equation 4.1 for the areal deep percolation rate. The analyses to be presented later in this paper will deal only with the processes occurring above the water table, in the vadose zone, and will not be directly involved with estimating the recharge from the Rio Salado to the underlying water-table aquifer. This paper is only dealing with field results and analyses for soil-moisture station 1. At a later date future researchers will compare and contrast the recharge rates for different soil types, vegetation, and slopes within the basin. At this time, however, the main interest is in quantifying the hydrologic processes that are occurring at soil-moisture station 1.

At soil-moisture station 1 the depth to the water table is approximately 6 meters. The soil-moisture instrumentation was placed relatively close to a stand of four-wing salt bush, approximately 0.8 meters away. From a pit dug in the area it has been estimated that the maximum rooting depth is about 1.5 meters. The assumption is being made that any downward flow gradient occurring below the root zone is contributing to the recharge of the saturated zone. There are a number of processes taking place within the soil profile between the land surface and the bottom of the root zone before any recharge flux is observed. These processes must be recognized before a full understanding can be made of the recharge process.

The land surface about soil-moisture station 1 is relatively level. This implies that both the runoff and interflow terms shown in equation 4.1 are probably negligible. Therefore these terms will be left out of the hydrologic analysis and the assumption is made that this will result in no substantial errors in evaluating the other hydrologic processes that occur.

The precipitation term in equation 4.1 can be estimated from the meteorological data collected at the site. It should be noted that the precipitation gauge at the site is collecting precipitation at a height of approximately 1.2 meters above land surface. The actual precipitation arriving at the land surface may be slightly less, due to evaporation processes. In arid

climates the evaporation potential on falling raindrops is generally quite large, due to relative humidity and advection effects. This process is assumed to be negligible between the height that precipitation is measured and the land surface. Therefore all the precipitation recorded will fall to the land surface and have the potential to either evaporate or infiltrate into the soil. Once this water has infiltrated past the land surface, it does not mean that the water must always travel downward through the soil profile. Evaporation at the soil surface may induce an upward gradient of water flow which also may evaporate.

This evaporation process at, or just below, the land surface is dependent upon temperature, relative humidity, solar radiation, wind velocity or advection, and the available moisture in the soil. There are empirical and theoretical methods for predicting the amount of potential evaporation from the soil. These methods generally employ the use of meteorological data to estimate some potential evaporation. The methods generally do not incorporate any soil-moisture characteristics and therefore may not accurately predict the actual evaporation rate under less than saturated conditions. The assumption made in deriving these relations is that the soil profile is never short of water (Doorenbos and Pruitt, 1977). Under natural flow conditions this is generally not the case. These methods of approximating the evaporation rate were developed for use with irrigated

agriculture. An overview of these methods is given in a subsequent section.

Part of this evaporation process is the movement of water vapor through the soil profile. Water vapor from soil moisture moves in the direction of higher temperature. Therefore it is assumed that in an arid environment, such as the site under study, water vapor will be traveling out of the soil profile during the day when surface temperatures are relatively high, and then downward into the soil profile at night when the soil surface is greatly cooled due to advection. This phenomenon has been discussed by Hillel (1980). From field observations it has been noted that there is dew forming during the night at the land surface. This is due to the cooling and condensing of water vapor in the atmosphere at lower night time air temperatures. Therefore it might be possible for this condensed water vapor to then flow into the soil profile. So evaporation processes may be greatly reduced during the night and may then influence other processes below the land surface. Evans and Thames (1981) state that in some arid environments moisture from dew can account for as much as 10% of the total moisture available in the soil profile. The other 90% of the moisture is derived from precipitation. Quantifying the potential effect of temperature and water vapor movement could prove to be a very difficult task, and is beyond the scope of this paper.

Below the land surface there is another part of the evapotranspiration phenomenon, the water uptake by plant roots, or transpiration. The amount of transpiration occurring from the plant is dependent upon the amount of soil moisture available, the soil texture, and soil-water chemistry. The more water available to a plant, the more it will transpire, to a point. Conversely, there generally exists some water content level that will not sustain plant life. The point at which the plant can no longer function in relation to water content and pressure head within the soil is often referred to as the permanent wilting point. Native vegetation in an arid or semi-arid environment is generally thought to have very high wilting points, on the order of -40 bars of pressure (Evans and Thames, 1981). A good discussion of the evapotranspiration phenomenon is presented by Jensen (1983).

Another part of the hydrologic budget as represented by equation 4.1 is the change in water storage with time. This factor is greatly influenced by the soil-water characteristics, the evapotranspiration effects, and the hydraulic characteristics of the soil.

The flow of water through a one-dimensional vertical profile of soil could be represented by the tension-based version of the Richard's equation:

$$C \frac{\partial \psi}{\partial t} = \frac{\partial}{\partial z} \left(K(\psi) \frac{\partial \psi}{\partial z} \right) - \frac{\partial K}{\partial z} - S \qquad (4.2)$$

where:

C = specific moisture capacity, or $\partial\theta/\partial\psi$, [1/L]

ψ = pressure head, [L]

t = time, [T]

z = depth, [L]

$K(\psi)$ = hydraulic conductivity as a function of pressure head, [L/T]

S = sources or sinks, [1/T]

This formulation, or an alternate form of it, has been used quite extensively to describe flow through the unsaturated zone.

The infiltration of water into the soil profile has been shown to displace the moisture already in the soil downward, and ahead of this infiltrated water. Warrick et al. (1971) and Dahiya et al. (1980) have both shown this type of result from experimental data. Warrick et al. (1971) have therefore suggested that ground-water recharge may occur even though the infiltrated water has not reached the water table. Quissenberry and Phillips (1976) contradict the findings of Warrick et al. (1971) when dealing with macropores. However, this is not the case at this study site.

It has been shown that the infiltration of water through the soil profile does not necessarily cause recharge. Smith (1967) demonstrated in theory that a wetting front could be completely absorbed within the soil profile without causing a recharge pulse

if the soil was initially very dry.

In addition to a wetting front advance occurring after a precipitation event, there is also a redistribution phenomenon taking place. The addition of infiltration water into the soil profile decreases the pressure head around the wetting front. As the wetting front advances, due to gravity forces and capillary pressures, the soil behind the wetting front generally increases in pressure head, or begins to dry out. The total head behind the wetting front may then become less than the total head within the wetting front. This causes a potential upward flow gradient behind and within the wetting front. Therefore capillary pressures act to redistribute this moisture above the wetting front, and dampen out the magnitude of the water content within the wetting front. Biswas et al. (1966) give a good discussion of this process, and also relate the history of research that has been done on this topic. Biswas et al. (1966) concluded that the rate of redistribution is a function of the initial water content in the soil profile and the hydraulic characteristics of the soil.

Hysteresis may have a pronounced effect on the redistribution phenomenon. A soil can be characterized hydraulically by its water content, pressure head, and hydraulic conductivity interrelationships. Generally, if a soil is under drainage conditions it has a specific pressure head versus water

content relation. During imbibition, or wetting, of the profile the pressure head is generally higher for the same water content value than during drainage conditions. This phenomenon implies that if the soil profile goes from wetting to drying conditions, or vice-versa, the pressure head may change significantly without a measureable change in water content. This hysteresis phenomenon will be shown graphically in a subsequent section. The hydraulic conductivity versus pressure head relation is also hysteretic with respect to wetting and drying. The hydraulic conductivity versus water content relation does not exhibit a hysteresis effect. These relationships must be well defined experimentally before any accurate predictions can be made of the infiltration and redistribution effects.

The deep percolation of infiltrated water through the vadose zone that recharges a water-table aquifer does not necessarily cause ground-water mounding. According to some numerical modeling results presented by Freeze (1969) the water-table elevation can be dropping even while recharge is occurring. Basically, these results imply that the ground-water outflow and discharges from the aquifer are greater than the recharge. A static water table implies a balance between inflow and outflow in the aquifer.

FIGURE 3 - The Weather Station and Surrounding Vegetation

The two additional rain gauges were set at opposite ends of the basin, one near the head of the basin on the south, and one in the river channel. The gauge in the river channel was identical to the one at the weather station. The third gauge is a weighing type with accuracy to 0.05 inches. The purpose of installing 3 rain gauges in an array was to determine whether or not the thunderstorms that track through the area have differing intensities and precipitation amounts in different parts of the basin. To date the differences appear to be negligible. However, as will be pointed out later, the precipitation for the period of record is below average, and therefore may not be indicative of any average meteorological events.

The recording observation wells were installed with New Mexico Tech's Mobile B-30 drill rig. The three recording wells, numbers 1, 3, and 4, were constructed of 6 inch diameter PVC pipe with 5 feet of number 20 slot PVC screen at the bottom. Well number 1 was installed at the weather station site. Well number 3 was installed just into the river channel. Well number 4 is located at the base of the slope along the floodplain to the south of the weather station. These three wells run a somewhat straightline perpendicular to the riverbed. Assuming the prevailing water-table gradient is mimicking the river channel gradient and flowing eastward toward the Rio Grande, then wells 1, 3, and 4 make a line that is perpendicular to the ground-water flow direction. Wells 5 and 6 radiate out from the weather

station in the east and west directions, respectively. This arrangement of wells should allow for easy utilization of Stallman's (1971) technique for computing ground-water recharge or discharge at a later date when a longer data base is obtained.

Well number 7 was drilled to a depth of refusal at the weather station site. A driller's log of this hole is presented in Appendix A. It is assumed that the refusal depth of 17.1 meters is the base of the phreatic aquifer. This means that there is approximately 14 meters of saturated thickness in this aquifer at this point. The drilling operation for this well revealed very coarse sands and cobbles throughout the saturated zone. This suggests that these fluvial deposits have a high permeability, and therefore make for a very good aquifer. Well number 7 was completed only to a depth of 10.7 meters, due to the refusal of the well point to be pushed through a cobble. Wells 5, 6, and 7 were each made of 2 inch diameter galvanized steel pipe with 3 feet of wire-wrapped number 20 slot screen at the bottom.

Well number 2 was installed in the river channel with the hopes of defining any hydraulic stream-aquifer interconnection during periods of high streamflow. The well was made of 2 inch diameter PVC pipe which was slotted with hacksaw cuts in the bottom 3 feet.

The soil-moisture station sites were chosen on the basis of soil type, slope, and vegetated cover. The station locations are shown by number in Figure 2. Each station consists of a set of tensiometers, ranging in depth from 30cm to 244cm below land surface. If the water table was shallower than 244cm the maximum depth was set just above the water table at the time of installation. The tensiometers were assembled in the laboratory. They were inserted with the aid of a tensiometer insertion tool. Special care was taken to ensure that the annular space was properly backfilled and that the porous cup was making good contact with the surrounding media. Proper saturation of the porous cup was also considered a crucial step in getting good contact with the porous media. From November 1982 through November 1983 site number 1 had mercury manometer tensiometers. From November 1983 to the present all stations were given tensiometers equipped with septum rubber stoppers for use with a portable field transducer for measuring pressure heads. Figure 4 shows a schematic of how these type of tensiometers are constructed. These tensiometers were constructed in the New Mexico Tech soils laboratory according to the specifications of Marthaler et al. (1983). It was deemed that the mercury manometer type of tensiometer was too delicate and cumbersome to maintain on a long term basis. Furthermore, potential environmental hazards associated with liquid mercury were avoided. One set of mercury tensiometers was maintained at site

number 1 for comparison with the pressure transducer type tensiometers. Good agreement was found between both types of tensiometers. Appendix A has tabulated and graphical sets of tensiometric data in the form of total hydraulic head versus time for both mercury manometer and pressure transducer type tensiometers. The pressure transducer setup is essentially the same as that outlined by Marthaler et al.(1983). A calibration procedure for the transducer is outlined in Appendix B.

Each soil-moisture station also included a neutron access tube. The latest neutron probe being used on this project for measuring moisture contents is made by Campbell Pacific Nuclear, model 503, and has a 50 millicurie americium-beryllium source. The previous neutron probe used was a Troxler model 3222 depth moisture gauge with a 10 millicurie source. Some electronic breakdowns occurred in the Troxler during the winter of 1983-1984 which were not repaired after a number of shop visits, and much down time. Therefore the new Campbell unit was put into use at the end of April 1984. A calibration procedure is outlined in Appendix C for the Campbell unit. The neutron access tubes were installed to a depth of 5.8 meters whenever possible. Exceptions occurred if the water table was shallower or bedrock was encountered. The tubes were set so as to keep them out of the saturated zone. The bottoms were capped with rubber stoppers to be sure that no moisture would seep into the aluminum tubes and possibly alter the water content readings.

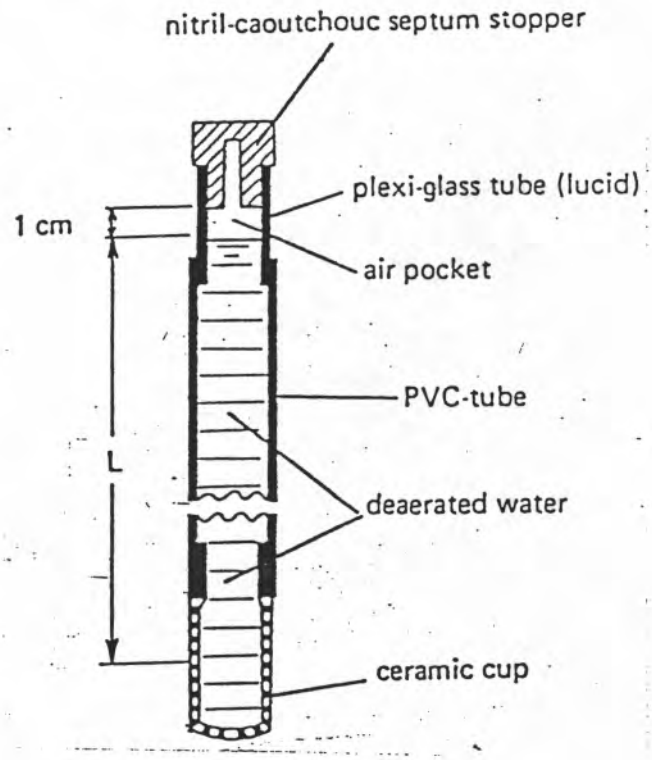

A) TENSIOMETER SETUP

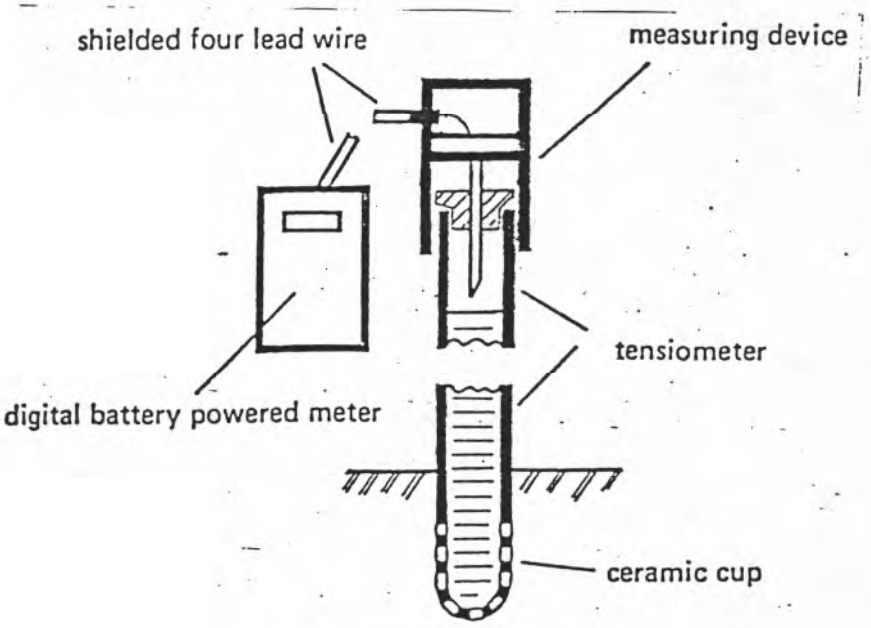

B) MONITORING SETUP

FIGURE 4 - Schematic of Tensiometer Used with the Portable Pressure Transducer

The aluminum access tubing was set by hand augering a 5cm diameter hole to the proper depth and backfilling with native material. Care was taken to ensure a proper and complete backfill occurred. Stations 11 and 12 required the use of the drill rig for their installation due to the size of the cobbles within the soil profile.

As stated earlier there were various reasons for selecting the sites for each soil-moisture station. Soil-mosture station 1 was established early on in November 1982. This station was set up near the previous research site used for borehole infiltration tests by Stephens et al. (1983). Extensive field and laboratory tests were conducted at the borehole infiltration test site to characterize the saturated hydraulic conductivity (Ks), unsaturated hydraulic conductivity versus pressure head relationship ($K-\psi$), volumetric water content versus pressure head relationship ($\theta-\psi$), grain size distribution, and spatial variability. The site is located in a soil type that is a transition zone from the sand dune, which is an unstable eolian deposit, and the fluvial deposits of the Holocene epoch along the floodplain. Figure 2 shows the numbered locations of all the soil-moisture stations. In addition to the tensiometer and neutron tube instrumentation there is also a set of subsurface temperature thermistors and an automated data acquisition system, employing a microprocessor, a scanning valve, and one pressure transducer, for logging tensiometer data. This data acquisition

system is decribed in detail by Tyler (1982). This site, with all its instrumentation and hydraulic data, is the one being used in this paper for analyses.

Stations 2, 3, 9, and 10 are located in the floodplain in the soil type listed by Machette (1978) as an alluvial deposit of the Holocene age. Figures 5 and 6 show photographs of sites 9 and 10, respectively. Station 9 is a good example of the instrumentation setup at a vegetated site; station 10 is a typical unvegetated site. Vegetation can be sparse in this basin, as evidenced in Figure 6. Each set of paired soil-moisture stations, vegetated and non-vegetated, were kept within 10 meters of each other. Stations 9 and 10 are located halfway between the weather station and the river channel. Stations 2 and 3 are located near the break in soil type between the alluvial floodplain deposits and the stabilized eolian sand deposits. Throughout the alluvial regime there is a noticeably finer grained surface soil texture, and correspondingly a greater plant density, than in the eolian deposits.

Stations 4, 5, 6, 7, and 8 are located in the eolian deposits of the Holocene age. Station 4 is located near the outcrop of the Santa Fe formation sandstone, a consolidated deposit. This is an axial stream deposit from the middle Pleistocene to middle Pliocene epoch that is slightly weathered at this location. The intent of setting the neutron tube at the

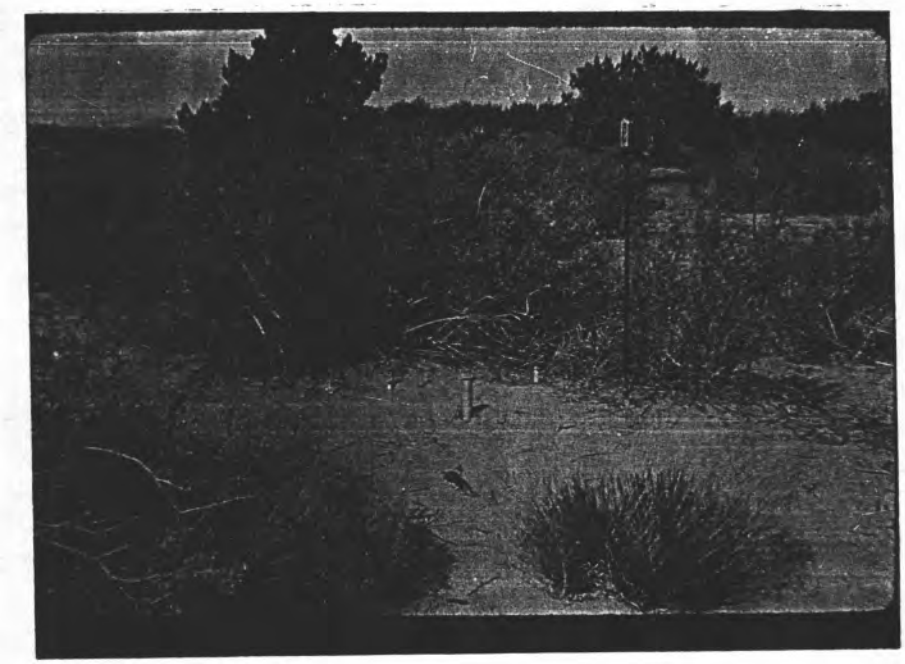

FIGURE 5 - Soil-Moisture Station 9, vegetated site

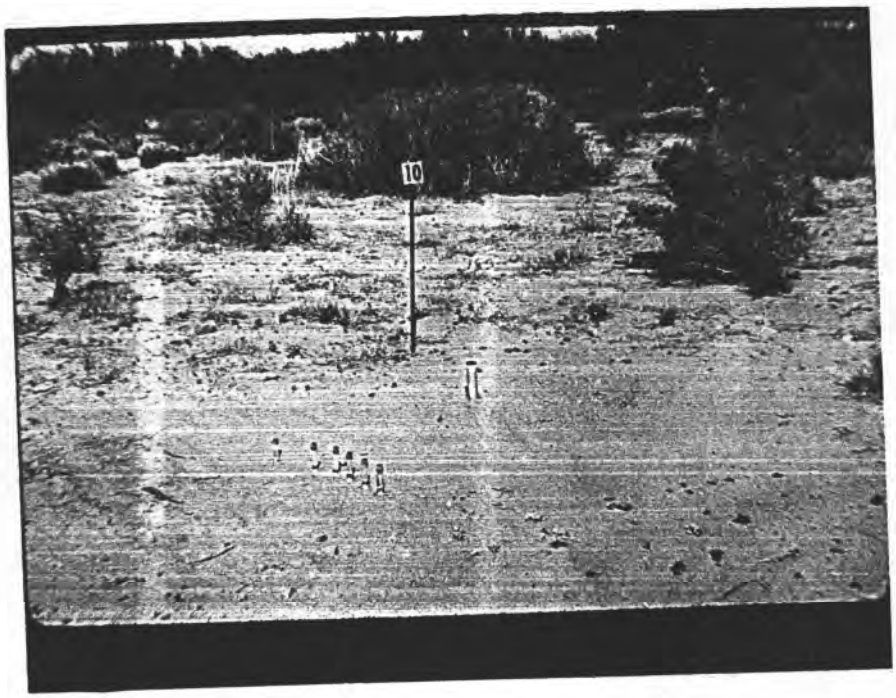

FIGURE 6 - Soil-Moisture Station 10, sparsely vegetated site

bedrock surface underlying the eolian deposits was that it might be possible to monitor some interflow over the bedrock within the unconsolidated material. The depth to bedrock at this point is roughly 3.5 meters, and the site is relatively close to observation well number 4.

Stations 5 and 6 are located at low elevations in this eolian deposit. Stations 7 and 8 are located high on the slope, and quite near the weighing-type rain gauge. The vegetated sites are 6 and 8, while stations 5 and 7 are non-vegetated.

Two stations, numbers 11 and 12, are located in an alluvial deposit of the upper Holocene age. They are located just inside the river channel bank. Station 11 is unvegetated and station 12 is vegetated.

The active dune on the southeast side of the basin was also instrumented. Stations 13, 14, and 15 define a transect across the dune from west to east. It was found that these dune sands are quite thick; the neutron tube augering going down to 5.8 meters and not encountering any consolidated material. This contrasts with Machette's estimate of a thickness usually less than 2 meters.

The axial stream deposits at the top of the basin could not be instrumented with available equipment due to their consolidated nature.

6. MONITORING PROCEDURES:

The instrumentation at the study site is monitored either continuously, via recording charts and cassettes, or semi-weekly through manual observations.

The three recording observation wells, hygrothermograph, three precipitation gauges, and the radiometer all have seven day recording charts and must be changed once a week. The evaporation pan instrumentation is read semi-weekly. The non-recording observation wells are also measured twice a week.

It was recommended by Dr. Lynn Gelhar of MIT (personal communication, 1983) that the soil-moisture stations be monitored every 4 to 5 days for the purpose of doing a time-series analysis on the data. To date there has not been a long enough period of record on the soil-moisture data to warrant doing a time-series analysis.

The tensiometers were therefore measured semi-weekly. It was felt that when 2 to 3 years worth of data has been collected a reasonable statistical analysis could be made. The tensiometers were serviced regularly and kept filled with de-aired, distilled water. The water was de-aired in the field by bubbling helium through it.

A small experiment had been run in the laboratory comparing different methods of de-airing water. The methods were boiling only, boiling and condensing the vapor, and bubbling helium through the sample. No methods were readily available to determine the concentrations of all dissolved gases in distilled water. It was decided that the best indicator of dissolved gas was analyzing for dissolved oxygen. The standard Winkler test was used for this determination. The percentage of dissolved oxygen removed from distilled water by each of the three methods was 75%, 75%, and 93%, respectively. Therefore, it was concluded that de-airing distilled water with diffused helium was a very effective method. It was also quite suitable for field applications. A tank of compressed helium was left at the research site for de-airing water on demand.

During the winter months it was found that temperatures were cold enough to freeze and crack the plastic tops on the tensiometers. This permitted the tensiometers to lose their vacuum and drain their contents out the cups, thus locally upsetting the natural flow field. It was felt that gathering winter tensiometric data was essential in determining recharge amounts, owing to winter precipitation in the form of sustained gentle rains and snow. Furthermore, there is an unknown amount of time required to route late summer or early autumn infiltration through the soil profile. Monitoring during the winter when transpiration is at a minimum is a critical element

of the data collection program. Therefore, laboratory experiments were carried out to determine the effects of substituting a fluid into the tensiometers that has a lower freezing temperature. The procedures and results of this experiment are outlined in Appendix D. In summary, it was found that using a 40% solution of ethylene glycol in de-aired, distilled water showed no differences in pressure head readings as compared to tensiometers filled with only distilled water. Therefore, this solution was used in the tensiometers during the winter months.

The water content profiles were taken at each soil-moisture station on a weekly basis. The first neutron tube was installed in November 1982. The total depth of the tube was 213cm. Measurements were made in 15cm increments from 30cm to 198cm of depth below land surface. In September 1983 this neutron access tube was replaced with a 5.8m deep tube. Measurements were made in 15cm increments from 30cm to 274cm depth, and in 30cm increments from 274cm to 549cm depths. It was found that monitoring with a neutron probe is very time consuming and tedious. Therefore roughly half the sites were measured each time a trip was made to the field. This minimized the time spent gathering data in any given day.

The subsurface temperature thermistors were monitored semi-weekly. So, too, were the micro-lysimeters. These micro-lysimeter canisters were set in triplicate and anlyzed according to Boast and Robertson (1982). A more detailed discussion of this method is presented elsewhere in this paper.

The bromide tracer tubes were monitored in accordance with precipitation events. The tubes were set between storms and pulled for analysis one to four days following the storms. Many questions arose in trying to implement this technique. Some of these questions and procedures are outlined elsewhere in this paper.

The automated data acquisition system was not installed at soil-mosture station 1 until the spring of 1984. This late installation was done to prevent the pressure transducer from freeezing, and possibly becoming damaged, during the winter months. The intent of using this automated data acquisition system was to better define any pressure pulse, or wetting front, that might occur in the soil profile as a result of a precipitation event. As the data will show later on, the winter and spring months were quite dry. The total precipitaion from January 5, 1984 to May 31,1984 was only 0.28cm. Therefore, this data system was not really put to the test and did not yield any worthwhile results. It is hoped that at a later date this equipment will collect some very valuable data toward

understanding the infiltration, redistribution, and recharge phenomena taking place at the research site.

The data collection did not stop at just weekly or semi-weekly measurements. If a precipitation event occurred that was of an appreciable size, additional trips were taken for site monitoring as frequently as daily. This afforded better resolution on the infiltration characteristics associated with different precipitation events while the automated data acquisition system was not in use.

7. FIELD TESTS:

The research site is comprised of four different mapped soil types. To date the only detailed analysis of soil texture and hydraulic properties has been done near soil-moisture station 1. This site was used previously by Stephens et al. (1983) in their investigations of borehole infiltration tests. Field test data are available from that project in the form of borehole tests, instantaneous profile tests, air-entry permeameter tests, and the double-tube method. These tests yield values and relationships between water content, pressure head, and unsaturated and saturated hydraulic conductivities. The methods being used in this report are utilizing data from an instantaneous profile test run at the site.

The instantaneous profile test entails the monitoring of the transient state internal drainage of a soil profile through the use of tensiometers and neutron probe logging. The method is based upon work done by Richards and Weeks (1953), Ogata and Richards (1957), Rose et al. (1965), and Watson (1966). The final procedure developed for field application was devised by Hillel et al. (1972).

The experiment is set up such that tensiometers are installed at various depths throughout a soil profile. A neutron access tube is installed relatively close to the tensiometer setup to obtain simultaneous readings of pressure head and water

content with depth and time during drainage. A berm is built around the instrumentation to facilitate the ponding of water over the site to wet up the profile to near saturation. When the profile has been wet to near saturation the ponding is ceased. The surface is then covered with plastic to prevent evaporation and the upward flow of water. The assumption is made that there exists only vertical downward flow during drainage. Measurements of water content and pressure head with time and depth will then allow the solution of the following governing flow equation:

$$\frac{\partial \theta}{\partial t} = \frac{\partial}{\partial z}\left[K(\theta)\frac{\partial H}{\partial z}\right] \qquad (7.1)$$

where θ is water content, $K(\theta)$ is the unsaturated hydraulic conductivity as a function of water content, t is time, z is depth, and H is total hydraulic head.

Hillel et al. (1972) developed a graphical procedure for solving this governing flow equation. Water content is plotted against time for each depth of measurement in the profile. A slope is then determined graphically from each curve for each time desired for output. This slope is a very critical parameter in the final determination of the unsaturated hydraulic conductivity. The change in moisture with time is then multiplied by the depth increment over which this change has taken place. This quantity represents a flux for that depth increment. The fluxes are then summed for each successively

deeper depth. Having obtained this Darcian flux for each depth the next step is to divide by the hydraulic gradient to obtain a value of unsaturated hydraulic conductivity. This is done for all depths at each output time desired. The result is a set of corresponding water content, pressure head, and unsaturated hydraulic conductivity values for each depth.

Another alternative to processing the instantaneous profile data by Hillel's method was devised by this author. A computer program was written to utilize regression techniques on the pressure head versus time, moisture content versus time, and total head versus depth relationships. These data could then be processed with the derived mathematical relationships instead of the graphical procedure outlined by Hillel et al. (1972). This mathematical technique yields results that are not as biased by personal manipulation of the data as in the graphical technique. However, the regression technique is only as good as the curve-fit that it yields. A poor curve-fit should yield a poor estimation of the unsaturated hydraulic conductivity. If care is taken to ensure that the curve-fits are good, the results from this computer program can be quite reliable, and much quicker to use than the graphical method. A discussion of this program, and a comparison of results, is presented in Appendix E. The program has only been tested against this one set of data and should be checked against new data as these tests are performed in the other soil types at the site.

The analysis of the instantaneous profile test data utilized tensiometric and water content data from the 30, 61, 91, 122, and 152cm depths. The soil profile here appeared homogeneous with only slight signs of stratification. The results of the graphical procedure are shown in the plot in Figure 7 of unsaturated hydraulic conductivity versus pressure head (commonly referred to as the $K-\psi$ relationship) for all five depths. One can see in Figure 7 that the unsaturated hydraulic conductivity may vary as much as one order of magnitude for the same pressure head between any two depths. Figure 8 shows the unsaturated hydraulic conductivity versus volumetric water content (sometimes referred to as the $K-\theta$ relationship) for the same test. This plot does not show the variability that the conductivity versus pressure head plot did. This would indicate that the unsaturated hydraulic conductivity is probably not as sensitive to changes in water content as it is to changes in pressure head. The conductivity versus water content relationship is relatively uneffected by hysteresis. Therefore a $K-\theta$ relationship could be used in analyzing both wetting and drainage data, even though it has been derived from a drainage type of test. The $K-\psi$ or $\theta-\psi$ relationships can have very pronounced differences for drainage and imbibition conditions, as will be shown later. Figures 7 and 8 show $K-\psi$ and $K-\theta$ relationships that are only slightly varied between any two depths. From this observation it might be safe to assume that the soil profile is relatively homogeneous between

the 30 and 152cm depths. This assumption will be very important in analyzing the field data to determine the recharge rate.

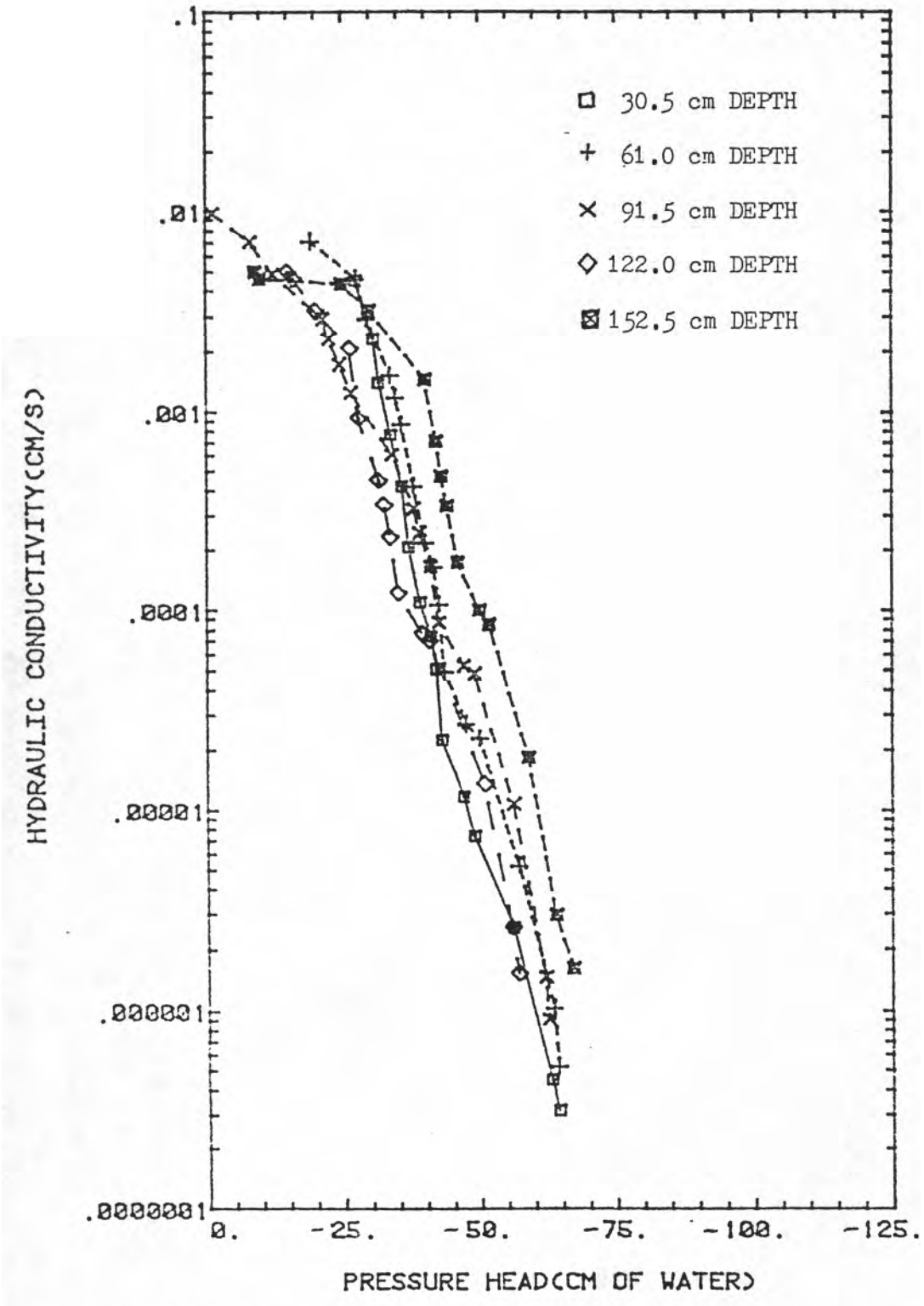

FIGURE 7 - K versus Pressure Head Data From Instantaneous Profile Test

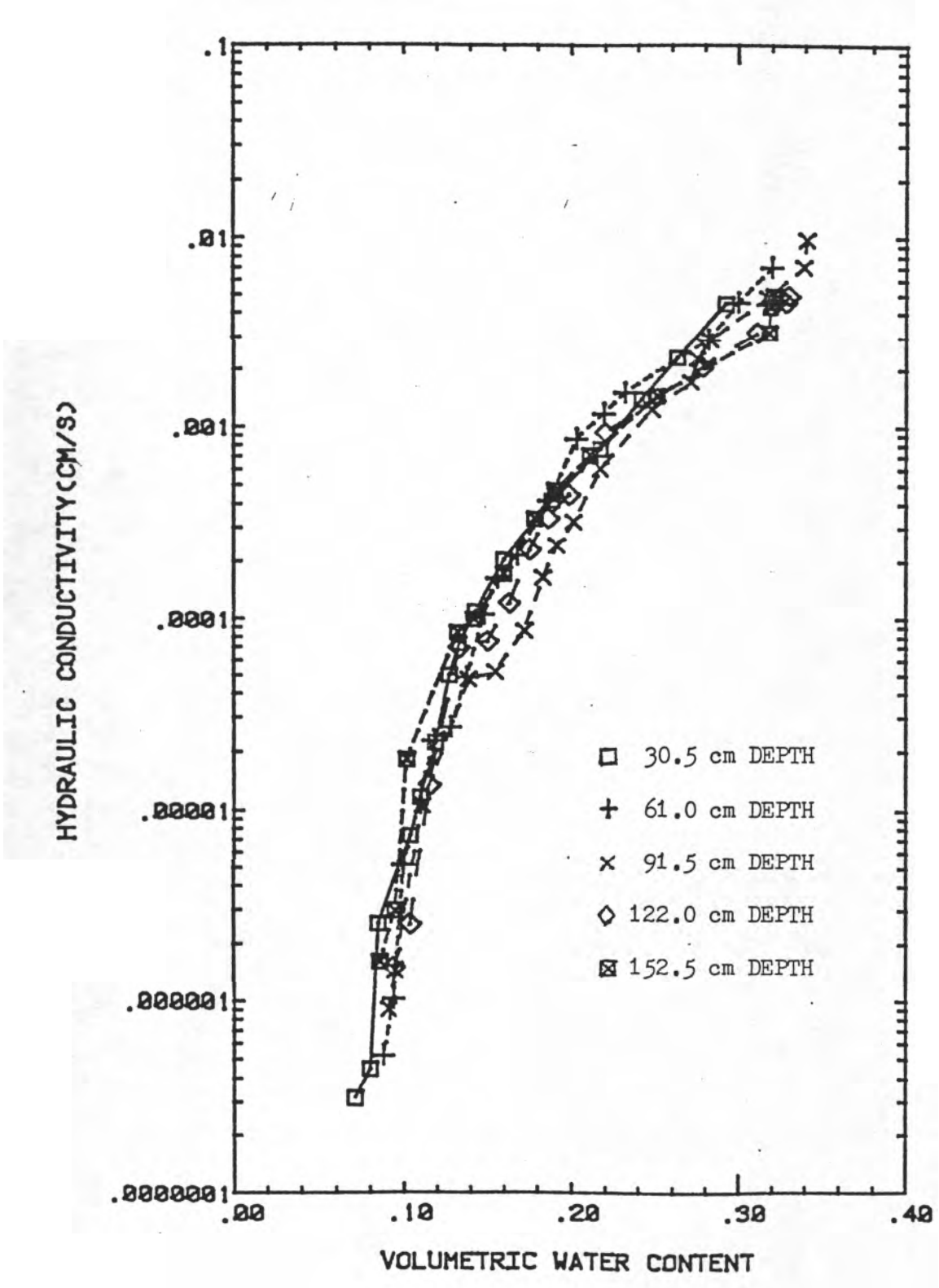

FIGURE 8 - K versus Water Content Data From Instantaneous Profile Test

8. LABORATORY TESTS:

There has been a significant amount of laboratory work done on soil samples collected from the research site used by Stephens et al. (1983) near soil-moisture station 1. Grain size was analyzed and the effects of spatial variability investigated. Saturated hydraulic conductivity estimates were determined with 100cc 'undisturbed' PF ring samples in a laboratory permeameter. It was found that the relatively small length of samples used in the laboratory permeameter were prone to disturbance through piping or wall effects. This led oftentimes to quite variable results.

In attempting to better estimate the saturated hydraulic conductivity of the soil the author helped a fellow graduate research assistant, Richard Rabold, build a new shelby tube permeameter for use in the laboratory. This permeameter utilizes a thin-walled steel tube of 41.88cm^2 cross-sectional area and 61cm length. Six tubes can be run at one time with either a constant head or falling head boundary condition at the top. Each tube is outfitted with a number of piezometers across its length for measuring head changes throughout the sample. These shelby tube samples were obtained with the aid of the New Mexico Tech Mobile B-30 drill rig. A continuous profile of soil samples was collected at soil-mosture station 1 from 0 to 5.33 meters. For a more in-depth discussion on the use of this shelby tube

permeameter refer to Rabold (1984).

The profile of depth versus saturated hydraulic conductivity near soil-moisture station 1 is shown in Figure 9. The individual plots of hydraulic conductivity versus time for each subsample within the shelby tubes are shown in Appendix F. The maximum hydraulic conductivity value obtained during infiltration in the permeameter for each plot in Appendix F was assumed to be the saturated hydraulic conductivity for that sample. Rabold (1984) calculated the error involved in estimating the saturated hydraulic conductivity with the shelby tube permeameter to be on the order of ± 10%.

Another laboratory analysis determined the soil-moisture characteristic curve (also referred to as the θ-ψ curve) in the 100cc 'undisturbed' soil samples(PF rings) using the hanging column method. The method was used for both imbibition and drainage. Figure 10 shows the results from the 30.5cm depth. The data from all depths analyzed is presented in Appendix F. An in-depth dicsussion on the use of the hanging column apparatus is given by Larson (1984).

Figure 10 shows the effect of hysteresis on the soil samples. This effect can be quite prominent when trying to understand infiltration, redistribution, and recharge phenomena. The fitted curves through the data in Figure 10 (and in Appendix F) were calculated with the use of an analytical model written by

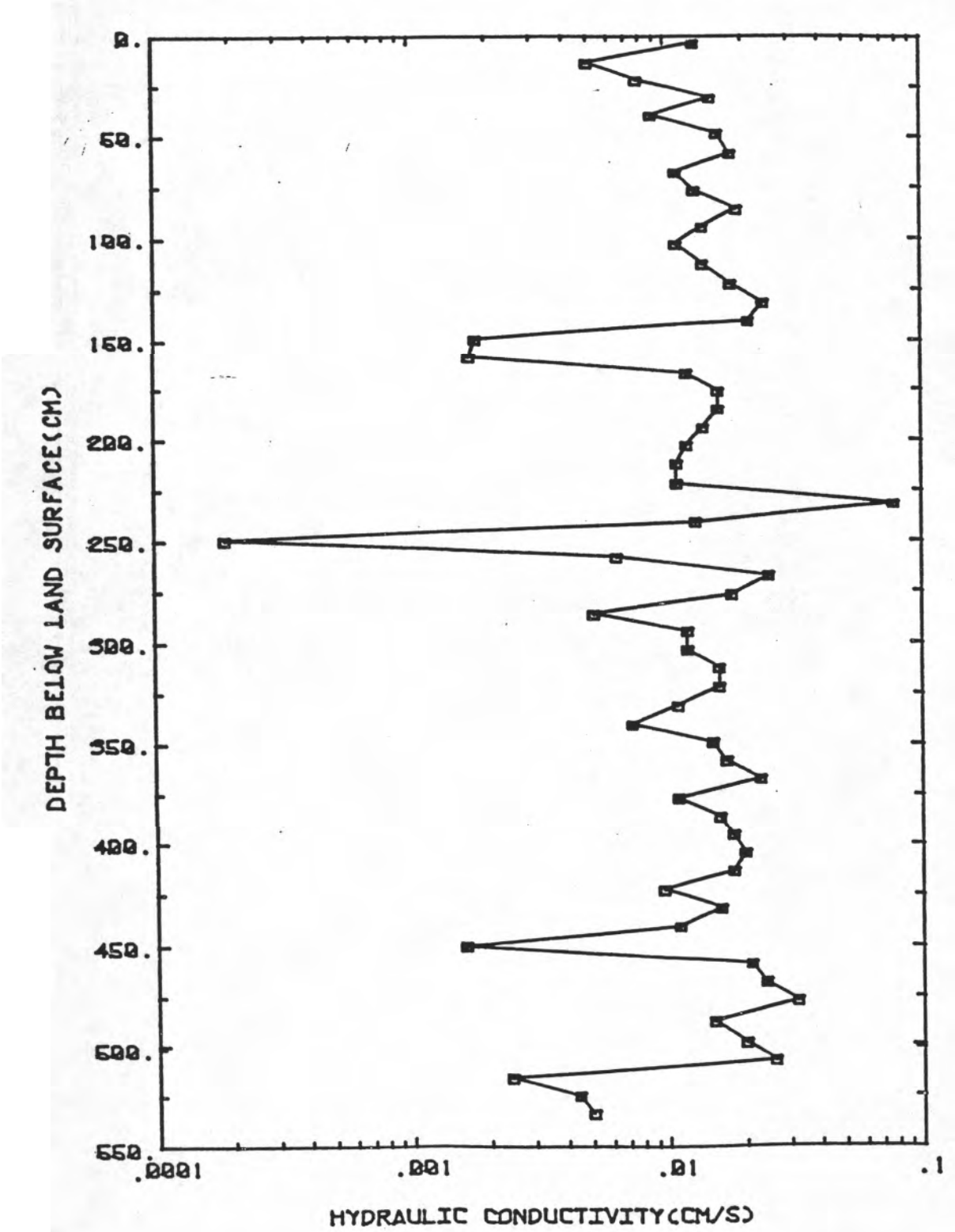

FIGURE 9 - Depth versus Saturated Hydraulic Conductivity from the Shelby Tube Permeameter

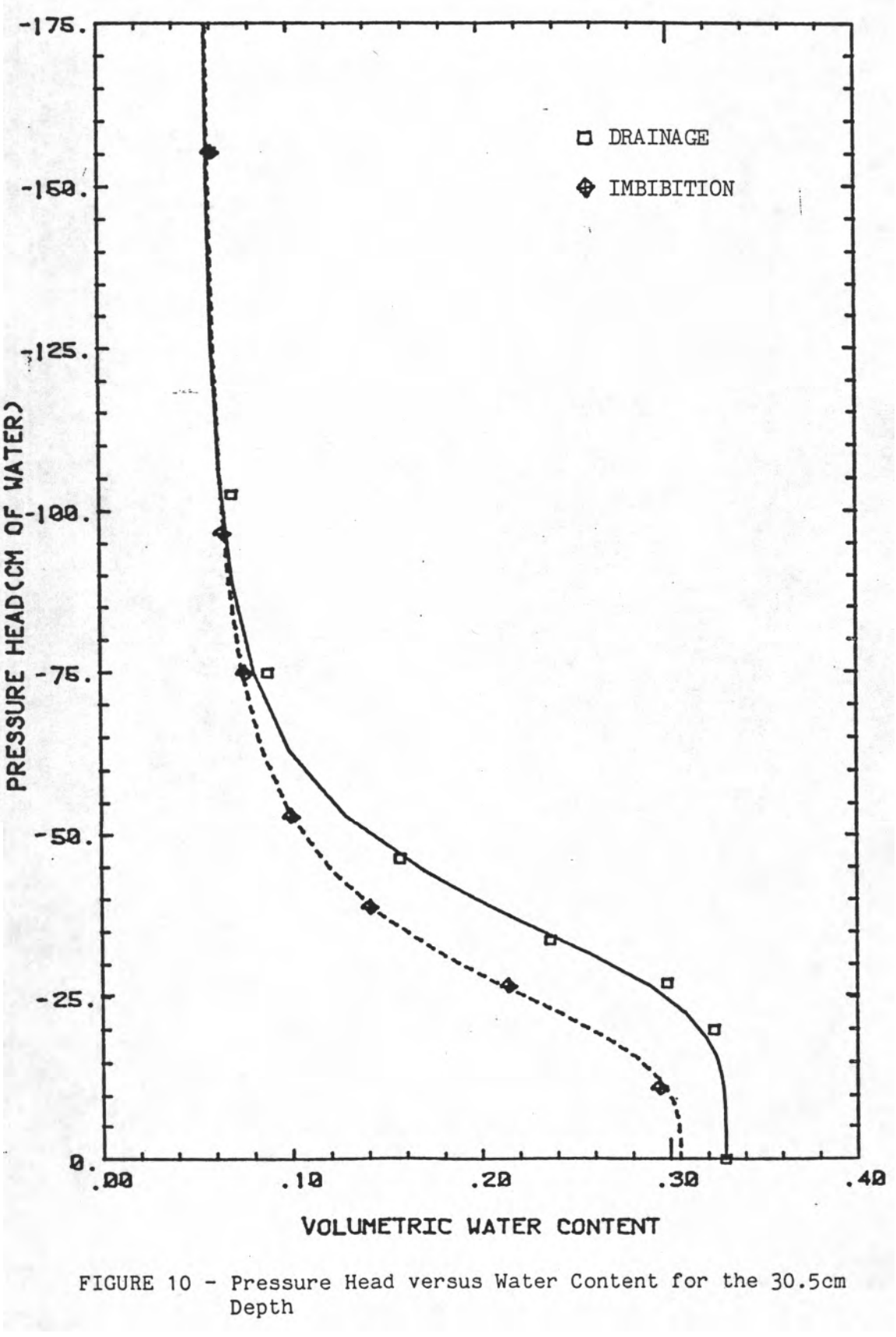

FIGURE 10 - Pressure Head versus Water Content for the 30.5cm Depth

van Genuchten (1978). This model uses a non-linear least-squares regression technique to generate a smooth curve-fit through the inputted θ-ψ data from the hanging column results. van Genuchten's model has essentially 3 different equations to choose from for use in the regression analysis. These 3 model options were developed in theory by Mualem and Burdine, and are discussed by van Genuchten (1978). The curve-fits presented in this report employ the 2 parameter Mualem approach. This curve-fitting was carried out to yield better input data for use in the numerical model, which will be discussed later.

9. METHODS OF ANALYSIS:

9.1 DARCY'S LAW APPROACH:

As mentioned in section 3, this report is concerned with estimating the deep percolation flux through the unsaturated zone that is recharging the ground-water table. The assumption is made that any downward flux of water below the root zone will eventually reach the water table. If an estimate can be made for this flux, then this is assumed to be the same recharge flux occurring at the water table. One method of estimating this flux is by the Darcy's law approach.

Darcy's law can be represented as:

$$q = K(\psi) \times i \qquad (9.1)$$

where q = Darcian flux, [L/T]

$K(\psi)$= unsaturated hydraulic conductivity as a function of pressure head, [L/T]

i = hydraulic gradient, also represented as dH/dZ, which is the change in total hydraulic head per length of flow path, [L/L].

The tensiometric data from soil-moisture station 1 will permit the calculation of the hydraulic gradient over a given time span. An average value of pressure head could also be obtained for the depths under consideration over the same time span. The corresponding value of unsaturated hydraulic conductivity may be obtained from the results of the

instantaneous profile test that was performed at the borehole infiltration test site used by Stephens et al. (1983). The effective hydraulic conductivity over the depths under consideration is estimated by employing a harmonic or geometric averaging scheme. A harmonic mean yields a value of the hydraulic conductivity representing a stratified medium. A geometric mean is appropriate for a relatively homogeneous medium.

The unsaturated hydraulic conductivity may also be estimated from the water content data obtained from the neutron probe logging of the aluminum access tubes at soil-moisture station 1. The Darcian flux could then be estimated from equation 9.1 by assuming a unit gradient within the profile under consideration.

9.2 TEMPERATURE GRADIENT METHOD:

Another method of analysis used for estimation of the recharge flux is the temperature gradient approach. Stallman (1963) was the first to introduce this method. The governing assumptions behind the derivation of this technique were that the porous media should be saturated, homogeneous, and isotropic. This method has been typically used to calculate seepage velocities through leaky confining layers into and out of confined aquifers. Boyle and Saleem (1979) give a good discussion on how to use this technique. Sammis et al. (1982) showed how this method could be used in the vadose zone with good results. Because the final result of this method is an estimate of the seepage velocity, it should not matter that the soil profile is not saturated. Knowing the water content in the soil will permit the calculation of the recharge flux.

This technique is being applied to the temperature data gathered from soil-moisture station 1 at relatively shallow depths; the 152, 183, and 213cm depths to be more specific. At these depths there may be diurnal temperature fluctuations, as well as seasonal changes. In any given season the temperature data has usually been collected at about the same time each day measurements were taken. This should minimize any diurnal fluctuations in the data. The data is to be analyzed as an average for each depth for the period of record. The assumption

is being made that averaging over the period of record will minimize any error associated with seasonal changes in temperature.

This method entails solving two separate equations to estimate the seepage velocity. The first equation to be used is solved iteratively for the term B, where:

$$\frac{Tz - To}{Tl - To} = \frac{\exp(Bz/L) - 1}{\exp(B) - 1} \qquad (9.2)$$

Tz = temperature at depth z

To = temperature at depth z = 0

Tl = Temperature at depth z = L

L = vertical distance over which temperatures are observed

This value of B is then used in the following equation to solve for the seepage velocity, Vz:

$$Vz = \frac{k\ B}{Co\ Po\ L} \qquad (9.3)$$

k = thermal conductivity of the medium

Po = density of the medium at field saturation

Co = specific heat of water

Having solved for the seepage velocity, the average water content, θ, could then be used to estimate the Darcian velocity, or recharge flux, from the following equation:

$$q = Vz \times \theta \qquad (9.4)$$

9.3 WATER BUDGET APPROACH

One approach taken in trying to quantify evapotranspiration rates is the water budget method. This method entails summing the water inputs and outputs through the soil profile and equating these to changes in water storage. The system under consideration is just a one dimensional cross-section within the soil profile. The equation characterizing flow in this system is as follows:

$$P - ET - RU - I - R = \int(d\theta/dt)dZ \qquad (9.5)$$

where :

P = precipitation rate, [L/T]

ET = evapotranspiration rate, [L/T]

RU = surface water runoff rate, [L/T]

I = interflow rate, [L/T]

R = recharge rate, [L/T]

$\int(d\theta/dt)dZ$ = the change in water content per unit time over some increment of depth, [L/T]

At this study site it was assumed that the surface water runoff is negligible. The interflow term in this equation is also assumed negligible, owing to the level terrain. Therefore these two terms will drop out of the governing equation. The precipitation rate is a known quantity from the site instrumentation. The term on the right side of equation 9.5 represents the change in water storage within the soil profile.

This quantity is estimated from the water content data obtained with the neutron probe. Being able to estimate either evapotranspiration or the recharge rate will permit solving for the final unknown quantity.

Quantifying evapotranspiration without the aid of a weighing lysimeter requires the use of empirical or theoretical equations. A description of the various mathematical equations now being used for this purpose is given in a subsequent section of this paper. Most all of these methods yield a potential evapotranspiration rate, and not an actual rate. Therefore an attempt will be made to quantify the recharge rate and solve for the evapotranspiration rate.

Estimation of the recharge rate was discussed previously in section 9.1. The results from the Darcian approach to calculating the recharge flux will be used as input to the water budget method of estimating the evapotranspiration flux. Once an estimate has been made for the recharge flux and the change in storage, equation 9.5 may be solved for the evapotranspiration rate.

9.4 THEORETICAL/EMPIRICAL EVAPOTRANSPIRATION ESTIMATES

Another approach to estimating the recharge flux is that of estimating the evapotranspiration demand with theoretically or empirically derived equations, and calculating the resultant recharge flux by solving equation 9.5. There has been much research into methods of estimating evapotranspiration from 1948 to the present. All of these methods employ the use of meteorological data to predict a potential, or reference crop, evapotranspiration rate. Other relationships have also been developed to estimate the actual evapotranspiration rate from this reference crop estimate.

The use of the term potential evapotranspiration has been discouraged by many researchers (Cuenca and Nicholson, 1982; Doorenbos and Pruitt, 1977; and Evans and Thames, 1981; to name but a few). This term implies that an estimate is being made of the maximum obtainable evapotranspiration rate. This rate may never be obtainable in nature due to atmospheric or soil-moisture conditions. The potential evapotranspiration prediction will vary over time due to changing meteorological conditions. Therefore calling it a potential evapotranspiration rate is not fully accurate. The evapotranspiration equations are actually predicting a rate relative to a reference crop evapotranspiration rate. This reference is being made to "the rate of evaporation from an extended surface of a short green crop, actively growing,

completely shading the ground, of uniform height, and not short of water" (Evans and Thames, 1981).

A number of methods for predicting reference crop evapotranspiration have been outlined by Doorenbos and Pruitt (1977). These include the Blaney - Criddle, radiation, Penman, modified Penman, and pan evaporation methods. The Blaney - Criddle equation is empirically based and utilizes only temperature and sunshine data. Doorenbos and Pruitt (1977) state that this method yields unacceptable results in high altitudes where there are cold nights and high daytime radiation levels. This is probably due to the empirical nature of the method, and the fact that there is a small amount of meteorological data being used in the calculations. The radiation method uses temperature and sunshine, cloudiness, or radiation data. Estimates of wind and humidity must also be made. In general, Doorenbos and Pruitt (1977) state that this method gives slightly better results than the Blaney-Criddle. The Penman method is theoretically based and uses temperature, humidity, wind, and sunshine duration or radiation. The modified Penman approach differs in that it has a modification to its aerodynamic term. The pan evaporation method utilizes the pan evaporation rate and an empirical coefficient to correct for side-wall heating of the pan and aerodynamic effects.

Other investigators have presented different methods over the years. Thornthwaite and Mather (1948) ulitized tepmperature and length of day in their formulation. Jensen and Haise (1963) used temperature and solar radiation. Priestley and Taylor (1972) focused their work on available energy. Their model requires a local calibration to measured evapotranspiration, such as with a weighing lysimeter. Jury and Tanner (1975) modified the advection term in the Priestley - Taylor correlation and reported slightly better results. Again, this method requires local calibraton. Extensive research has been carried out by Morton (1969,1975) into predicting evaporation and evapotranspiration. The meteorological data requirements for use in his formulation are more extensive than this project can provide.

Each one of these methods has been used in site specific locations with reportedly good results. According to Shouse et al.(1980) in an arid environment, such as the one under study for this project, the best results are obtained with equations utilizing an advective term. These investigators analyzed differences between the modified Penman, radiation, Priestley-Taylor, modified Priestley-Taylor, and pan evaporation methods. They found that the modified Penman and modified Priestley-Taylor correlations gave the best results in an arid climate in California for irrigated agricultural crops. Van Bavel (1966) concluded from experiments performed at Phoenix,

Arizona that the Penman method adequately accounted for advection in an arid environment. He calculated excellent correlations between the Penman predictions and lysimeter results for open water, saturated soil, and irrigated alfalfa.

Jensen (1974) investigated the use of 16 different methods for estimating potential evapotranspiration in a variety of climates. He concluded that there is no one method that is universally adequate under all climatic conditions.

The instrumentation and data from this project are not adequate to calibrate one of the above mentioned models that requires calibration. The equations without advection terms are unsuitable for this research site. Therefore, the modified Penman approach will be used in this analysis and applied without calibration. For ease of calculations a numerical model written by Gupta et al., as presented in Appendix III of Doorenbos and Pruitt (1977), is being used. This model calculates reference crop evapotranspiration results for the 5 methods previously mentioned under Doorenbos and Pruitt (1977).

The actual evapotranspiration rate can be estimated from the reference crop evapotranspiration rate. Boonyatharokul and Walker (1979) outlined essentially 3 different methods for predicting actual evapotranspiration using the following relation:

$$ETa = Kc \times Etrc \qquad (9.6)$$

where ETa = actual evapotranspiration rate, Etrc = reference crop evapotranspiration rate, and Kc = crop stage coefficient. Kc is predicted by any of 3 different empirical relationships. The equations are presented as follows:

$$Kc = (1.0 - (Dp/Dt)^{**}m)^{**}n \quad (9.7)$$

$$Kc = (\log (1.0 + 100(1-(Dp/Dt))))/(\log 101) \quad (9.8)$$

$$Kc = ((Dt-Dp)/Dt) / b \quad (9.9)$$

where:

$$m = 0.02841 + 4.316x(1/Ro) + 0.07592x(Ksat/RoxETrc) \quad (9.10)$$

$$n = 8.777 - 32.40xRm + 8.709x(1/Ro) + 0.028x(Ksat/(RoxETrc)) \quad (9.11)$$

$$b = 0.4229 + 0.1572xRo - 0.00790x(Ksat/ETrc) + 0.00006x(Ksat/Etrc)^2 \quad (9.12)$$

Dp represents the depleted available moisture from the entire root zone. Dt is the total available moisture in the root zone. Ksat is the saturated hydraulic conductivity. Ro is the value of the water uptake distribution at the soil surface, assumed to be 1.8 for a deep water-table condition. Rm is the distance from the soil surface to the centroid of the area under the water uptake distribution curve, assumed to be 0.3667. The parameters m,n, and b are empirical constants whose mathematical relationships in equations 9.10, 9.11, and 9.12 were developed by regression techniques. Boonyatharokul and Walker (1979) have indicated that the term b is often assumed to be 0.5, instead of using equation 9.12.

9.5 MICRO-LYSIMETER EXPERIMENTS:

A relatively new technique for estimating evaporation from bare soil has been used at the research site from March 1984 through May 1984. This method is explained in detail by Boast and Robertson (1982). Basically, this method utilizes a "micro-lysimeter", a scaled-down version of a weighing lysimeter, to measure water losses in a soil column due to evaporation.

The micro-lysimeter columns used in this study are run in triplicate. These columns are made from PVC pipe that are 7.5cm in diameter and 15cm in length. Each column is installed in the field by pushing it into the soil until the column is nearly full. The column of soil is then pulled from the surrounding soil and the bottom capped with a rubber stopper. The weight of the entire column is measured and then it is placed back into the soil with the top of the column flush with land surface. This is done to minimize any turbulent wind effects and to allow the natural atmospheric conditions to prevail over the tops of the columns. The columns are then left for 3 to 4 days and then pulled and weighed again. From the calculated difference in weight between the two weighings the evaporation rate can be estimated from the columns. The results from the three columns are averaged together to help minimize errors.

9.6 BROMIDE TRACER EXPERIMENTS:

Another experimental technique applied in this study is the use of a bromide tracer in measuring average water particle velocities, or seepage velocities, after natural precipitation events. The basic concept involved here has been employed by other researchers, such as Jury et al. (1982) and Saffigna et al. (1977).

Bromide is a highly soluble ion which very rarely occurs in nature in any appreciable amounts. It is easily detected with the use of a relatively inexpensive bromide electrode. For these reasons it is quite suitable for use in these experiments.

The initial phases of this experiment delt with much trial and error in establishing some acceptable procedures for bromide tracer tests. Jury et al. (1982) and Saffigna et al. (1977) utilized the drainage water from weighing lysimeters or water samples from porous cup soil-moisture samplers to analyze for bromide concentration while doing leaching experiments. The technique being used in this study is slightly different.

Some 15cm diameter PVC columns were installed at the field site by driving them into the soil until the top of each column is flush with land surface. The top 1cm of soil is then removed from the column and 5.0g of bromide are distributed over this surface in the form of $CaBr_2 2H_2O$. The previously removed

soil is then placed on top of the column again. Placing the bromide 1cm below land surface ensures that the bromide will not be blown away by the wind over the columns. The columns are then left in place until after a precipitation event occurs. A few days after the event the columns are pulled from the soil, capped at both ends, then brought back to the laboratory for analysis.

As soon as the columns are brought into the lab they are sectioned off in 1cm intervals, the soil samples placed in beakers, weighed, then put in the oven to dry. After 24 hours of drying at 105 °C the samples are taken out and weighed. This weighing and drying sequence permits the determination of the water content of each sample in the soil profile.

The next step is to add a certain volume of distilled water and ISA (Ionic Strength Adjuster) solution to each soil sample. Each sample is then stirred thoroughly, and while stirring is still underway the bromide electrode is lowered into the solution to determine the bromide concentration. Calculations are then made to determine the concentration of bromide in moles/kg for each depth in the soil profile.

The water content profile should show a sharp breakoff in elevated water content back to the initial levels of water content at a depth that corresponds to the wetting front. This depth should correspond to the value Z obtained from the following relation:

$$Z = (K(\theta o) \times t)/(\theta o - \theta i) \qquad (9.13)$$

where $K(\theta o)$ is the hydraulic conductivity behind the wetting front in units of [L/T], t is the time over which infiltration has occurred, θo is the volumetric water content behind the wetting front, and θi is the initial water content.

The bromide concentration profile should show the maximum depth of infiltration of the bromide salt due to the precipitation. This will be shallower than the wetting front, owing to some initial water in the profile being pushed ahead of the infiltrating water. Therefore, the vertical extent of the bromide salt should be an indication of the actual depth of infiltration of the precipitation. The depth of infiltration of the bromide may be approximated with the following equation:

$$Z = (K(\theta o) \times t)/(\theta o) \qquad (9.14)$$

10. RESULTS OF FIELD WORK

10.1 PRESENTATION OF FIELD DATA

Data collected at the research site comes in a variety of forms including recording charts, cassette tapes, and handwritten forms. The data analyzed for this report is limited to that collected prior to May 31,1984; this record was considered of sufficient length to evaluate seasonal effects and still be manageable for a master's degree study.

The charts from the recording instruments are not presented in this report. They are, however, available for inspection at the Geoscience Department here at Tech. The manually collected information for most all of the other instrumentation is presented in Appendix A. These data are presented in graphical, as well as tabular form, in relation to time.

Figure 11 shows a plot of total hydraulic head versus time. The total head data were from soil-moisture station 1. The plot is for the period of record that the precipitation gauge was in operation. It can be seen from this plot that the deeper depth tensiometers are measuring lower total heads than the shallower tensiometers. This would indicate a general downward frow gradient during the whole period of record. Therefore there must be a recharge flux occurring when data below the root zone show

downward flux potentials.

Figure 12 shows a plot of volumetric water content versus time for the 30.5cm depth from soil-moisture station 1. The data is shown for only the first year of data collection, November 1982 through October 1983. As mentioned previously difficulties were encountered in the use of the Troxler neutron probe during the 1983-1984 winter season. The probe required frequent repairs and the calibration characteristics may have changed during this time. Therefore the water content data collected during this time frame may be of questionable accuracy. Total hydraulic head and volumetric water content data versus time have been plotted and tabulated in Appendix A for soil-moisture station 1.

Sub-surface temperature thermistors were installed at soil-moisture station 1. Figure 13 shows a plot of temperature versus time for the 30.5cm depth for the first year of data collection, November 1982 through October 1983. Appendix A includes all the temperature data.

Figure 14 shows a plot of water level elevation versus time for observation well number 1. The observation well data is also presented in Appendix A. Each well was leveled in to a survey marker at the refuge. An assumed elevation was given to this marker and all well elevations were determined relative to the survey marker.

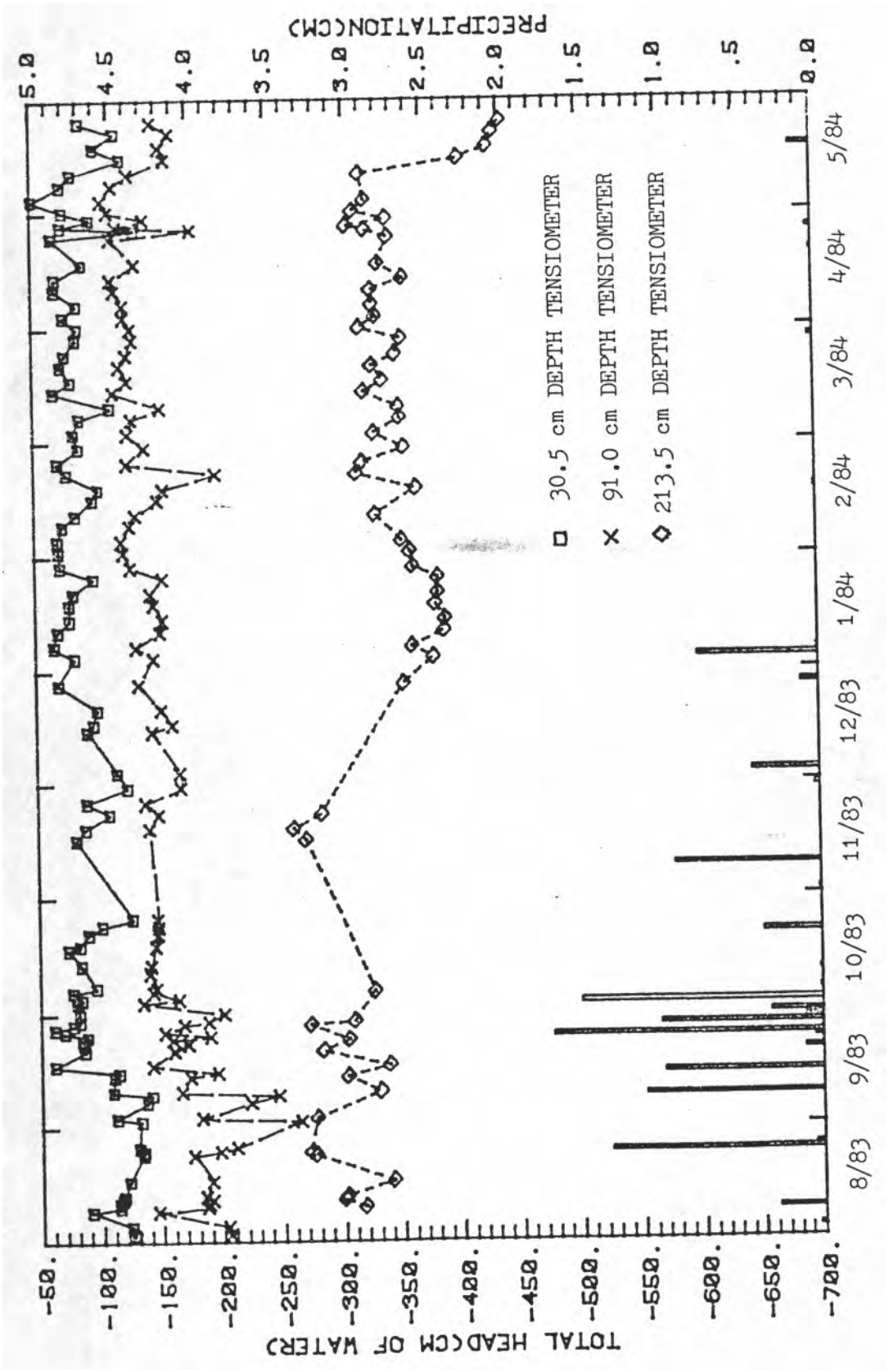

FIGURE 11 - Total Head and Precipitation versus Time

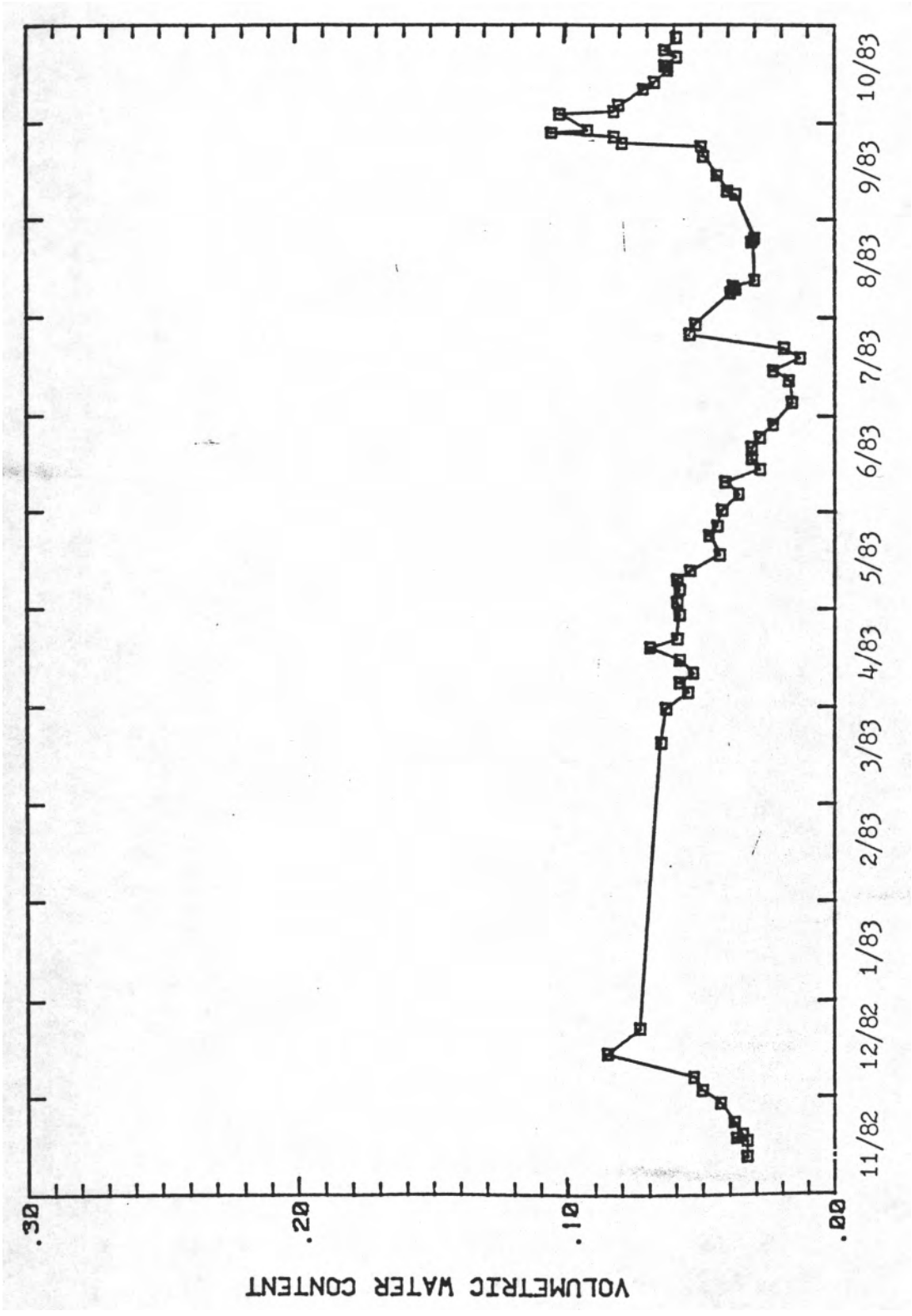

FIGURE 12 - Water Content versus Time for the 30.5cm Depth

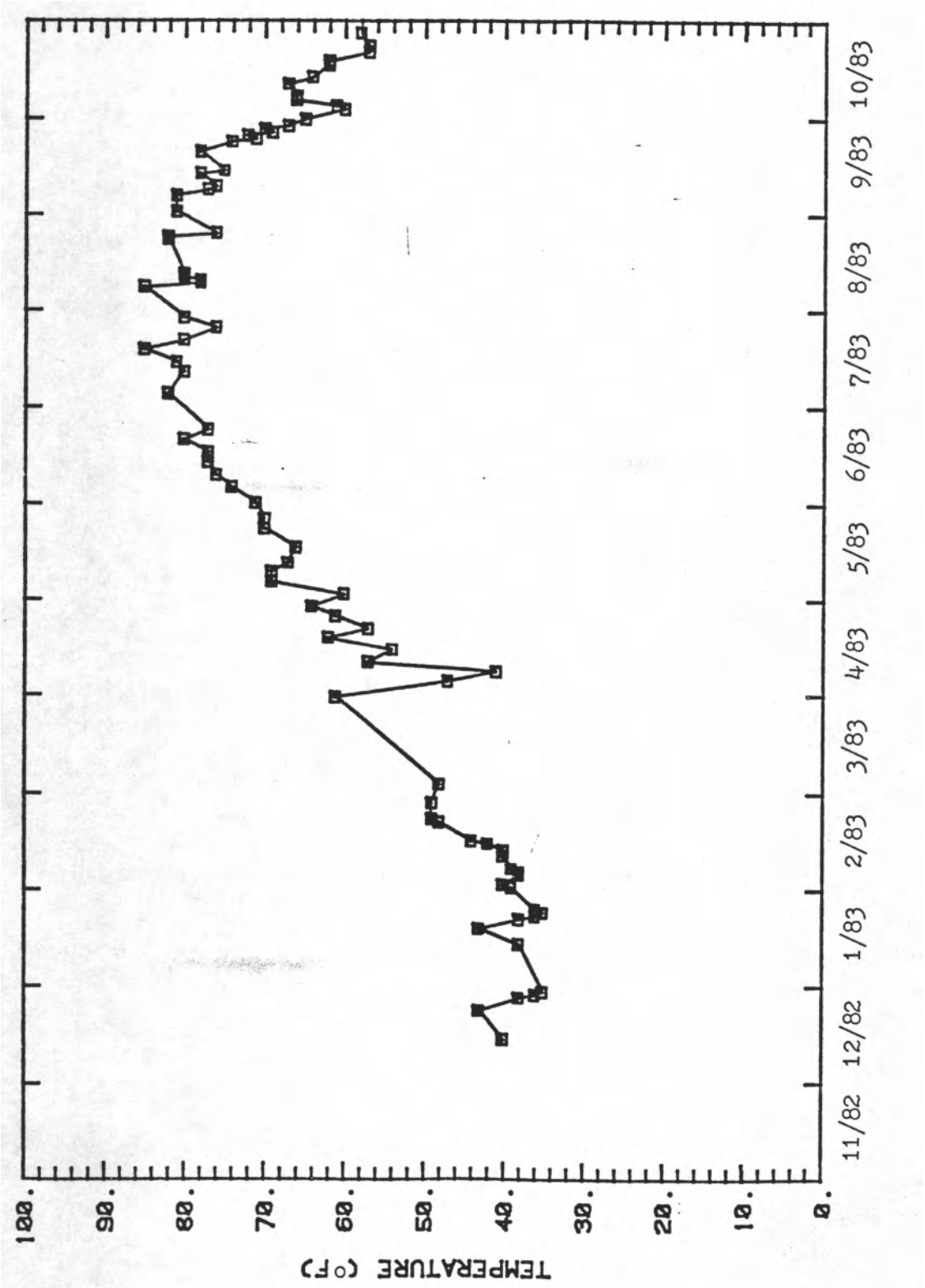

FIGURE 13 - Temperature versus Time for the 30.5cm Depth

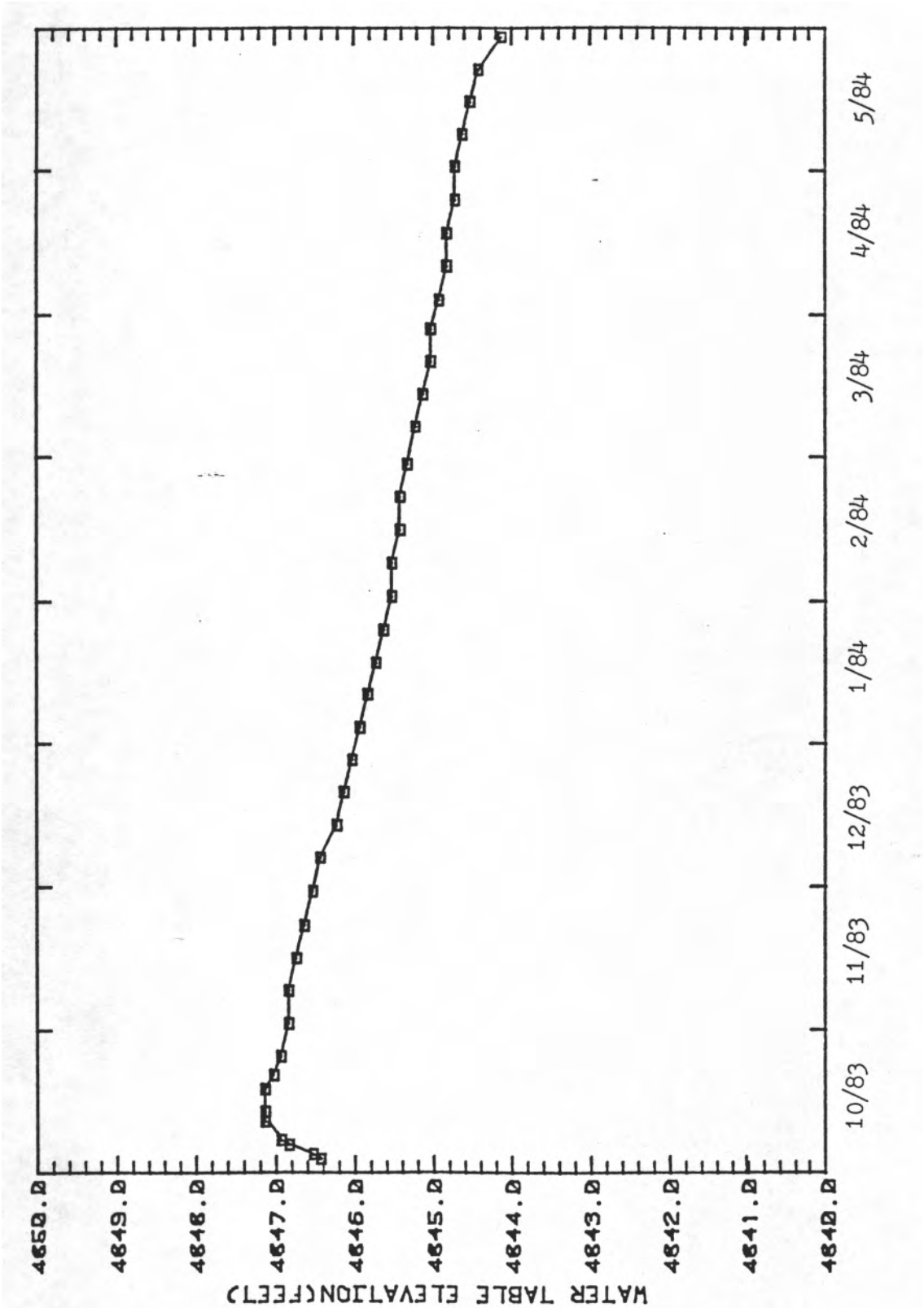

FIGURE 14 - Water Level Elevation versus Time for Observation Well Number 1

The micro-lysimeter experiments were initiated in March 1984 and continued through the present. Figure 15 shows the results in the form of evaporation rate versus time.

The pan evaporation rate as a function of time is shown in Figure 16. These rates were obtained by dividing the total amount of water evaporated from the pan over the time span between measurements, generally 3 to 4 days. Figure 17 shows the wind velocity versus time for the same time period at a height of 30cm above land surface adjacent to the pan. The maximum and minimum evaporation pan temperatures are shown in Figure 18 against time.

Theoretical and empirical methods of evaluating this data to make estimates of evaporation, transpiration, and recharge rates will be presented in a subsequent section.

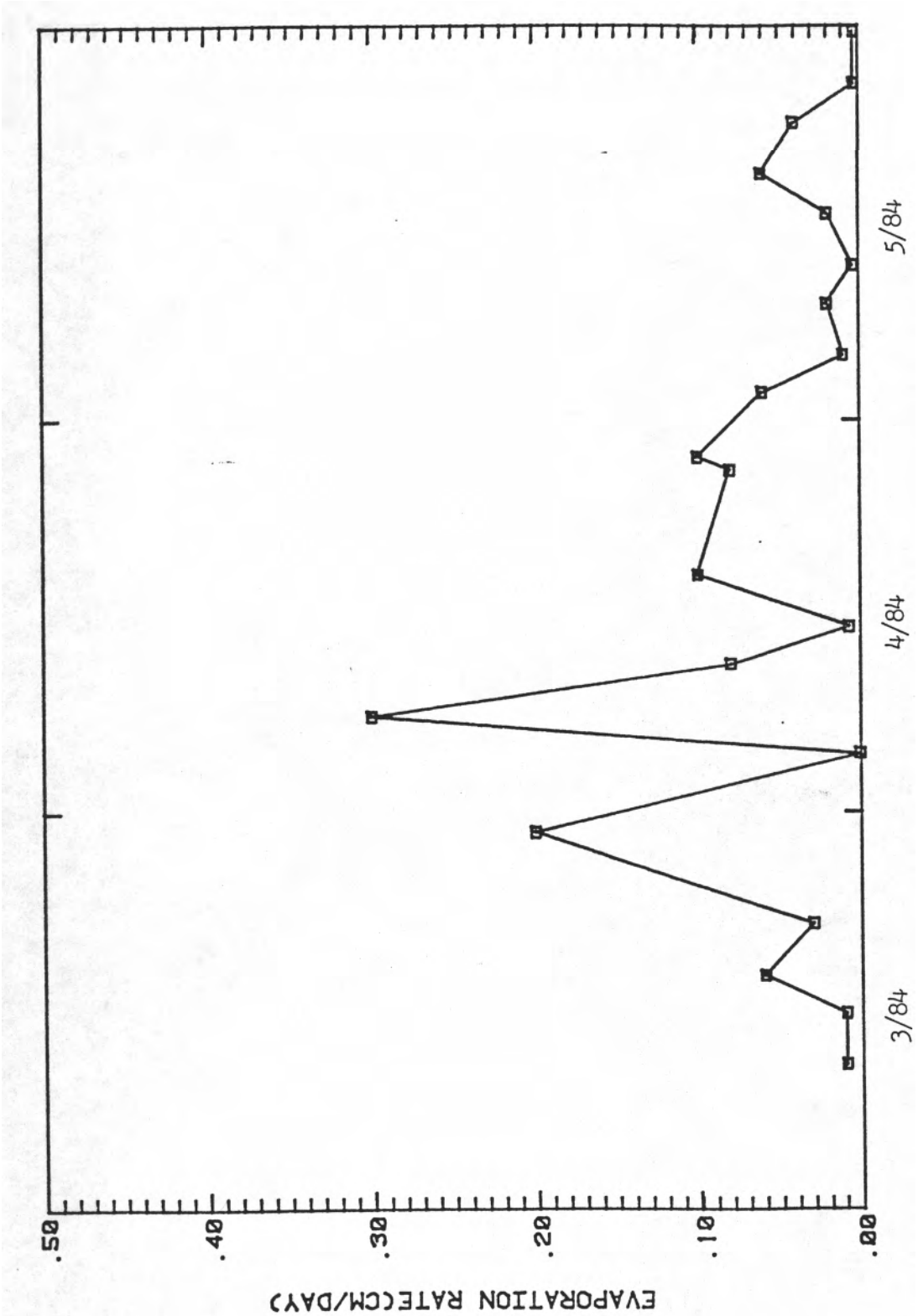

FIGURE 15 - Evaporation Rate versus Time from Micro-lysimeter Data

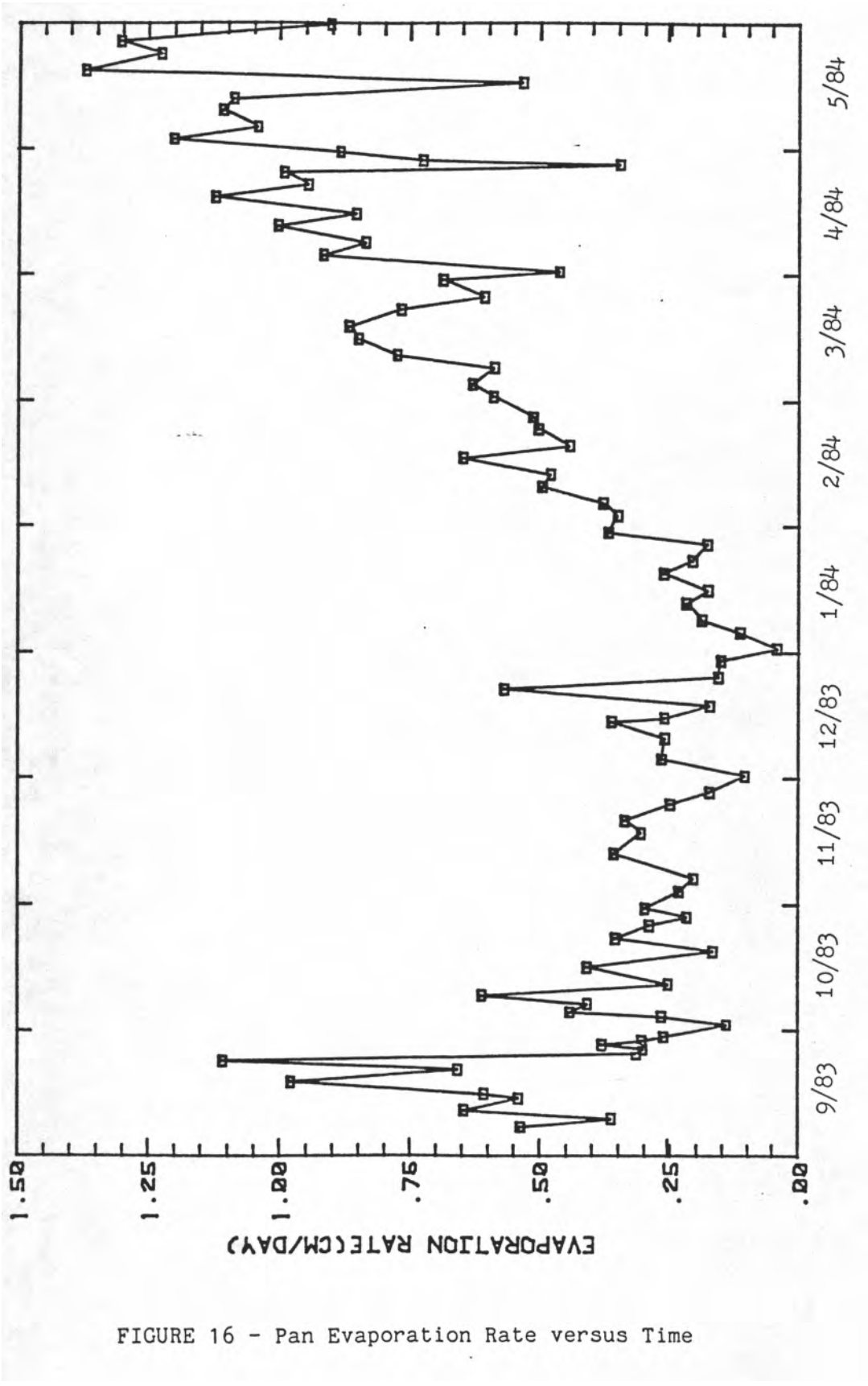

FIGURE 16 - Pan Evaporation Rate versus Time

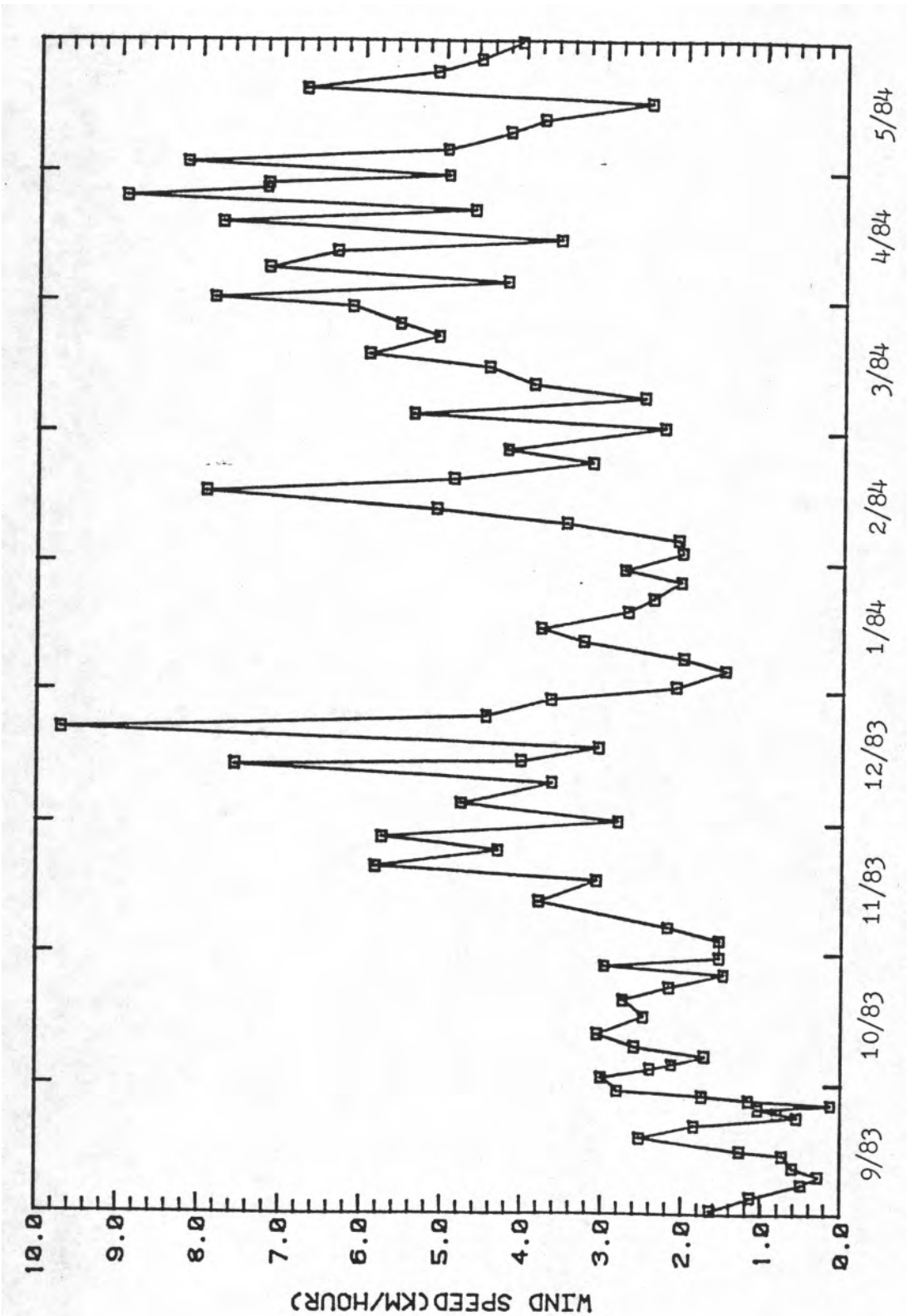

FIGURE 17 - Wind Velocity versus Time from Anemometer

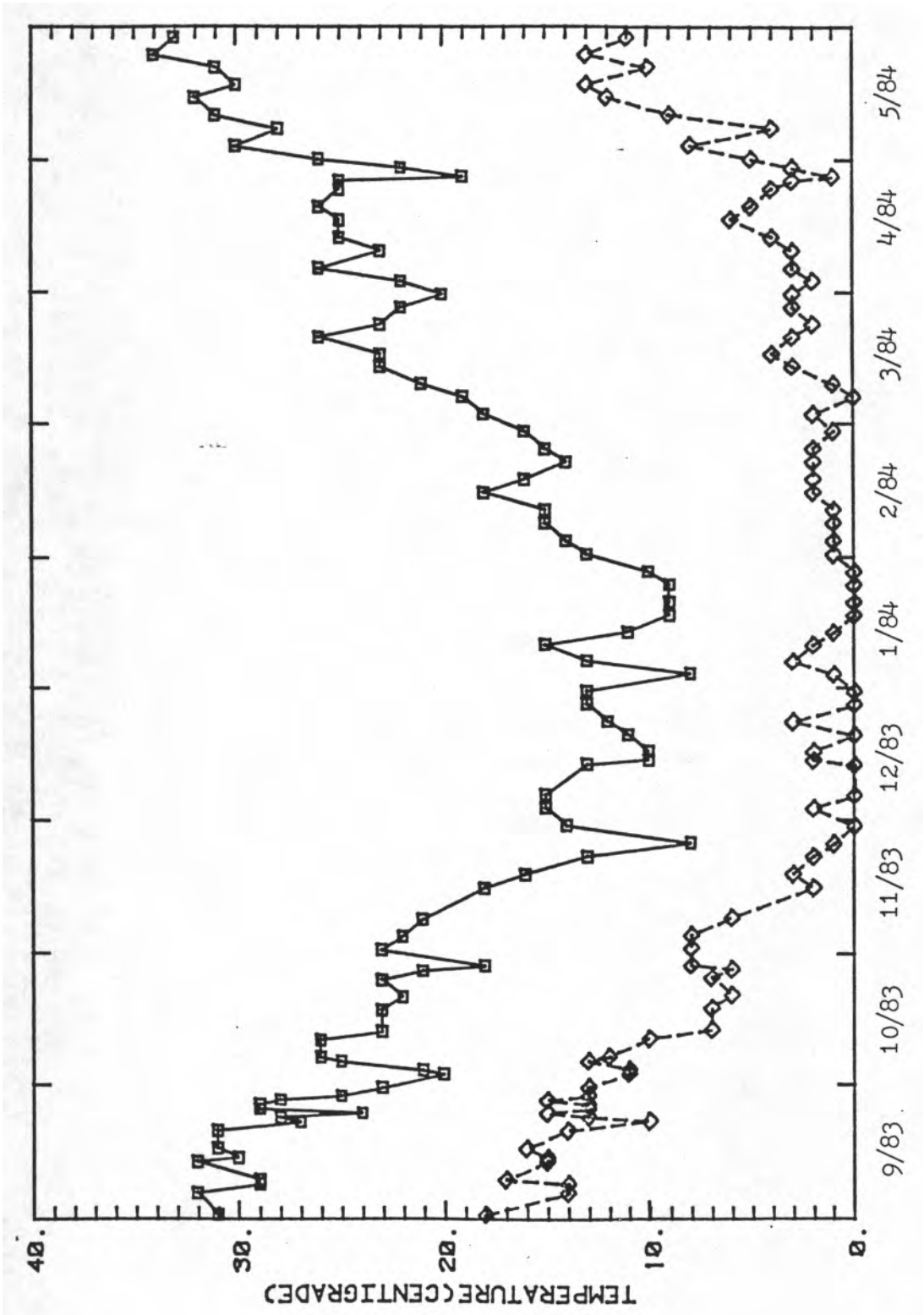

FIGURE 18 - Maximum and Minimum Pan Temperatures versus Time

10.2 RECHARGE CALCULATIONS

10.2.1 DARCY'S LAW APPROACH

For purposes of estimating a recharge flux the tensiometric data is used to calculate the average pressure head and hydraulic gradient for the 183, 213, and 244cm depths. These values are -84cm and 0.94, respectively, over the entire period of record, November 1982 through May 1984. From this average pressure head value an estimate could be made of the average unsaturated hydraulic conductivity from a characteristic K-ψ relationship.

Section 7 presented the results from an instantaneous profile test. It was recognized that this soil profile, from the 30 to 152cm depths, was relatively homogeneous. With this in mind, the K-ψ data from all five depths in Figure 7 was combined and an exponential regression analysis performed on all the data. The result was a coefficient of determination (R^2 value) of 0.88 with the following relation:

$$K(\psi) = 0.5601 \times EXP [\psi \times (0.2030)] \qquad (10.1)$$

From this relation and the average pressure head (ψ) of -84cm, the average hydraulic conductivity was estimated to be 2.20×10^{-8} cm/sec. Using this value of K in Darcy's equation (equation 9.1) yields a flux value of 2.07×10^{-8} cm/sec., or 0.65 cm/year.

To calculate the seepage velocity associated with this recharge flux the average water content would need to be estimated over the same depth range. This average is approximately 0.06. From the relation $V = \bar{q}/\theta$ comes an average seepage velocity of 10.8 cm/year below the 1.5m depth.

In order to compare the calculated recharge flux with the precipitation rate for the same period of record some additional precipitation data needs to be estimated. The soil-moisture data obtained at the site is from November 1982 through May 1984. The precipitation data that was collected at the site is for the period from August 1983 through May 1984. An estimate can be made for precipitation from November 1982 through July 1983 by averaging the data in the National Oceanic and Atmospheric Administration's (NOAA) monthly summaries. The records from Socorro and Bernardo were averaged to provide these estimates. Magdalena and Gran Quivera's records were not included in this averaging scheme due to their significantly greater altitudes. The floodplain locations of Bernardo and Socorro were thought to be more representative of the rain patterns occurring at the Sevilleta research site. Referring back to Figure 1 one can see the relative locations of these sites. Figure 19 shows a plot of this averaged precipitation data versus time.

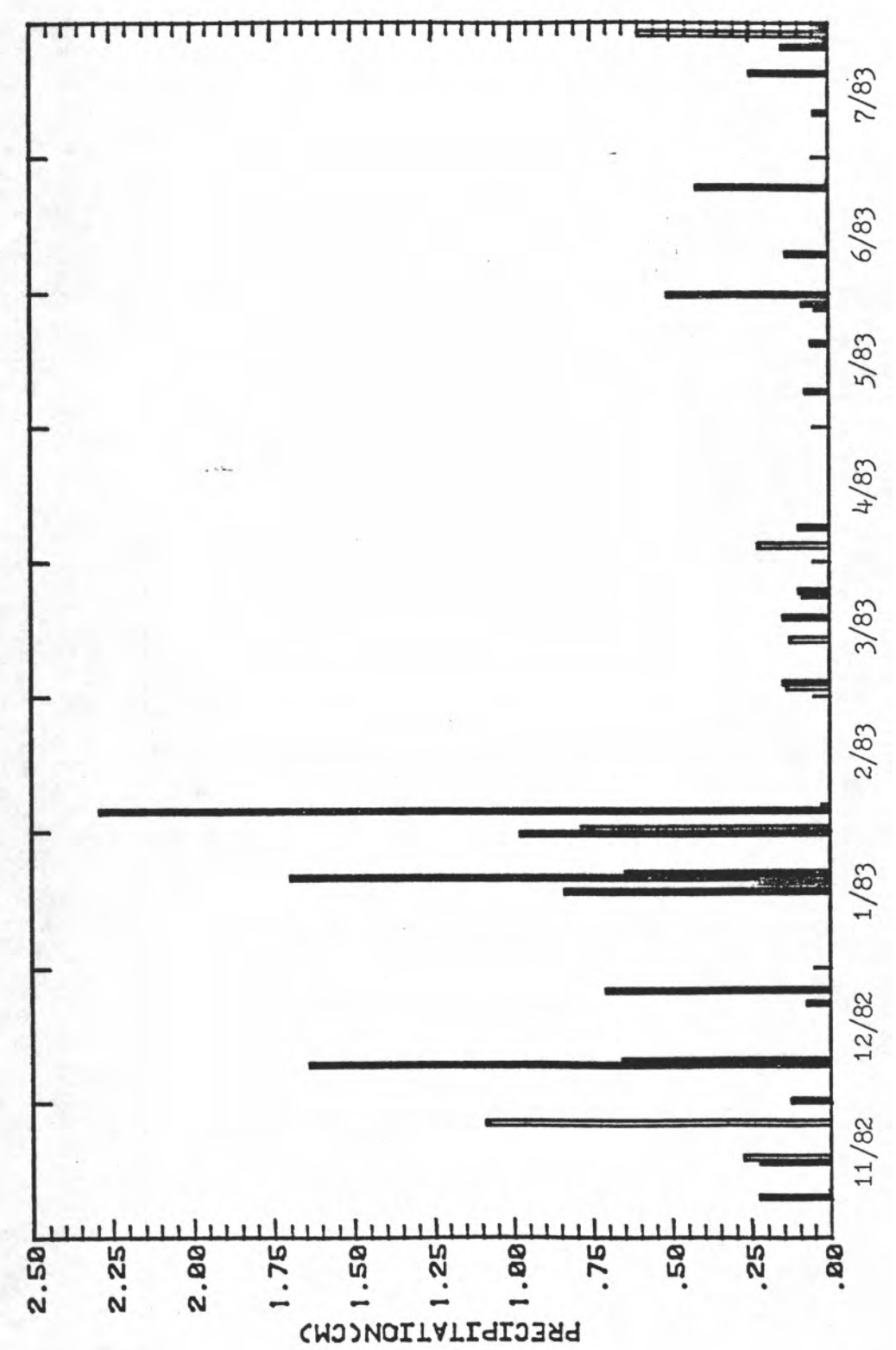

FIGURE 19 - Estimated Precipitation versus Time

The averaged precipitation data and the recorded precipitation data yield a precipition rate of 17.7 cm/year for the period of record. Comparing this rate with Socorro's 30 year average (1941 - 1970, from 1982 NOAA summary) of 20.1 cm/year it can be seen that the period from November 1982 to May 1984 might be 12% below the normal precipitation rate. Also note that the calculated recharge rate of 0.65 cm/year is 3.7% of the actual precipitation rate of 17.8 cm/year for this period of record.

A crucial point to consider in evaluating this recharge estimate is the estimation of the unsaturated hydraulic conductivity. This is typically a very difficult parameter to measure accurately. Flühler et al. (1976) suggest that the instantaneous profile method can give errors on the order of 20 to 30% of the actual K value in moist soils, and as much as 100% error in drier soils. Considering only the bandwidth of data that is shown in Figure 7 for the K-ψ estimates a range of values could be made for the estimated recharge flux. Figure 20 shows two lines approximating the limits of the calculated K-ψ data from the instantaneous profile test. Using the average pressure head of -84cm and a gradient of 0.94, two separate flux estimates could be made from the K-ψ limits. These values are 0.14 cm/year and 0.74 cm/year. These two estimates of recharge are 0.8% and 4.2% of the average precipitation rate for the same period of record, respectively.

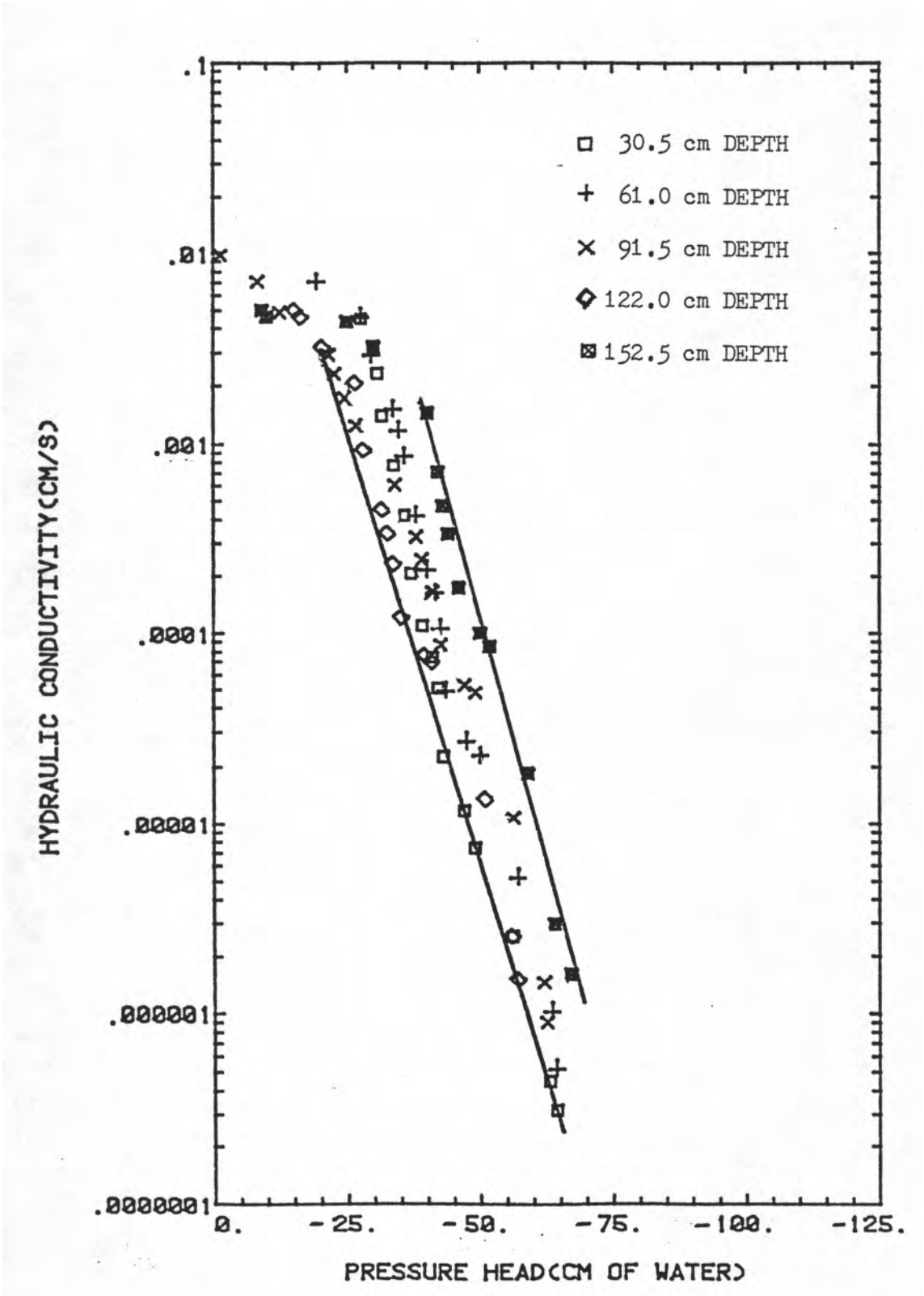

FIGURE 20 - K versus Pressure Head Data from the Instantaneous Profile Test with Estimated Limits on the Data

It can be seen from these estimates that the range of calculated recharge rates from 0.14 to 0.74 cm/year, ± 10 to 15% (from Flühler et al., 1976) is quite large. Therefore let it suffice to say that the estimate of 0.65 cm/year is an estimate that does have some error associated with it.

The recharge estimate just presented represents a gross averaging of the pressure head data below the root zone for the period of record, 11/82 through 5/84, from which an approximate Darcian flux was estimated. The pressure head data was generally collected on a semi-weekly basis. Averaging these data over shorter time increments might demonstrate the seasonality of the recharge process. The flux estimates from this averaging technique might also be compared with the precipitation records to obtain a crude estimate of the lag response time between precipitation events and recharge to the water table.

The pressure head data below the 150cm depth was averaged on a monthly basis, for each depth of tensiometric measurement. Determinations of the hydraulic gradient and unsaturated hydraulic conductivity were made from these data. The unsaturated hydraulic conductivity is estimated using equation 10.1. The effective hydraulic conductivity was then estimated from a harmonic and geometric averaging scheme, as mentioned in section 9.1. The Darcian flux was then calculated from equation 9.1. Figure 21 shows the results of these calculations for both

the harmonically and geometrically averaged flux estimates.

As mentioned in the previous section the estimation of the unsaturated hydraulic conductivity is a very sensitive part of this analysis. The unsaturated hydraulic conductivity is directly proportional to the recharge flux. Prior to the flux calculations just mentioned a detailed analysis was carried out with the intent of approximating a characteristic $K-\psi$ relationship for each depth of the profile from which pressure head measurements were taken. flux. The instantaneous profile test only gave results for the 30 through 152cm depths. It was felt that a better approximation could be made for the 183, 213, and 244cm depth $K-\psi$ relationships than just averaging the instantaneous profile data and assuming the soil profile to be homogeneous.

The method employed to estimate the $K-\psi$ relationships was that of van Genuchten(1978). His model was used to run a non-linear least-squares regression on the $\theta-\psi$ values generated from the hanging columns, previously discussed in section 8. A resulting curve-fit of the Mualem 2-parameter model option was shown in Figure 9. This model also predicted the unsaturated hydraulic conductivity associated with these $\theta-\psi$ values. The results from this analysis were questionable. Figure 22 shows a $K-\psi$ plot for the instantaneous profile data versus van Genuchten's predicted data for the 91cm depth. The model tended

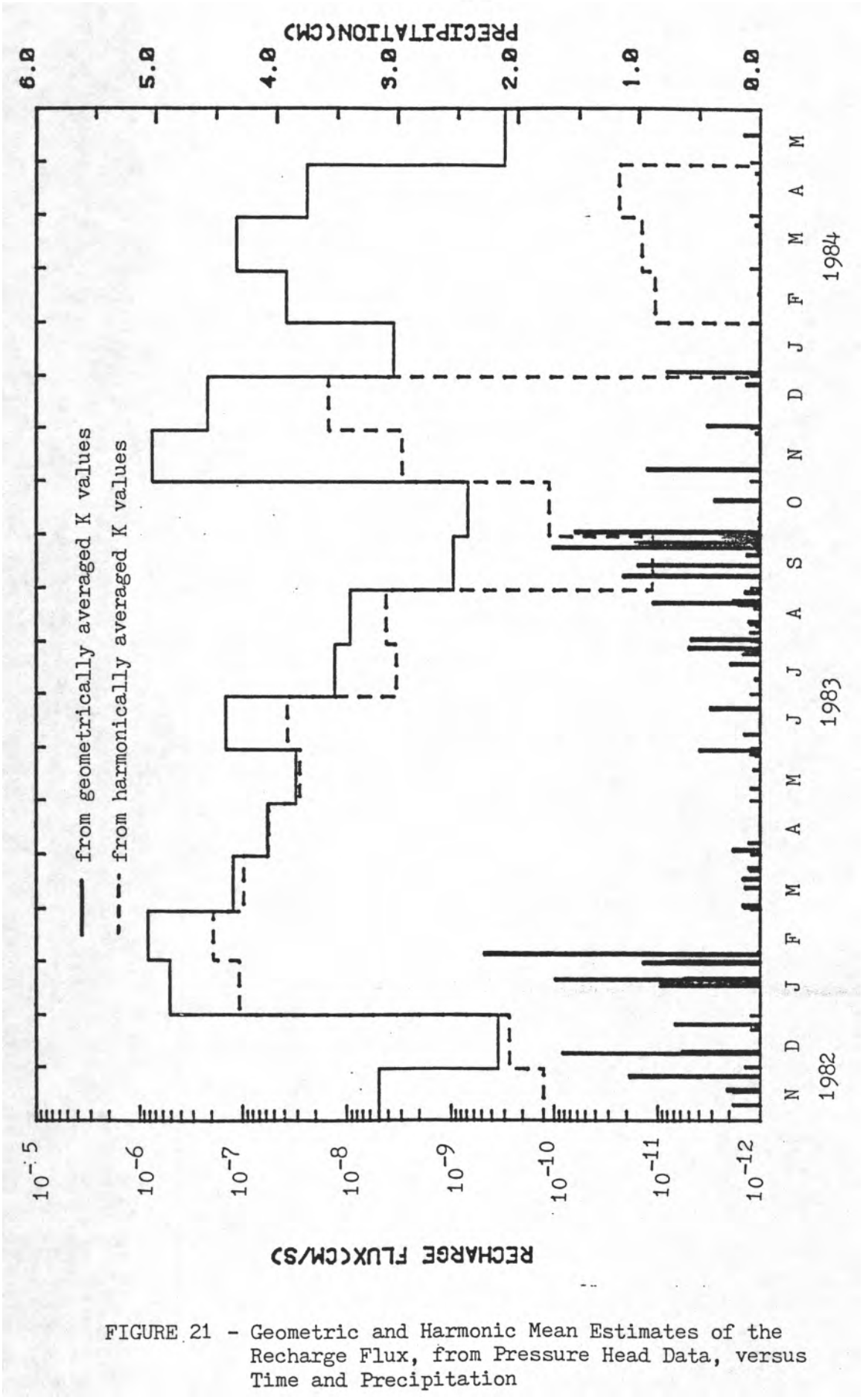

FIGURE 21 - Geometric and Harmonic Mean Estimates of the Recharge Flux, from Pressure Head Data, versus Time and Precipitation

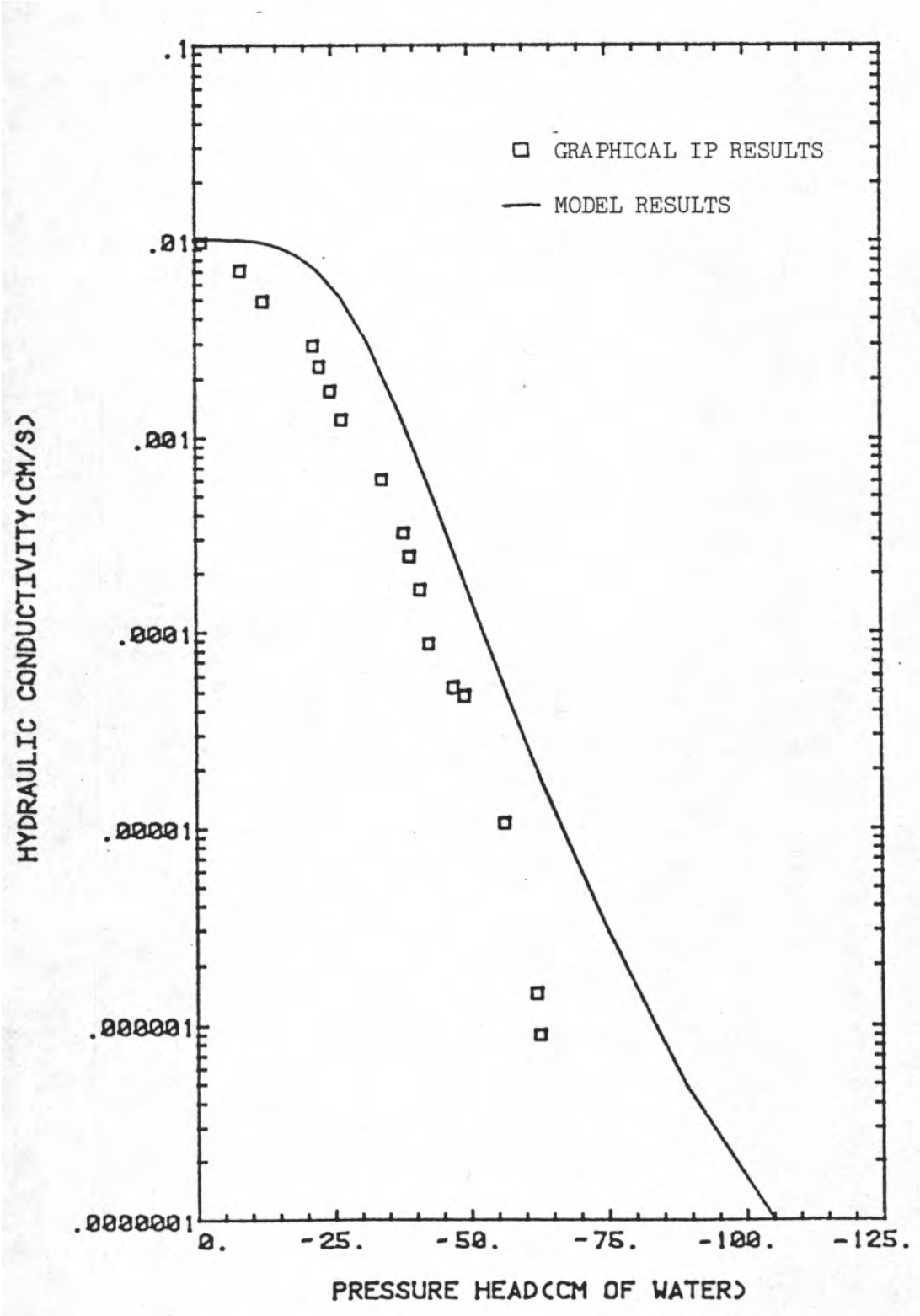

FIGURE 22 - K versus Pressure Head Data for the 91.0cm Depth, Instantaneous Profile and Mualem's Model Results

to overestimate the hydraulic conductivity as compared to the field data. Many attempts were made with van Genuchten's model to obtain a good K-ψ relationship. The best results were used to calculate the recharge flux. These recharge results were totally inadequate. The predicted recharge rates for the period of record were many times greater than the actual precipitation rate.

Knowing that the empirical estimation of the K-ψ relationships would not be useful the assumption was made that the medium is homogeneous. The results from the exponential curve-fit to the instantaneous profile data shown in equation 10.1 were then utilized to calculate the recharge flux.

The water content data can also be used to obtain a separate estimate of the recharge flux. The governing equation of flow is still that of Darcy's law, equation 9.1. However, in this approach the unsaturated hydraulic conductivity is estimated from a K-θ relationship. This relationship was calculated from the K-θ data obtained from the instantaneous profile test spoken of earlier. The K-θ data for water content values less than or equal to 0.14 were used in a regression to obtain the following result with a coefficient of determination (R^2 value) of 0.79:

$$K(\theta) = 6.79 \times 10^{-10} \times \exp[83.84 \times (\theta)] \qquad (10.2)$$

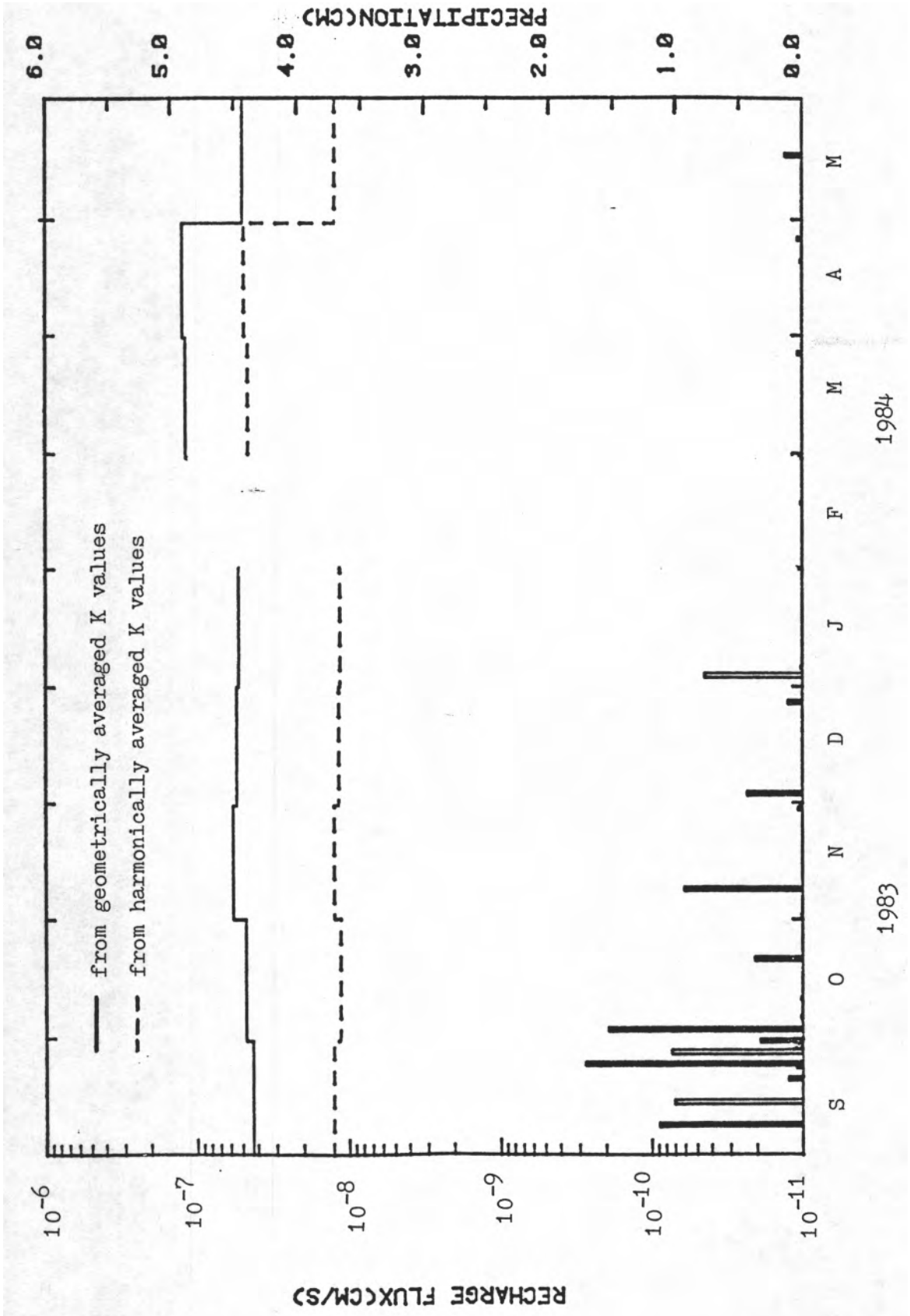

FIGURE 23 - Geometric and Harmonic Mean Estimates of the Recharge Flux, from Water Content Data, versus Time and Precipitation

The water content data between the 2.75m and 4.88m depths was utilized in determining hydraulic conductivity estimates. This depth interval was used because it was felt that it was sufficiently below the root zone and above the capillary fringe associated with water table fluctuations and should therefore be most representative of the recharge flux. The water content values for each depth were averaged on a monthly basis. The time span over which measurements were made at these depths was from September 1983 through May 1984. The depth increments of water content values were then averaged harmonically and geometrically to obtain an estimate of the effective unsaturated hydraulic conductivity. The hydraulic gradient was assumed to be equal to unity. The recharge flux was then calculated using Darcy's law, equation 9.1. The results of this analysis are shown in Figure 23.

Averaging the results of the pressure head derived recharge estimates for the nineteen months of record yields average recharge rates of 0.90 and 4.73 cm/year for both the harmonically and geometrically averaged cases, respectively. These estimates correspond to 5.1% and 26.6% , respectively, of the precipitation rate for the same period of record. The same type of results for the water content derived recharge estimates are 0.65 and 2.13 cm/year for both the harmonic and geometric mean cases. These values are 4.8% and 15.7% of the precipitation rate for this shorter time period of observation. For comparative purposes

between the pressure head and water content derived recharge estimates, the recharge flux for the pressure head case between September 1983 and May 1984 is about 0.063 to 3.99 cm/year. This corresponds to between 0.5% and 29.3% of the precipitation rate during this relatively short time period.

Assuming an average water content in the profile of 0.06, and these same estimates of the recharge rate, estimates of the average particle velocity can be made. For the pressure head derived case the seepage velocities would be 15.0 and 78.8 cm/year. If this were the range of seepage rates occurring between the land surface and the water table, at a depth of 6 meters, the time for precipitation to travel this distance might be between 7.6 and 40.0 years. This same type of approach could be used on the water content derived recharge flux estimates. In this case the seepage velocity might be between 10.8 and 35.6 cm/year, and the travel time would be on the order of 16.9 to 55.8 years.

10.2.2 TEMPERATURE GRADIENT METHOD

Another method of analysis used for estimation of the recharge flux is the temperature gradient approach. This method was outlined in Section 9.3. This technique is being applied to the temperature data gathered from soil-moisture station 1 at relatively shallow depths; the 152, 183, and 213cm depths to be more specific. The data is to be analyzed as an average for each depth for the period of record. The assumption is being made that averaging over the period of record will minimize any error associated with seasonal changes in temperature.

Average temperatures (To,Tz, and Tl) at the 152, 183, and 213cm depths are 54, 55, and 56 degrees Fahrenheit, for the period from November 3,1983 to May 29,1984. Solving equation 9.3 iteratively for B yields a value of 0.040.

From Birch et al. (1942) the thermal conductivity is estimated to be 2.09 x 10-3 cal/sec cm C. The density is taken to be 2.06 g/cc from the 'undisturbed' soil samples used in the hanging column experiments. Co is 1.00054 cal/g/ C and L equals 61cm. The resulting estimate of seepage velocity from equation 9.4 is 6.65 x 10^{-7} cm/sec, or 21.0 cm/year. Assuming an average water content of 0.06 yields a calculated recharge flux of 1.26 cm/year. This amounts to approximately 7.1% of the actual precipitation rate for the period of record.

10.3 EVAPOTRANSPIRATION ESTIMATES

10.3.1 WATER BUDGET APPROACH

One approach taken in trying to quantify evapotranspiration is the water budget method. This method entails summing the water inputs and outputs through the soil profile and equating them with the change in water storage. The system under consideration is a one dimensional vertical cross-section within the soil profile, from land surface to about 197cm in depth. The recharge flux was estimated previously in section 10.1. The recharge flux values corresponding to the pressure head data of harmonically and geometrically averaged hydraulic conductivities are used in this analysis of the water budget so as to bracket the range of evapotranspiration rates that might occur. The water content derived flux estimates were not utilized due to the limited length of data available. The change in water storage in the soil profile was estimated from the neutron probe water content data. These calculations of the change in water storage were made on a monthly basis for the entire period of record, November 1982 through May 1984.

Table 1 shows the results of the water budget calculations for both cases where the recharge flux was estimated from the pressure head data. The change in storage estimation shown in Table 1 indicates a loss in soil water for a negative quantity,

and a gain in soil water for a positive quantity, between land surface and the 197cm depth. The table also gives estimates of the evapotranspiration rate, which is calculated by solving equation 9.5.

Looking more closely at this monthly data it can be seen that the months with relatively high precipitation rates do not necessarily have large recharge rates. This observation seems to suggest that there is a lag time associated with any pressure pulse that may induce a recharge flux. This concept could be better understood through the use of a numerical model or a time-series analysis of the tensiometric and water content data.

The average change in water storage is calculated to be an increase of 1.14 cm/year. This value may be questionable, because there were several months during which the neutron probe was not in use and no change in storage could be estimated. estimated at 22.7 cm/year. The average water content between the 137cm and 197cm depths at the beginning of this season was 2.4%. The soil profile within this zone has not been as dry since, even though the precipitation from January 1984 through May 1984 was only 0.28cm. The average water content between the 137cm and 197cm depths at the end of May 1984 was 5.6%. The neutron access tube at soil-moisture station 1 was installed at the end of November 1982. It may be that the soil used as backfill material around the access tube was quite dry, and required quite some

TABLE 1 - Water Budget Results

Month	Precipitation Rate (cm/sec)	(dO/dt)*dz (cm/sec)	Recharge[1] Rate (cm/sec)	Evapotrans-[1] piration Rate (cm/sec)	Recharge[2] Rate (cm/sec)	Evapotrans-[2] piration Rate (cm/sec)
11/82	7.14×10^{-7}	1.77×10^{-7}	1.22×10^{-10}	5.37×10^{-7}	4.80×10^{-9}	5.32×10^{-7}
12/82	1.24×10^{-6}	1.30×10^{-6}	2.67×10^{-10}	-6.03×10^{-8}	3.37×10^{-10}	-5.83×10^{-8}
1/83	1.95×10^{-6}	-	1.07×10^{-7}	-	5.05×10^{-7}	-
2/83	9.55×10^{-7}	-	1.93×10^{-7}	-	8.23×10^{-7}	-
3/83	2.84×10^{-7}	-	9.58×10^{-8}	-	1.21×10^{-7}	-
4/83	1.43×10^{-7}	-1.50×10^{-7}	5.59×10^{-8}	2.37×10^{-7}	5.71×10^{-8}	2.36×10^{-7}
5/83	2.95×10^{-7}	-8.40×10^{-7}	2.77×10^{-8}	1.11×10^{-6}	3.00×10^{-8}	1.11×10^{-6}
6/83	2.20×10^{-7}	-	3.73×10^{-8}	-	1.44×10^{-7}	-
7/83	4.37×10^{-7}	-2.31×10^{-7}	3.26×10^{-9}	6.65×10^{-7}	1.26×10^{-8}	6.55×10^{-7}
8/83	6.57×10^{-7}	-9.07×10^{-8}	4.15×10^{-9}	7.44×10^{-7}	9.01×10^{-9}	7.39×10^{-7}
9/83	2.15×10^{-6}	1.46×10^{-6}	1.11×10^{-11}	6.90×10^{-7}	9.13×10^{-10}	6.87×10^{-7}
10/83	7.32×10^{-7}	1.45×10^{-7}	1.10×10^{-10}	5.87×10^{-7}	6.64×10^{-10}	5.86×10^{-7}
11/83	3.86×10^{-7}	8.24×10^{-8}	2.92×10^{-9}	3.01×10^{-7}	7.50×10^{-7}	-4.46×10^{-7}
12/83	2.09×10^{-7}	5.41×10^{-8}	1.49×10^{-8}	1.40×10^{-7}	2.10×10^{-7}	-5.51×10^{-8}
1/84	2.99×10^{-7}	-	9.54×10^{-15}	-	3.43×10^{-9}	-
2/84	7.98×10^{-9}	-	1.05×10^{-11}	-	3.77×10^{-8}	-
3/84	1.49×10^{-8}	1.15×10^{-8}	1.40×10^{-11}	3.39×10^{-9}	1.13×10^{-7}	-1.10×10^{-7}
4/84	2.31×10^{-8}	-8.71×10^{-7}	2.33×10^{-11}	8.94×10^{-7}	2.32×10^{-8}	8.71×10^{-7}
5/84	5.23×10^{-8}	-5.78×10^{-7}	2.50×10^{-15}	6.30×10^{-7}	2.85×10^{-10}	6.30×10^{-7}

1 - Based upon harmonic mean of K in determining the recharge rate
2 - Based upon geometric mean of K in determining the recharge rate

time to equilibrate with the surrounding soil. A new neutron access tube was installed in September 1983. The same type of phenomenon may have occurred with this new backfill material as evidenced previously. These observations imply that the change in storage estimations may be erroneous for periods immediately following the installation of a neutron access tube.

Over a long period of time the average change in water storage should be close to zero. The evapotranspiration rate will then be approximately equal to the difference between the average precipitation rate and the average recharge rate. Due to the lack of water content data over the full period of record the assumption is made that the evapotranspiration rate may be approximated as the difference just described.

The evapotranspiration rate is estimated to be between 13.1 and 16.9 cm/year. The maximum evapotranspiration rate for a salt bush as reported by Evans and Thames (1981) was 0.2 cm/day, or 73.0 cm/year. This range of rates is intuitively reasonable, considering the fact that the water content around the salt bush is not near saturation, it is approximately 6%, and therefore the actual evapotranspiration rate should be considerably less than the potential. The evapotranspiration rates shown in Table 1 are sometimes negative. This could imply that water has moved into the shallow soil horizon from deep within the soil profile and was taken up as evapotranspiration. This phenomenon is not

deemed likely due to the downward hydraulic gradients calculated from the tensiometric data. A more likely cause for the calculated evapotranspiration being negative is that of measurement error. The neutron probe is only good to ± 1.8% water content (refer to Troxler's users manual). This could mean a substantial difference in the calculated change in storage. Also, Flühler et al. (1976) concluded that the estimate of unsaturated hydraulic conductivity from an instantaneous profile test could be in error by as much as 100%. This fact implies that the estimate of the recharge flux may have some error associated with it. Therefore, if the change in storage and recharge estimates are suspected to be in error, then the solution of equation 9.5 should produce an evapotranspiration estimate that has some error associated with it.

10.3.2 THEORETICAL/EMPIRICAL EVAPOTRANSPIRATION ESTIMATES

Another approach to estimating the recharge flux is that of estimating the evapotranspiration demand with theoretically or empirically derived equations and solving equation 9.5 for the recharge flux. For ease of calculations a numerical model written by Gupta et al., as presented in Appendix III of Doorenbos and Pruitt (1977), has been employed. This model calculates reference crop evapotranspiration results for the 5 methods previously mentioned under Doorenbos and Pruitt (1977) in Section 9.4.

Table 2 shows the averaged meteorological data inputs for the numerical model as obtained from field measurements. The computed values of evapotranspiration by each method are presented in Table 3. As mentioned previously the modified Penman approach is assumed to yield the best results for the research site under study. The calculated reference crop evapotranspiration rate for the period of meteorological record, September 1983 through May 1984, is 0.76 cm/day. One can see from Table 3 that the other methods of predicting evapotranspiration yield markedly different results from the modified Penman approach.

Having obtained an estimate of the reference crop evapotranspiration rate, an estimate of the actual evapotranspiration rate can also be made. Boonyatharokul and

TABLE 2

Meteorological Data

Month	RHmin (%)	RHmax (%)	Tmin (^{o}F)	Tmax (^{o}F)	Atm. Press. (mm Hg)	Radiation (cal/day)	Wind Speed (km/hr)	Pan Evap. (cm/d)	Sunshine Hours
9/83	30	70	55	80	645	1022	1.14	0.498	12
10/83	25	65	45	77	645	1022	2.35	0.320	11
11/83	25	60	35	60	645	922	3.77	0.244	10
12/83	25	60	30	50	645	850	4.84	0.273	10
1/84	25	58	20	58	645	893	2.48	0.193	10
2/84	20	45	25	62	645	994	4.09	0.475	10
3/84	20	45	30	70	645	1094	4.56	0.704	11
4/84	18	45	35	75	645	1224	6.32	0.824	12
5/84	18	40	45	85	645	1195	4.88	1.083	13

TABLE 3

Theoretical/Empirical Evapotranspiration Estimates*

Month	Blaney-Criddle Method	Radiation Method	Penman Method	Modified Penman Method	Pan Evaporation Method
9/83	0.469	1.132	0.877	0.830	0.326
10/83	0.388	1.122	0.858	0.786	0.203
11/83	0.237	0.893	0.682	0.683	0.150
12/83	0.158	0.740	0.581	0.610	0.164
1/84	0.137	0.733	0.547	0.565	0.120
2/84	0.246	0.948	0.719	0.598	0.272
3/84	0.367	1.162	0.883	0.851	0.400
4/84	0.527	1.436	1.112	0.928	0.450
5/84	0.695	1.535	1.172	0.997	0.601
Average	0.358	1.078	0.825	0.761	0.298

* - All values are in units of cm/day.

Walker (1979) outlined essentially 3 different methods for predicting actual evapotranspiration using equation 9.6.

Some averaging of the field data is needed as input to equations 9.7 through 9.12. The saturated hydraulic conductivity is approximately 0.01 cm/sec. Averaging the maximum and minimum water contents for all depths within the root zone for the period 9/83 through 5/84 and taking the difference between the two values gives us a Dp value of 0.055. Taking an average of the maximum and minimum water contents for the entire period of record, 11/82 through 5/84, and calculating the difference yields a Dt value of 0.066. Substituting these values into equations 9.7 through 9.12 yields Kc values of 0.998, 1.57, and 0.0024 respectively. The corresponding values of actual evapotranspiration would be 277, 436, and 0.67 cm/year. The first two values are 15.6 and 24.6 times greater than the actual precipitation rate for the same period of record. The third value of 0.67 cm/year implies that the recharge rate is 17.0 cm/year, or 96.2% of the precipitation rate. All three predictions appear to be questionable. Boonyatharokul and Walker (1977) also state that the term b is often assumed to be 0.5. Substituting b=0.5 into equation 9.9 yields a Kc value of 0.333 and the actual evapotranspiration rate to be 92.6 cm/year. This value is 5.2 times the precipitation rate. This result is also questionable.

In order to estimate whether or not these equations could yield reasonable results some additional calculations will be made. The assumption is made that the empirical constants, Ksat, ETa, and Dp, are all valid. The average evapotranspiration rate from the water budget method in Section 10.3.1 for the same period of record, September 1983 through May 1984, was calculated to be 9.95 cm/year. This corresponds to a Kc value of 0.0359. The three equations, 9.7, 9.8, and 9.9, are now solved for Dt, the total available moisture, yielding values of 0.0571, 0.0551, and -0.037, respectively. The first and second values agree quite well with observed field moisture conditions. The third value has no meaning in the context of total available moisture held within a depth of 150cm. Equation 9.9 was also evaluated using b equal to 0.5 and solved for Dt; obtaining a value of 0.056. This value appears to agree quite well with observed field moisture conditions. The neutron probe method of measuring the water content in the soil can be in error by as much as ± 0.018 (refer to the Troxler users manual). The initial estimate of Dt is within this error tolerance of the three estimated Dt values of 0.0571, 0.0551, and 0.056. Therefore one might conclude that equations 9.7, 9.8, and 9.9 (with b equal to 0.5) could yield acceptable estimates of the actual evapotranspiration rate. In as much as field measured meteorological and soil-moisture data used as input produced unreasonable values of evapotranspiration, it appears that improved estimates of

available moisture are needed for the research site under study. Another factor to consider is how good an estimate of the reference crop evapotranspiration the modified Penman method yields. Evaluating this estimate would require comparison to some observed field test conditions, with the likes of a weighing lysimeter. This type of equipment was not installed at the site due to monetary constraints. Most all of the empirical relationships used in this section were derived for use with irrigated agricultural crops and may have some limitations when applied to natural vegetation and soil-water environments.

10.3.3 MICRO-LYSIMETER EXPERIMENTS.

The micro-lysimeter technique being used at the research site was outlined in Section 9.5. This method was developed and discussed in detail by Boast and Robertson (1982).

The micro-lysimeter columns being used in this study are being analyzed in triplicate, and the results averaged together to help minimize errors. The calculated evaporation rates from these field experiments were shown in Figure 15 previously. The average monthly rates for 3/84, 4/84, and 5/84 were 1.79, 2.85, and 0.77 cm/month, respectively. If these results are extended to a yearly rate the values would be 21.1, 34.7, and 9.0 cm/year. The March and April evaporation rates are higher than the yearly precipitation rate. The estimate for May was only half the precipitation rate. The evaporation rate can be quite low during some periods and quite high during others. This is acceptable if the long term average evaporation rate is less than or equal to the precipitation rate.

When one considers that very little precipitation occurred during the period from January 1984 through May 1984, only 0.28cm, then these relatively large estimates of actual evaporation seem erroneous. There may be some problems inherent in this technique for which some hypotheses can be made.

The human error involved with any manual field measurements is always something to consider. However, these columns are being analyzed in triplicate and the results are averaged. It is assumed that this averaging technique minimizes the impact of human error on the results.

Another factor to consider might be the wall or boundary effects of each column. The conductance of heat through the PVC column may artificially upset the evaporation process within each column. Also because the bottom of the column is capped, there is no hydraulic connection with the surrounding or underlining soil. A sealed container of this type may impede the natural air and water-vapor transport through the soil column. As discussed by Hillel (1980), water-vapor movement within the near surface soil profile is downward at night and upward during the day, due to temperature gradients. Field observations during the cool of the morning indicate that dew condenses at the soil surface. Therefore there is a potential for water to move into the soil profile during some portion of the day. The net effect is presumed to be water loss from the profile. However, if the bottom cap and side-walls of the column impede the movement of water vapor, then the downward flow of moisture at night may be impeded. This would lead to a more pronounced evaporation flux, which may account for the large values that have been reported.

A better understanding of the physics behind unsaturated flow, vapor transport, and heat transport is needed to accurately solve this problem. A trial solution might be to use larger diameter columns to minimize wall and air entrapment effects. This would necessitate the use of a larger capacity weighing scale which would mean sacrificing some accuracy. There is a need for more research into this technique, as it does appear to be a relatively easy and economical method for predicting the actual evaporation rate.

10.4 INFILTRATION ESTIMATES

10.4.1 BROMIDE TRACER EXPERIMENTS:

Another experimental technique being applied in this study is the use of a bromide tracer in measuring average water particle velocities, or seepage velocities, after natural precipitation events. The basic concept involved here has been employed by other researchers, such as Jury et al. (1982) and Saffigna et al. (1977). The approach used for this project was outlined in Section 9.6.

Figure 24 shows the depth versus water content profile for a column that was installed November 29, 1983 and removed December 16, 1983. A precipitation event of 0.44cm was recorded on December 3, 1983. Figure 25 shows the depth versus bromide concentration for the same column. One can see from Figure 25 that the bromide has moved down to approximately 20cm in depth. Figure 24, however, shows a wetted profile down to a depth of about 26cm. This type of water content profile is consistent with the general theory of infiltration in which it is supposed that the wetting front pushed along some background moisture to yield higher water contents ahead of the infiltrated precipitation. Therefore the infiltrated water has percolated to the 20cm depth, but the wetting front has pushed ahead of itself enough water to show a wetted profile to a depth of 26cm.

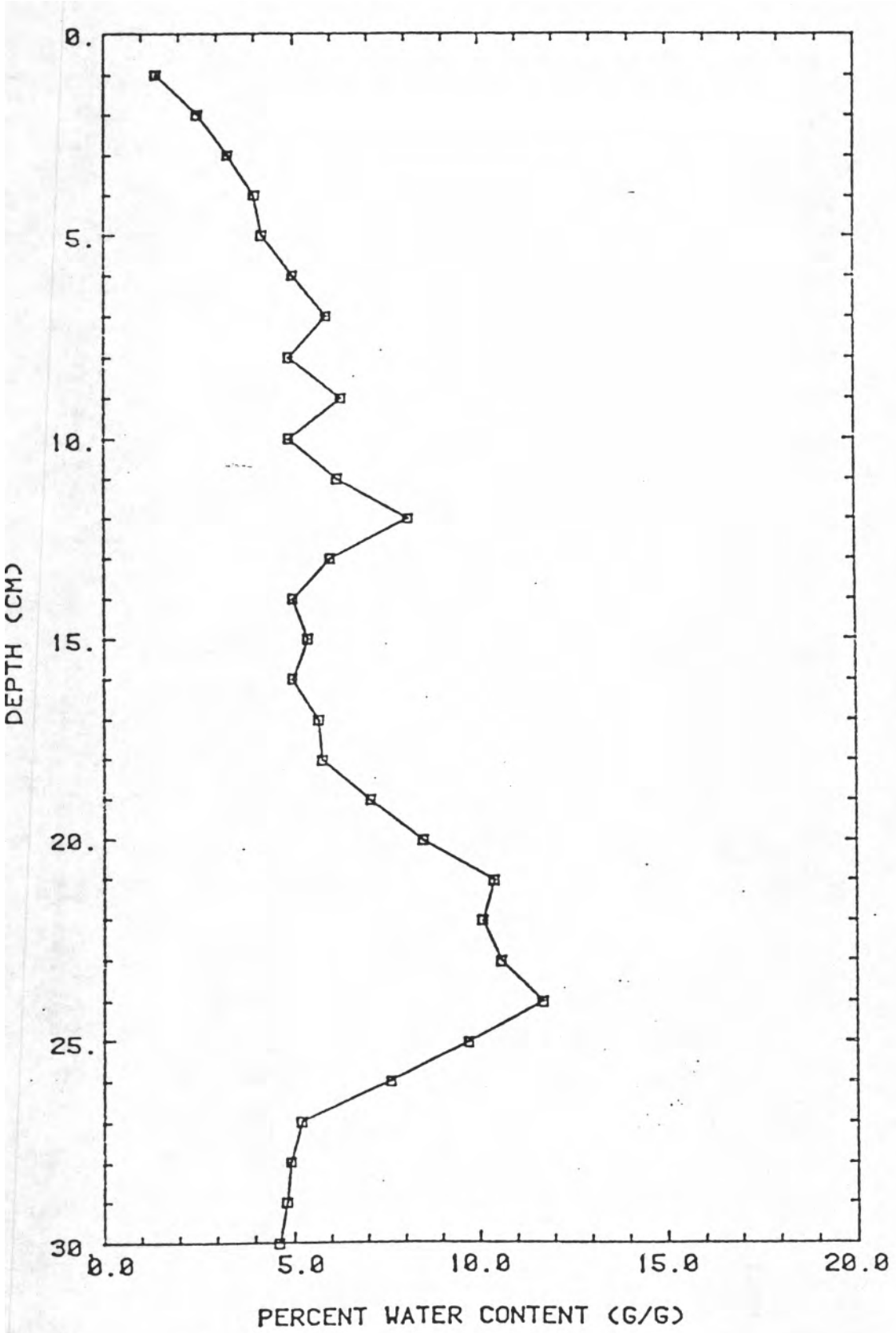

Figure 24. Water Content Versus Depth at Site 1. The field experiment began November 29,1983 and terminated December 16,1983. The only precipitation during this time occurred on December 3,1983.

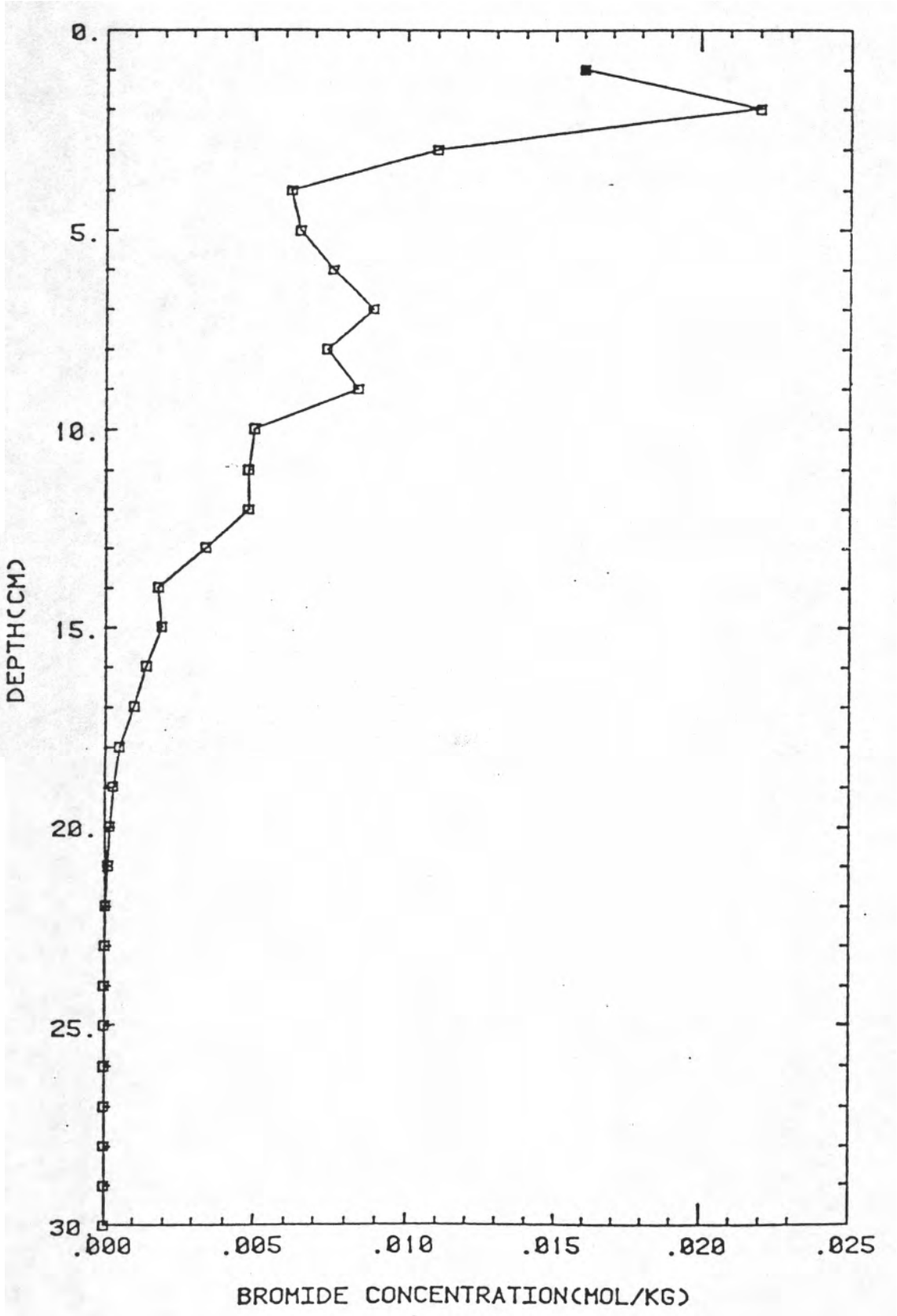

Figure 25. Bromide Concentration Versus Depth at Site 1. The field experiment began November 29, 1983 and terminated December 16, 1983. The only precipitation during this time occurred on December 3.

Assuming that the water content behind the wetting front was 12% and the initial water content was 5%, then equations 9.13 and 9.14 could be solved for depth and compared to the observed wetting front and bromide depths. The time parameter used in both equations is assumed to be the time between the precipitation event and the time that the soil column was pulled from the field, 13 days. The unsaturated hydraulic conductivity is estimated from a regression analysis of the instantaneous profile K-θ data. A power curve-fit to the K-θ data resulted in a coefficient of determination (R^2 value) of 0.96 and the following relation:

$$K(\theta) = 9.77 \times (\theta)^{**}6.21 \qquad (10.3)$$

These data are then substituted into equation 9.13 and 9.14 to obtain estimates of the theoretical wetting front depth and bromide depth. These values are 300cm and 175cm, respectively. The actual depths of 26cm and 20cm do not correlate with the theoretical predictions. It may be that the time parameter was incorrect. The actual time taken for the wetting front and bromide to reach the observed depths may have been considerably shorter than the 13 days between the precipitation event and the excavation of the soil column. The water content behind the wetting front may have been larger than that observed upon excavation of the soil column. The water within the soil profile may have redistributed after infiltration into the soil.

Some problems arose in some of the other tests done with this method. Diffusion of the bromide salt was apparent during periods of no precipitation. Quantifying the amount and characteristics of this diffusion process became a major concern. Research into this subject is still being carried out by other investigators here at Tech. Until we can quantify a dispersion coefficient associated with the scale of our problem we can not accurately predict any infiltration characteristics of the soil in our area based on this method. At a later date we hope to infer some general infiltration and redistribution characteristics at our site from different rainfall amounts and intensities.

11. NUMERICAL SIMULATION

11.1 MODEL DESCRIPTION:

Apart from the hydrologic estimates an attempt was made to simulate the unsaturated flow with the use of a numerical computer model. There are many computer codes available for doing this. Finding one that can best approximate the natural flow phenomenon of the study site, that is available for use, and has a documented user's guide, was a difficult task.

Ideally the model being used should be able to simulate one-dimensional unsaturated flow. It should also be able to approximate wetting and drying through the use of soil-moisture characteristic curves. This also means that the scanning curves must be approximated. The model would also be able to account for transpiration within the entire root zone. Evaporation across the soil surface should be approximated. Finally, the upper and lower boundaries may be specified as either prescribed flux or prescribed head conditions.

Oster (1982) gives a comprehensive list of the published unsaturated flow models. He outlines whether or not each code is proprietary, has a user's guide, and has documented results. He then evaluates and describes each model that he feels deserves additional attention.

Of all the codes listed in Oster (1982) only two were readily available for use on this project that even came close to meeting the modeling needs stated above. TRUST by Reisenauer et al. (1982) can handle most of these needs except simulating transpiration. UNSAT2 by Davis and Neuman (1983) does handle transpiration but does not account for hysteresis. It was not considered feasible, for this masters thesis, to modify either one of these codes to fit all the modeling needs outlined above. Therefore some concessions had to be made.

Considering the proximity of soil-moisture station 1 to a stand of salt bush it was decided that simulating transpiration was more important than accounting for hysteresis. It is realized that either approach, simulating either transpiration or hysteresis, while neglecting the other, may lead to gross errors in the model predictions because the model is not truly simulating all facets of the natural flow system. However, a modeling effort is just a sophistocated tool to help better understand a given flow problem, and is only as good an approximation as the data that goes into it. Therefore great care must be exercised in evaluating the results of a modeling effort. Having confidence in the data input may provide confidence in the model output, and vice-versa.

UNSAT2 is a relatively easy code to use. It is a 2-dimensional variably saturated flow model. The basic governing flow equation is given as:

(11.1)

$$L(h) = \underbrace{\sum_{i=1}^{3}\sum_{j=1}^{3}\frac{\partial}{\partial x_i}\left[K^r(h)K^s_{ij}\frac{\partial h}{\partial x_j}\right]}_{\text{Advection}} + \underbrace{\sum_{i=1}^{3}\frac{\partial}{\partial x_i}K^r(h)K^s_{i3}}_{\text{Drainage}} - \underbrace{[C(h)+\beta S_s]\frac{\partial h}{\partial t}}_{\text{Storage}} - \underbrace{S}_{\text{Source/Sink}} = 0$$

where L = quasilinear differential operator defined in the flow region,

x_i = spatial coordinates (i=1,2,3 with x_3 the vertical),

K^r = relative hydraulic conductivity ($0 \leq K^r \leq 1$),

K^s_{ij} = hydraulic conductivity tensor at saturation,

h = pressure head,

C = specific moisture capacity = $\frac{d\theta}{dh}$,

θ = volumetric moisture content,

β = 0 in unsaturated zone and 1 in saturated zone,

S_s = specific storage,

t = time, and

S = sink term.

Within this equation there is a source term which may be defined in terms of a transpiration uptake by the following relation:

S = Kr x K11s x (h - hr) x b' (11.2)

where hr is the pressure head in the plant roots, and b' is the root effectiveness function. The term b' is basically an empirical relationship, and must be determined by model calibration. The Galerkin finite element solution scheme is used in this model to solve the governing equation via an iteration procedure.

11.2 MODEL DESCRETIZATION:

After choosing the type of model to be used the flow domain must now be discretized in order to facilitate the data input into the model. As mentioned previously, UNSAT2 is a 2-dimensional model, and for this project it is intended that only a 1-dimensional vertical flow simulation needs to be done. This can be accomplished by utilizing one column of rectangular elements throughout the flow domain. Rectangular elements are required within the root zone, and for ease of use this scheme was continued throughout the whole soil profile being simulated.

A graphical representation of the soil column and the finite element mesh used for this problem is shown in Figure 26. It can be seen from this graph that the first centimeter of depth below land surface is given 0.25cm grid spacings. The next 2 centimeters of depth have 0.5cm grid spacings. From the 3cm depth to the 60cm depth a 1cm spacing is used. Two centimeter spacings are then used from 60 through 296cm. From 296 to 300cm a reversal of the same grid spacing used in the top 4cm of the model is used. The total column length of the model is 3 meters using 192 elements. The width of the column is taken to be 1cm.

As mentioned previously it is assumed that the maximum rooting depth of the four winged salt bush near soil-moisture station 1 is 1.5 meters. Therefore the model will be used to simulate root uptake to a depth of 1.5 meters. In doing so it is

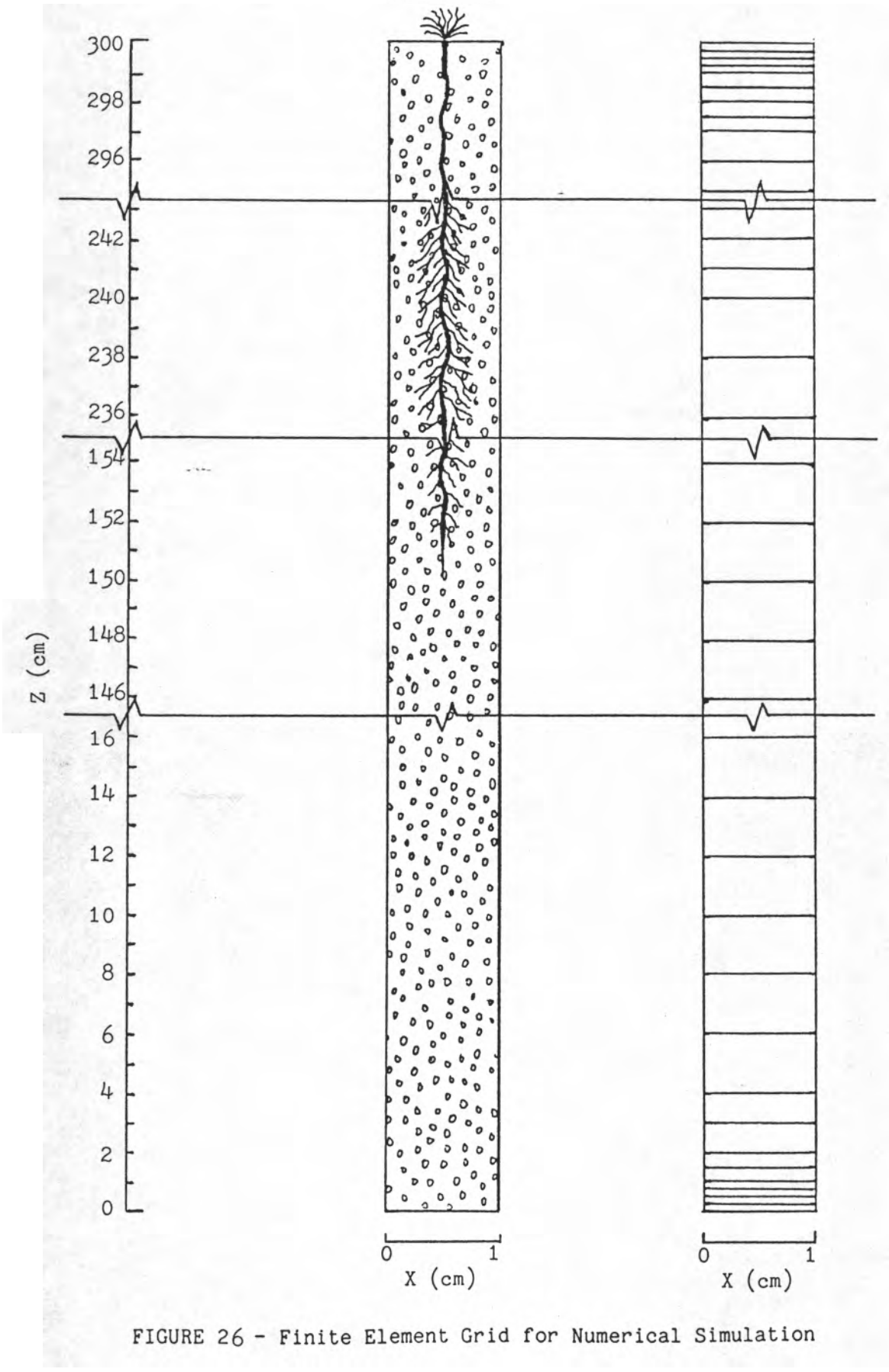

FIGURE 26 - Finite Element Grid for Numerical Simulation

assumed that any downward flux of water below this root zone, as simulated by the model, will be the same flux that is recharging the water table.

The model requires the input of the θ-ψ and K-θ relationships. The entire profile being simulated is assumed to be homogeneous and isotropic. Therefore averaged relationships of θ-ψ and K-θ are to be input in tabular form. These relationships must be monotonic; there will be no capillary fringe and therefore the air entry pressure is essentially zero. The θ-ψ relationship is obtained from the instantaneous profile data spoken of in Section 7. Figure 27 shows the instantaneous profile data plotted against the average θ-ψ relationship that is being used as model input. In order for the model to yield stable results the specific moisture capacity plotted against water content must be a smooth line, and also must be monotonic. Figure 28 shows a plot of specific moisture capacity versus water content as generated by UNSAT2 from the input θ-ψ relation. The K-θ relationship was also obtained from the instantaneous profile data. Figure 29 is a K-θ plot of the instantaneous profile data versus the power curve-fit to this data. Equation 10.3 expressed this relationship in the form of a power curve. The average saturated hydraulic conductivity is estimated to be 0.01 cm/sec, from the shelby tube experiments discussed in Section 8. The model requires the input of an empirical root density function in order to simulate transpiration. This relation is obtained

through calibration of the model to some observed data.

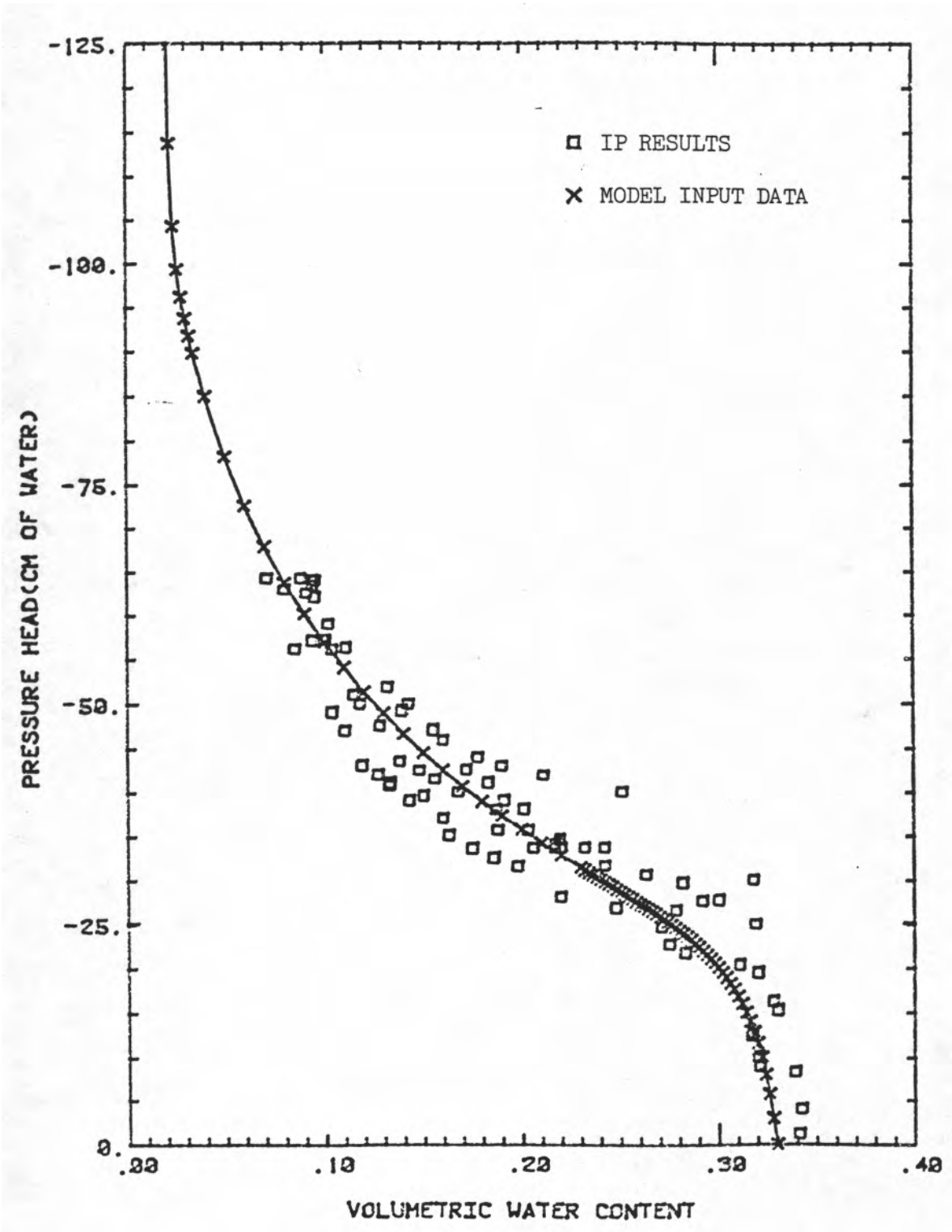

FIGURE 27 - Pressure Head versus Water Content, from Instantaneous Profile Data and the Average Model Input

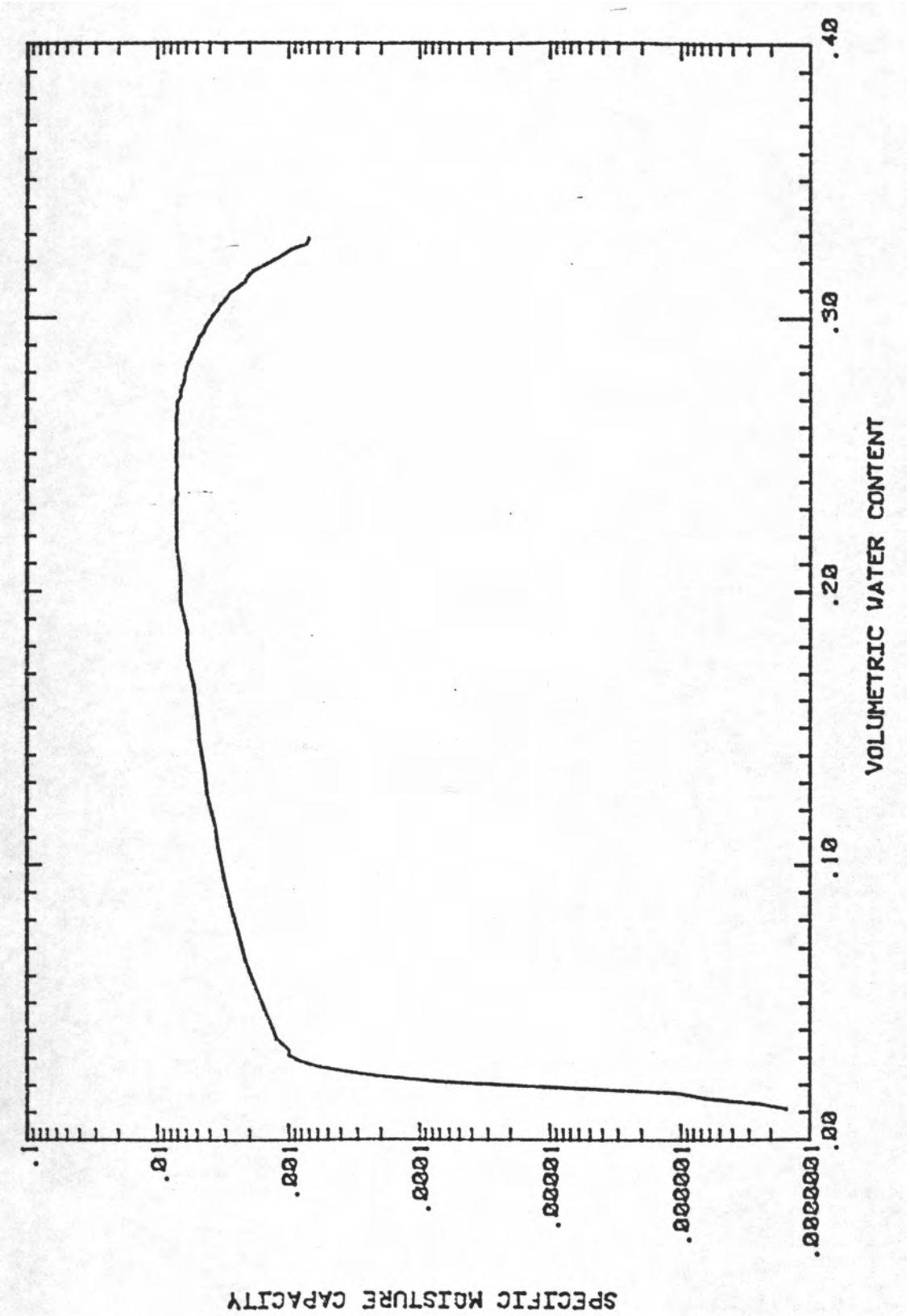

FIGURE 28 - Specific Moisture Capacity versus Water Content Generated by UNSAT2 from Input θ-ψ

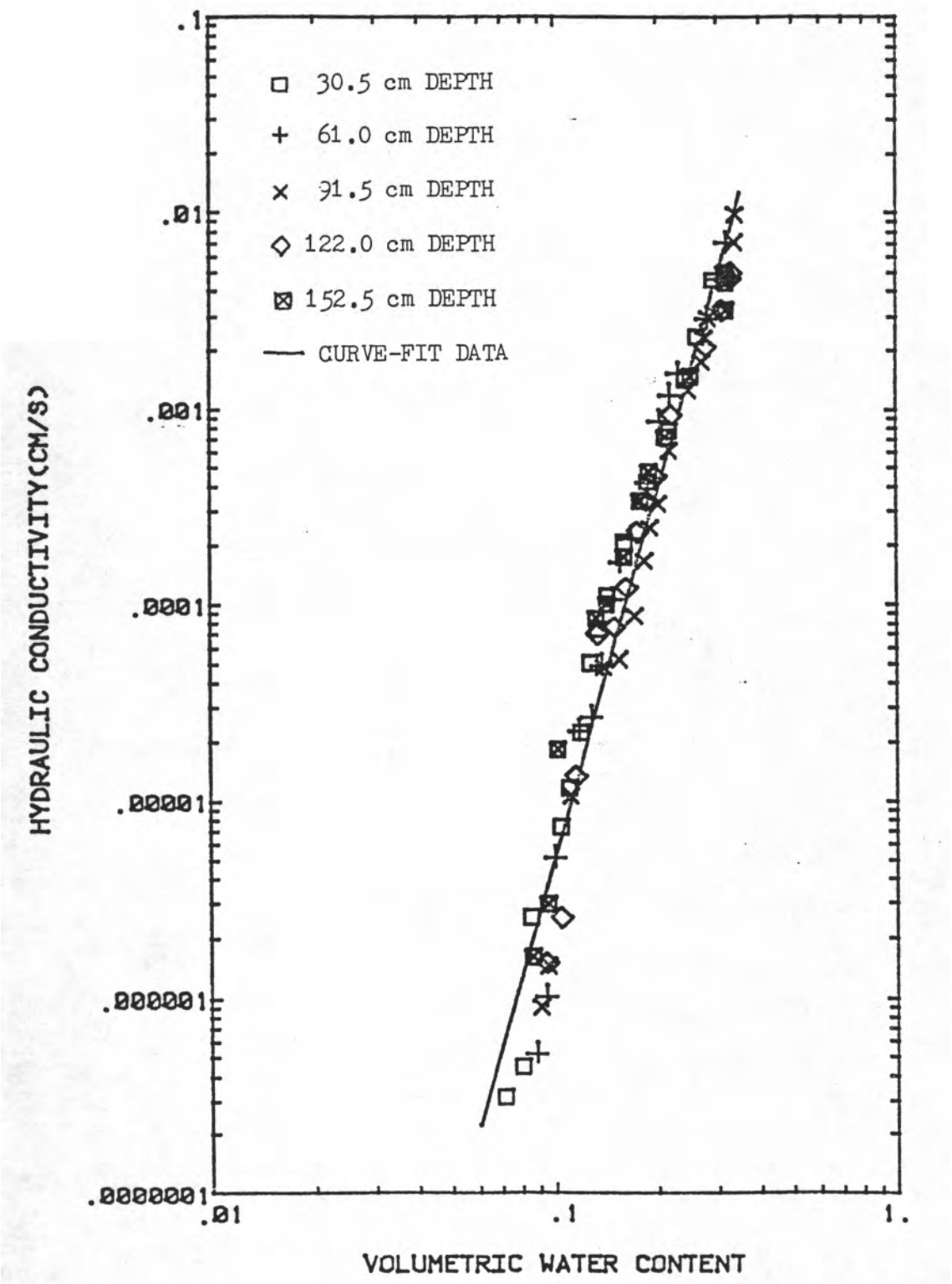

FIGURE 29 - K versus Water Content, Instantaneous Profile Data versus Power Curve-Fit Data

11.3 MODEL CALIBRATION:

Before the discretized model input data can be used for simulating long term infiltration and recharge phenomena, a calibration must be performed. The averaged input values of water content, pressure head, and hydraulic conductivity are assumed to be the best values available. Therefore, no calibration of these parameters is warranted. However, the root density function used in the model to simulate transpiration is obtained by calibrating the model to a set of observed data.

The calibration of the transpiration data is to be carried out for steady state conditions. The UNSAT2 code used for this simulation was modified for use in steady state analyses by Dr. Jim Yeh while he was at New Mexico Tech a few years ago. Therefore, it was felt that a check was needed on the numerical results for the two model options to be used, both the steady and transient state conditions.

To check the steady state solution scheme a hypothetical test case was set up. The top boundary condition in the model was given a constant total head value of 0cm of water. The bottom boundary was also given a prescribed total head of 0cm. This scheme is representative of a soil profile above a static water table that has no sources or sinks being applied to it. Under these conditions the total head throughout the unsaturated soil profile will be 0cm, and there is no flow occurring. This

implies that the pressure head at any point within the soil profile should be equal in magnitude, but opposite in sign, to the elevation head. If this is true then the depth versus water content profile from the model output should take on the same shape as the pressure head versus water content relation used in the model input. Figure 30 shows the results from this test case. The results match quite well. Therefore it is assumed that the modified UNSAT2 code does yield acceptable results for a steady state simulation with constant head boundary conditions. It should be recognized that the code was not modified to simulate prescribed flux boundary conditions for the steady state case.

A check on the numerical results of a transient simulation is also required for the model to be used for a predictive analysis. This test case involves simulating a constant head boundary condition at both the top and bottom of the soil column being simulated. The bottom boundary is set equal to some water content value that is used throughout the soil profile as an initial water content. The top boundary is set equal to saturation. The wetting front profiles for different times can then be compared to a Philip's quasi-analytical solution for the same soil type and boundary conditions. The Philip's solution used for this analysis was programmed as a computer model by Dr. Peter Huyakorn when he was at New Mexico Tech a few years ago. His code was modified by this author to accept generalized input

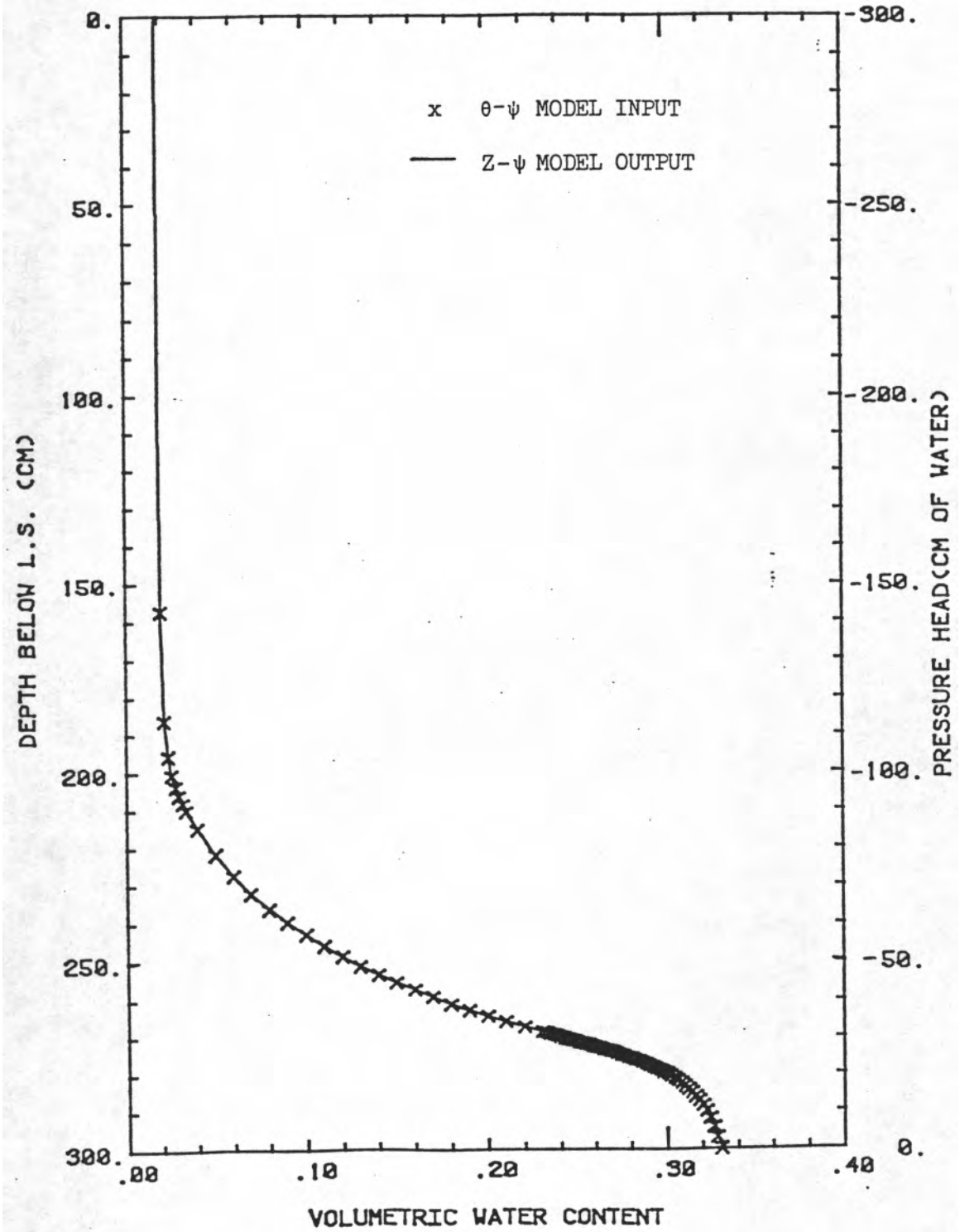

FIGURE 30 - Pressure Head and Depth versus Water Content Profiles from a Steady State Test Simulation with UNSAT2, Constant Head Boundary Conditions at the Top and Bottom of the Soil Column

information for whatever soil type that is needed. The results of this transient test case are shown in Figure 31. The two solutions are in good agreement with each other. Therefore the UNSAT2 code could yield adequate results for transient simulations.

As mentioned above, the calibration of the root density function for simulating transpiration was done for steady state conditions. It was felt that calibration of the transpiration and evaporation functions in the model could not be accomplished adequately for a discrete set of transient data. There was no observed data applicable to calibrating a transient simulation when there was only transpiration occurring and no evaporation occurring. Simulating the actual inputs and outputs through the soil profile, while adjusting the root density function and evaporation potential to match observed data over a finite time frame, was considered too cumbersome a task. Besides, any calibration of the transpiration and evaporation functions in the model to a discrete set of data would only be applicable for use in transient simulations during the same period of the year under simulation. The intent of simulating the natural flow phenomenon with UNSAT2 was to ultimately use the model for long term predictions of the recharge flux. Ideally this would mean that a calibration of the transpiration and evaporation functions should be carried out for different seasons of the year, as these effects change due to changing meteorological and soil-moisture

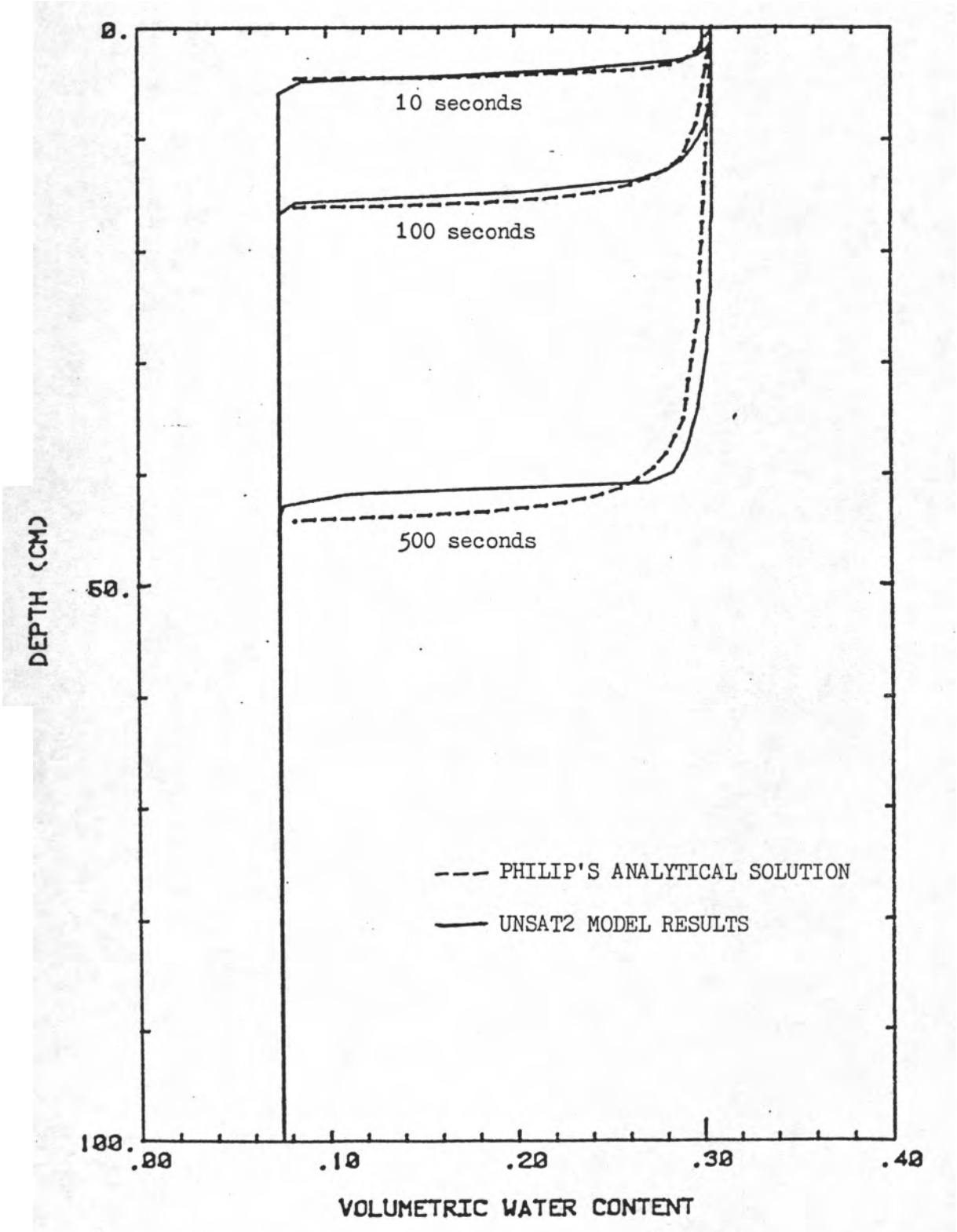

FIGURE 31 - Depth versus Water Content for a Transient State Test Simulation with UNSAT2, Philip's Analytical versus UNSAT2 Numerical Results

conditions. This type of analysis was considered to be too costly and time consuming for this study. Therefore some assumptions had to be made.

The water budget results from Section 10.3.1 were assumed to be correct for the period under study, November 1982 through May 1984. The recharge rate reported in Table 1 was assumed to be equivalent to the long term average recharge rate. In calibrating the transpiration function this rate was held constant. This was done by prescribing a constant pressure head of -80cm of water at the bottom of the soil column under simulation. This was essentially the same average pressure head observed for the Darcy's Law approach from Section 10.2.1. As long as the transpiration rate was not too large this outflow rate of approximately 3.0×10^{-8} cm/sec was maintained.

As mentioned previously, UNSAT2 is incapable of simulating a constant flux boundary condition in a steady state simulation. Therefore, a constant head boundary condition was applied at the soil surface and the resultant flux across that boundary was used in analyzing the data. This flux across the top of the model is dependent upon the transpiration uptake below it. Therefore, there appears to be a delicate balance between the constant head boundary condition at the soil surface and the transpiration function.

The root density function is an empirical relation set up by Neuman in UNSAT2 to simulate transpiration. It is not truly related to the actual root density in the sense that a quantification of the root density in the soil will be the root density function. It is more of an empirical mathematical relation which produces an effect that is similar to that observed from plants. The physics of water uptake by plants is not understood well enough to develop a theoretically based mathematical relationship for simulating transpiration. Therefore this empirical relationship was formed utilizing a root density function.

Feddes et al. (1975) utilized UNSAT2 for simulating transpiration from an irrigated agricultural crop. They concluded that, for the crop under study, an exponential decay of the root density function with depth worked best. This approach was taken in trying to simulate root uptake in this semi-arid naturally vegetated condition. The root density function and the constant head boundary condition were adjusted until the mass balance of the model output was small. The pressure head profile was sought to match the average pressure head profile for the period of record at soil-moisture station 1, November 1982 through May 1984. The condition sought for final calibration was one in which the flux across the land surface boundary was equivalent to the sum of the transpiration and outflow (or recharge) rates from the model. The transpiration rate was

assumed to be 90% of the evapotranspiration rate calculated in Section 10.3.1. This percentage was chosen because of the close proximity of the soil-moisture station instrumentation to a stand of salt bush. No better information was available for use in determining the transpiration function. This may have been the goal of this calibration attempt, but it was not attained. Many attempts were made to achieve this end, but all failed. In order to simulate a transpiration rate that was 90%, 50%, or even 30% of the evapotranspiration rate from the water budget results, the resultant pressure head profile was always too dry within the top portion of the root zone. The root zone was assumed to extend from 15 to 150cm below land surface, based upon field observations. Therefore this exponential decay function for the root density, which is at a maximum at the top of the root zone, was assumed to be inadequate for the simulation of soil-moisture station 1 flow conditions.

A new relationship was devised which is just a slight modification to the approach by Feddes et al. (1975). This relation also involves an exponential decay function; only this time the maximum root density value is at the center of the root zone and the exponential decay is both upwards and downwards from the center. This allows the gradual uptake of water from transpiration with depth instead of the sharp increase imposed with the previous method. Even this new functional relationship may yield questionable results. However, in the course of many

more attempts at a calibration of the transpiration function a solution was settled upon. In order to keep the same outflow, or recharge rate of 3.0×10^{-8} cm/sec from the base of the model, the resultant transpiration rate was 1.9×10^{-8} cm/sec. This estimation of the long term transpiration rate is only about 3.5% of the estimated overall evapotranspiration rate. Therefore the evaporation potential is much greater in the area of site instrumentation than the transpiration. The model setup was such that the final constant pressure head at the soil surface was -40cm of water, and the resultant pressure head profile was in relatively good agreement with the observed average pressure head profile. Figure 32 shows the results of this calibration. Figure 33 shows the root density function in relation to depth. The results of this calibration have rather interesting implications. In order to simulate the same observed pressure head profile and recharge flux the transpiration rate was relatively small, only 3.4% of the precipitation rate for the period of record, November 1982 through May 1984. This result assumes that there is no net change in water storage during this time frame. The implication of the evaporation flux being much larger than the transpiration rate may not be far from reality. Evans and Thames (1981) have observed that the lateral extent of the roots of a desert hackberry bush near Santa Rita, Arizona was never more than 1 meter. A desert hackberry bush is similar to a salt bush in appearance, size, and maximum observed

evapotranspiration (according to Evans and Thames, 1981). One might assume that they have similar root structures. This being the case, and soil-moisture station 1 located just under 1 meter from a salt bush, then the low transpiration rate predicted in this calibration is not unreasonable.

Another implication of these results comes from the finalized constant head boundary condition at the soil surface. Under steady state conditions this result implies that if there were no other stresses on the soil system (such as evaporation) a constant pressure head of -40cm of water is sufficient to sustain the plant water demand within the root zone. In reality there is a greater precipitation flux at the land surface than was simulated in this calibration. There is also an evaporation flux. It is assumed that this additional precipitation is equal in magnitude, but opposite in sign, to the evaporation flux. Essentially this means that the precipitation flux not accounted for in this steady state transpiration calibration is intercepted within the near surface soil profile by evaporation processes. This should allow the subsurface profile to be essentially the same as that shown in Figure 32, except within the near surface profile where evaporation is a factor. UNSAT2 is not capable of simulating the combined effects of precipitation, evaporation and transpiration under steady state conditions. Therefore a calibration will not be performed on the evaporation function used at the top of the model.

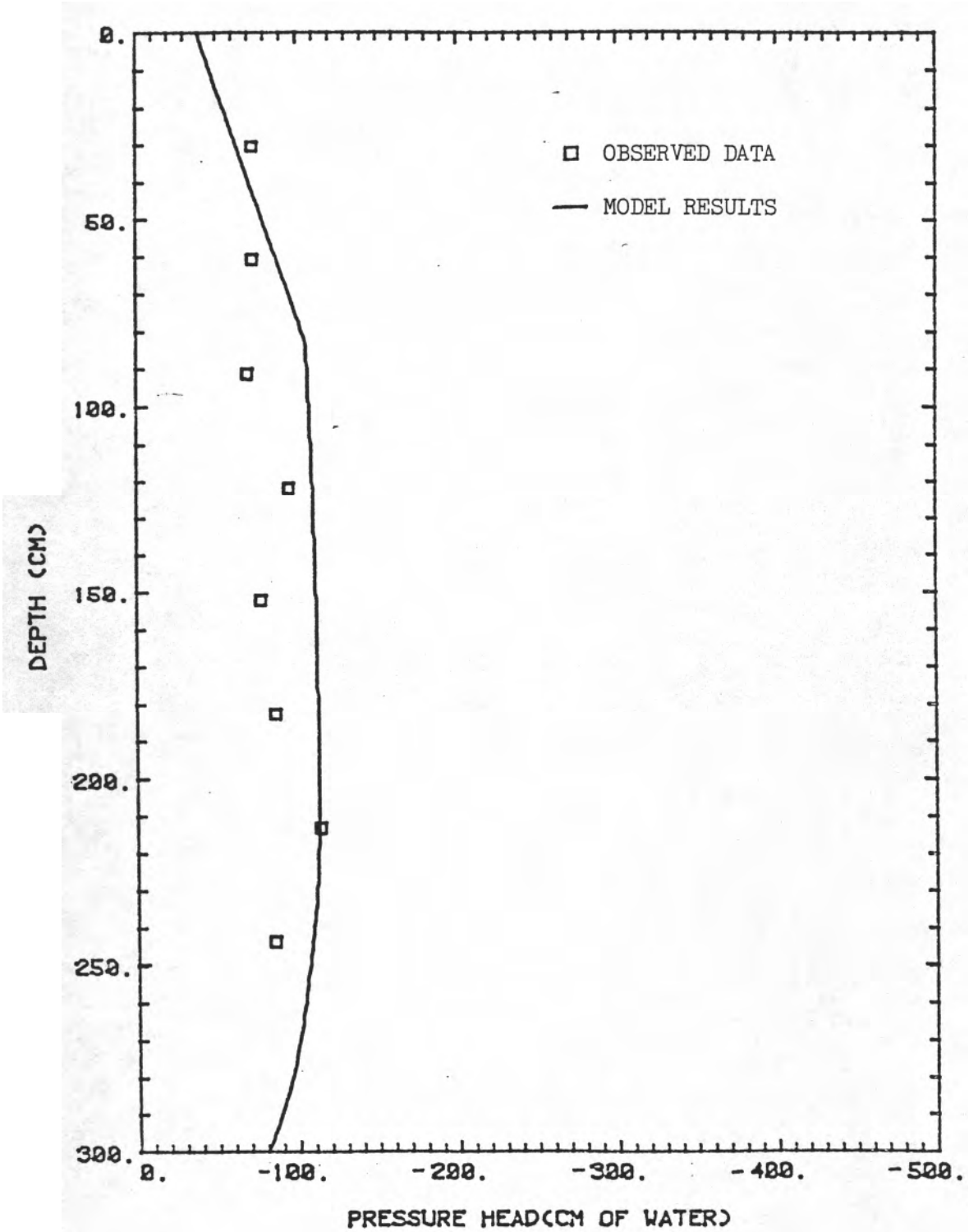

FIGURE 32 - Pressure Head versus Depth Profile for a Steady State Calibration of the Root Density Function for Transpiration, UNSAT2 Results versus Observed Data

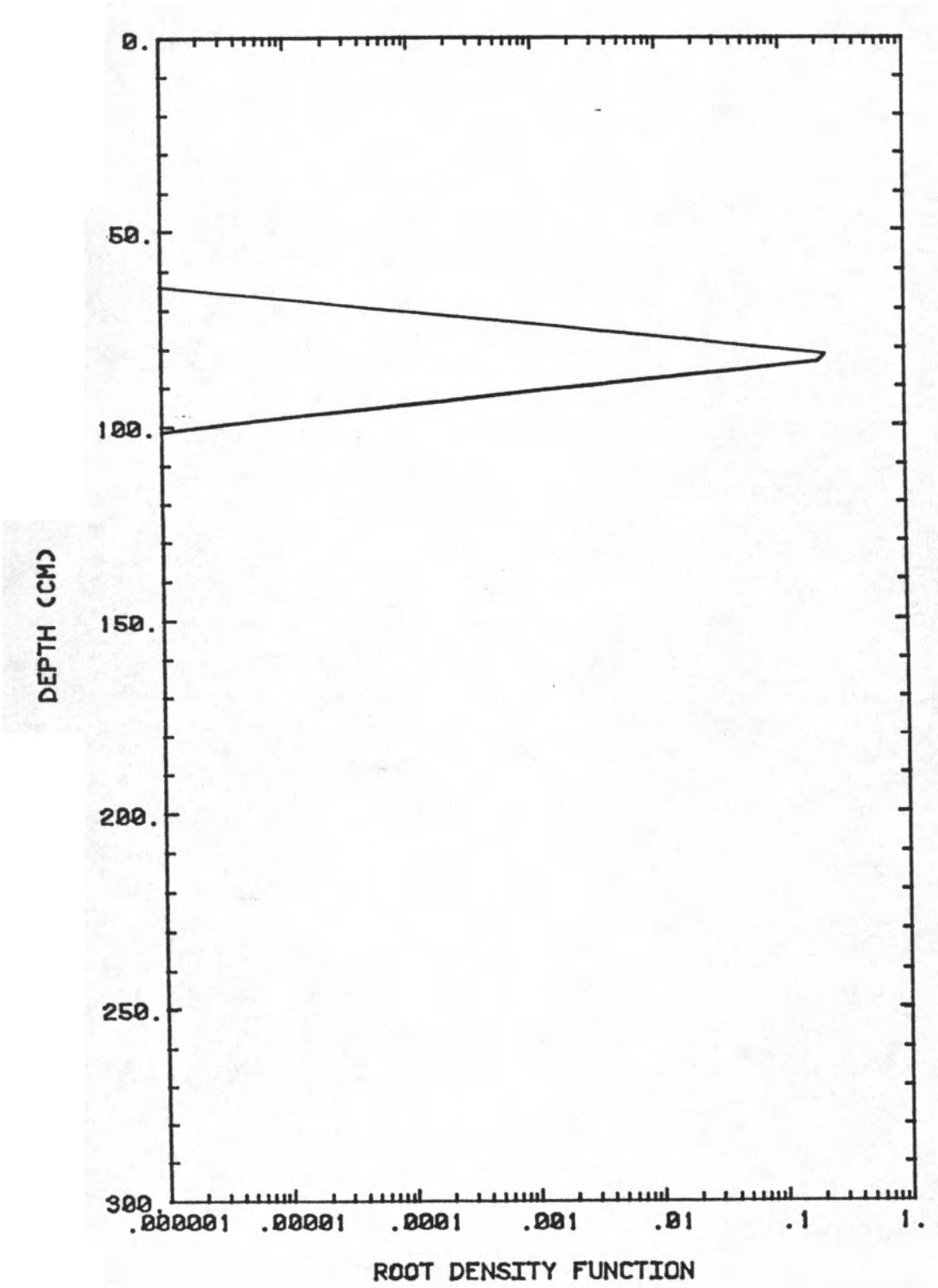

FIGURE 33 - Depth versus the Finalized Root Density Function for the UNSAT2 Model Input

The average results from this calibration procedure could then be used for a verification and prediction procedure. The root density function could be left the same for any simulation. The potential transpiration could be varied to simulate differing root uptakes during different times of the year. This approach will be explored in the verification procedure.

11.4 MODEL VERIFICATION:

Before attempting any predictive work with this calibrated model setup, a verification to an observed set of transient data is needed. This verification procedure is done in order to qualitatively evaluate the prediction results that will be discussed in the next section. For this case a simulation of a precipitation event, followed by a couple of days of infiltration, was performed. The observed data is from September 23, 1983 through September 26, 1983. On September 23, 1983 a storm of 1.74cm was recorded at the research site over a 6 hour period. This corresponds to an average precipitation rate of 8.06×10^{-5} cm/sec over the 6 hour period.

The observed data consisted of water content and pressure head profiles collected at soil-moisture station 1 before, one day after, and two days after the event. The pressure head data was discontinuous with depth, due to the inoperation of some tensiometers. Therefore the water content profile was used as the observed data, and converted to corresponding pressure head values with the ψ-θ relation used in the model input. The observed data collected before the precipitation event was used as the starting pressure head profile for the model simulation. The data collected one and two days after the event are hopefully matched by the UNSAT2 results to verify the model setup validity.

Figure 34 shows the results from this verification simulation. Many attempts were made at correctly inputting the evaporation potential. This evaporation function did not have any significant influence on the model response between the 40 and 100cm depths. The model results appear to be in relatively good agreement with the observed data. The data set being analyzed for this verification of the model was from a relatively wet period of the year. The period from July through September averages about 52% of the yearly precipitation rate (according to the NOAA summaries for Socorro, NM). The transpiration potential should be higher than the long term average during periods when the soil profile is relatively wet. Therefore the potential transpiration value used for this verification procedure was increased from the average value used in the calibration procedure. A verification to a set of precipitation and infiltration data during a drier season would require a lower value of potential transpiration. However, as pointed out previously, the period from January 1984 through May 1984 was quite dry, with a total precipitation of only 0.28cm. The observed data from this period did not lend itself to the verification procedure. It is hoped that for the long term predictive case that this transpiration function will yield acceptable results. The prediction phase of this modeling effort will be carried out over the wet and dry seasons. Therefore it is hoped that a good estimate of the potential transpiration and

evaporation can be obtained to yield adequate results. Otherwise the model may predict excessive wetting or drying of the soil profile in relation to actual soil-moisture profiles.

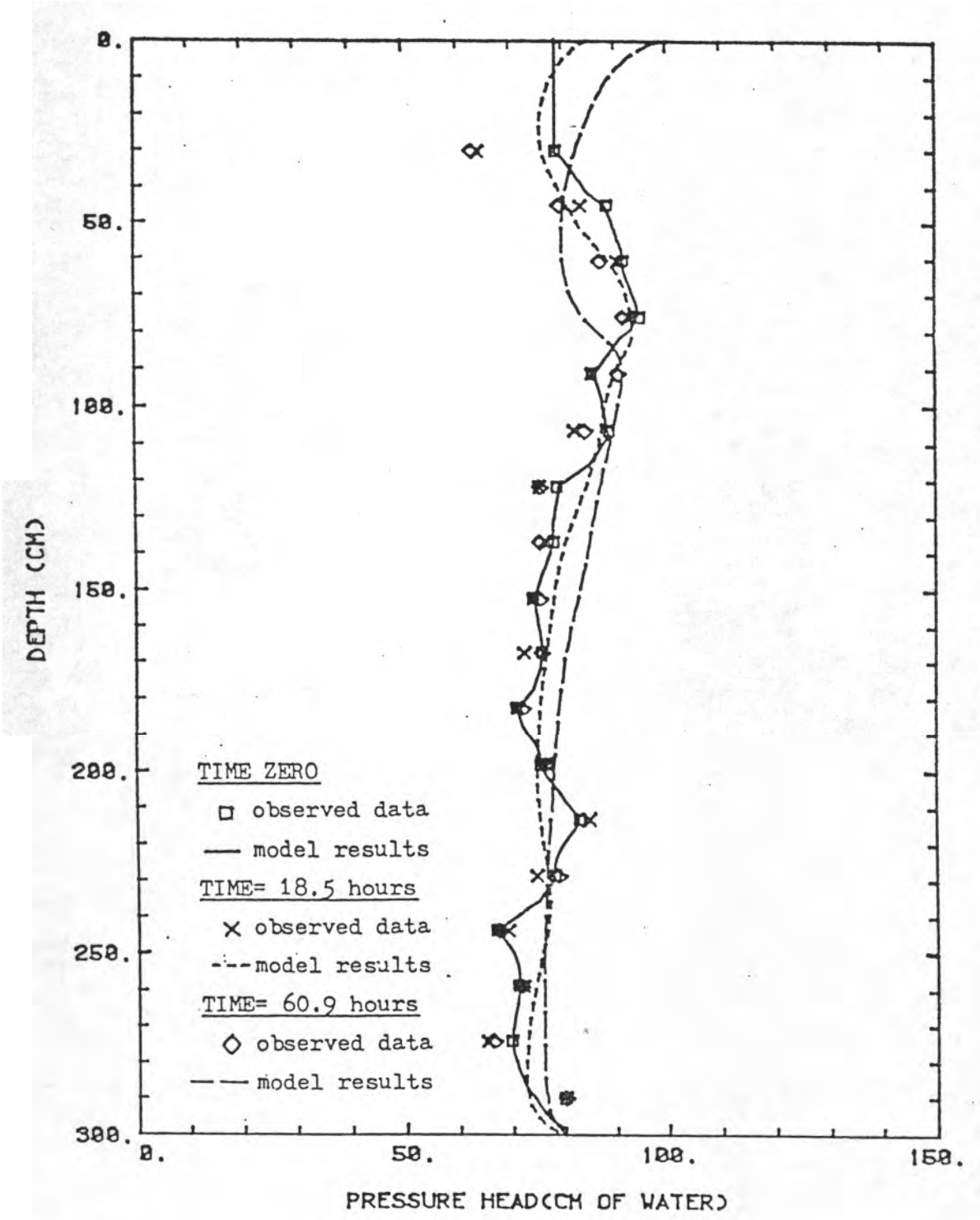

FIGURE 34 - Verification of model results, simulating a 4 hour storm of 8.06×10^{-5} cm/sec, and subsequent infiltration and redistribution.

11.5 POTENTIAL MODEL USE:

The model setup just spoken of may be used to predict infiltration and evapotranspiration phenomena associated with the soil profile under investigation. A long term simulation of the average precipitation events that occur at the research site might shed some insight on the seasonal behaviour of the recharge flux. This type of simulation might also show what length of lag times there may be between precipitation events and the associated recharge flux to the water table. A study of infiltration phenomena might also be done for varying initial moisture conditions and varying magnitudes and durations of precipitation events. This type of study might determine what types of precipitation events are important to inducing recharge and what events have a negligible impact. Because of time and budgetary constraints these types of analyses were not carried out in this study, but may be continued by another researcher.

12. SUMMARY:

An extensive amount of instrumentation and monitoring equipment was installed within a small drainage basin in a semi-arid lowland. This equipment is being used to measure and predict the hydrologic processes occurring at this site. The methods presented in this paper are specifically related to estimating the natural ground-water recharge flux and the evapotranspiration rate. A Darcy's Law approach yielded an estimated recharge flux of between 0.90 and 4.73 cm/year for a pressure head based evaluation. This corresponds to about 5.1% to 26.6% of the precipitation rate for the period of record, November 1982 through May 1984. The seepage velocity associated with this recharge flux was between 15.0 and 78.8 cm/year below the root zone. A water content based analysis using Darcy's law over the period September 1983 to May 1984 yielded a recharge flux estimate between 0.65 and 2.13 cm/year. The corresponding seepage velocity would be between 10.8 and 35.6 cm/year. This estimate of the recharge flux is between 4.8% and 15.7% of the precipitation rate over the period of record for which data was collected. A temperature gradient method was used to calculate a recharge rate of 1.26 cm/year, or 7.1% of the precipitation rate. The seepage velocity for this method is calculated to be 21.0 cm/year. Averaging the estimated recharge rates from the pressure head derived case and the temperature gradient method yields a value of 2.30 cm/year. The average seepage velocity is

about 38.3 cm/year. Assuming this seepage velocity is representative of the long term water particle velocity throughout the soil profile, and the depth to water at the site under investigation is 6 meters, then it takes approximately 15.7 years for water to travel from the land surface to the water table.

An estimate of the evapotranspiration rate was made from a water budget method. The calculated values were between 13.1 and 16.9 cm/year, or 73.4% and 94.9% of the precipitation rate over the period November 1982 through May 1984. Estimates of actual evapotranspiration rate were made from an approximation of the potential, or reference crop, evapotranspiration rate. The best estimates of input parameters were made and the resultant estimation of actual evapotranspiration was inadequate. A subsequent evaluation of the methods suggested that with minor modifications of estimating the input parameters to these models some good results could probably be obtained.

Two experimental field techniques were evaluated. The 'micro-lysimeter' technique was used to directly measure actual evaporation. The results appeared to be over-estimates of the evaporation rate. This technique appears to have potential as an inexpensive method of estimating actual evaporation and deserves more attention. Bromide tracer experiments were carried out to measure wetting front advances after natural precipitation

events. A number of technical problems and questions arose from this analysis which need to be addressed before any conclusive results can be obtained.

A numerical model was employed to simulate the unsaturated flow at the study site. A test of the steady state and transient simulation options was made, with good results. A calibration of the transpiration uptake was done against observed data. A verification of the model results was also carried out against observed data for a specific precipitation event, and subsequent infiltration and redistribution. Some recommendations are given for future predictive work that could be carried out with this calibrated model.

13. RECOMMENDATIONS FOR FURTHER RESEARCH:

Data collection at this research site should be carried out for as long as possible. This data could be analyzed over the long term with the methods presented in this paper. A long term data base would also lend itself to a time-series analysis. Another approach would be a more detailed numerical analysis utilizing this long term data instead of making approximations as was done above.

This site should also lend itself to some analyses with isotopes of oxygen, hydrogen, and chlorine to estimate seepage velocities and evaporation fluxes. An isotopic analysis could also be used in conjunction with stream gauging of the Rio Salado to determine recharge rates from the river to the phreatic aquifer.

Installing two weighing lysimeters at the site could help determine the actual evapotranspiration. One lysimeter should be set up with native vegetation, the other with a bare surface. This should facilitate the estimation of the amount of both evaporation and transpiration as separate, but related, quantities.

Temperature thermistors should be installed at deeper depths, and at more soil-moisture stations, than currently exists at the site. Monitoring of the heat flux across the soil profile

should be done at different soil types within the basin to approximate water and water vapor loss from the soil. Quantification of the water vapor loss from the soil profile could prove to be significant.

A statistical analysis should be done on the reliability of the data that is being used in the methods for estimating the recharge flux. An estimate of error involved with each reported result is in order.

Comparing and contrasting the hydrologic processes occurring in different soil types, slopes, and vegetative cover was a goal outlined in the original proposal for this project, which as yet has not been accomplished.

Additional computer modeling work should be carried out with the aid of the calibrated model. Determinations of long term recharge rates and infiltration characteristics could be made with this model, given the time and computer dollars. A better understanding of the time lag concept might also be obtained from this effort. A time-series analysis might also prove to be beneficial in understanding the time-lag phenomenon.

REFERENCES

Birch, A.F., J.F. Schairer, and H.C. Spicer, 1942, Handbook of Physical Constants, Geological Society of America Special Paper 36, 325 pp.

Biswas, T.D., D.R. Nielsen, and J.W. Biggar, 1966, Redistribution of Soil Water after Infiltration, Water Resources Research, v. 2, no. 3, p. 513-524.

Boast, C.W. and T.M. Robertson, 1982, A "Micro-Lysimeter" Method for Determining Evaporation from Bare Soil: Description and Laboratory Evaluation, Soil Science Society of America Journal, v. 46, p. 689-696.

Boonyatharokul, W. and W.R. Walker, 1979, Evapotranspiration Under Depleting Soil Moisture, American Society of Civil Engineers, Journal of Irrigation and Drainage, v. 105, no. IR4, p. 391-402.

Boyle, J.M. and Z.A. Saleem, 1979, Determination of Recharge Rates using Temperature-Depth Profiles in Wells, Water Resources Research, v. 15, no. 6, p. 1616-1622.

Cuenca, R.H. and M.T. Nicholson, 1982, Application of Penman Equation Wind Function, American Society of Civil Engineers, Journal of Irrigation and Drainage, v. 108, no. IR1, p. 13-23.

Dahiya, I.S., M. Singh, M. Singh, and S. Hajrasuliha, 1980, Simultaneous Transport of Surface-Applied Salts and Water Through Unsaturated Soils as Affected by Infiltration, Redistribution, and Evaporation, Soil Science Society of America Journal, v. 44, no. 2, p. 223-227.

Davis, L.A. and S.P. Neuman, 1983, Documentation and User's Guide: UNSAT2 Variably Saturated Flow Model (Including 4 Example Problems), Final Report, WWL/TM-1791-1, Water Waste and Land, Inc., Fort Collins, Colorado.

Dincer, T., A. Al-Mugrin, and U. Zimmerman, 1974, Study of the Infiltration and Recharge through Sand Dunes in Arid Zones with Special Reference to the Stable Isotopes and Thermonuclear Tritium, Journal of Hydrology, v. 23, p. 79-109.

Doorenbos, J. and W.O. Pruitt, 1977, Guidelines for Predicting Crop Water Requirements, Irrigation and Drainage Paper 24, F.A.O. United Nations, Rome, Italy, 144 pp.

Enfield, C.G., J.J.C. Hsieh, and A.W. Warrick, 1973, Evaluation of Water Flux above a Deep Water Table using Thermocouple Psychrometers, Soil Science Society of

America Proceedings, v. 37, p. 968-970.

Evans, D.D. and J.L. Thames (editors), 1981, Water in Desert Ecosystems, Dowden, Hutchinson and Ross, Inc., Stroudsburg, Pa., 280 pp.

Feddes, R.A., S.P. Neuman, and E. Bresler, 1975, Finite Element Analysis of Two-Dimensional Flow in Soils Considering Water Uptake by Roots: II. Field Applications, Soil Science Society of America Proceedings, v. 39, p. 231-237.

Flühler, H., M.S. Ardakani, and L.H. Stolzy, 1976, Error Propagation in Determining Hydraulic Conductivities from Successive Water Content and Pressure Head Profiles, Soil Science Society of America Journal, v. 40, p. 830-836.

Freeze, R.A., 1969, The Mechanism of Natural Ground-Water Recharge and Discharge, 1. One-dimensional, Vertical, Unsteady, Unsaturated Flow above a Recharging or Discharging Ground-Water Flow System, Water Resources Research, v. 5, no. 1, p. 153-171.

Gupta, S.K., K.K. Tanji, D.R. Nielsen, J.W. Biggar, C.S. Simmons, and J.L. MacIntyre, 1978, Field Simulation of Soil-Water Movement with Crop Water Extraction, University of California, Department of Land, Air and Water Resources, Water Science and Engineering Paper No. 4013, 121 pp.

Hanks, R.J., A. Klute, and E. Bresler, 1969, A Numeric Method for Estimating Infiltration, Redistribution, Drainage and Evaporation of Water from Soil, Water Resources Research, v. 5, p. 1064-1069.

Hawley, J.W., 1983, Site Identification for Low-Level Radioactive Waste Disposal in New Mexico, Report to the Radioactive Waste Consultation Committee of the New Mexico State Legislature, February 18, 1983.

Higuchi, M., 1984, Numerical Simulation of Soil-Water Flow During Drying in a Nonhomogeneous Soil, Journal of Hydrology, v. 71, p. 303-334.

Hillel, D., V.D. Krentos, and Y. Stylianou, 1972, Procedure and Test of an Internal Drainage Method for Measuring Soil Hydraulic Characteristics In Situ, Soil Science, v. 114, no. 5, p. 395-400.

Hillel, D., 1980, Fundamentals of Soil Physics, Academic

Press, New York, 411 pp.

Jensen, K.H., 1983, Simulation of Water Flow in the Unsaturated Zone including the Root Zone, Institute of Hydrodynamics and Hydraulic Engineering, Technical University of Denmark, Series Paper No. 33, 259 p.

Jensen, M.E. and H.R. Haise, 1963, Estimating Evapotranspiration and Solar Radiation, American Society of Civil Engineers Journal of Irrigation and Drainage, v. 89, p. 15-41.

Jensen, M.E. (editor), 1974, Consumptive Use of Water and Irrigation Water Requirements, A report prepared by Technical Communications on Irrigation Water Requirements, Irrigation and Drainage Division, American Society of Civil Engineers, New York.

Jury, W.A. and C.B. Tanner, 1975, Advection Modification of the Priestley and Taylor Evapotranspiration Formula, Agronomy Journal, v. 67, p. 840-842.

Jury, W.A., L.H. Stolzy, and P. Shouse, 1982, A Field Test of the Transfer Function Model for Predicting Solute Transport, Water Resources Research, v. 18, no. 2, p. 369-375.

Kirkham, R.R. and G.W. Gee, 1983, Measurement of Unsaturated Flow Below the Root Zone at an Arid Site, Proceedings of Conference on Characterization and Monitoring of the Vadose Zone, National Water Well Association.

Klute, A., R.E. Danielson, D.R. Linden, and P. Hamaker, 1972, Ground-Water Recharge as affected by Surface Vegetation and Management, Colorado State University, Colorado Water Resources Research Institute Completion Report, No. 41, 48 pp.

Krishnamurthi, N., D.K. Sunada, and R.A. Longenbaugh, 1977, Mathematical Modeling of Natural Groundwater Recharge, Water Resources Research, v. 13, no. 4, p. 720-724.

Larson, M., 1984, A Comparison of Empirical/Theoretical, Laboratory, and Field Techniques in Evaluating Unsaturated Hydraulic Properties of Mill Tailings, unpublished master's thesis, New Mexico Institute of Mining and Technology, Socorro, NM.

Longenbaugh, R.A., 1975, Computer Estimates of Natural Recharge from Soil Moisture Data, High Plains of Colorado, Colorado State University, Colorado Water Resources Research Institute Completion Report Series No. 64, 58 pp.

Longmire, P.A., B.M. Gallaher, and J.W. Hawley, 1981, Geological, Geochemical, and Hydrological Criteria for Disposal of Hazardous Wastes in New Mexico, New Mexico Geological Society, Special Publication No. 10, p. 93-102.

Machette, M.N., 1978, Geologic Map of the San Acacia Quadrangle, Socorro County, New Mexico, USGS Geologic Quadrangle Map GQ-1415.

Marthaler, H.P., W. Vogelsanger, F. Richard, and P.J. Wierenga, 1983, A Pressure Transducer for Field Tensiometers, Soil Science Society of America Journal, v. 47, p. 624-627.

Maxey, G.B. and T.E. Eakin, 1949, Ground Water in White River Valley, White Pine, Nye, and Lincoln Counties, Nevada, Nevada State Engineer, Water Resources Bulletin, No. 8, 59 pp.

McKim, H.L., R.L. Bert, R.W. McGaw, R.T. Atkins, and J. Ingersoll, 1976, Development of a Remote Reading Tensiometer/Transducer System for Use in Subfreezing Temperatures, Proceedings of 2nd Conference on Soil-Water Problems in Cold Regions, Edmonton, Alberta, Canada, p. 31-45.

Meyboom, P., 1966, Estimates of Ground-Water Recharge on the Prairies, Symposium on Hydraulic Resources of Canada, Water Resources of Canada, University of Toronto Press.

Morton, F.I., 1969, Potential Evaporation as a Manifestation of Regional Evaporation, Water Resources Research, v. 5, no. 6, p. 1244-1255.

Morton, F.I., 1975, Estimating Evaporation and Transpiration from Climatological Observations, Journal of Applied Meteorology, v. 14. p. 488-497.

Ogata, G. and L.A. Richards, 1957, Water Content Changes Following Irrigation of Bare Field Soil that is Protected from Evaporation, Soil Science Society of America Proceedings, v. 21, p. 355-356.

Oster, C.A., 1982, Review of Ground-Water Flow and Transport Models in the Unsaturated Zone, Pacific Northwest Laboratory, NUREG/CR-2917, PNL-4427.

Priestley, C.H.B. and R.J. Taylor, 1972, On the Assessment of Surface Hear Flux and Evaporation using Large-Scale Parameters, Monthly Weather Review, v. 100, p. 81-92.

Quissenberry, V.L. and R.E. Phillips, 1976, Percolation of

Surface Applied Water in the Field, Soil Science Society of America Journal, v. 40, p. 484-489.

Rabold, R.R., 1984, The Results of a Borehole Infiltration Test with a Shallow Water Table, unpublished master's thesis, New Mexico Institute of Mining and Technology, Socorro, NM.

Reddel, D.L., 1967, Distribution of Ground-Water Recharge, Technical Report No. AER 66-67 DLR91, Agricultural Engineering Department, Colorado State University, Fort Collins, Colorado.

Reisenauer, A.E., K.T. Key, T.N. Narasimhan, and R.W. Nelson, 1982, TRUST: A Computer Program for Variably Saturated Flow in Multidimensional, Deformable Media, Pacific Northwest Laboratory, NUREG/CR-2360, PNL-3975, Government Printing Office, Washington, D.C.

Richards, S.J. and L.V. Weeks, 1953, Capillary Conductivity Values from Moisture Yield and Tension Measurements on Soil Columns, Soil Science Society of America Proceedings, v. 17, p. 206-209.

Rose, C.W., W.R. Stern, and J.E. Drummond, 1965, Determination of Hydraulic Conductivity as a Function of Depth and Water Content for Soil In Situ, Australian Journal of Soil Research, v. 3, p. 1-9.

Saffigna, P.G., D.R. Keeney, and C.B. Tanner, 1977, Lysimeter and Field Measurements of Chloride and Bromide Leaching in an Uncultivated Loamy Sand, Soil Science Society of America Journal, v. 41, p. 478-482.

Sammis, T.W., D.D. Evans, and A.W. Warrick, 1982, Comparison of Methods to Estimate Deep Percolation Rates, Water Resources Bulletin, v. 18, no. 3, p. 465-470.

Shouse, P., W.A. Jury, and L.H. Stolzy, 1980, Use of Deterministic and Empirical Models to Predict Potential Evapotranspiration in an Advective Environment, Agronomy Journal, v. 72, p. 994-998.

Smith, W.O., 1967, Infiltration in Sands and its Relation to Ground-Water Recharge, Water Resources Research, v. 3, no. 2, p. 539-555.

Stallman, R.W., 1963, Computation of Ground-Water Velocity from Temperature Data, in USGS Water Supply Paper 1544-H, p. 36-46.

Stallman, R.W., 1971, Aquifer-Test Design, Observation and

Data Analysis, Techniques of Water Resources Investigations of the USGS, Chapter B1, Government Printing Office, Washington, D.C.

Stephens, D.B., S.P. Neuman, S. Tyler, K. Lambert, D. Watson, R. Knowlton, E. Byers, and S. Yates, 1983, Insitu Determination of Hydraulic Conductivity in the Vadose Zone using Borehole Infiltration Tests, Technical Completion Report, Project B-073-NMEX, NM Water Resources Research Institute, Las Cruces, NM, 165 pp.

Thornthwaite, C.W. and J.R. Mather, 1948, Instructions and Tables for Computing Potential Evapotranspiration and the Water Balance, in Publications in Climatology: Laboratory of Climatology, v. 10, no. 3, 311 pp.

Van Bavel, C.H.M., 1966, Potential Evaporation: The Combination Concept and Its Experimental Verification, Water Resources Research, v. 2, p. 455-467.

van Genuchten, R., 1978, Calculating the Unsaturated Hydraulic Conductivity with a New Closed-Form Analytical Model, Department of Civil Engineering Research Report 78-WR-08, Princeton University, Princeton, New Jersey.

Warrick, A., J.W. Biggar, and D.R. Nielsen, 1971, Simultaneous Solute and Water Transfer for Unsaturated Soil, Water Resources Research, v. 7, p. 1216-1225.

Watson, K.K., 1966, An Instantaneous Profile Method for Determining the Hydraulic Conductivity of Unsaturated Porous Materials, Water Resources Research, v. 2, no. 4, p. 709-715.

Watson, P., P. Sinclair, and R. Waggoner, 1976, Quantitative Evaluation of a Method for Estimating Recharge to the Desert Basins of Nevada, Journal of Hydrology, v. 31, p. 335-357.

Winograd, I.J., 1981, Radioactive Waste Disposal in Thick Unsaturated Zones, Science, v. 212, no. 4502, p. 1457-1463.

APPENDIX A

FIELD DATA

Evaporation Rate versus Time from the Micro-lysimeter Experiments.

Date	Evaporation Rate (cm/day)
03/11/84	1.2E-02
03/15/84	1.1E-02
03/18/84	6.0E-02
03/22/84	2.6E-02
03/29/84	1.8E-01
04/05/84	7.3E-04
04/08/84	2.7E-01
04/12/84	8.2E-02
04/15/84	7.4E-03
04/19/84	1.3E-01
04/27/84	7.6E-02
04/28/84	1.0E-01
05/03/84	5.7E-02
05/06/84	1.4E-02
05/10/84	2.2E-02
05/13/84	3.6E-03
05/17/84	1.8E-02
05/20/84	6.2E-02
05/24/84	4.0E-02
05/27/84	2.7E-03
05/31/84	3.0E-03

Pan Evaporation versus Time Data from Weather Station.

Date	Evaporation Rate (cm/day)	Date	Evaporation Rate (cm/day)	Date	Evaporation Rate (cm/day)
09/07/83	0.535	11/20/83	0.335	03/01/84	0.588
09/09/83	0.360	11/24/83	0.248	03/04/84	0.628
09/11/83	0.643	11/27/83	0.172	03/08/84	0.536
09/14/83	0.539	12/01/83	0.105	03/11/84	0.772
09/15/83	0.605	12/05/83	0.264	03/15/84	0.847
09/18/83	0.975	12/10/83	0.258	03/18/84	0.864
09/21/83	0.656	12/14/83	0.361	03/22/84	0.764
09/23/83	1.104	12/15/83	0.259	03/25/84	0.605
09/25/83	0.313	12/18/83	0.172	03/29/84	0.685
09/26/83	0.300	12/22/83	0.566	04/01/84	0.462
09/27/83	0.378	12/25/83	0.155	04/05/84	0.913
09/28/83	0.302	12/29/83	0.150	04/08/84	0.833
09/29/83	0.260	01/01/84	0.042	04/12/84	1.000
10/02/83	0.139	01/05/84	0.113	04/15/84	0.851
10/04/83	0.264	01/08/84	0.186	04/19/84	1.120
10/05/83	0.440	01/12/84	0.216	04/22/84	0.942
10/07/83	0.406	01/15/84	0.175	04/25/84	0.988
10/09/83	0.610	01/19/84	0.260	04/27/84	0.346
10/12/83	0.252	01/22/84	0.205	04/28/84	0.724
10/16/83	0.407	01/26/84	0.176	04/30/84	0.882
10/20/83	0.165	01/29/84	0.366	05/03/84	1.199
10/23/83	0.352	02/02/84	0.349	05/06/84	1.039
10/26/83	0.288	02/05/84	0.376	05/10/84	1.104
10/28/83	0.216	02/09/84	0.494	05/13/84	1.084
10/30/83	0.297	02/12/84	0.478	05/17/84	0.532
11/03/83	0.231	02/16/84	0.647	05/20/84	1.368
11/06/83	0.204	02/19/84	0.442	05/24/84	1.222
11/12/83	0.356	02/23/84	0.501	05/27/84	1.301
11/17/83	0.304	02/26/84	0.512	05/31/84	0.900

Minimum Evaporation Pan Temperature versus Time from the Weather Station.

Date	Temperature (°C)	Date	Temperature (°C)	Date	Temperature (°C)
09/01/83	18.	11/15/83	2.	02/28/84	1.
09/06/83	14.	11/18/83	3.	03/02/84	2.
09/08/83	14.	11/22/83	2.	03/06/84	0.
09/09/83	17.	11/25/83	1.	03/09/84	1.
09/13/83	15.	11/29/83	0.	03/13/84	3.
09/14/83	15.	12/03/83	2.	03/16/84	4.
09/16/83	16.	12/06/83	0.	03/20/84	3.
09/20/83	14.	12/13/83	0.	03/23/84	2.
09/22/83	10.	12/14/83	2.	03/27/84	3.
09/23/83	13.	12/16/83	2.	03/30/84	3.
09/24/83	15.	12/20/83	0.	04/03/84	2.
09/25/83	13.	12/23/83	3.	04/06/84	3.
09/26/83	13.	12/27/83	0.	04/10/84	3.
09/27/83	15.	12/30/83	0.	04/13/84	4.
09/28/83	13.	01/03/84	1.	04/17/84	6.
09/30/83	13.	01/06/84	3.	04/20/84	5.
10/03/83	11.	01/10/84	2.	04/24/84	4.
10/04/83	11.	01/13/84	1.	04/26/84	3.
10/06/83	13.	01/17/84	0.	04/27/84	1.
10/07/83	12.	01/20/84	0.	04/29/84	3.
10/11/83	10.	01/24/84	0.	05/01/84	5.
10/13/83	7.	01/27/84	0.	05/04/84	8.
10/18/83	7.	01/31/84	1.	05/08/84	4.
10/21/83	6.	02/03/84	1.	05/11/84	9.
10/25/83	7.	02/07/84	1.	05/15/84	12.
10/27/83	6.	02/10/84	1.	05/18/84	13.
10/28/83	8.	02/14/84	2.	05/22/84	10.
11/01/83	8.	02/17/84	2.	05/25/84	13.
11/04/83	8.	02/21/84	2.	05/29/84	11.
11/08/83	6.	02/24/84	2.		

Maximum Evaporation Pan Temperature versus Time from the Weather Station.

Date	Temperature (°C)	Date	Temperature (°C)	Date	Temperature (°C)
09/01/83	31.	11/15/83	18.	02/28/84	16.
09/06/83	32.	11/18/83	16.	03/02/84	18.
09/08/83	29.	11/22/83	13.	03/06/84	19.
09/09/83	29.	11/25/83	8.	03/09/84	21.
09/13/83	32.	11/29/83	14.	03/13/84	23.
09/14/83	30.	12/03/83	15.	03/16/84	23.
09/16/83	31.	12/06/83	15.	03/20/84	26.
09/20/83	31.	12/13/83	13.	03/23/84	23.
09/22/83	27.	12/14/83	10.	03/27/84	22.
09/23/83	28.	12/16/83	10.	03/30/84	20.
09/24/83	24.	12/20/83	11.	04/03/84	22.
09/25/83	29.	12/23/83	12.	04/06/84	26.
09/26/83	29.	12/27/83	13.	04/10/84	23.
09/27/83	28.	12/30/83	13.	04/13/84	25.
09/28/83	25.	01/03/84	8.	04/17/84	25.
09/30/83	23.	01/06/84	13.	04/20/84	26.
10/03/83	20.	01/10/84	15.	04/24/84	25.
10/04/83	21.	01/13/84	11.	04/26/84	25.
10/06/83	25.	01/17/84	9.	04/27/84	19.
10/07/83	26.	01/20/84	9.	04/29/84	22.
10/11/83	26.	01/24/84	9.	05/01/84	26.
10/13/83	23.	01/27/84	10.	05/04/84	30.
10/18/83	23.	01/31/84	13.	05/08/84	28.
10/21/83	22.	02/03/84	14.	05/11/84	31.
10/25/83	23.	02/07/84	15.	05/15/84	32.
10/27/83	21.	02/10/84	15.	05/18/84	30.
10/28/83	18.	02/14/84	18.	05/22/84	31.
11/01/83	23.	02/17/84	16.	05/25/84	34.
11/04/83	22.	02/21/84	14.	05/29/84	33.
11/08/83	21.	02/24/84	15.		

Precipitation versus Time from the Tipping Bucket Rain Gauge at the Weather Station.

Date	Precipitation (cm)
08/03/83	0.01
08/08/83	0.30
08/24/83	1.36
08/25/83	0.06
09/08/83	1.14
09/14/83	1.02
09/20/83	0.12
09/23/83	0.06
09/24/83	1.72
09/25/83	0.02
09/27/83	1.04
09/28/83	0.12
09/30/83	0.34
10/03/83	1.54
10/06/83	0.02
10/11/83	0.02
10/21/83	0.36
11/01/83	0.02
11/08/83	0.94
11/29/83	0.04
12/03/83	0.44
12/27/83	0.12
01/03/84	0.72
01/05/84	0.02
02/17/84	0.02
03/27/84	0.04
04/20/84	0.02
04/26/84	0.04
05/18/84	0.14

Neutron Probe Calibration data from Drainage Experiment

Neutron Probe Reading	Volumetric Water Content (cc/cc)
0.1073	0.0701
0.1116	0.0599
0.1271	0.0776
0.1388	0.0939
0.1506	0.0989
0.1541	0.0943
0.1668	0.1284
0.1793	0.1105
0.1894	0.1469
0.2364	0.1912
0.2405	0.1907
0.2941	0.2295
0.2961	0.2479
0.3061	0.2247

Soil Temperature versus Time for the 61.0cm Depth at Soil-moisture Station 1

Date	Temperature (°F)
12/14/82	42.
12/23/82	43.
12/27/82	43.
12/28/82	42.
12/29/82	42.
01/13/83	42.
01/18/83	42.
01/21/83	42.
01/22/83	41.
01/23/83	40.
01/24/83	39.
01/31/83	43.
02/01/83	41.
02/04/83	42.
02/05/83	41.
02/06/83	41.
02/10/83	41.
02/12/83	42.
02/14/83	43.
02/15/83	44.
02/21/83	46.
02/22/83	47.
02/27/83	47.
03/04/83	49.
03/31/83	55.
04/05/83	52.
04/08/83	48.
04/11/83	52.
04/15/83	52.
04/19/83	57.
04/22/83	56.
04/26/83	60.
04/29/83	62.
05/03/83	61.
05/07/83	66.
05/10/83	66.
05/13/83	67.
05/18/83	65.
05/24/83	68.
05/27/83	70.
06/01/83	72.
06/06/83	73.
06/10/83	74.
06/14/83	75.
06/17/83	75.
06/21/83	78.
06/24/83	78.
07/05/83	79.
07/12/83	81.
07/15/83	80.
07/19/83	82.
07/22/83	81.
07/26/83	79.
07/29/83	78.
08/08/83	82.
08/09/83	81.
08/10/83	80.
08/11/83	80.
08/12/83	81.
08/23/83	83.
08/24/83	82.
08/25/83	81.
09/01/83	82.
09/06/83	83.
09/08/83	81.
09/09/83	80.
09/13/83	81.
09/14/83	81.
09/20/83	80.
09/23/83	77.
09/24/83	75.
09/25/83	74.
09/26/83	74.
09/27/83	74.
09/28/83	73.
09/30/83	71.
10/03/83	67.
10/04/83	67.
10/06/83	68.
10/07/83	69.
10/11/83	69.
10/13/83	69.
10/17/83	67.
10/18/83	66.
10/21/83	64.
10/23/83	64.
10/27/83	63.
11/01/83	63.
11/03/83	63.
11/04/83	63.
11/15/83	57.
11/18/83	55.
11/22/83	53.
11/25/83	50.
11/29/83	47.
12/03/83	47.
12/06/83	47.
12/16/83	46.
12/20/83	44.
12/23/83	46.
12/27/83	44.
12/30/83	42.
01/03/84	42.
01/06/84	42.
01/10/84	43.
01/13/84	42.
01/20/84	39.
01/24/84	38.
01/27/84	39.
01/31/84	41.
02/03/84	42.
02/07/84	42.
02/10/84	43.
02/14/84	44.
02/17/84	45.
02/21/84	43.
02/28/84	45.
03/02/84	47.
03/06/84	46.
03/09/84	47.
03/13/84	51.
03/16/84	53.
03/20/84	53.
03/23/84	54.
03/27/84	54.
03/30/84	54.
04/03/84	53.
04/06/84	57.
04/10/84	57.
04/13/84	59.
04/17/84	61.
04/20/84	64.
04/24/84	62.
04/26/84	64.
04/27/84	59.
05/01/84	60.
05/04/84	65.
05/15/84	71.
05/18/84	70.
05/22/84	72.
05/25/84	74.
05/29/84	76.

Soil Temperature versus Time for the 91.5cm Depth at Soil-moisture Station 1

Date	Temperature (°F)
12/14/82	44.
12/23/82	44.
12/27/82	45.
12/28/82	45.
12/29/82	44.
01/13/83	42.
01/18/83	43.
01/21/83	43.
01/22/83	43.
01/23/83	42.
01/24/83	41.
01/31/83	43.
02/01/83	42.
02/04/83	42.
02/05/83	42.
02/06/83	42.
02/10/83	41.
02/12/83	42.
02/14/83	42.
02/15/83	43.
02/21/83	45.
02/22/83	46.
02/27/83	46.
03/04/83	48.
03/31/83	53.
04/05/83	53.
04/08/83	49.
04/11/83	50.
04/15/83	50.
04/19/83	54.
04/22/83	54.
04/26/83	56.
04/29/83	58.
05/03/83	59.
05/07/83	62.
05/10/83	63.
05/13/83	63.
05/18/83	63.
05/24/83	64.
05/27/83	65.
06/01/83	68.
06/06/83	69.
06/10/83	70.
06/14/83	71.
06/17/83	71.
06/21/83	73.
06/24/83	74.
07/05/83	75.
07/12/83	77.
07/15/83	76.
07/19/83	77.
07/22/83	78.
07/26/83	77.
07/29/83	76.
08/08/83	79.
08/09/83	79.
08/10/83	78.
08/11/83	78.
08/12/83	78.
08/23/83	80.
08/24/83	80.
08/25/83	79.
09/01/83	79.
09/06/83	79.
09/08/83	79.
09/09/83	79.
09/13/83	78.
09/14/83	78.
09/20/83	77.
09/23/83	76.
09/24/83	76.
09/25/83	75.
09/26/83	74.
09/27/83	74.
09/28/83	74.
09/30/83	73.
10/03/83	70.
10/04/83	69.
10/06/83	69.
10/07/83	69.
10/11/83	69.
10/13/83	69.
10/17/83	68.
10/18/83	67.
10/21/83	66.
10/23/83	65.
10/27/83	65.
11/01/83	64.
11/03/83	63.
11/04/83	63.
11/15/83	59.
11/18/83	58.
11/22/83	56.
11/25/83	53.
11/29/83	51.
12/03/83	50.
12/06/83	50.
12/16/83	48.
12/20/83	47.
12/23/83	47.
12/27/83	47.
12/30/83	46.
01/03/84	44.
01/06/84	44.
01/10/84	45.
01/13/84	44.
01/20/84	42.
01/24/84	41.
01/27/84	41.
01/31/84	42.
02/03/84	43.
02/07/84	43.
02/10/84	44.
02/14/84	44.
02/17/84	45.
02/21/84	45.
02/28/84	46.
03/02/84	46.
03/06/84	47.
03/09/84	47.
03/13/84	49.
03/16/84	51.
03/20/84	52.
03/23/84	53.
03/27/84	53.
03/30/84	53.
04/03/84	53.
04/06/84	55.
04/10/84	55.
04/13/84	57.
04/17/84	58.
04/20/84	61.
04/24/84	60.
04/26/84	61.
04/27/84	60.
05/01/84	59.
05/04/84	62.
05/15/84	67.
05/18/84	67.
05/22/84	68.
05/25/84	70.
05/29/84	72.

Soil Temperature versus Time for the 122.0cm Depth at Soil-moisture Station 1

Date	Temperature (°F)
12/14/82	50.
12/23/82	48.
12/27/82	46.
12/28/82	46.
12/29/82	46.
01/13/83	43.
01/18/83	43.
01/21/83	43.
01/22/83	43.
01/23/83	43.
01/24/83	42.
01/31/83	42.
02/01/83	42.
02/04/83	42.
02/05/83	42.
02/06/83	42.
02/10/83	41.
02/12/83	42.
02/14/83	41.
02/15/83	43.
02/21/83	44.
02/22/83	45.
02/27/83	44.
03/04/83	46.
03/31/83	50.
04/05/83	52.
04/08/83	49.
04/11/83	49.
04/15/83	49.
04/19/83	51.
04/22/83	51.
04/26/83	53.
04/29/83	55.
05/03/83	56.
05/07/83	58.
05/10/83	59.
05/13/83	59.
05/18/83	60.
05/24/83	60.
05/27/83	61.
06/01/83	64.
06/06/83	65.
06/10/83	66.
06/14/83	67.
06/17/83	67.
06/21/83	68.
06/24/83	69.
07/05/83	70.
07/12/83	72.
07/15/83	72.
07/19/83	72.
07/22/83	73.
07/26/83	73.
07/29/83	72.
08/08/83	74.
08/09/83	74.
08/10/83	73.
08/11/83	73.
08/12/83	73.
08/23/83	75.
08/24/83	75.
08/25/83	75.
09/01/83	74.
09/06/83	75.
09/08/83	75.
09/09/83	75.
09/13/83	74.
09/14/83	74.
09/20/83	73.
09/23/83	73.
09/24/83	73.
09/25/83	72.
09/26/83	72.
09/27/83	71.
09/28/83	71.
09/30/83	70.
10/03/83	68.
10/04/83	68.
10/06/83	67.
10/07/83	67.
10/11/83	67.
10/13/83	67.
10/17/83	65.
10/18/83	65.
10/21/83	65.
10/23/83	63.
10/27/83	63.
11/01/83	61.
11/03/83	61.
11/04/83	61.
11/15/83	58.
11/18/83	57.
11/22/83	55.
11/25/83	53.
11/29/83	51.
12/03/83	50.
12/06/83	49.
12/16/83	47.
12/20/83	46.
12/23/83	46.
12/27/83	46.
12/30/83	45.
01/03/84	44.
01/06/84	43.
01/10/84	44.
01/13/84	43.
01/20/84	42.
01/24/84	41.
01/27/84	40.
01/31/84	40.
02/03/84	41.
02/07/84	41.
02/10/84	41.
02/14/84	42.
02/17/84	42.
02/21/84	42.
02/28/84	43.
03/02/84	43.
03/06/84	44.
03/09/84	44.
03/13/84	45.
03/16/84	46.
03/20/84	48.
03/23/84	49.
03/27/84	49.
03/30/84	49.
04/03/84	49.
04/06/84	51.
04/10/84	51.
04/13/84	52.
04/17/84	53.
04/20/84	55.
04/24/84	55.
04/26/84	56.
04/27/84	57.
05/01/84	54.
05/04/84	56.
05/15/84	60.
05/18/84	61.
05/22/84	62.
05/25/84	63.
05/29/84	65.

Soil Temperature versus Time for the 152.5cm Depth at Soil-moisture Station 1

Date	Temperature (°F)
12/14/82	53.
12/23/82	50.
12/27/82	50.
12/28/82	50.
12/29/82	50.
01/13/83	46.
01/18/83	46.
01/21/83	46.
01/22/83	46.
01/23/83	46.
01/24/83	46.
01/31/83	45.
02/01/83	45.
02/04/83	45.
02/05/83	45.
02/06/83	45.
02/10/83	43.
02/12/83	45.
02/14/83	44.
02/15/83	45.
02/21/83	47.
02/22/83	47.
02/27/83	47.
03/04/83	48.
03/31/83	52.
04/05/83	53.
04/08/83	52.
04/11/83	51.
04/15/83	51.
04/19/83	52.
04/22/83	52.
04/26/83	53.
04/29/83	55.
05/03/83	57.
05/07/83	59.
05/10/83	59.
05/13/83	60.
05/18/83	61.
05/24/83	61.
05/27/83	62.
06/01/83	65.
06/06/83	66.
06/10/83	67.
06/14/83	68.
06/17/83	68.
06/21/83	69.
06/24/83	70.
07/05/83	71.
07/12/83	73.
07/15/83	73.
07/19/83	74.
07/22/83	74.
07/26/83	74.
07/29/83	74.
08/08/83	75.
08/09/83	75.
08/10/83	75.
08/11/83	75.
08/12/83	75.
08/23/83	77.
08/24/83	77.
08/25/83	77.
09/01/83	76.
09/06/83	77.
09/08/83	77.
09/09/83	77.
09/13/83	77.
09/14/83	77.
09/20/83	76.
09/23/83	76.
09/24/83	76.
09/25/83	75.
09/26/83	75.
09/27/83	75.
09/28/83	75.
09/30/83	74.
10/03/83	73.
10/04/83	72.
10/06/83	71.
10/07/83	71.
10/11/83	71.
10/13/83	71.
10/17/83	70.
10/18/83	69.
10/21/83	69.
10/23/83	68.
10/27/83	67.
11/01/83	66.
11/03/83	66.
11/04/83	66.
11/15/83	63.
11/18/83	63.
11/22/83	61.
11/25/83	60.
11/29/83	58.
12/03/83	56.
12/06/83	56.
12/16/83	53.
12/20/83	53.
12/23/83	52.
12/27/83	52.
12/30/83	51.
01/03/84	50.
01/06/84	50.
01/10/84	50.
01/13/84	49.
01/20/84	48.
01/24/84	47.
01/27/84	47.
01/31/84	46.
02/03/84	47.
02/07/84	47.
02/10/84	47.
02/14/84	47.
02/17/84	47.
02/21/84	47.
02/28/84	48.
03/02/84	48.
03/06/84	48.
03/09/84	49.
03/13/84	49.
03/16/84	50.
03/20/84	51.
03/23/84	52.
03/27/84	53.
03/30/84	53.
04/03/84	53.
04/06/84	54.
04/10/84	54.
04/13/84	55.
04/17/84	56.
04/20/84	58.
04/24/84	58.
04/26/84	59.
04/27/84	58.
05/01/84	58.
05/04/84	60.
05/15/84	62.
05/18/84	63.
05/22/84	64.
05/25/84	65.
05/29/84	67.

Soil Temperature versus Time for the 183.0cm Depth at Soil-moisture Station 1

Date	Temperature (°F)
12/14/82	56.
12/23/82	52.
12/27/82	55.
12/28/82	54.
12/29/82	55.
01/13/83	51.
01/18/83	50.
01/21/83	50.
01/22/83	50.
01/23/83	50.
01/24/83	50.
01/31/83	49.
02/01/83	49.
02/04/83	49.
02/05/83	48.
02/06/83	48.
02/10/83	46.
02/12/83	47.
02/14/83	46.
02/15/83	47.
02/21/83	48.
02/22/83	48.
02/27/83	48.
03/04/83	49.
03/31/83	53.
04/05/83	53.
04/08/83	52.
04/11/83	52.
04/15/83	51.
04/19/83	52.
04/22/83	51.
04/26/83	53.
04/29/83	54.
05/03/83	55.
05/07/83	57.
05/10/83	57.
05/13/83	57.
05/18/83	59.
05/24/83	60.
05/27/83	60.
06/01/83	62.
06/06/83	63.
06/10/83	65.
06/14/83	65.
06/17/83	65.
06/21/83	67.
06/24/83	67.
07/05/83	69.
07/12/83	70.
07/15/83	70.
07/19/83	71.
07/22/83	71.
07/26/83	72.
07/29/83	72.
08/08/83	73.
08/09/83	73.
08/10/83	73.
08/11/83	73.
08/12/83	73.
08/23/83	74.
08/24/83	75.
08/25/83	75.
09/01/83	75.
09/06/83	75.
09/08/83	75.
09/09/83	75.
09/13/83	75.
09/14/83	75.
09/20/83	75.
09/23/83	75.
09/24/83	75.
09/25/83	74.
09/26/83	74.
09/27/83	74.
09/28/83	74.
09/30/83	74.
10/03/83	73.
10/04/83	73.
10/06/83	72.
10/07/83	72.
10/11/83	71.
10/13/83	71.
10/17/83	70.
10/18/83	70.
10/21/83	69.
10/23/83	69.
10/27/83	68.
11/01/83	67.
11/03/83	67.
11/04/83	67.
11/15/83	65.
11/18/83	64.
11/22/83	63.
11/25/83	62.
11/29/83	61.
12/03/83	59.
12/06/83	58.
12/16/83	56.
12/20/83	55.
12/23/83	55.
12/27/83	54.
12/30/83	54.
01/03/84	53.
01/06/84	52.
01/10/84	52.
01/13/84	51.
01/20/84	50.
01/24/84	50.
01/27/84	49.
01/31/84	49.
02/03/84	48.
02/07/84	48.
02/10/84	48.
02/14/84	48.
02/17/84	49.
02/21/84	48.
02/28/84	49.
03/02/84	49.
03/06/84	49.
03/09/84	49.
03/13/84	49.
03/16/84	50.
03/20/84	51.
03/23/84	51.
03/27/84	52.
03/30/84	53.
04/03/84	53.
04/06/84	54.
04/10/84	54.
04/13/84	54.
04/17/84	55.
04/20/84	56.
04/24/84	57.
04/26/84	57.
04/27/84	57.
05/01/84	57.
05/04/84	59.
05/15/84	60.
05/18/84	61.
05/22/84	62.
05/25/84	62.
05/29/84	64.

Soil Temperature versus Time for the 213.5cm Depth at Soil-moisture Station 1

Date	Temperature (°F)
11/03/83	68.
11/04/83	68.
11/15/83	66.
11/18/83	66.
11/22/83	65.
11/25/83	64.
11/29/83	63.
12/03/83	62.
12/06/83	61.
12/16/83	58.
12/20/83	58.
12/23/83	57.
12/27/83	56.
12/30/83	56.
01/03/84	55.
01/06/84	55.
01/10/84	54.
01/13/84	54.
01/20/84	53.
01/24/84	52.
01/27/84	52.
01/31/84	51.
02/03/84	51.
02/07/84	51.
02/10/84	51.
02/14/84	50.
02/17/84	51.
02/21/84	50.
02/28/84	51.
03/02/84	51.
03/06/84	51.
03/09/84	51.
03/13/84	51.
03/16/84	51.
03/20/84	51.
03/23/84	52.
03/27/84	53.
03/30/84	53.
04/03/84	53.
04/06/84	54.
04/10/84	54.
04/13/84	55.
04/17/84	56.
04/20/84	56.
04/24/84	56.
04/26/84	57.
04/27/84	57.
05/01/84	57.
05/04/84	59.
05/15/84	59.
05/18/84	60.
05/22/84	61.
05/25/84	62.
05/29/84	63.

Water Content versus Time for the 30.5cm depth at Soil-moisture Station 1

Date	Water Content	Date	Water Content	Date	Water Content
11/12/82	0.033	06/21/83	0.031	10/18/83	0.063
11/17/82	0.033	06/24/83	0.028	10/21/83	0.059
11/18/82	0.037	06/28/83	0.023	10/23/83	0.063
11/19/82	0.035	07/05/83	0.016	10/27/83	0.059
11/23/82	0.038	07/12/83	0.017	11/01/83	0.058
11/29/82	0.043	07/15/83	0.023	11/04/83	0.052
12/03/82	0.050	07/19/83	0.013	11/18/83	0.063
12/07/82	0.053	07/22/83	0.019	11/25/83	0.057
12/14/82	0.065	07/26/83	0.054	11/29/83	0.060
12/22/82	0.073	07/29/83	0.052	12/03/83	0.059
03/20/83	0.065	08/08/83	0.039	12/06/83	0.065
03/31/83	0.063	08/09/83	0.037	12/14/83	0.058
04/05/83	0.055	08/10/83	0.038	12/16/83	0.063
04/08/83	0.058	08/12/83	0.030	12/20/83	0.060
04/11/83	0.053	08/24/83	0.031	12/23/83	0.064
04/15/83	0.058	08/25/83	0.030	12/27/83	0.062
04/19/83	0.069	09/08/83	0.037	12/30/83	0.067
04/22/83	0.059	09/09/83	0.040	01/03/84	0.059
04/29/83	0.058	09/14/83	0.044	01/06/84	0.076
05/03/83	0.059	09/20/83	0.049	01/10/84	0.069
05/07/83	0.058	09/23/83	0.050	01/13/84	0.069
05/10/83	0.059	09/24/83	0.079	03/09/84	0.071
05/13/83	0.054	09/26/83	0.082	03/13/84	0.066
05/18/83	0.043	09/27/83	0.105	03/23/84	0.062
05/24/83	0.047	09/28/83	0.092	03/27/84	0.064
05/27/83	0.044	10/03/83	0.102	04/03/84	0.066
06/01/83	0.042	10/04/83	0.082	04/06/84	0.062
06/06/83	0.036	10/06/83	0.080	05/01/84	0.048
06/10/83	0.041	10/11/83	0.071	05/04/84	0.045
06/14/83	0.028	10/13/83	0.067	05/15/84	0.040
06/17/83	0.031	10/17/83	0.062	05/22/84	0.037
				05/29/84	0.036

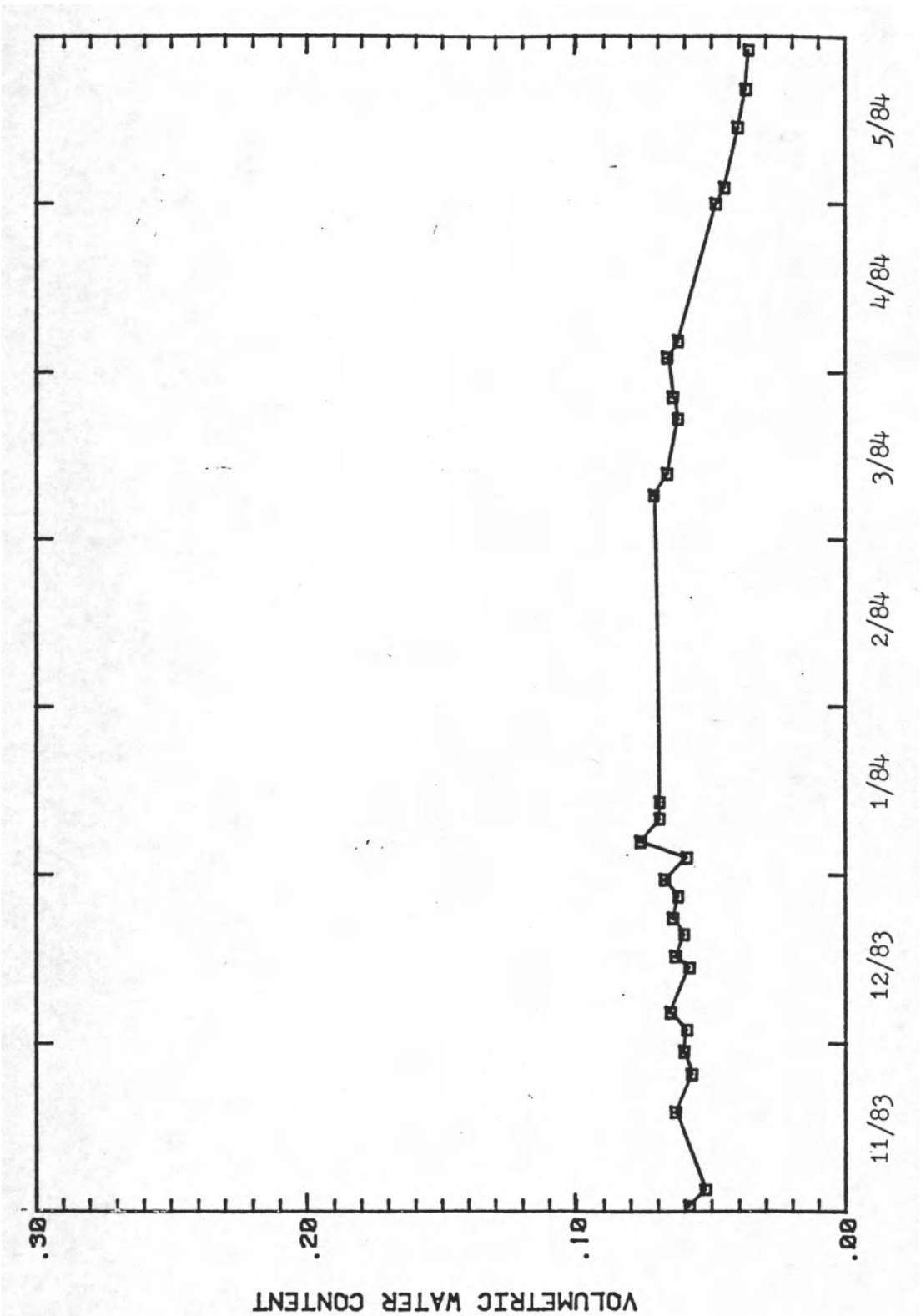

Water Content versus Time for the 30.5 cm depth at Soil-moisture Station 1.

Water Content versus Time for the 61.0cm depth at Soil-moisture Station 1

Date	Water Content
11/12/82	0.069
11/17/82	0.073
11/18/82	0.070
11/19/82	0.067
11/23/82	0.076
11/29/82	0.073
12/03/82	0.070
12/07/82	0.067
12/14/82	0.110
12/22/82	0.104
03/20/83	0.083
03/31/83	0.079
04/05/83	0.073
04/08/83	0.081
04/11/83	0.071
04/15/83	0.074
04/19/83	0.079
04/22/83	0.078
04/29/83	0.067
05/03/83	0.067
05/07/83	0.075
05/10/83	0.073
05/13/83	0.060
05/18/83	0.059
05/24/83	0.059
05/27/83	0.057
06/01/83	0.054
06/06/83	0.052
06/10/83	0.041
06/14/83	0.046
06/17/83	0.040
06/21/83	0.044
06/24/83	0.035
06/28/83	0.038
07/05/83	0.035
07/12/83	0.035
07/15/83	0.034
07/19/83	0.029
07/22/83	0.037
07/26/83	0.033
07/29/83	0.028
08/08/83	0.032
08/09/83	0.035
08/10/83	0.023
08/12/83	0.033
08/24/83	0.033
08/25/83	0.033
09/08/83	0.029
09/09/83	0.033
09/14/83	0.030
09/20/83	0.029
09/23/83	0.036
09/24/83	0.033
09/26/83	0.037
09/27/83	0.040
09/28/83	0.042
10/03/83	0.103
10/04/83	0.118
10/06/83	0.104
10/11/83	0.096
10/13/83	0.093
10/17/83	0.088
10/18/83	0.097
10/21/83	0.099
10/23/83	0.086
10/27/83	0.090
11/01/83	0.081
11/04/83	0.086
11/18/83	0.082
11/25/83	0.066
11/29/83	0.078
12/03/83	0.078
12/06/83	0.084
12/14/83	0.069
12/16/83	0.070
12/20/83	0.071
12/23/83	0.078
12/27/83	0.079
12/30/83	0.079
01/03/84	0.067
01/06/84	0.074
01/10/84	0.075
01/13/84	0.084
03/09/84	0.086
03/13/84	0.086
03/23/84	0.083
03/27/84	0.083
04/03/84	0.086
04/06/84	0.083
05/01/84	0.073
05/04/84	0.071
05/15/84	0.067
05/22/84	0.064
05/29/84	0.060

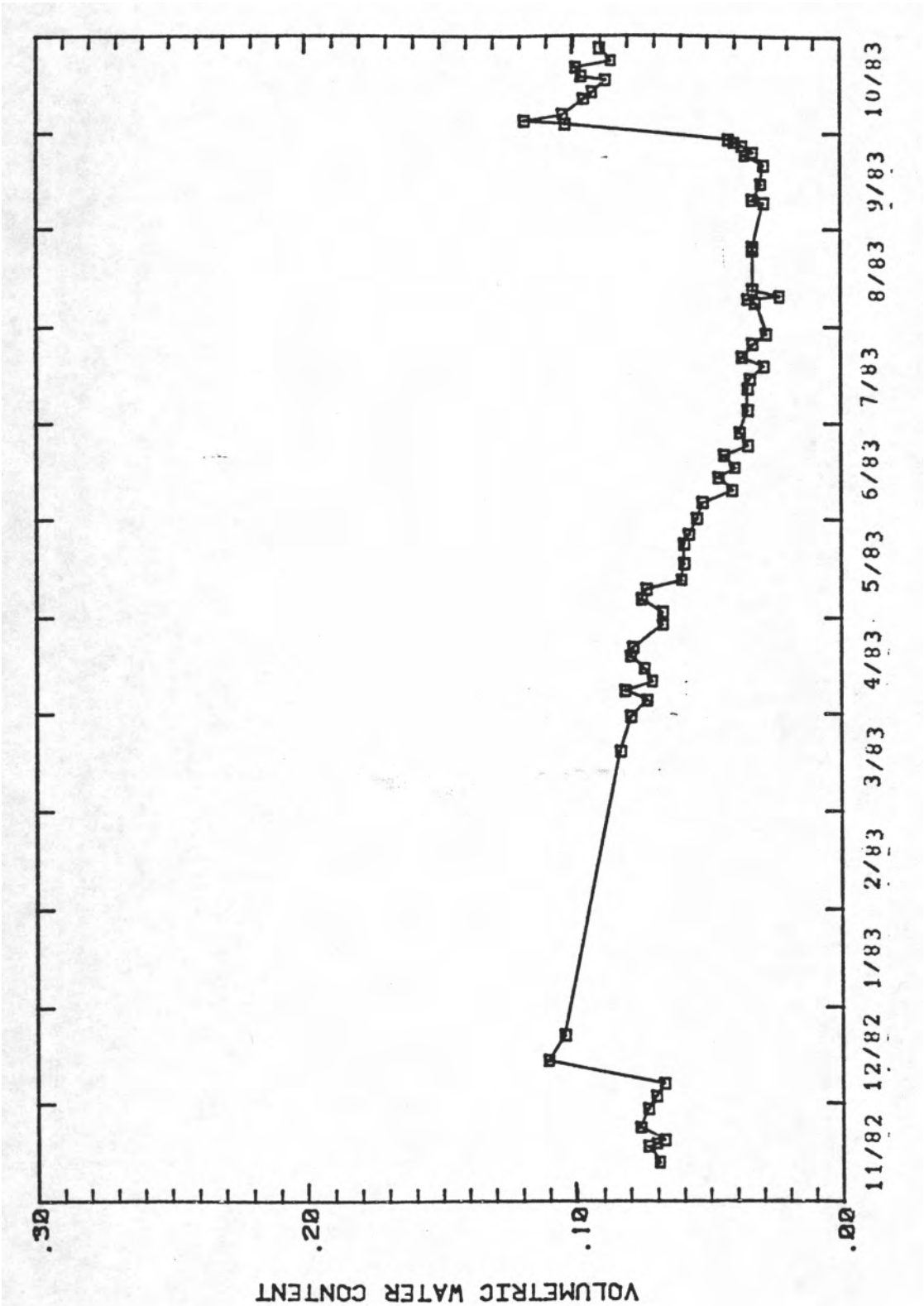

Water Content versus Time for the 61.0cm depth at Soil-moisture Station 1

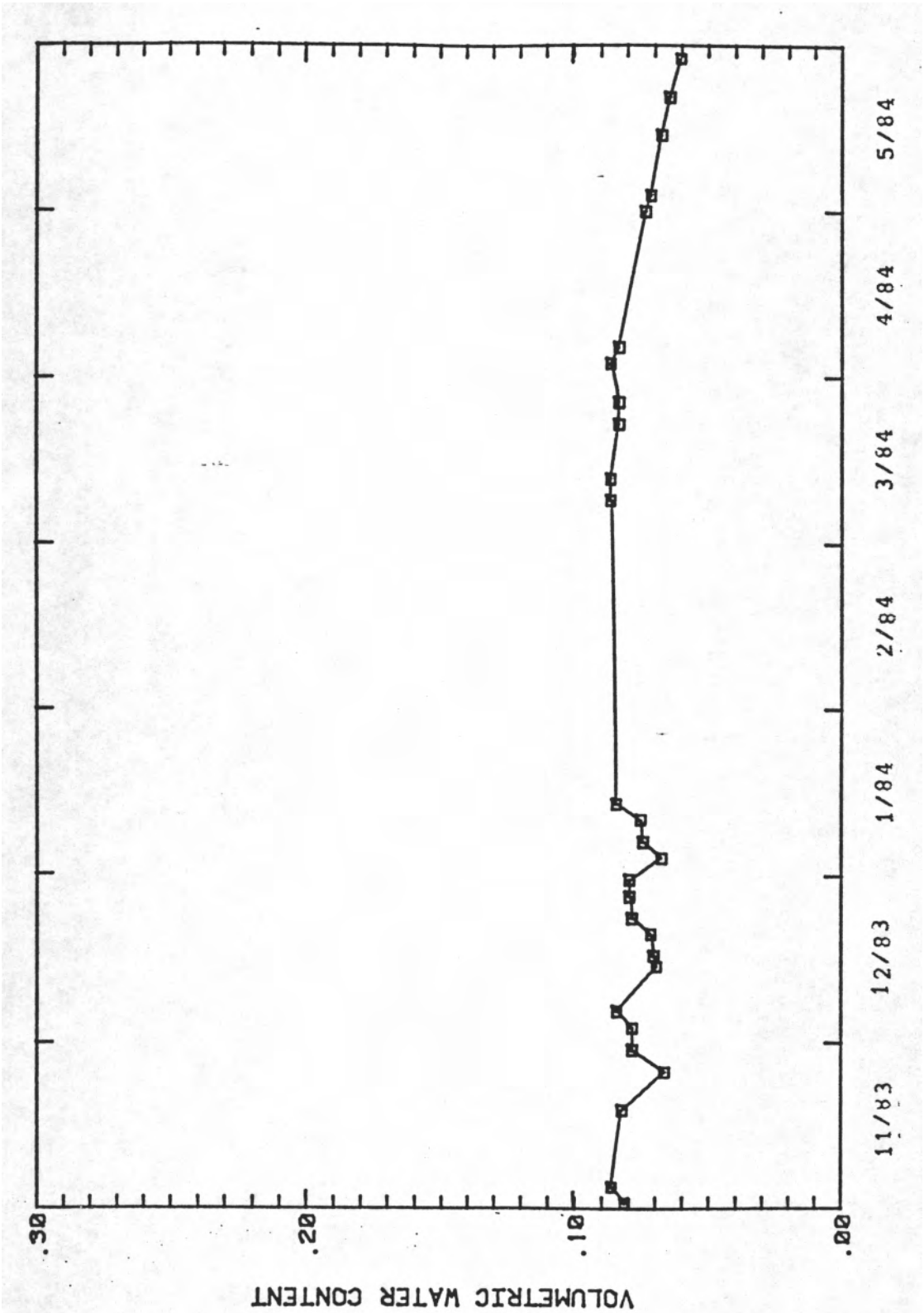

Water Content versus Time for the 61.0cm depth at Soil-moisture Station 1

Water Content versus Time for the 91.5cm depth at Soil-moisture Station 1

Date	Water Content
11/12/82	0.061
11/17/82	0.067
11/18/82	0.065
11/19/82	0.064
11/23/82	0.065
11/29/82	0.062
12/03/82	0.061
12/07/82	0.060
12/14/82	0.071
12/22/82	0.098
03/20/83	0.083
03/31/83	0.076
04/05/83	0.076
04/08/83	0.071
04/11/83	0.068
04/15/83	0.075
04/19/83	0.073
04/22/83	0.068
04/29/83	0.074
05/03/83	0.071
05/07/83	0.064
05/10/83	0.067
05/13/83	0.064
05/18/83	0.061
05/24/83	0.063
05/27/83	0.060
06/01/83	0.060
06/06/83	0.060
06/10/83	0.055
06/14/83	0.056
06/17/83	0.051
06/21/83	0.048
06/24/83	0.051
06/28/83	0.048
07/05/83	0.040
07/12/83	0.041
07/15/83	0.039
07/19/83	0.043
07/22/83	0.032
07/26/83	0.030
07/29/83	0.036
08/08/83	0.032
08/09/83	0.036
08/10/83	0.034
08/12/83	0.038
08/24/83	0.038
08/25/83	0.034
09/08/83	0.041
09/09/83	0.035
09/14/83	0.034
09/20/83	0.036
09/23/83	0.033
09/24/83	0.039
09/26/83	0.033
09/27/83	0.030
09/28/83	0.033
10/03/83	0.033
10/04/83	0.033
10/06/83	0.040
10/11/83	0.058
10/13/83	0.066
10/17/83	0.068
10/18/83	0.074
10/21/83	0.071
10/23/83	0.072
10/27/83	0.077
11/01/83	0.070
11/04/83	0.070
11/18/83	0.069
11/25/83	0.076
11/29/83	0.079
12/03/83	0.071
12/06/83	0.076
12/14/83	0.071
12/16/83	0.080
12/20/83	0.074
12/23/83	0.072
12/27/83	0.066
12/30/83	0.077
01/03/84	0.073
01/06/84	0.074
01/10/84	0.079
01/13/84	0.073
03/09/84	0.084
03/13/84	0.083
03/23/84	0.083
03/27/84	0.082
04/03/84	0.086
04/06/84	0.079
05/01/84	0.074
05/04/84	0.074
05/15/84	0.067
05/22/84	0.066
05/29/84	0.061

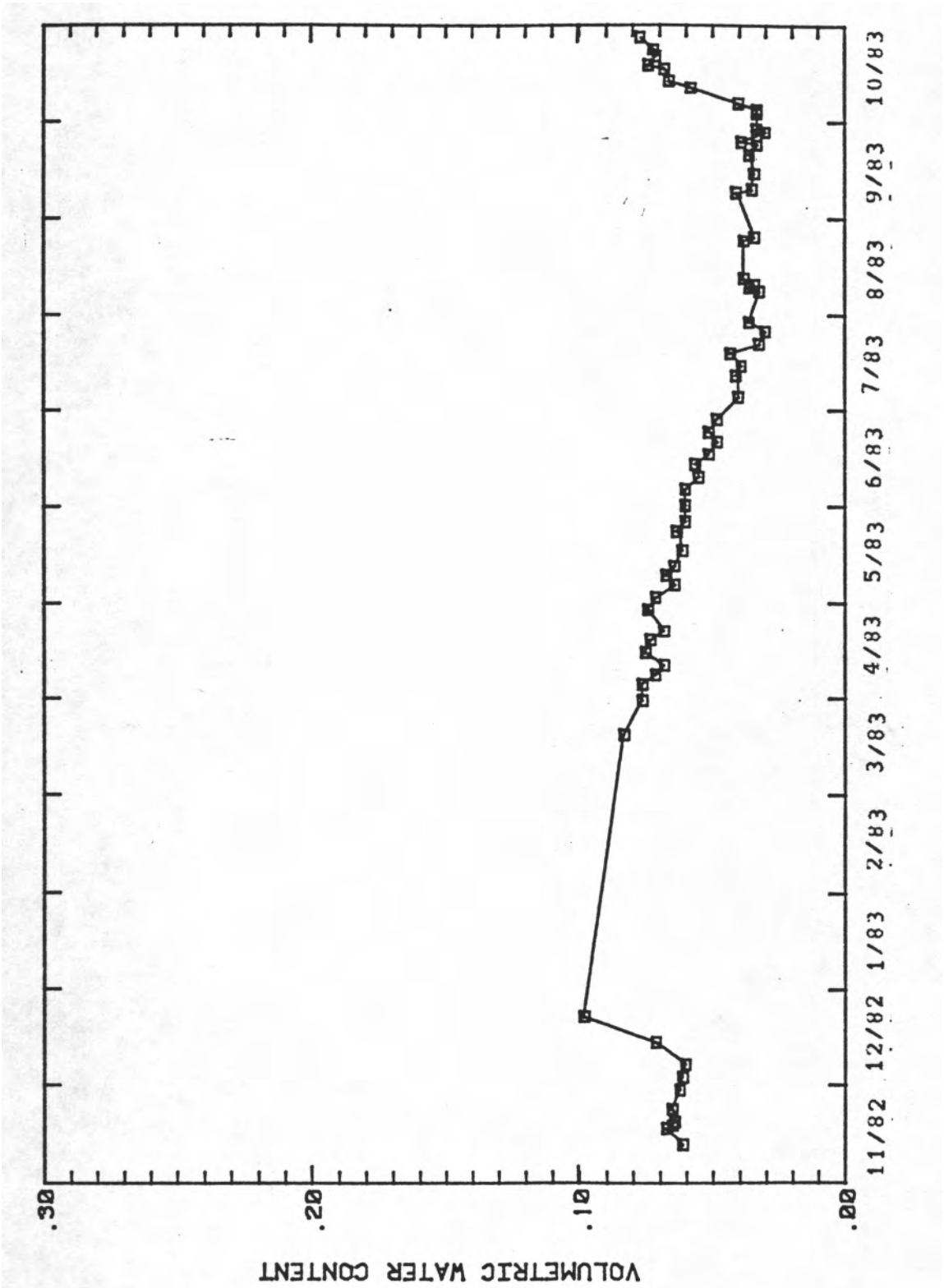

Water Content versus Time for the 91.5cm depth at Soil-moisture Station 1

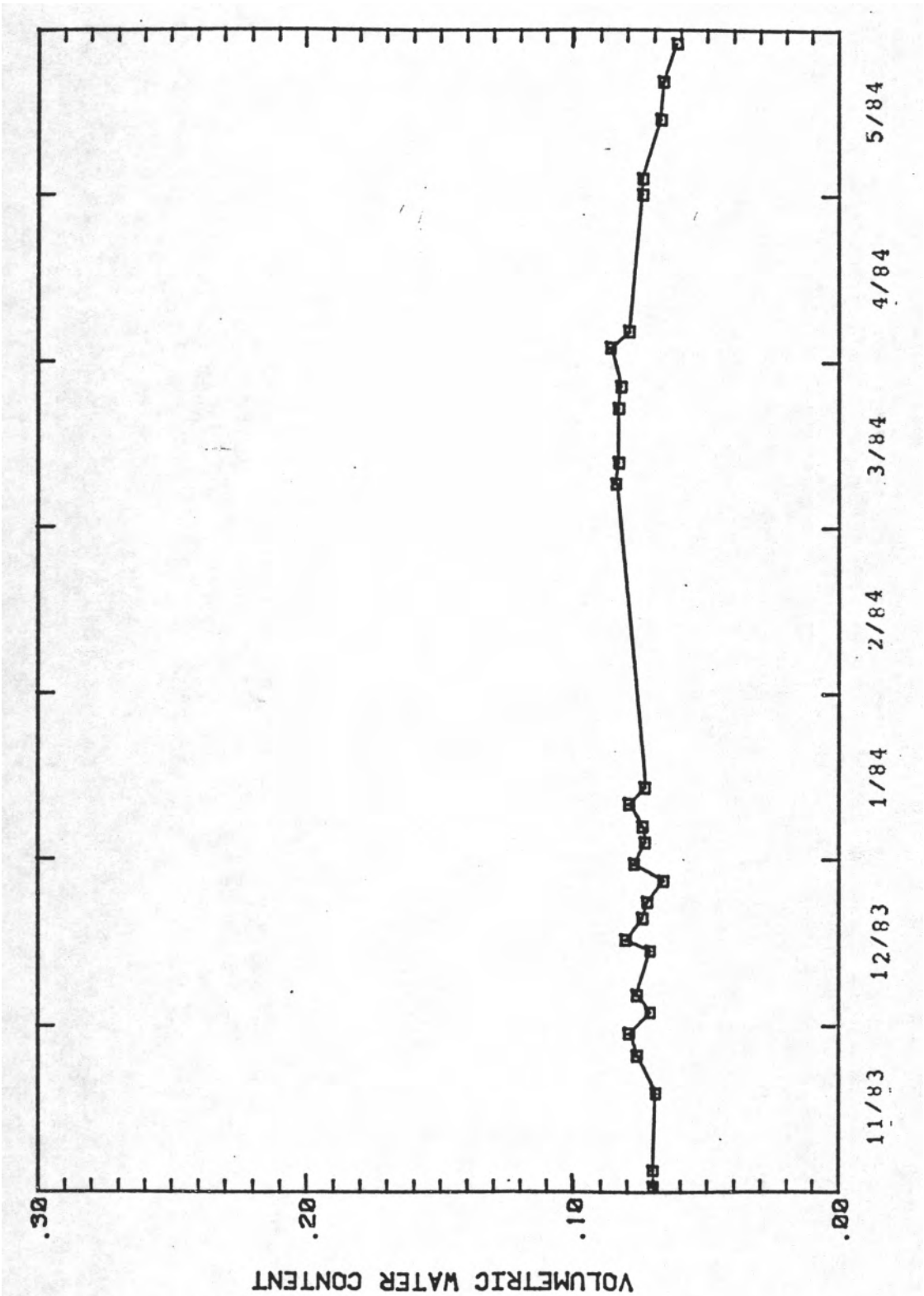

Water Content versus Time for the 91.5cm depth at Soil-moisture Station 1

Water Content versus Time for the 122.0cm depth at Soil-moisture Station 1

Date	Water Content	Date	Water Content	Date	Water Content
11/12/82	0.042	06/28/83	0.064	11/01/83	0.054
11/17/82	0.045	07/05/83	0.059	11/18/83	0.065
11/18/82	0.044	07/12/83	0.052	11/25/83	0.068
11/19/82	0.048	07/15/83	0.059	11/29/83	0.068
11/23/82	0.045	07/19/83	0.050	12/03/83	0.066
11/29/82	0.046	07/22/83	0.050	12/06/83	0.069
12/03/82	0.042	07/26/83	0.044	12/14/83	0.073
12/07/82	0.045	07/29/83	0.052	12/16/83	0.068
12/14/82	0.046	08/08/83	0.048	12/20/83	0.066
12/22/82	0.051	08/09/83	0.042	12/23/83	0.067
03/20/83	0.097	08/10/83	0.040	12/27/83	0.067
03/31/83	0.082	08/12/83	0.054	12/30/83	0.072
04/05/83	0.088	08/24/83	0.050	01/03/84	0.060
04/08/83	0.083	08/25/83	0.055	01/06/84	0.066
04/11/83	0.080	09/08/83	0.048	01/10/84	0.073
04/15/83	0.076	09/09/83	0.043	01/13/84	0.063
04/19/83	0.072	09/14/83	0.047	03/09/84	0.065
04/22/83	0.078	09/20/83	0.048	03/13/84	0.086
04/29/83	0.084	09/23/83	0.050	03/23/84	0.086
05/03/83	0.085	09/24/83	0.051	03/27/84	0.087
05/07/83	0.085	09/26/83	0.051	04/03/84	0.089
05/10/83	0.087	09/27/83	0.041	04/06/84	0.088
05/13/83	0.085	09/28/83	0.048	05/01/84	0.082
05/18/83	0.086	10/03/83	0.046	05/04/84	0.082
05/24/83	0.076	10/04/83	0.049	05/15/84	0.076
05/27/83	0.077	10/06/83	0.048	05/22/84	0.077
06/01/83	0.070	10/11/83	0.044	05/29/84	0.071
06/06/83	0.075	10/13/83	0.044		
06/10/83	0.068	10/17/83	0.049		
06/14/83	0.070	10/18/83	0.055		
06/17/83	0.073	10/21/83	0.056		
06/21/83	0.066	10/23/83	0.050		
06/24/83	0.071	10/27/83	0.049		

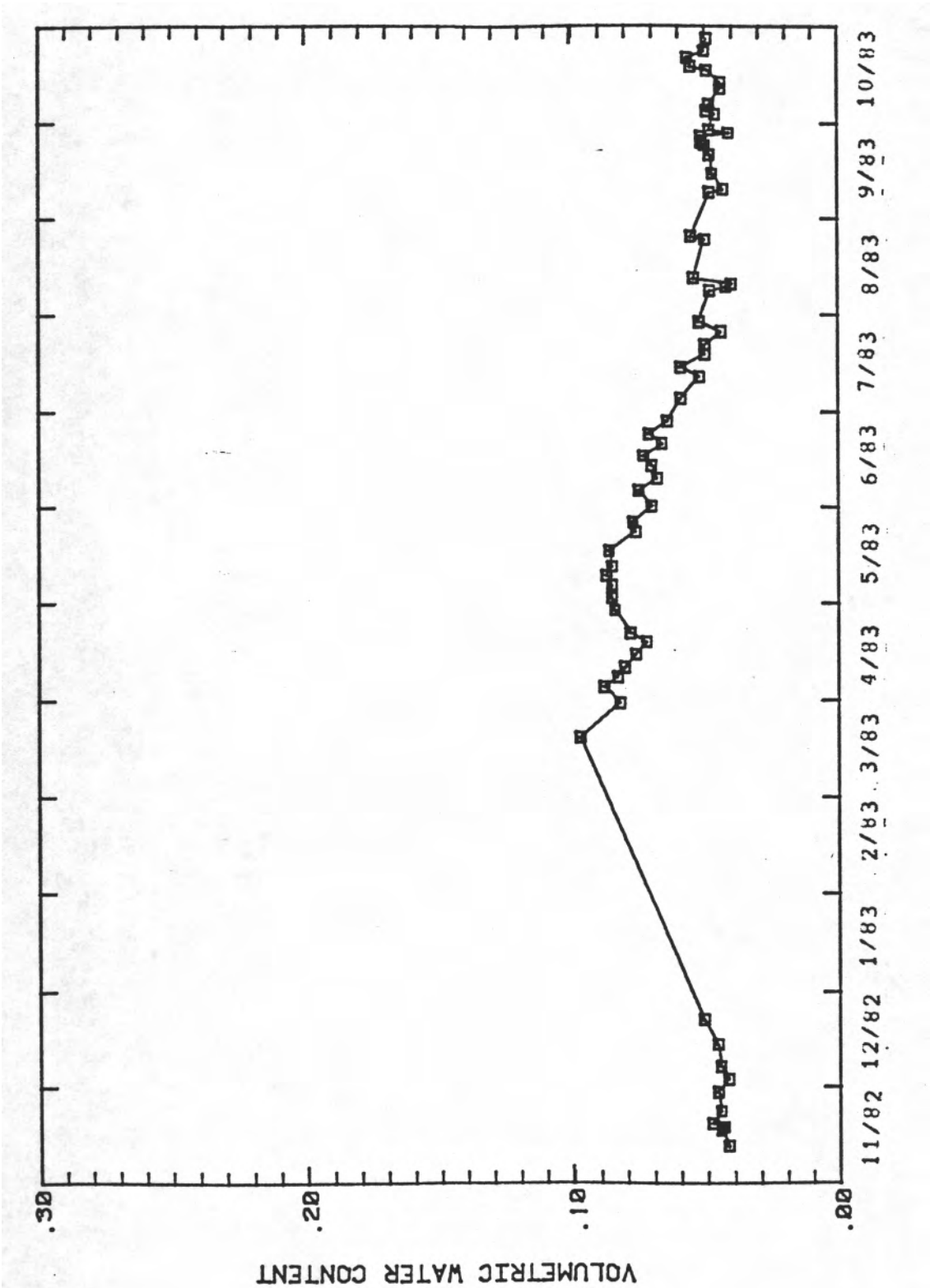

Water Content versus Time for the 122.0cm depth at Soil-Moisture Station 1

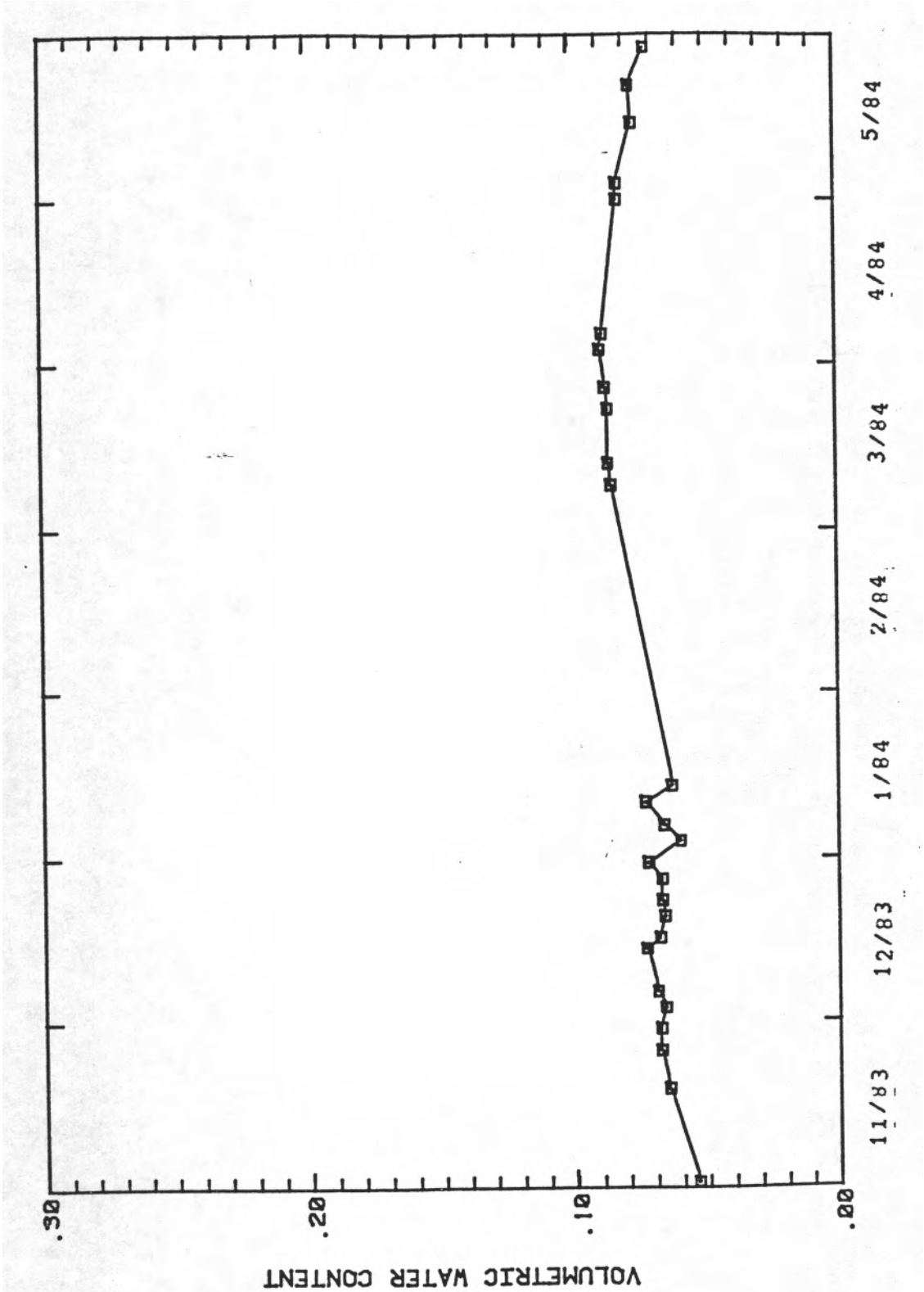

Water Content versus Time for the 122.0cm depth at Soil-moisture Station 1

Water Content versus Time for the 152.5cm deptn at Soil-moisture Station 1

Date	Water Content	Date	Water Content	Date	Water Content
11/12/82	0.020	06/28/83	0.054	11/01/83	0.050
11/17/82	0.023	07/05/83	0.054	11/18/83	0.058
11/18/82	0.022	07/12/83	0.052	11/25/83	0.053
11/19/82	0.021	07/15/83	0.050	11/29/83	0.055
11/23/82	0.019	07/19/83	0.048	12/03/83	0.049
11/29/82	0.019	07/22/83	0.046	12/06/83	0.049
12/03/82	0.025	07/26/83	0.048	12/14/83	0.058
12/07/82	0.023	07/29/83	0.045	12/16/83	0.057
12/14/82	0.019	08/08/83	0.046	12/20/83	0.053
12/22/82	0.024	08/09/83	0.045	12/23/83	0.044
03/20/83	0.096	08/10/83	0.046	12/27/83	0.050
03/31/83	0.080	08/12/83	0.035	12/30/83	0.054
04/05/83	0.081	08/24/83	0.042	01/03/84	0.058
04/08/83	0.081	08/25/83	0.043	01/06/84	0.059
04/11/83	0.086	09/08/83	0.056	01/10/84	0.059
04/15/83	0.076	09/09/83	0.059	01/13/84	0.056
04/19/83	0.076	09/14/33	0.056	03/09/84	0.069
04/22/83	0.067	09/20/83	0.060	03/13/84	0.068
04/29/83	0.070	09/23/83	0.055	03/23/84	0.069
05/03/83	0.071	09/24/83	0.057	03/27/84	0.072
05/07/83	0.075	09/26/83	0.051	04/03/84	0.073
05/10/83	0.076	09/27/83	0.059	04/06/84	0.072
05/13/83	0.069	09/28/83	0.046	05/01/84	0.062
05/18/83	0.068	10/03/83	0.058	05/04/84	0.072
05/24/83	0.066	10/04/83	0.054	05/15/84	0.058
05/27/83	0.067	10/06/83	0.055	05/22/84	0.060
06/01/83	0.067	10/11/83	0.051	05/29/84	0.057
06/06/83	0.066	10/13/83	0.058		
06/10/83	0.062	10/17/83	0.056		
06/14/83	0.065	10/18/83	0.056		
06/17/83	0.054	10/21/83	0.051		
06/21/83	0.059	10/23/83	0.058		
06/24/83	0.059	10/27/83	0.058		

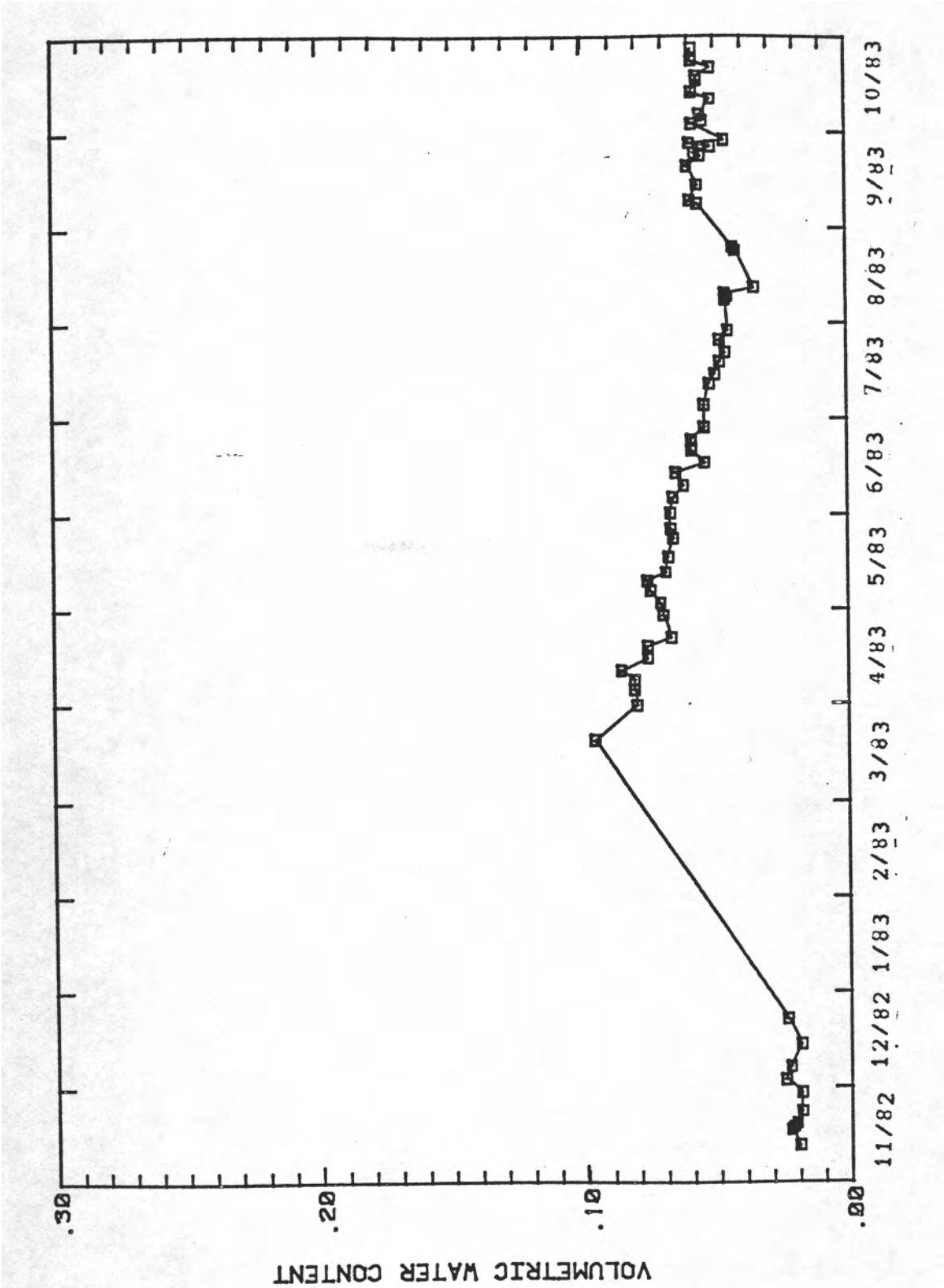

Water Content versus Time for the 152.5cm depth at Soil-moisture Station 1

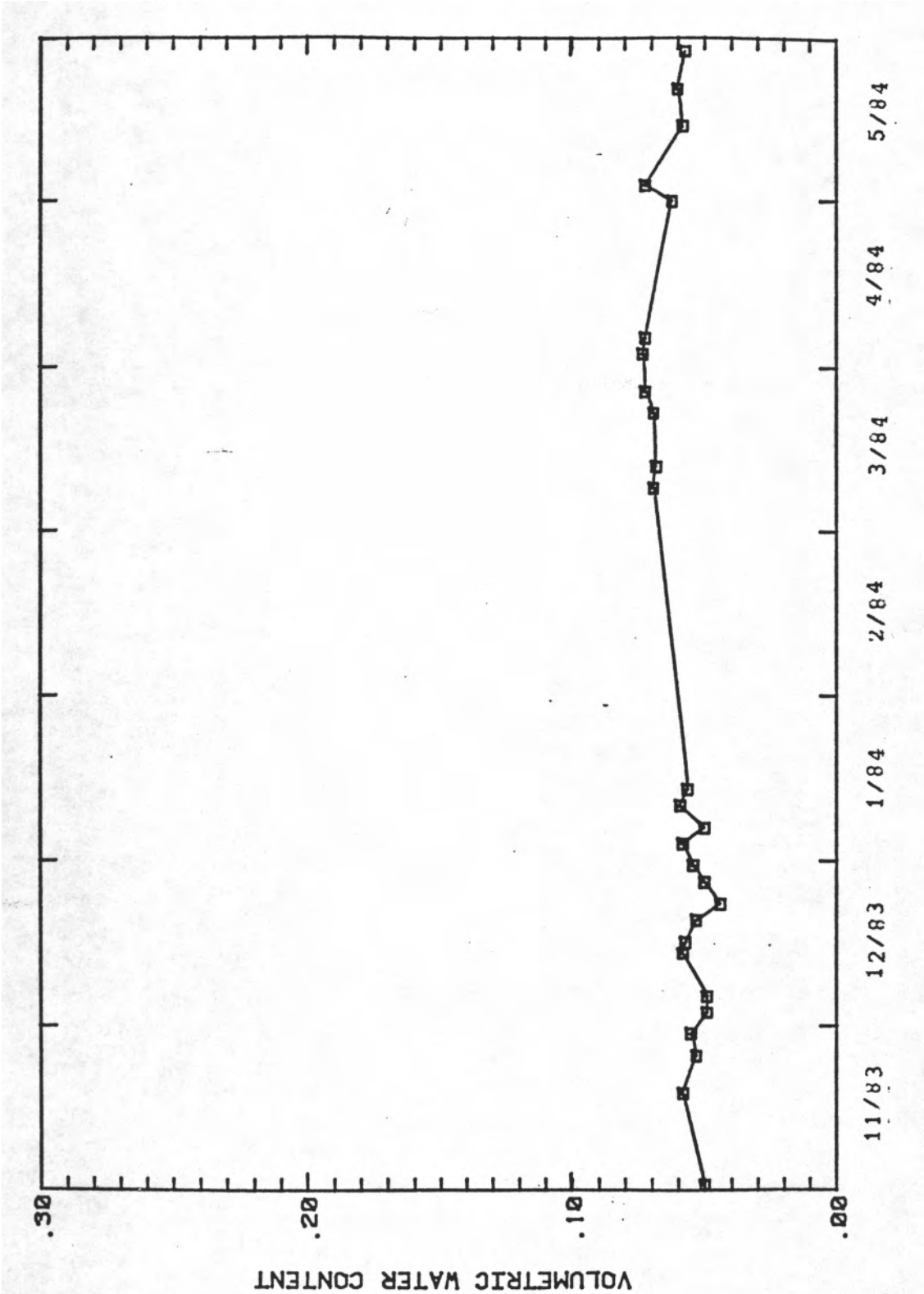

Water Content versus Time for the 152.5cm depth at Soil-moisture Station 1

Water Content versus Time for the 183.0cm depth at Soil-moisture Station 1

Date	Water Content
11/12/82	0.022
11/17/82	0.025
11/18/82	0.023
11/19/82	0.021
11/23/82	0.020
11/29/82	0.024
12/03/82	0.022
12/07/82	0.021
12/14/82	0.023
12/22/82	0.024
03/20/83	0.107
03/31/83	0.101
04/05/83	0.100
04/08/83	0.098
04/11/83	0.104
04/15/83	0.098
04/19/83	0.095
04/22/83	0.097
04/29/83	0.087
05/03/83	0.099
05/07/83	0.095
05/10/83	0.090
05/13/83	0.085
05/18/83	0.089
05/24/83	0.095
05/27/83	0.086
06/01/83	0.084
06/06/83	0.080
06/10/83	0.082
06/14/83	0.076
06/17/83	0.078
06/21/83	0.076
06/24/83	0.079
06/28/83	0.076
07/05/83	0.054
07/12/83	0.062
07/15/83	0.064
07/19/83	0.050
07/22/83	0.053
07/26/83	0.055
07/29/83	0.050
08/08/83	0.050
08/09/83	0.047
08/10/83	0.052
08/12/83	0.047
08/24/83	0.049
08/25/83	0.057
09/08/83	0.057
09/09/83	0.062
09/14/83	0.055
09/20/83	0.068
09/23/83	0.058
09/24/83	0.063
09/26/83	0.061
09/27/83	0.061
09/28/83	0.050
10/03/83	0.053
10/04/83	0.057
10/06/83	0.060
10/11/83	0.059
10/13/83	0.055
10/17/83	0.061
10/18/83	0.056
10/21/83	0.051
10/23/83	0.058
10/27/83	0.059
11/01/83	0.059
11/18/83	0.062
11/25/83	0.057
11/29/83	0.057
12/03/83	0.051
12/06/83	0.060
12/14/83	0.050
12/16/83	0.059
12/20/83	0.056
12/23/83	0.059
12/27/83	0.054
12/30/83	0.058
01/03/84	0.049
01/06/84	0.051
01/10/84	0.052
01/13/84	0.057
03/09/84	0.065
03/13/84	0.063
03/23/84	0.062
03/27/84	0.065
04/03/84	0.066
04/06/84	0.064
05/01/84	0.054
05/04/84	0.054
05/15/84	0.053
05/22/84	0.055
05/29/84	0.053

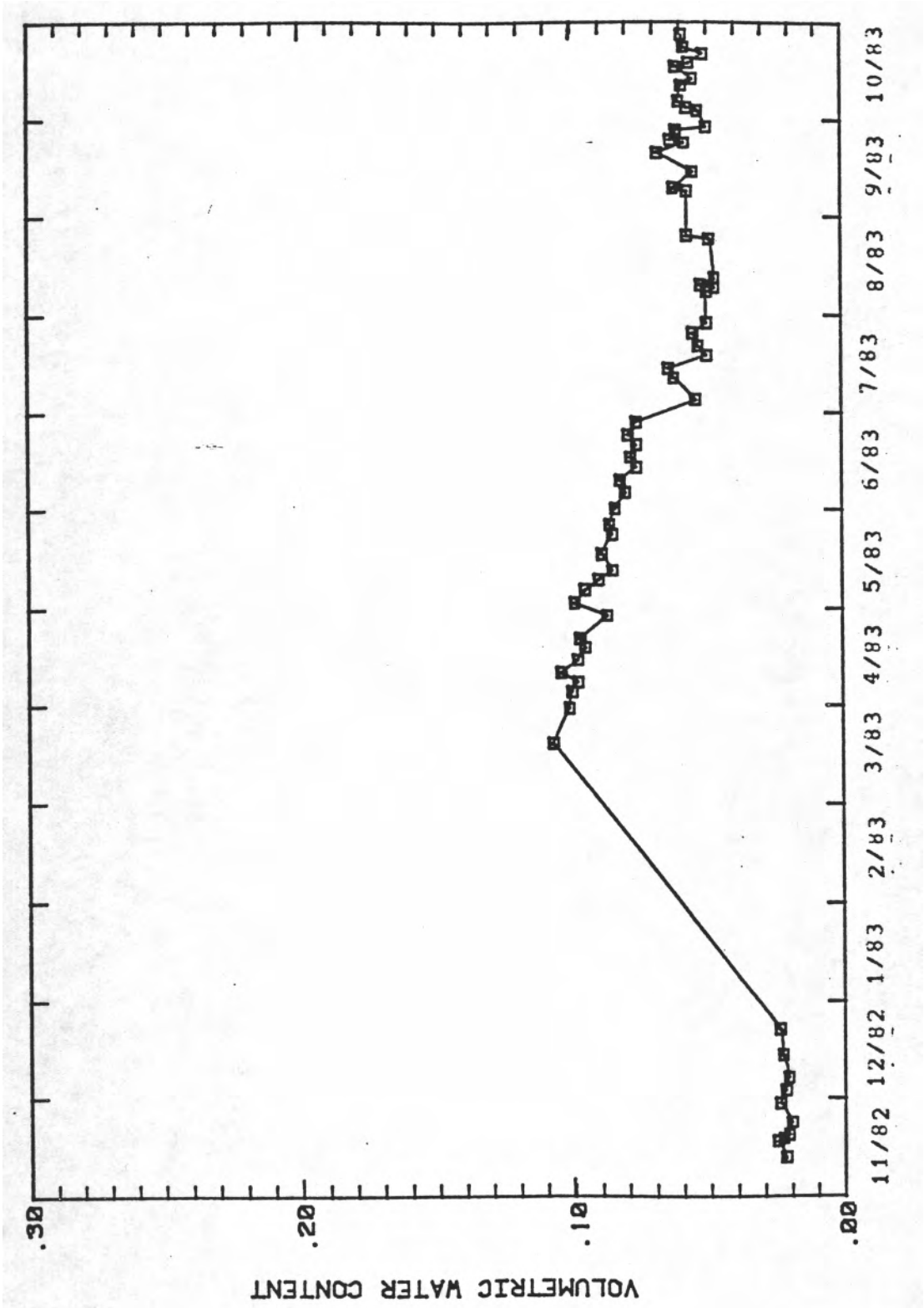

Water Content versus Time for the 183.0cm depth at Soil-moisture Station 1

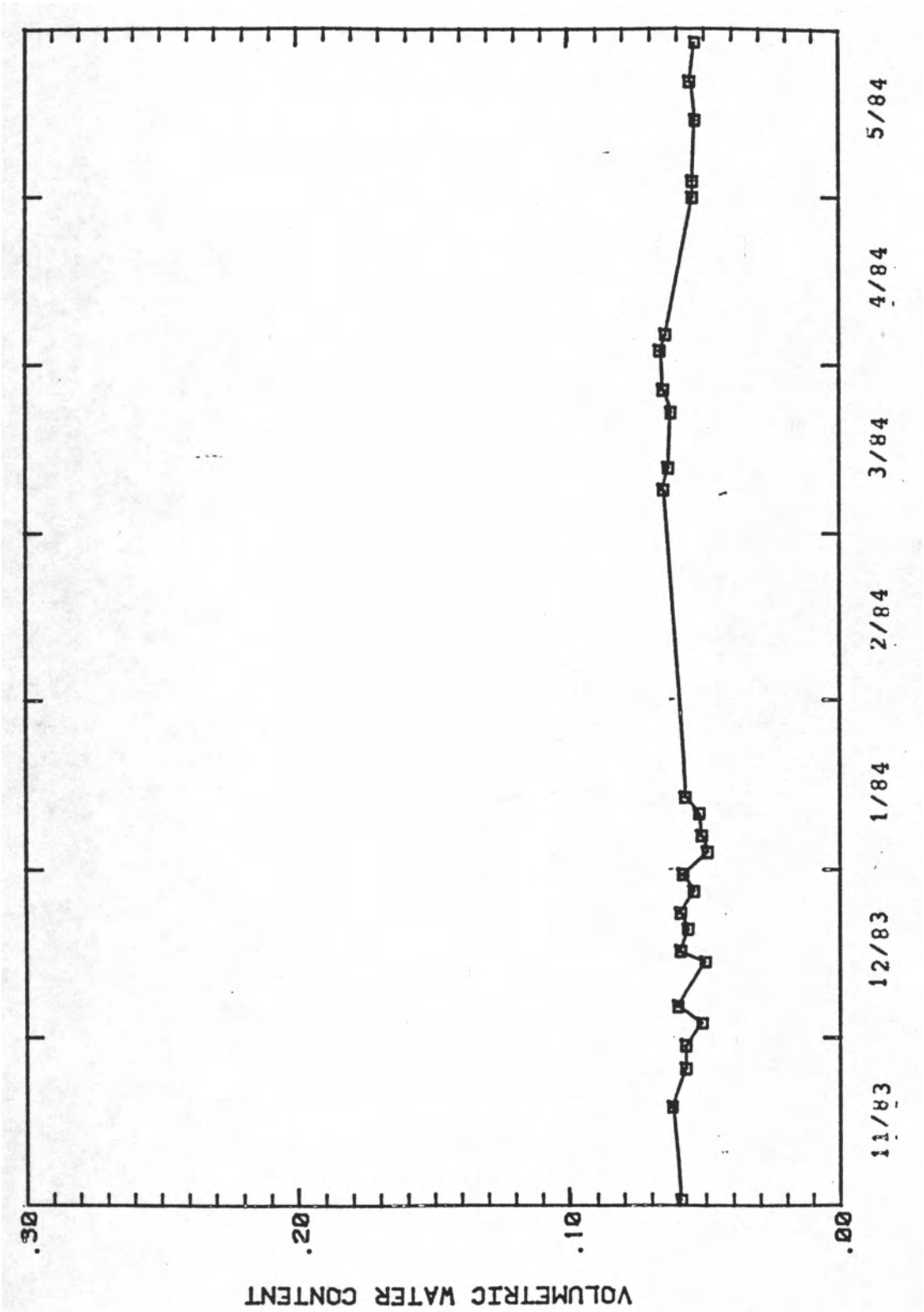

Water Content versus Time for the 183.0cm deptn at Soil-moisture Station 1

Water Content versus Time for the 213.5cm depth at Soil-moisture Station 1

Date	Water Content	Date	Water Content
09/08/83	0.039		
09/09/83	0.044		
09/14/83	0.046		
09/20/83	0.045		
09/23/83	0.041		
09/24/83	0.040		
09/26/83	0.042		
09/27/83	0.043		
09/28/83	0.046		
10/03/83	0.039		
10/04/83	0.044		
10/06/83	0.042		
10/11/83	0.046		
10/13/83	0.048		
10/17/83	0.036		
10/18/83	0.048		
10/21/83	0.045		
10/23/83	0.042		
10/27/83	0.042		

Water Content versus Time for the 213.5cm depth at Soil-moisture Station 1

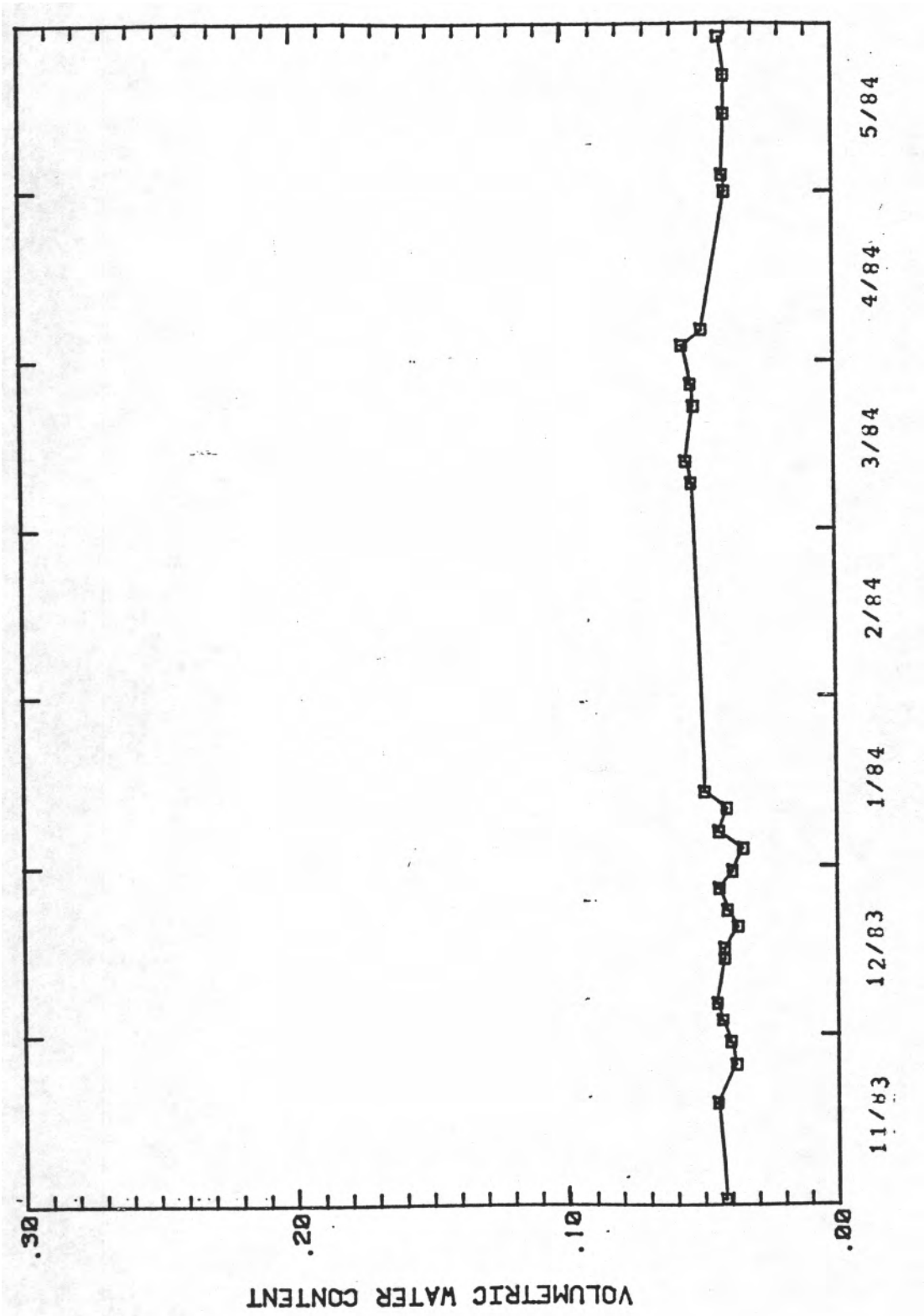

Water Content versus Time for the 213.5cm depth at Soil-moisture Station 1

Water Content versus Time for the 244.0cm depth at Soil-moisture Station 1

Date	Water Content
09/08/83	0.073
09/09/83	0.076
09/14/83	0.072
09/20/83	0.070
09/23/83	0.074
09/24/83	0.067
09/26/83	0.071
09/27/83	0.072
09/28/83	0.076
10/03/83	0.066
10/04/83	0.067
10/06/83	0.073
10/11/83	0.070
10/13/83	0.069
10/17/83	0.068
10/18/83	0.069
10/21/83	0.067
10/23/83	0.063
10/27/83	0.070
11/01/83	0.061
11/18/83	0.073
11/25/83	0.068
11/29/83	0.071
12/03/83	0.067
12/06/83	0.072
12/14/83	0.068
12/16/83	0.073
12/20/83	0.065
12/23/83	0.068
12/27/83	0.069
12/30/83	0.065
01/03/84	0.066
01/06/84	0.078
01/10/84	0.074
01/13/84	0.071
03/09/84	0.077
03/13/84	0.078
03/23/84	0.076
03/27/84	0.077
04/03/84	0.075
04/06/84	0.078
05/01/84	0.068
05/04/84	0.067
05/15/84	0.067
05/22/84	0.066
05/29/84	0.064

Water Content versus Time for the 244.0cm depth at Soil-moisture Station 1

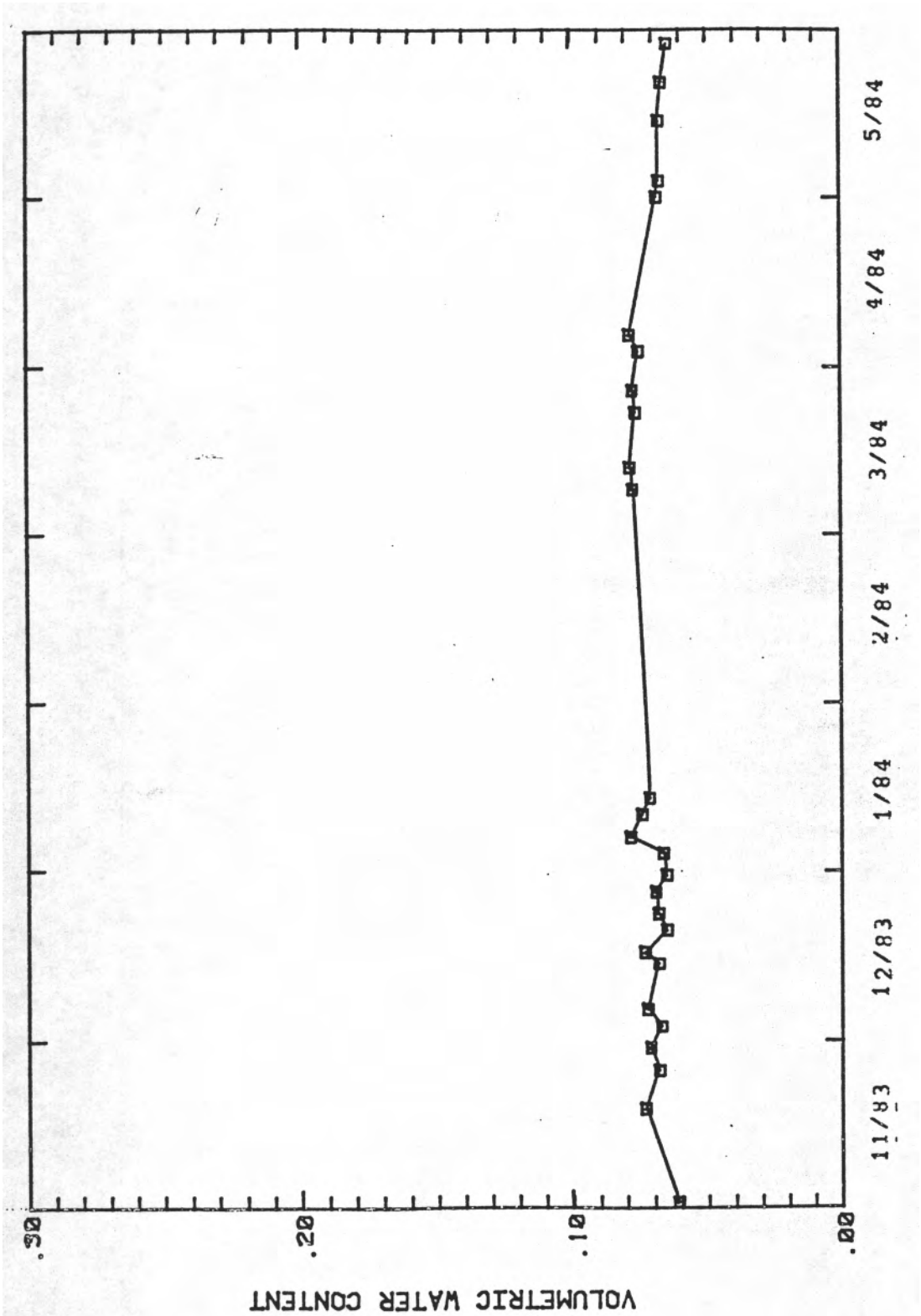

Water Content versus Time for the 244.0cm deptn at Soil-moisture Station 1

Water Content versus Time for the 274.5cm depth at Soil-moisture Station 1

Date	Water Content
09/08/83	0.077
09/09/83	0.077
09/14/83	0.079
09/20/83	0.066
09/23/83	0.067
09/24/83	0.076
09/26/83	0.074
09/27/83	0.080
09/28/83	0.076
10/03/83	0.073
10/04/83	0.071
10/06/83	0.076
10/11/83	0.078
10/13/83	0.071
10/17/83	0.065
10/18/83	0.076
10/21/83	0.071
10/23/83	0.070
10/27/83	0.082
11/01/83	0.067
11/04/83	0.067
11/18/83	0.077
11/25/83	0.072
11/29/83	0.076
12/03/83	0.071
12/06/83	0.068
12/14/83	0.066
12/16/83	0.070
12/20/83	0.068
12/23/83	0.070
12/27/83	0.072
12/30/83	0.068
01/03/84	0.059
01/06/84	0.069
01/10/84	0.076
01/13/84	0.078
03/09/84	0.080
03/13/84	0.077
03/23/84	0.075
03/27/84	0.076
04/03/84	0.077
04/06/84	0.077
05/01/84	0.066
05/04/84	0.066
05/15/84	0.065
05/22/84	0.064
05/29/84	0.063

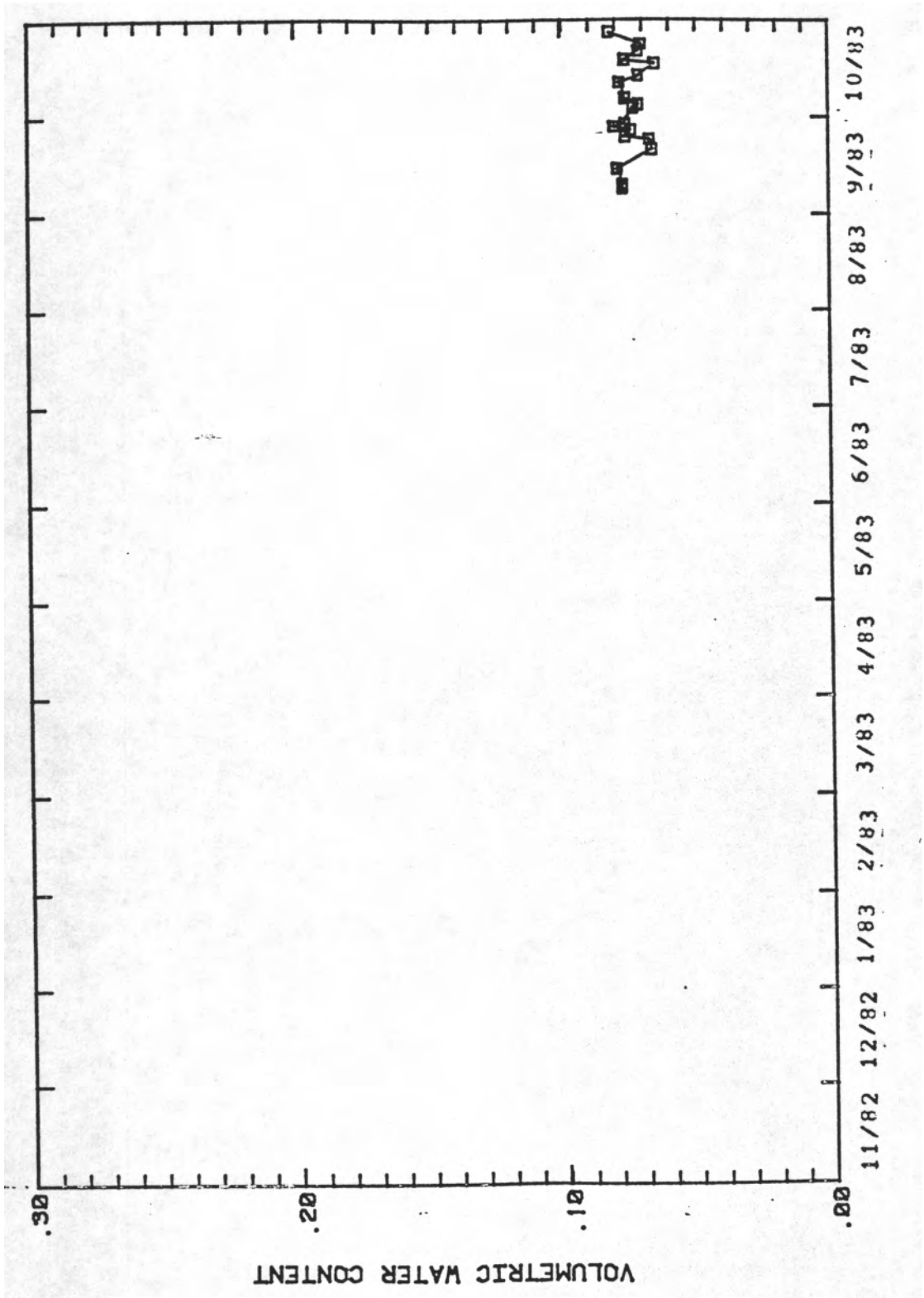

Water Content versus Time for the 274.5cm depth at Soil-moisture Station 1

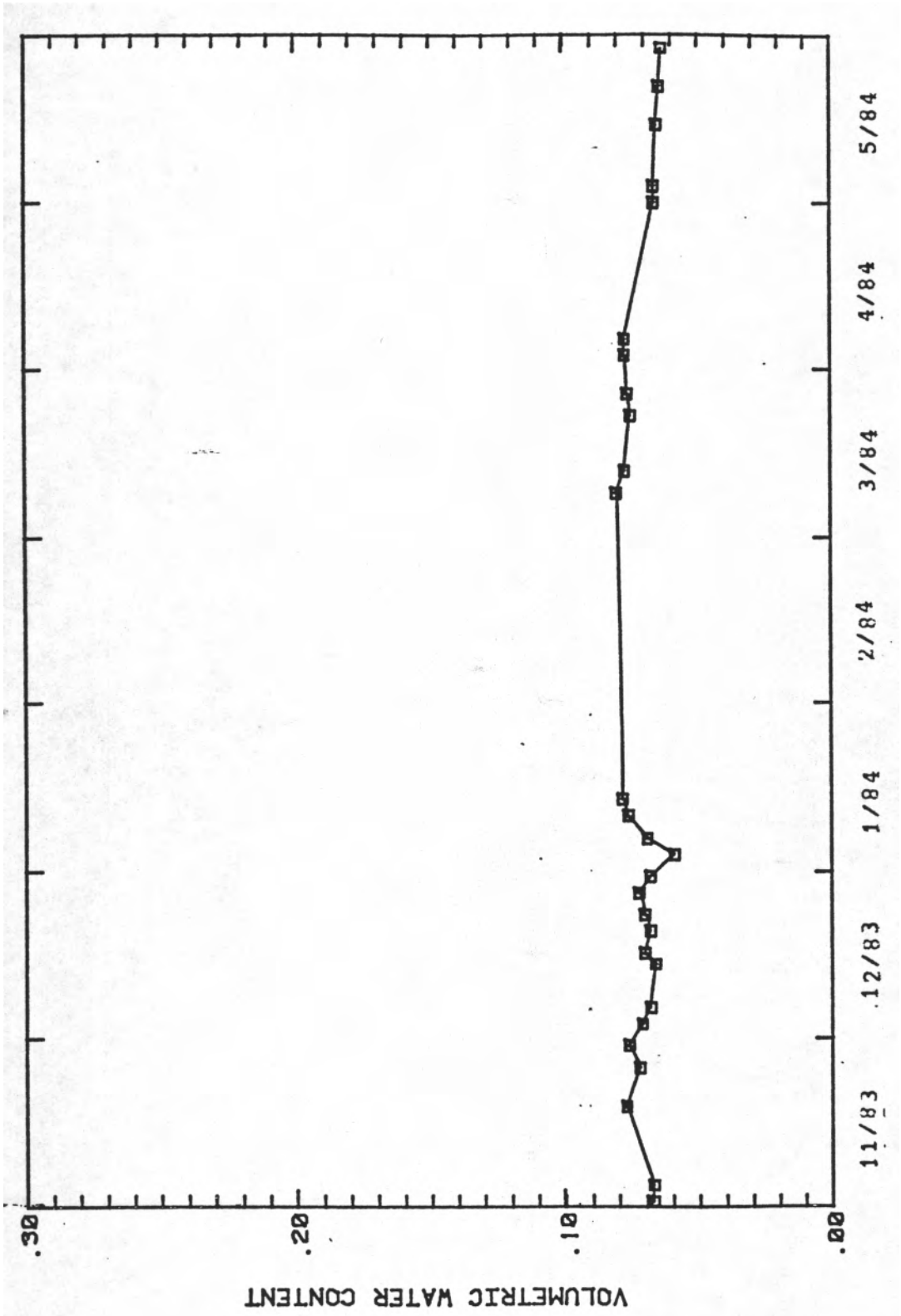

Water Content versus Time for the 274.5cm depth at Soil-moisture Station 1

Water Content versus Time for the 305.0cm depth at Soil-moisture Station 1

Date	Water Content
09/08/83	0.043
09/09/83	0.044
09/14/83	0.043
09/20/83	0.045
09/23/83	0.038
09/24/83	0.040
09/26/83	0.038
09/27/83	0.040
09/28/83	0.043
10/03/83	0.042
10/04/83	0.053
10/06/83	0.040
10/11/83	0.048
10/13/83	0.042
10/17/83	0.038
10/18/83	0.042
10/21/83	0.042
10/23/83	0.042
10/27/83	0.033
11/01/83	0.040
11/04/83	0.035
11/16/83	0.040
11/25/83	0.040
11/29/83	0.035
12/03/83	0.041
12/06/83	0.040
12/14/83	0.038
12/16/83	0.038
12/20/83	0.046
12/23/83	0.039
12/27/83	0.037
12/30/83	0.032
01/03/84	0.033
01/06/84	0.042
01/10/84	0.037
01/13/84	0.042
03/09/84	0.055
03/13/84	0.055
03/23/84	0.056
03/27/84	0.056
04/03/84	0.054
04/06/84	0.057
05/01/84	0.040
05/04/84	0.040
05/15/84	0.039
05/22/84	0.040
05/29/84	0.039

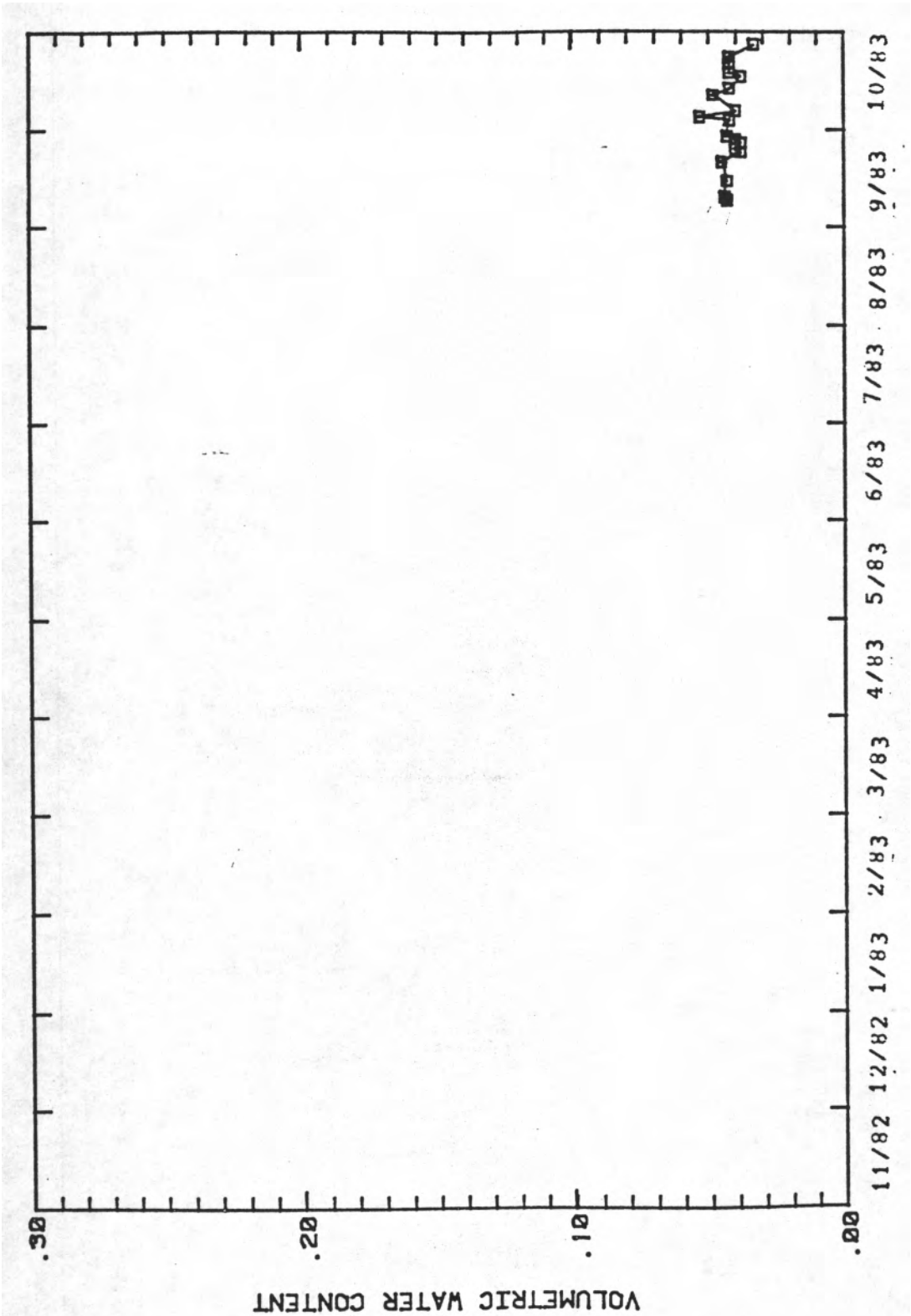

Water Content versus Time for the 305.0cm depth at Soil-moisture Station 1

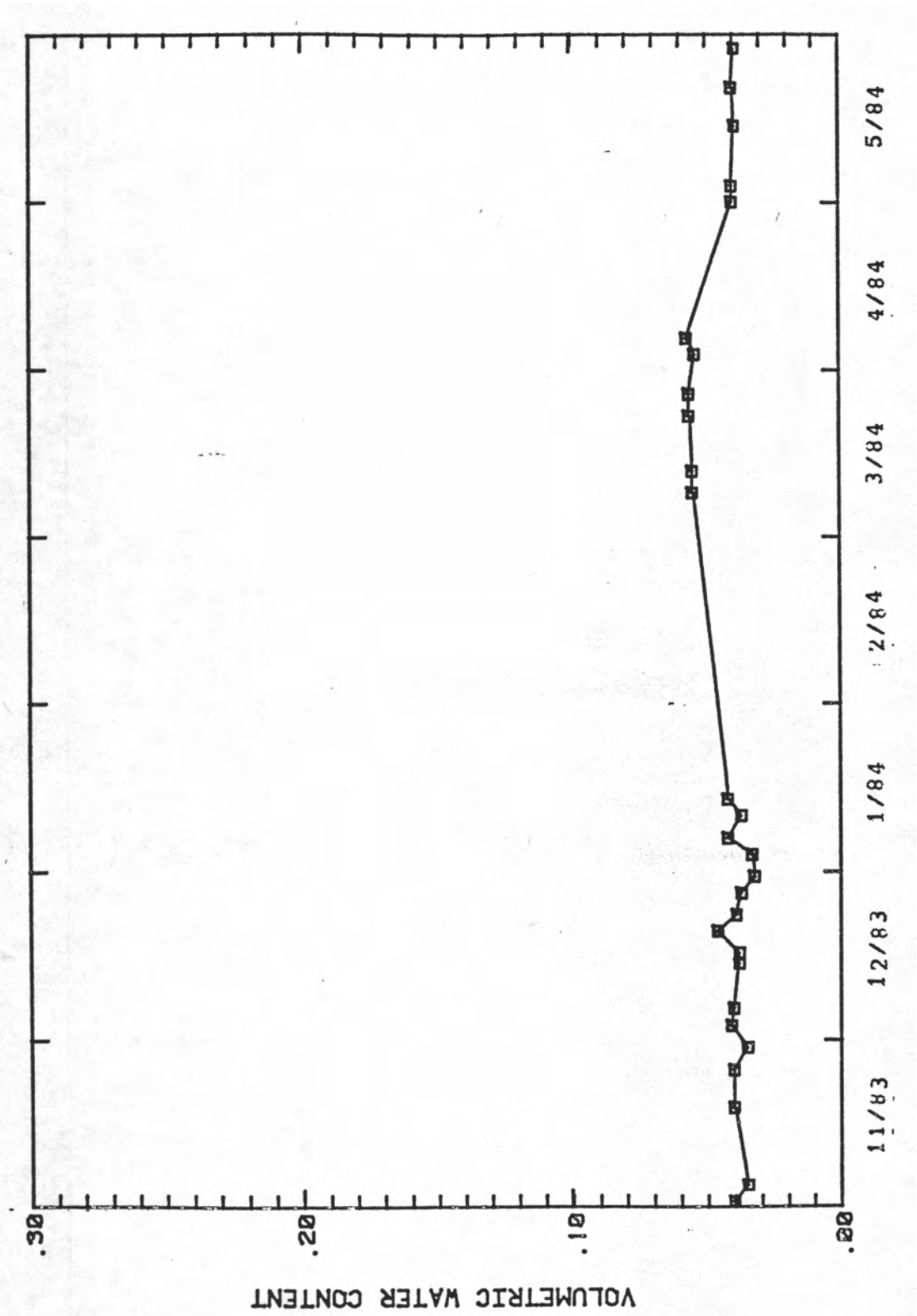

Water Content versus Time for the 305.0cm depth at Soil-moisture Station 1

Water Content versus Time for the 335.5cm deptn at Soil-moisture Station 1

Date	Water Content
09/08/83	0.033
09/09/83	0.034
09/14/83	0.029
09/20/83	0.034
09/23/83	0.034
09/24/83	0.036
09/25/83	0.034
09/26/83	0.033
09/27/83	0.033
09/28/83	0.035
10/03/83	0.032
10/04/83	0.033
10/06/83	0.030
10/11/83	0.032
10/13/83	0.035
10/17/83	0.031
10/18/83	0.035
10/21/83	0.037
10/23/83	0.042
10/27/83	0.036
11/01/83	0.033
11/04/83	0.074
11/18/83	0.038
11/25/83	0.036
11/29/83	0.038

Date	Water Content
12/03/83	0.031
12/06/83	0.028
12/14/83	0.033
12/16/83	0.033
12/20/83	0.038
12/23/83	0.028
12/27/83	0.032
12/30/83	0.033
01/03/84	0.032
01/06/84	0.033
01/10/84	0.038
01/13/84	0.034
03/09/84	0.049
03/13/84	0.047
03/23/84	0.046
03/27/84	0.048
04/03/84	0.047
04/06/84	0.047
04/10/84	0.049
05/01/84	0.036
05/04/84	0.034
05/15/84	0.036
05/22/84	0.037
05/29/84	0.035

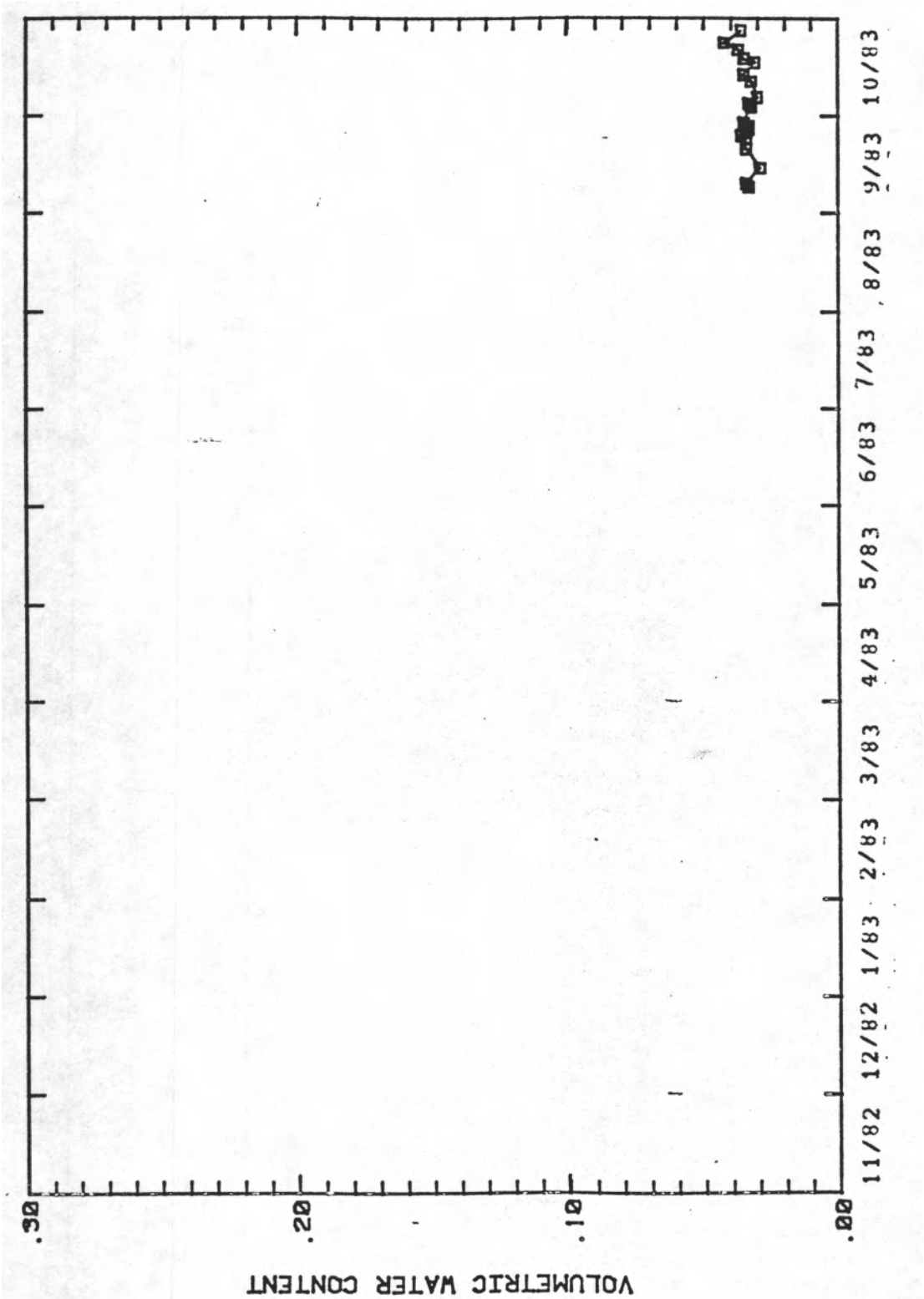

Water Content versus Time for the 335.5cm depth at Soil-moisture Station 1

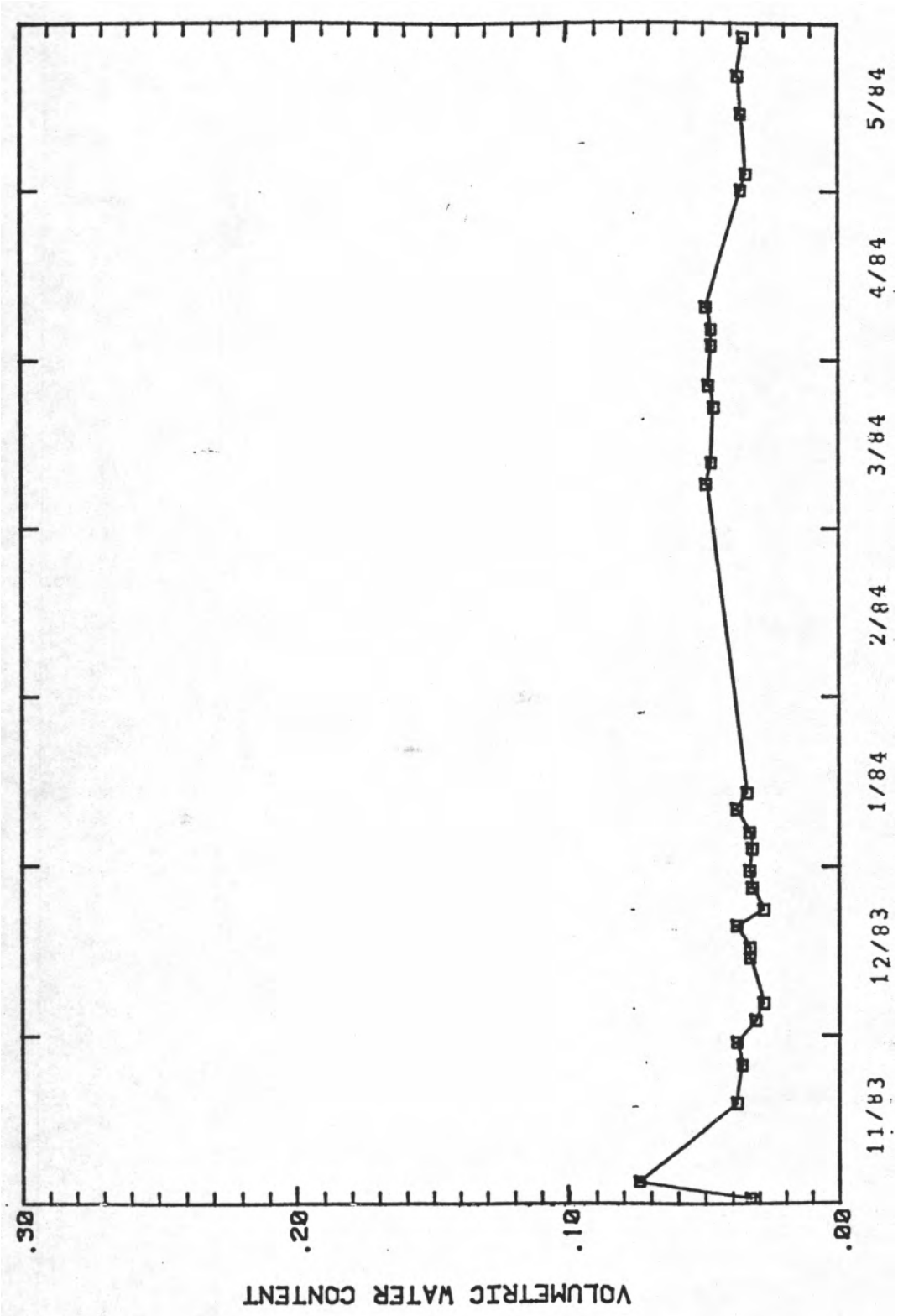

Water Content versus Time for the 335.5cm depth at Soil-moisture Station 1

Water Content versus Time for the 366.0cm depth at Soil-moisture Station 1.

Date	Water Content
09/08/83	0.035
09/09/83	0.031
09/14/83	0.030
09/20/83	0.031
09/23/83	0.029
09/24/83	0.029
09/25/83	0.029
09/26/83	0.037
09/27/83	0.032
09/28/83	0.027
10/03/83	0.030
10/04/83	0.031
10/06/83	0.034
10/11/83	0.029
10/13/83	0.028
10/17/83	0.028
10/18/83	0.033
10/21/83	0.031
10/23/83	0.027
10/27/83	0.033
11/01/83	0.026
11/04/83	0.033
11/18/83	0.034
11/25/83	0.024
11/29/83	0.029
12/03/83	0.029
12/06/83	0.032
12/14/83	0.032
12/16/83	0.025
12/20/83	0.030
12/23/83	0.033
12/27/83	0.025
12/30/83	0.026
01/03/84	0.025
01/06/84	0.026
01/10/84	0.031
01/13/84	0.032
03/09/84	0.044
03/13/84	0.044
03/23/84	0.044
03/27/84	0.042
04/03/84	0.046
04/06/84	0.044
04/10/84	0.044
05/01/84	0.031
05/04/84	0.030
05/15/84	0.029
05/22/84	0.030
05/29/84	0.029

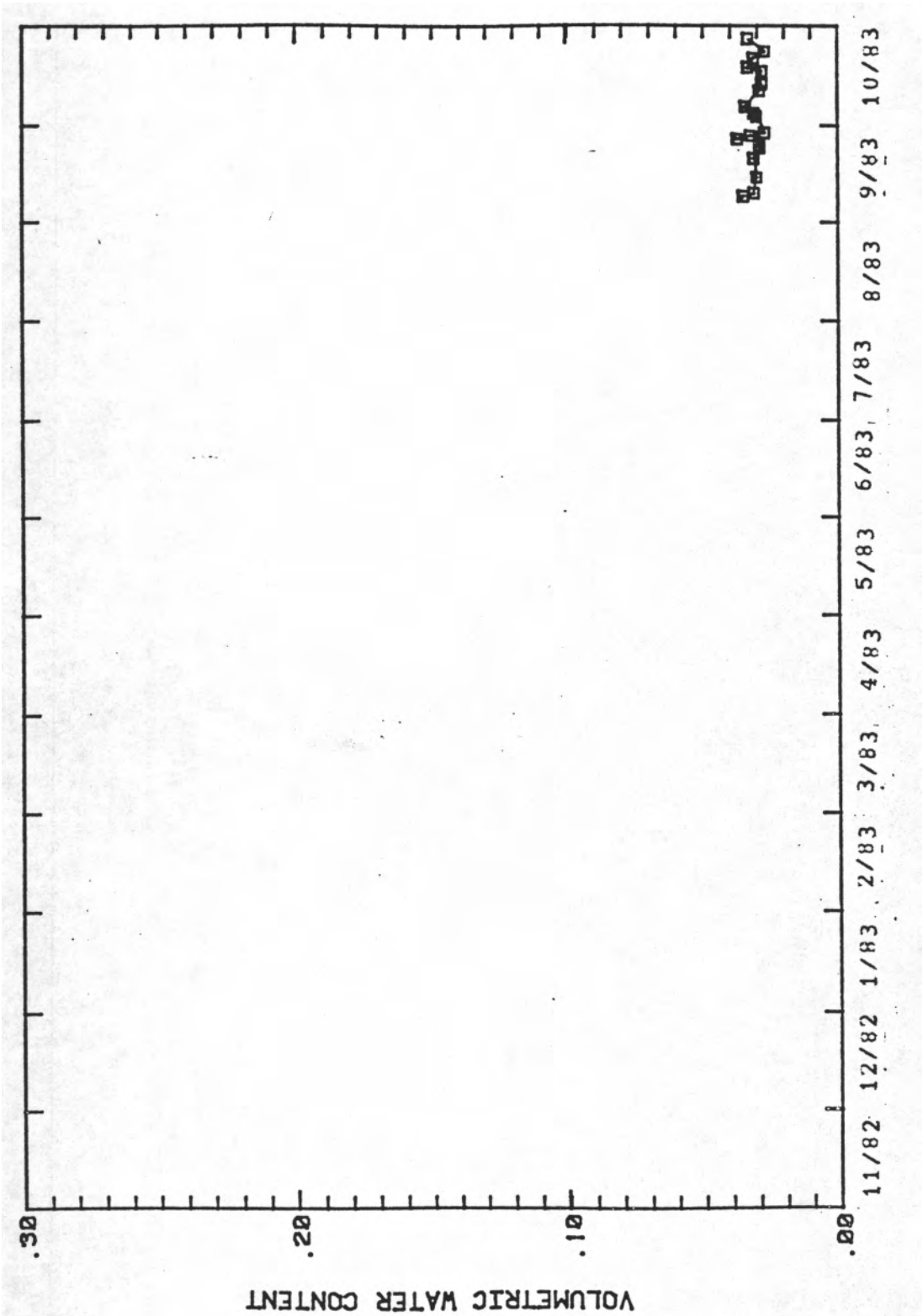

Water Content versus Time for the 366.0cm depth at Soil-moisture Station 1

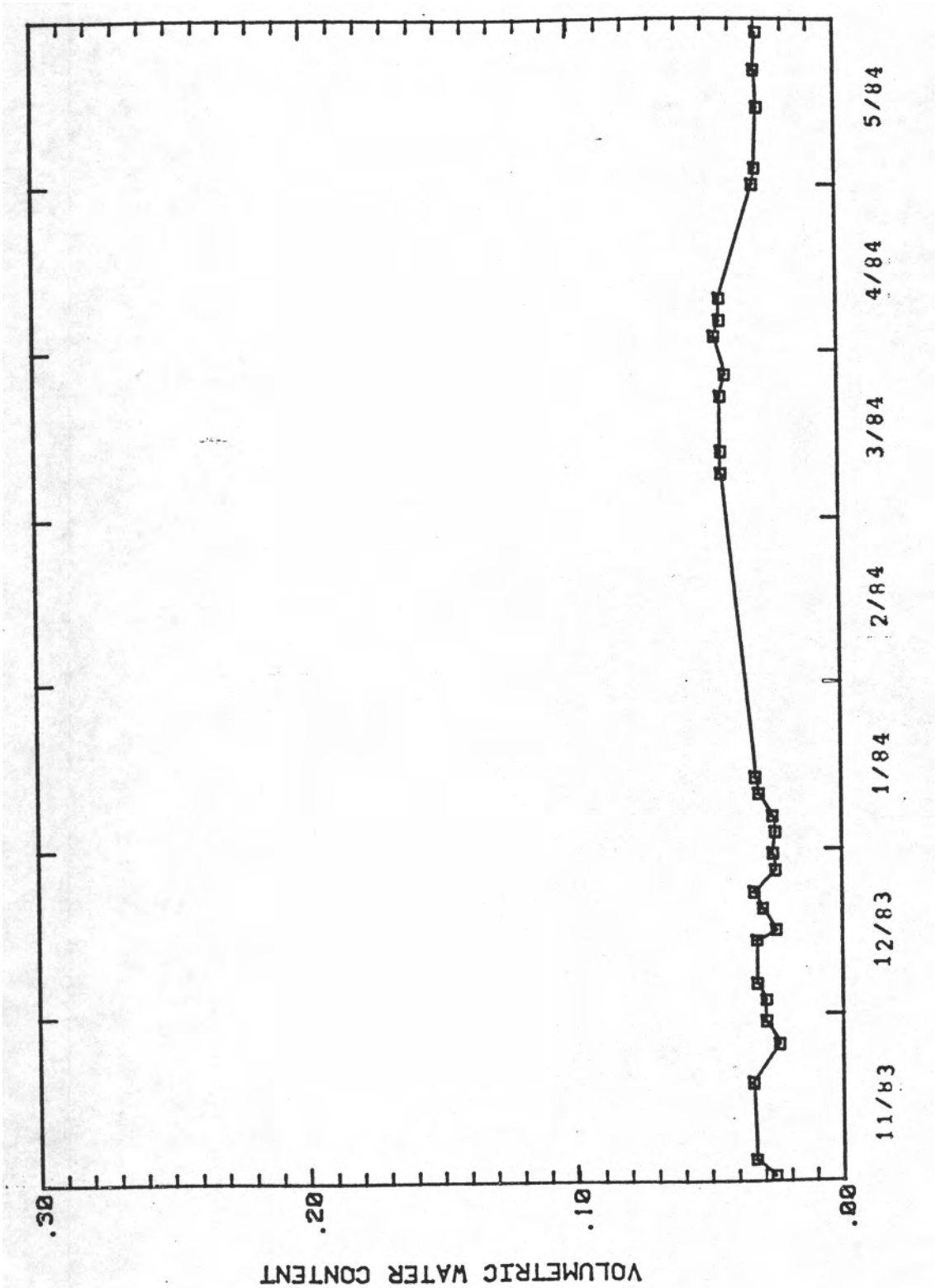

Water Content versus Time for the 366.0cm depth at Soil-moisture Station 1

Water Content versus Time for the 396.5cm depth at Soil-moisture Station 1

Date	Water Content
09/08/83	0.022
09/09/83	0.016
09/14/83	0.018
09/20/83	0.016
09/23/83	0.015
09/24/83	0.016
09/25/83	0.018
09/26/83	0.016
09/27/83	0.019
09/28/83	0.019
10/03/83	0.011
10/04/83	0.015
10/06/83	0.011
10/11/83	0.013
10/13/83	0.014
10/17/83	0.012
10/18/83	0.011
10/21/83	0.021
10/23/83	0.021
10/27/83	0.016
11/01/83	0.019
11/04/83	0.017
11/18/83	0.012
11/25/83	0.015
11/29/83	0.018
12/03/83	0.015
12/06/83	0.024
12/14/83	0.012
12/16/83	0.016
12/20/83	0.013
12/23/83	0.016
12/27/83	0.015
12/30/83	0.018
01/03/84	0.016
01/06/84	0.012
01/10/84	0.016
01/13/84	0.017
03/09/84	0.033
03/13/84	0.033
03/23/84	0.036
03/27/84	0.033
04/03/84	0.035
04/06/84	0.034
04/10/84	0.035
05/01/84	0.017
05/04/84	0.016
05/15/84	0.016
05/22/84	0.016
05/29/84	0.016

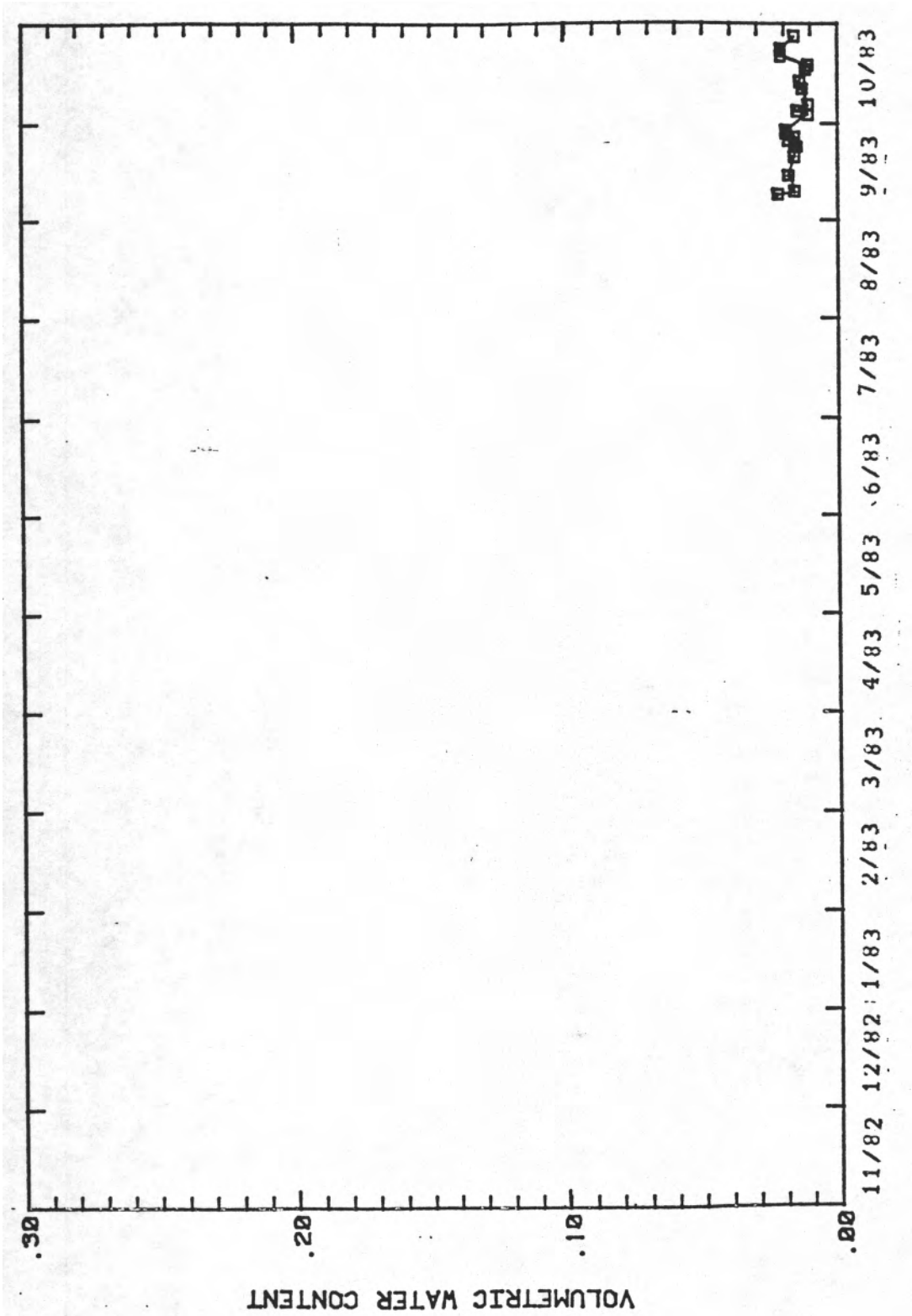

Water Content versus Time for the 396.5cm depth at Soil-moisture Station 1

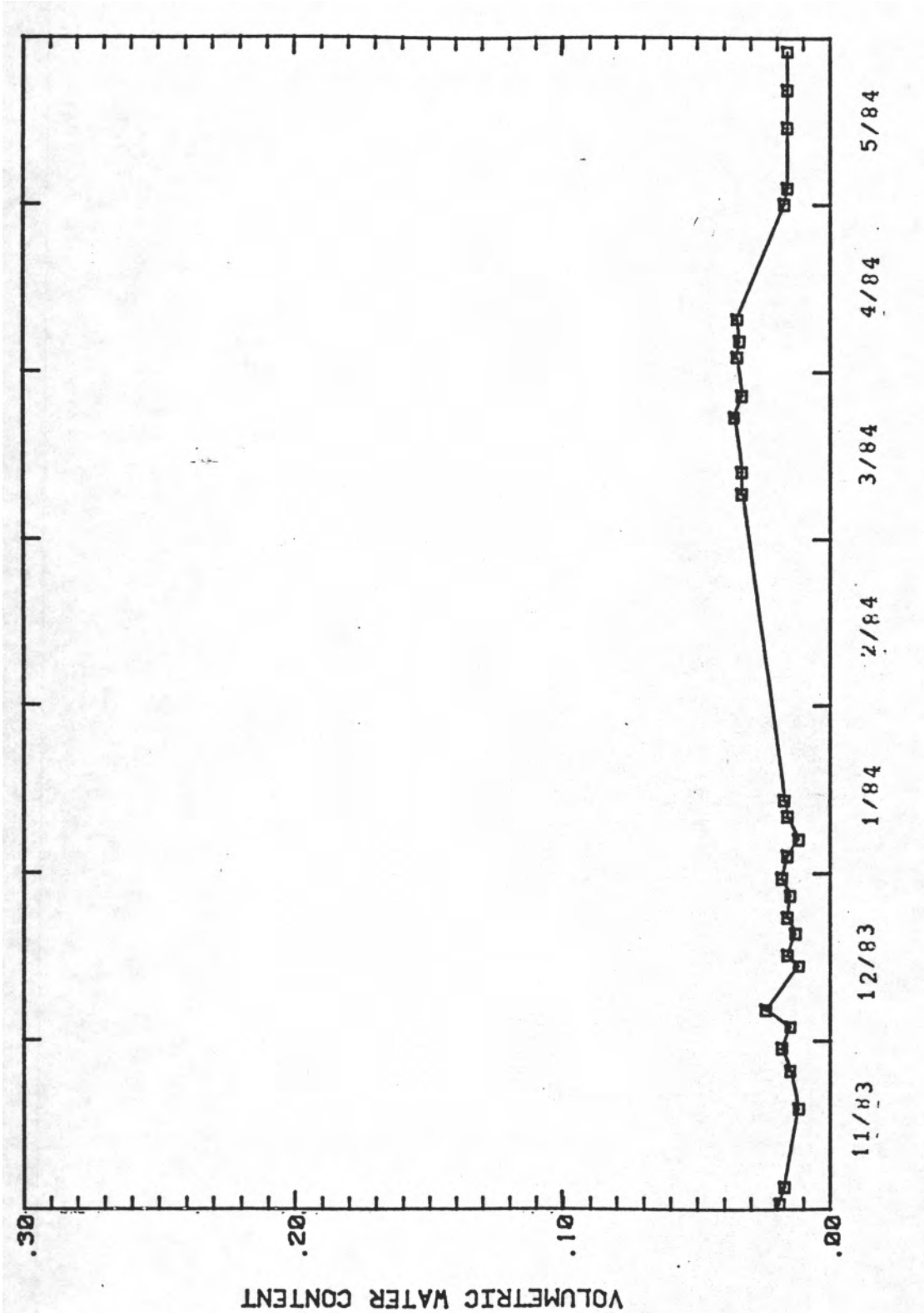

Water Content versus Time for the 396.5cm depth at Soil-moisture Station 1

Water Content versus Time for the 427.0cm deptn at Soil-moisture Station 1

Date	Water Content
09/08/83	0.065
09/09/83	0.065
09/14/83	0.063
09/20/83	0.069
09/23/83	0.063
09/24/83	0.077
09/25/83	0.066
09/26/83	0.073
09/27/33	0.076
09/28/83	0.072
10/03/83	0.070
10/04/83	0.071
10/06/83	0.078
10/11/83	0.074
10/13/83	0.080
10/17/83	0.075
10/18/83	0.072
10/21/83	0.080
10/23/83	0.031
10/27/83	0.082
11/01/83	0.078
11/04/83	0.080
11/18/83	0.084
11/25/83	0.083
11/29/83	0.084
12/03/83	0.081
12/06/83	0.079
12/14/83	0.079
12/16/83	0.087
12/20/83	0.084
12/23/83	0.079
12/27/83	0.087
12/30/83	0.085
01/03/84	0.085
01/06/84	0.087
01/10/84	0.058
01/13/84	0.068
03/09/84	0.078
03/13/84	0.077
03/23/84	0.075
03/27/84	0.077
04/03/84	0.079
04/06/84	0.079
04/10/84	0.078
05/01/84	0.075
05/04/84	0.075
05/15/84	0.073
05/22/84	0.076
05/29/84	0.076

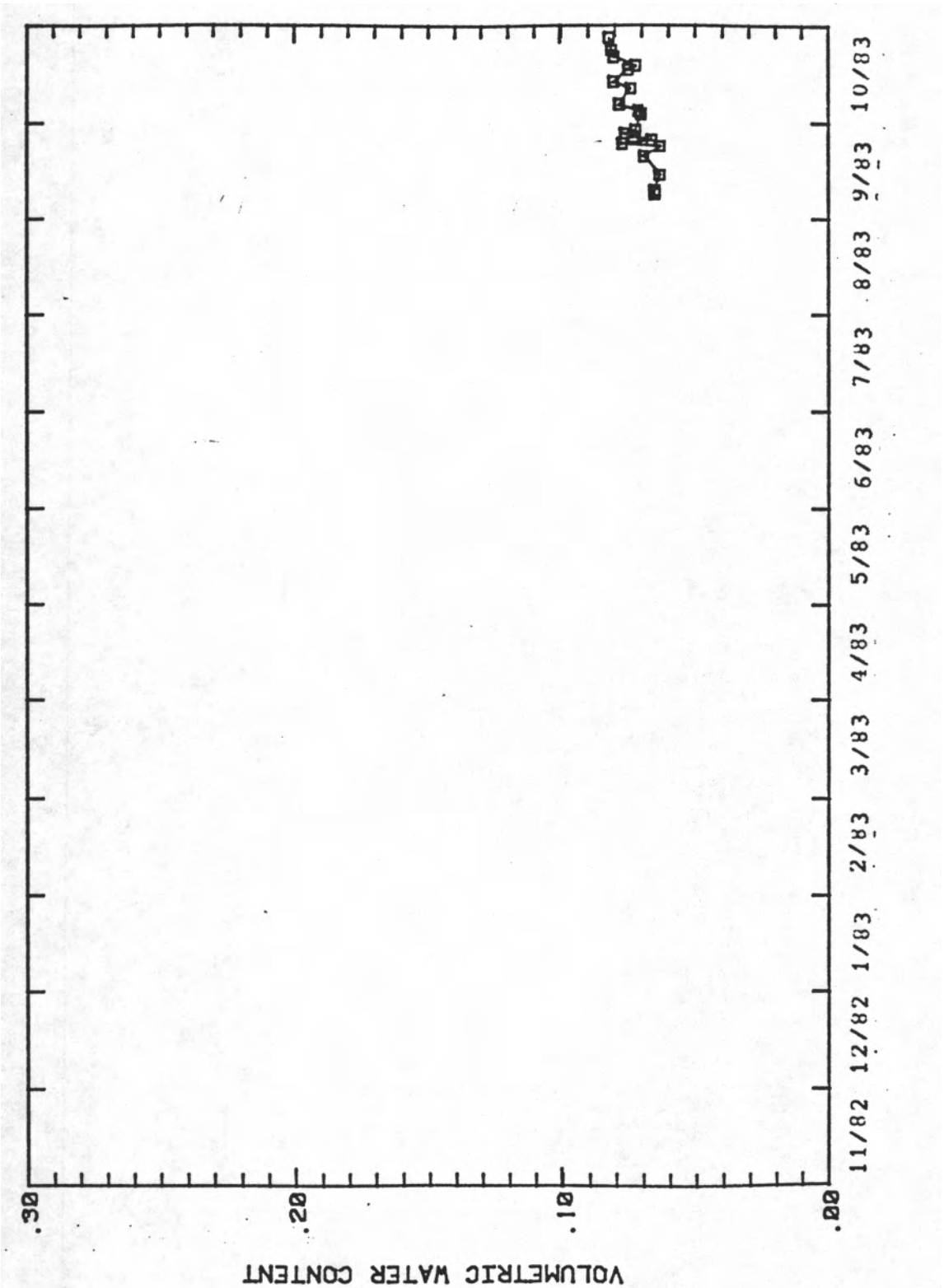

Water Content versus Time for the 427.0cm depth at Soil-moisture Station 1

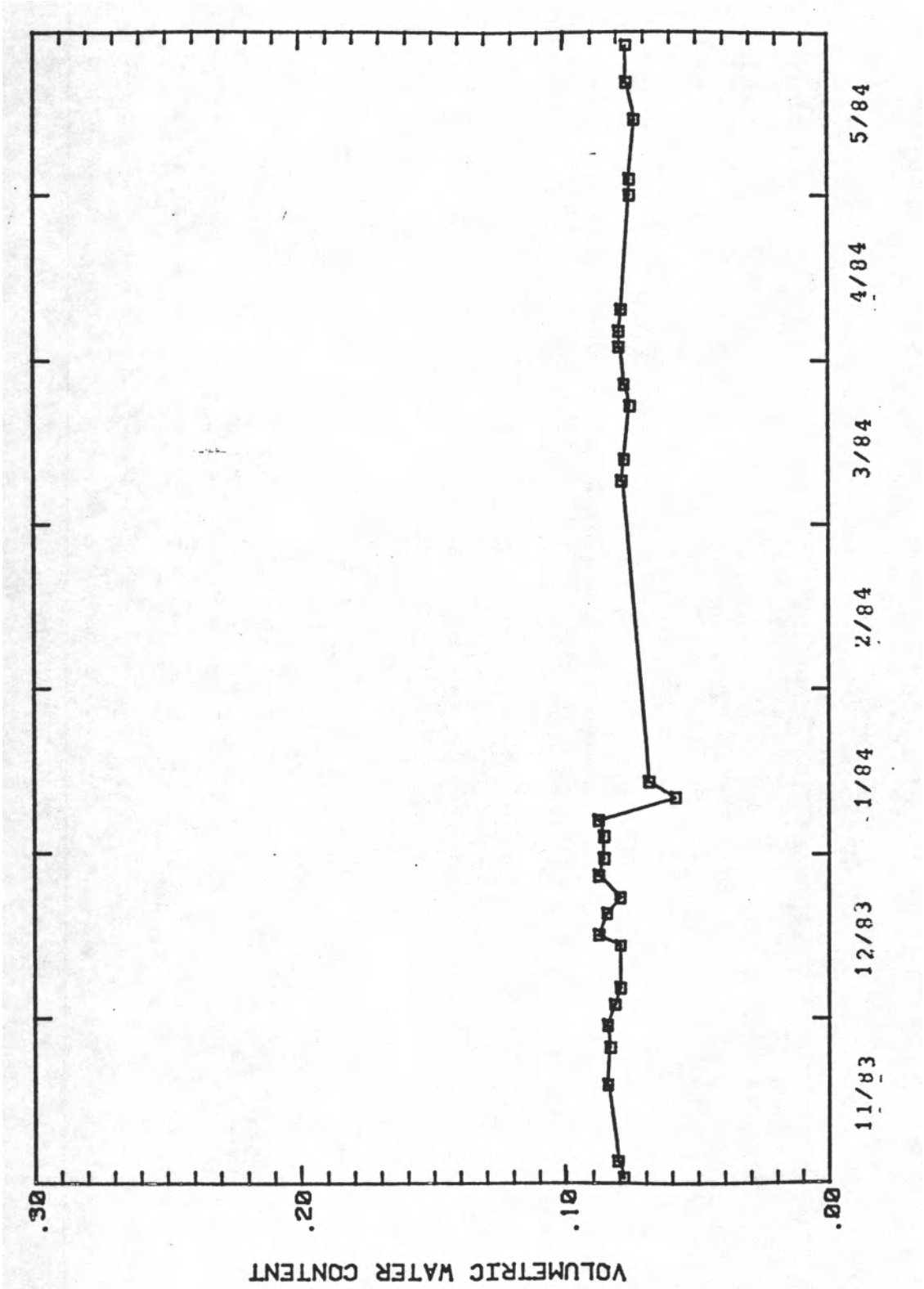

Water Content versus Time for the 427.0cm depth at Soil-moisture Station 1

Water Content versus Time for the 457.5cm depth at Soil-moisture Station 1

Date	Water Content
09/08/83	0.076
09/09/83	0.088
09/14/83	0.086
09/20/83	0.084
09/23/83	0.076
09/24/83	0.085
09/25/83	0.079
09/26/83	0.084
09/27/83	0.084
09/28/83	0.084
10/03/83	0.088
10/04/83	0.089
10/06/83	0.083
10/11/83	0.093
10/13/83	0.093
10/17/83	0.096
10/18/83	0.097
10/21/83	0.093
10/23/83	0.095
10/27/83	0.099
11/01/83	0.093
11/04/83	0.088
11/18/83	0.097
11/25/83	0.091
11/29/83	0.094
12/03/83	0.092
12/06/83	0.094
12/14/83	0.098
12/16/83	0.101
12/20/83	0.097
12/23/83	0.101
12/27/83	0.098
12/30/83	0.097
01/03/84	0.093
01/06/84	0.101
01/10/84	0.092
01/13/84	0.095
03/09/84	0.095
03/13/84	0.094
03/23/84	0.095
03/27/84	0.098
04/03/84	0.100
04/06/84	0.097
04/10/84	0.097
05/01/84	0.100
05/04/84	0.099
05/15/84	0.099
05/22/84	0.100
05/29/84	0.099

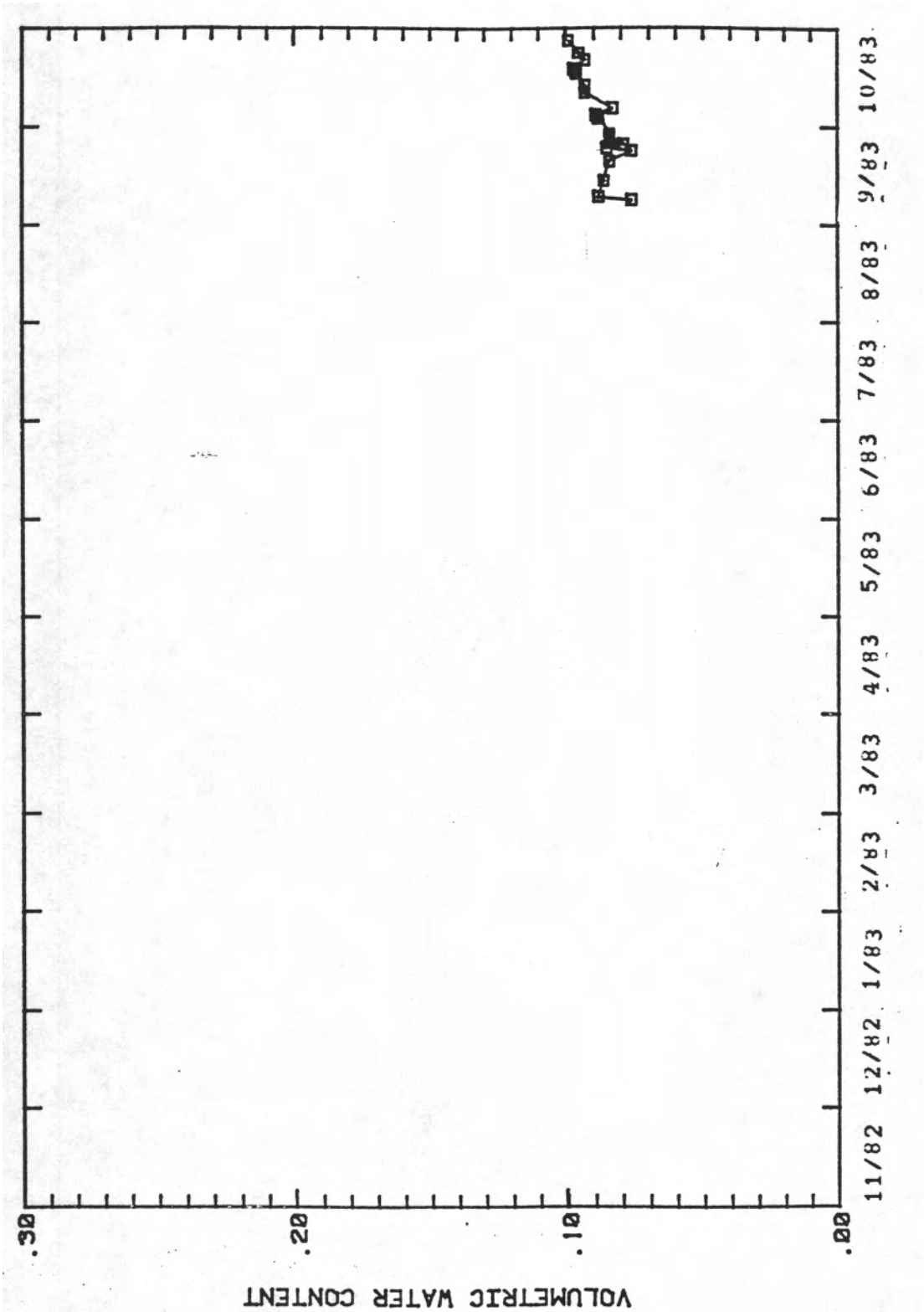

Water Content versus Time for the 457.5cm depth at Soil-moisture Station 1

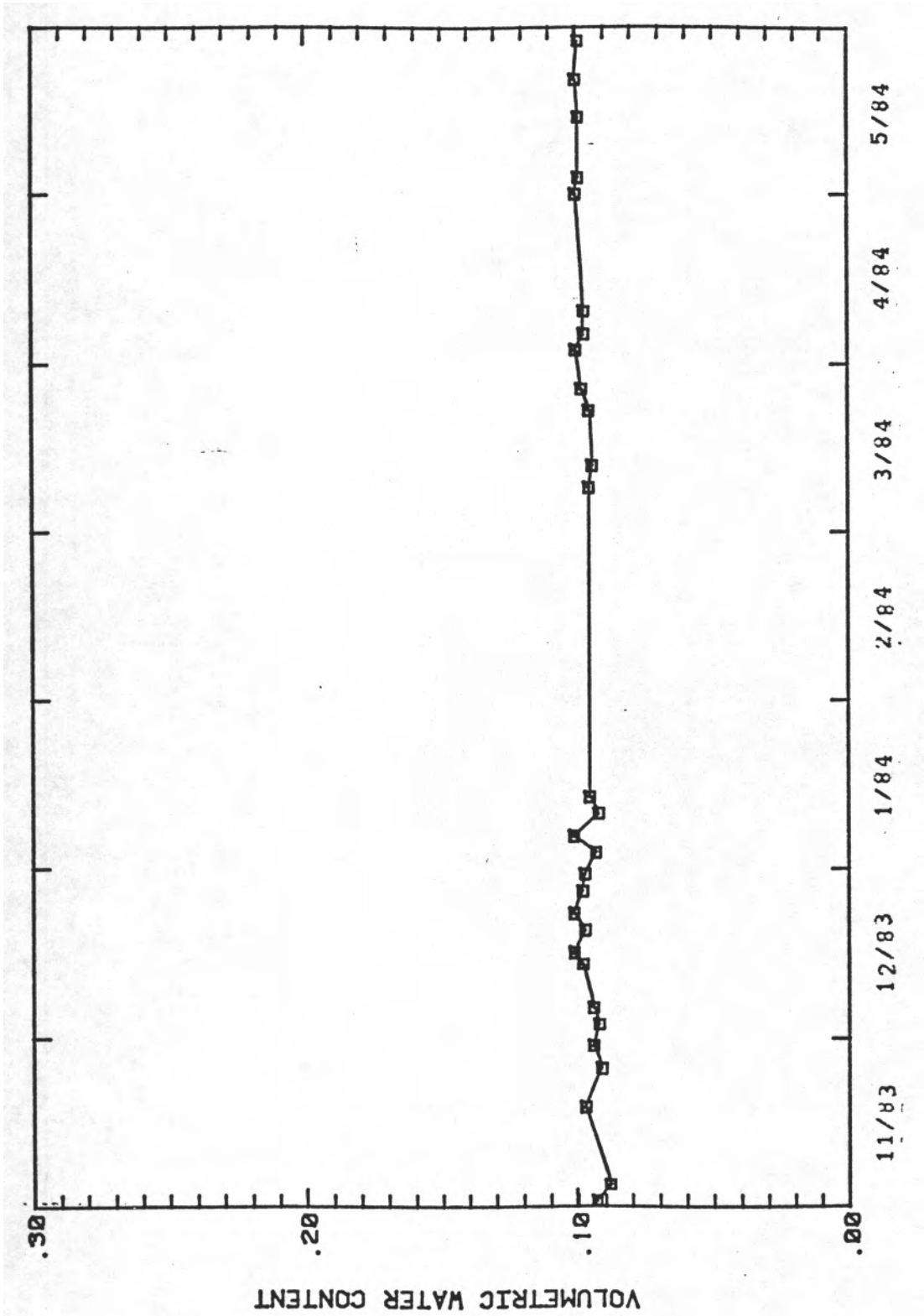

Water Content versus Time for the 457.5cm depth at Soil-moisture Station 1.

Water Content versus Time for the 488.0cm depth at Soil-moisture Station 1

Date	Water Content
09/08/83	0.043
09/09/83	0.042
09/14/83	0.043
09/20/83	0.043
09/23/83	0.041
09/24/83	0.040
09/25/83	0.043
09/26/83	0.043
09/27/83	0.046
09/28/83	0.042
10/03/83	0.038
10/04/83	0.040
10/06/83	0.041
10/11/83	0.037
10/13/83	0.044
10/17/83	0.042
10/18/83	0.043
10/21/83	0.046
10/23/83	0.049
10/27/83	0.037
11/01/83	0.052
11/04/83	0.047
11/18/83	0.053
11/25/83	0.049
11/29/83	0.045
12/03/83	0.055
12/06/83	0.055
12/14/83	0.053
12/16/83	0.049
12/20/83	0.044
12/23/83	0.050
12/27/83	0.059
12/30/83	0.053
01/03/84	0.046
01/06/84	0.049
01/10/84	0.052
01/13/84	0.074
03/09/84	0.060
03/13/84	0.061
03/23/84	0.058
03/27/84	0.061
04/03/84	0.060
04/06/84	0.057
04/10/84	0.058
05/01/84	0.046
05/04/84	0.046
05/15/84	0.046
05/22/84	0.046
05/29/84	0.045

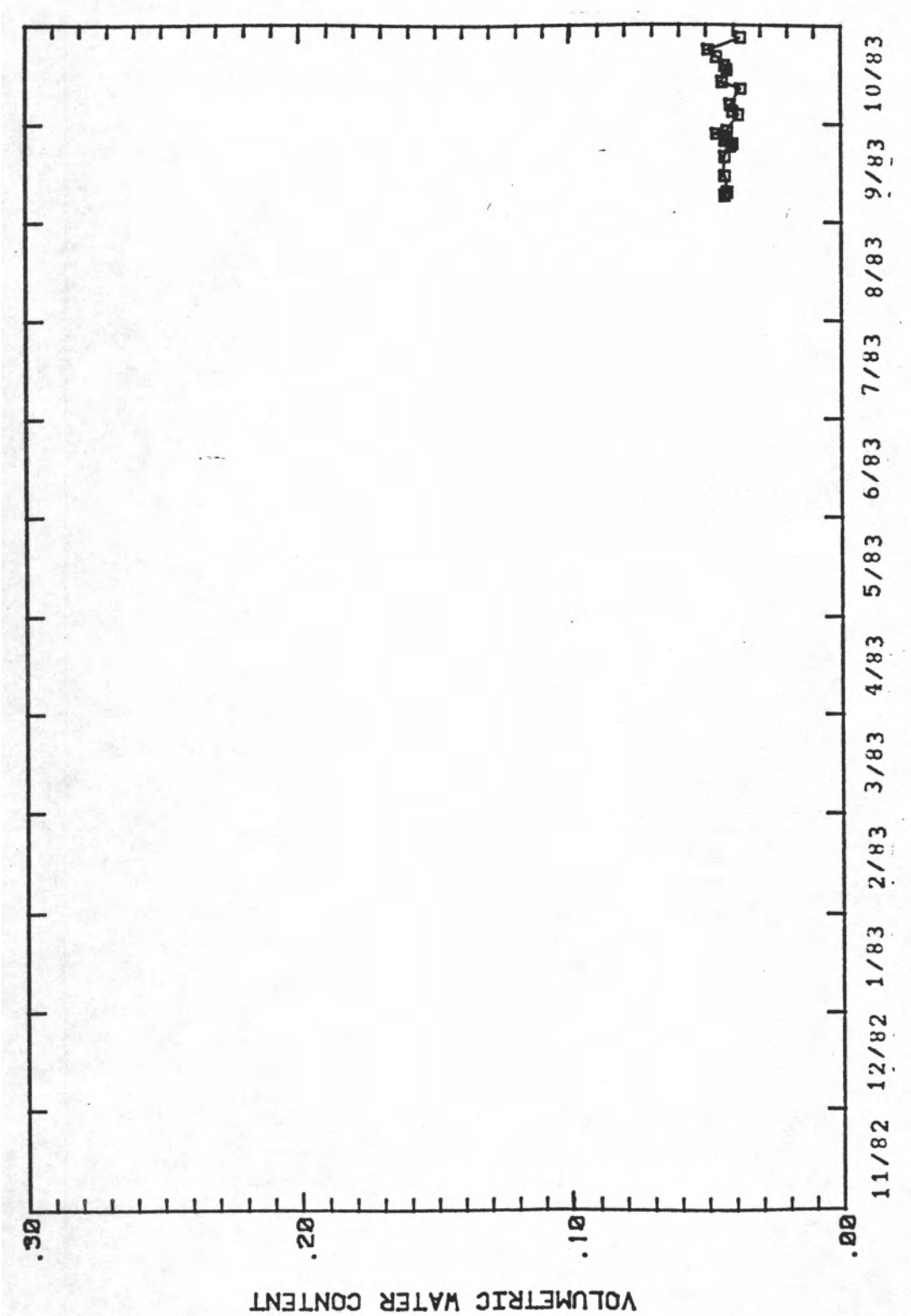

Water Content versus Time for the 488.0cm deptn at Soil-moisture Station 1

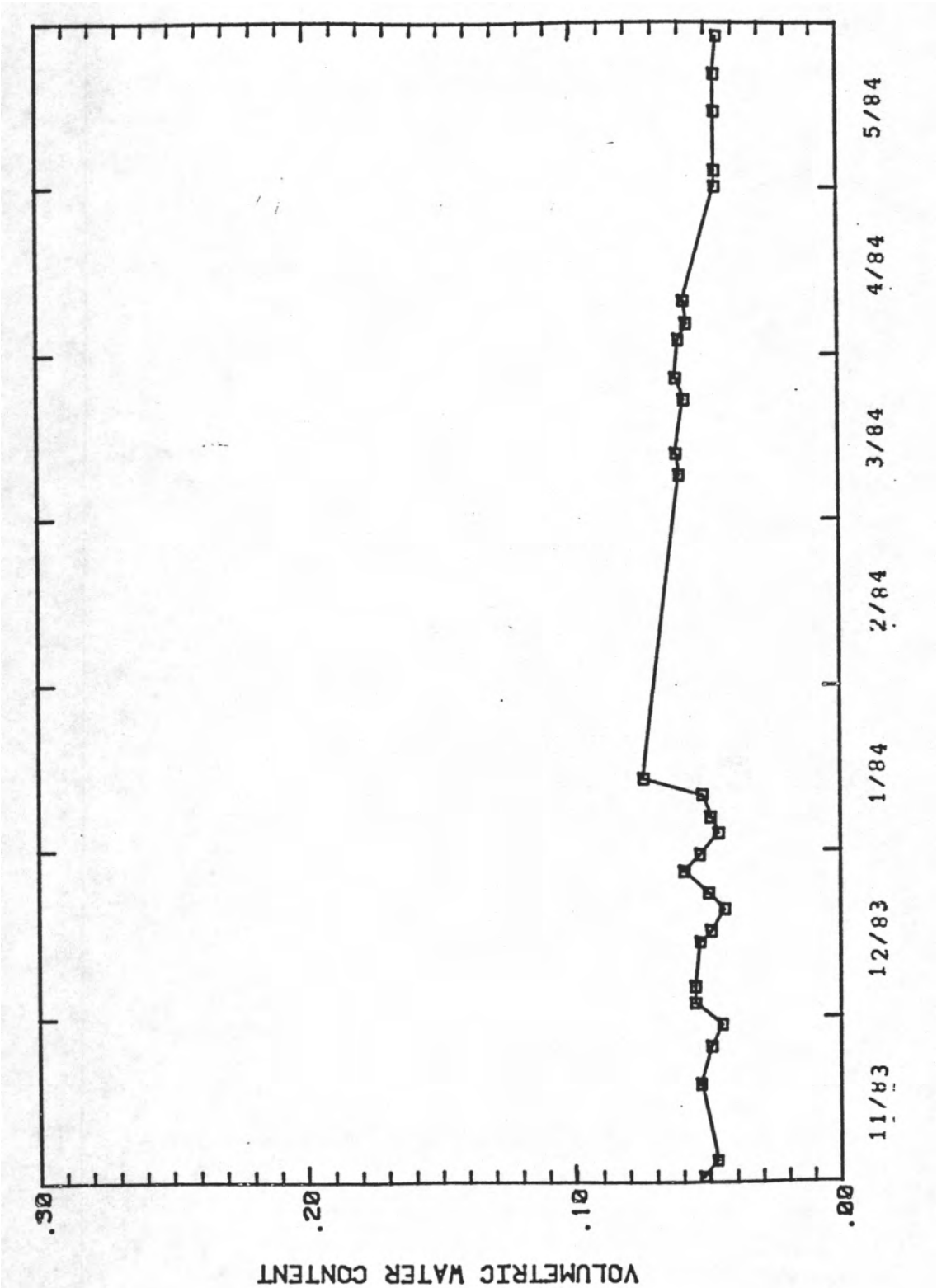

Water Content versus Time for the 488.0cm depth at Soil-moisture Station 1

Water Content versus Time for the 518.5cm depth at Soil-moisture Station 1

Date	Water Content
09/08/83	0.061
09/09/83	0.065
09/14/83	0.067
09/20/83	0.064
09/23/83	0.064
09/24/83	0.059
09/25/83	0.059
09/26/83	0.054
09/27/83	0.065
09/28/83	0.073
10/03/83	0.059
10/04/83	0.075
10/06/83	0.088
10/11/83	0.103
10/13/83	0.113
10/17/83	0.118
10/18/83	0.126
10/21/83	0.132
10/23/83	0.122
10/27/83	0.126
11/01/83	0.118
11/04/83	0.126
11/18/83	0.118
11/25/83	0.103
11/29/83	0.107
12/03/83	0.102
12/06/83	0.119
12/14/83	0.102
12/16/83	0.102
12/20/83	0.096
12/23/83	0.114
12/27/83	0.100
12/30/83	0.110
01/03/84	0.097
01/06/84	0.105
01/10/84	0.082
01/13/84	0.076
03/09/84	0.077
03/13/84	0.080
03/23/84	0.076
03/27/84	0.075
04/03/84	0.077
04/06/84	0.076
04/10/84	0.072
05/01/84	0.070
05/04/84	0.069
05/15/84	0.068
05/22/84	0.069
05/29/84	0.069

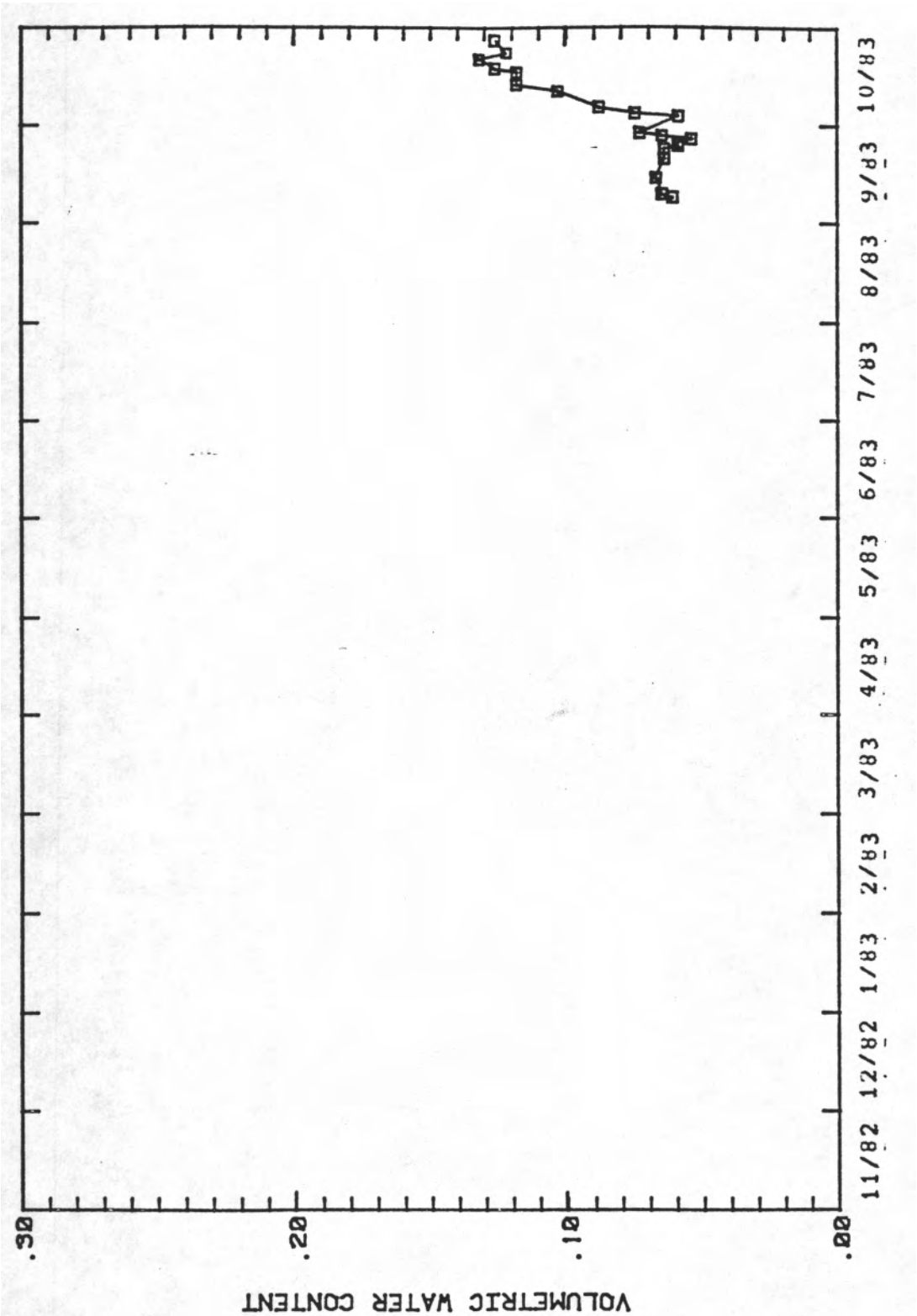

Water Content versus Time for the 518.5cm depth at Soil-moisture Station 1

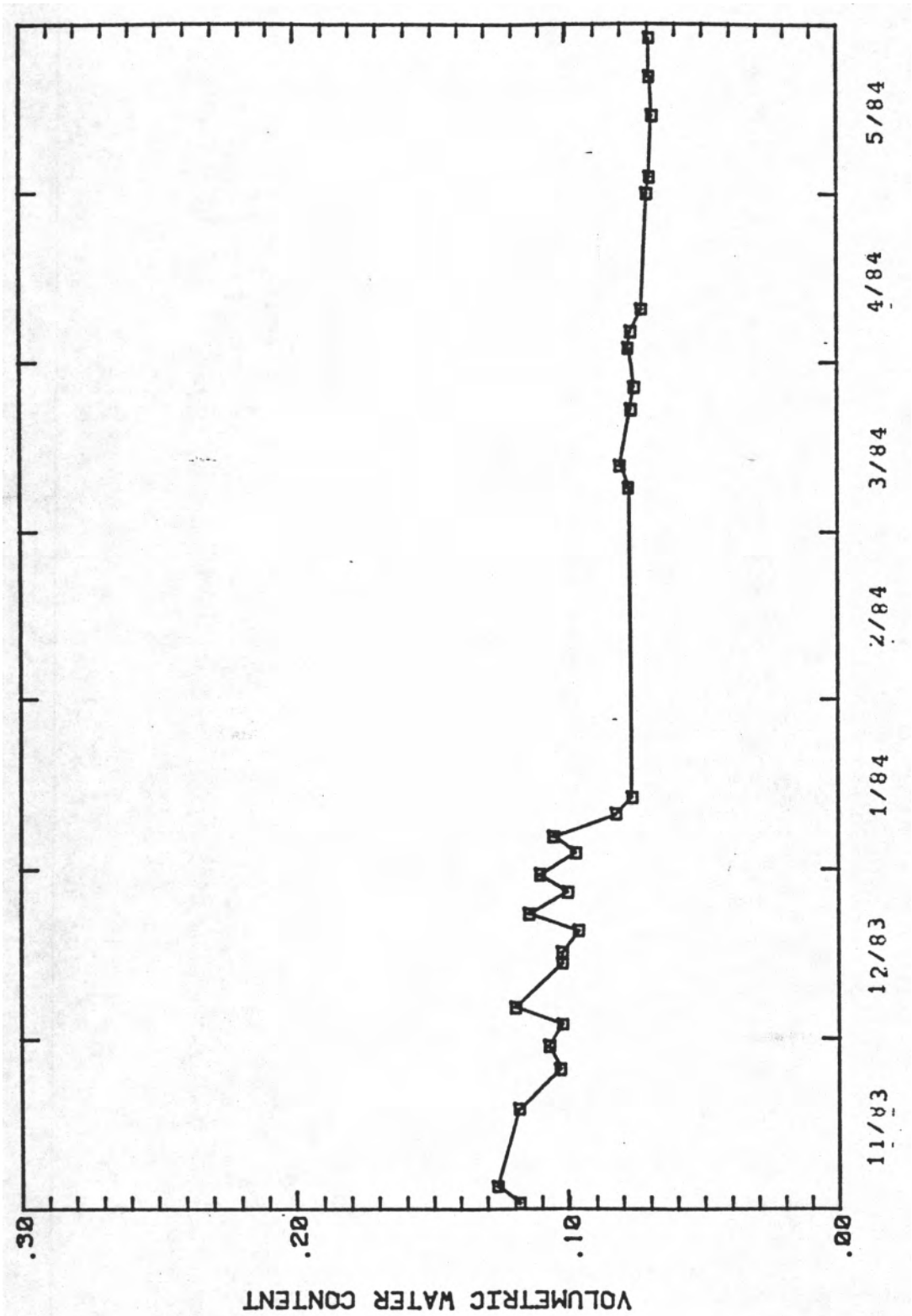

Water Content versus Time for the 518.5cm deptn at Soil-moisture Station 1

Water Content versus Time for the 549.0cm depth at Soil-moisture Station 1

Date	Water Content
09/08/83	0.077
09/09/83	0.069
09/14/83	0.083
09/20/83	0.101
09/23/83	0.111
09/24/83	0.115
09/25/83	0.114
09/26/83	0.110
09/27/83	0.111
09/28/83	0.120
10/03/83	0.144
10/04/83	0.158
10/06/83	0.209
10/11/83	0.277
10/13/83	0.286
10/17/83	0.283
10/18/83	0.297
10/21/83	0.296
10/23/83	0.297
10/27/83	0.300
11/01/83	0.280
11/04/83	0.287
11/18/83	0.274
11/25/83	0.256
11/29/83	0.247
12/03/83	0.255
12/06/83	0.231
12/14/83	0.222
12/16/83	0.223
12/20/83	0.211
12/23/83	0.216
12/27/83	0.222
12/30/83	0.199
01/03/84	0.202
01/06/84	0.203
01/10/84	0.162
01/13/84	0.167
03/09/84	0.115
03/13/84	0.114
03/23/84	0.110
03/27/84	0.110
04/03/84	0.111
04/10/84	0.108
05/01/84	0.096
05/04/84	0.068
05/15/84	0.090
05/22/84	0.090
05/29/84	0.065

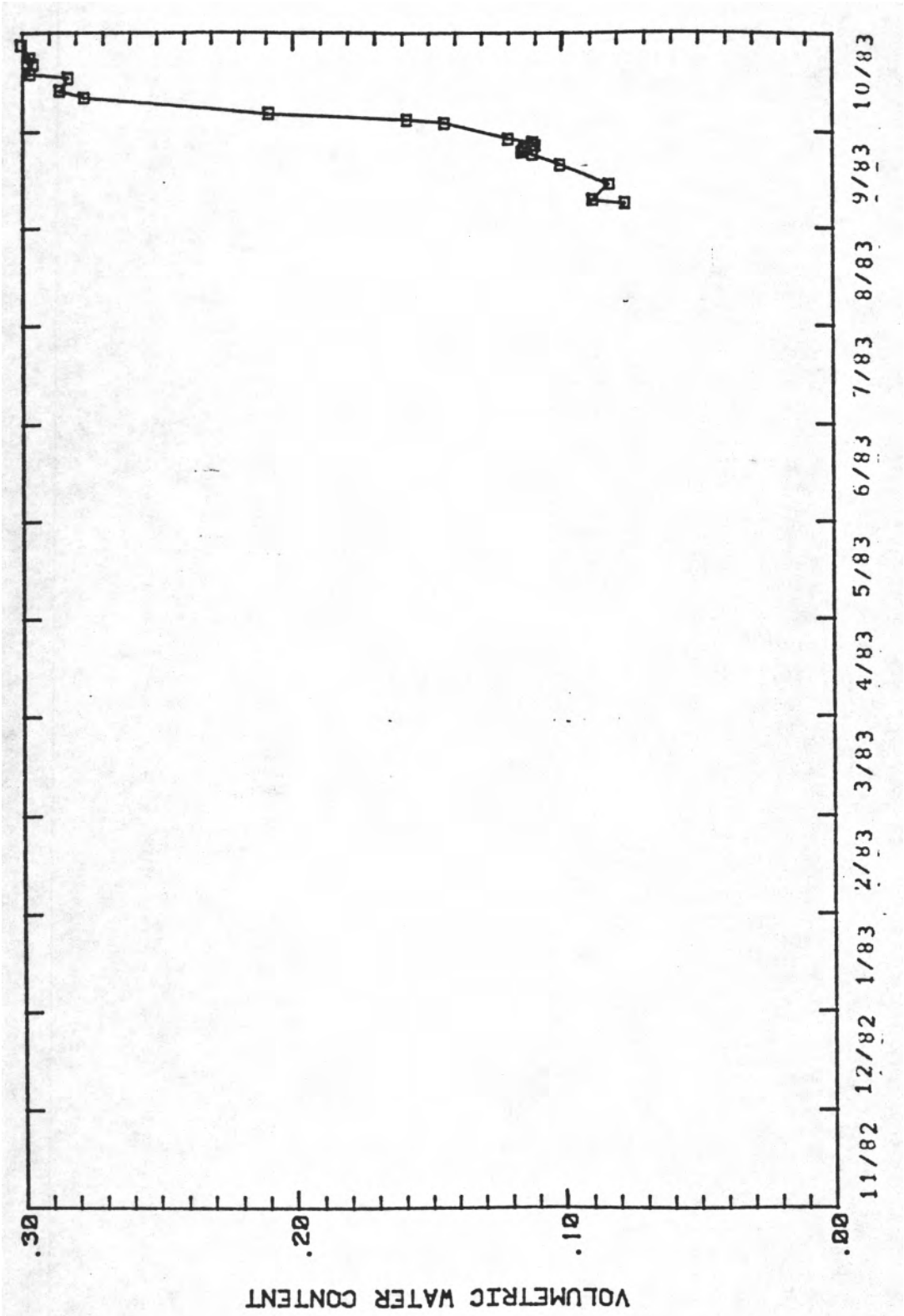

Water Content versus Time for the 549.0cm depth at Soil-moisture Station 1

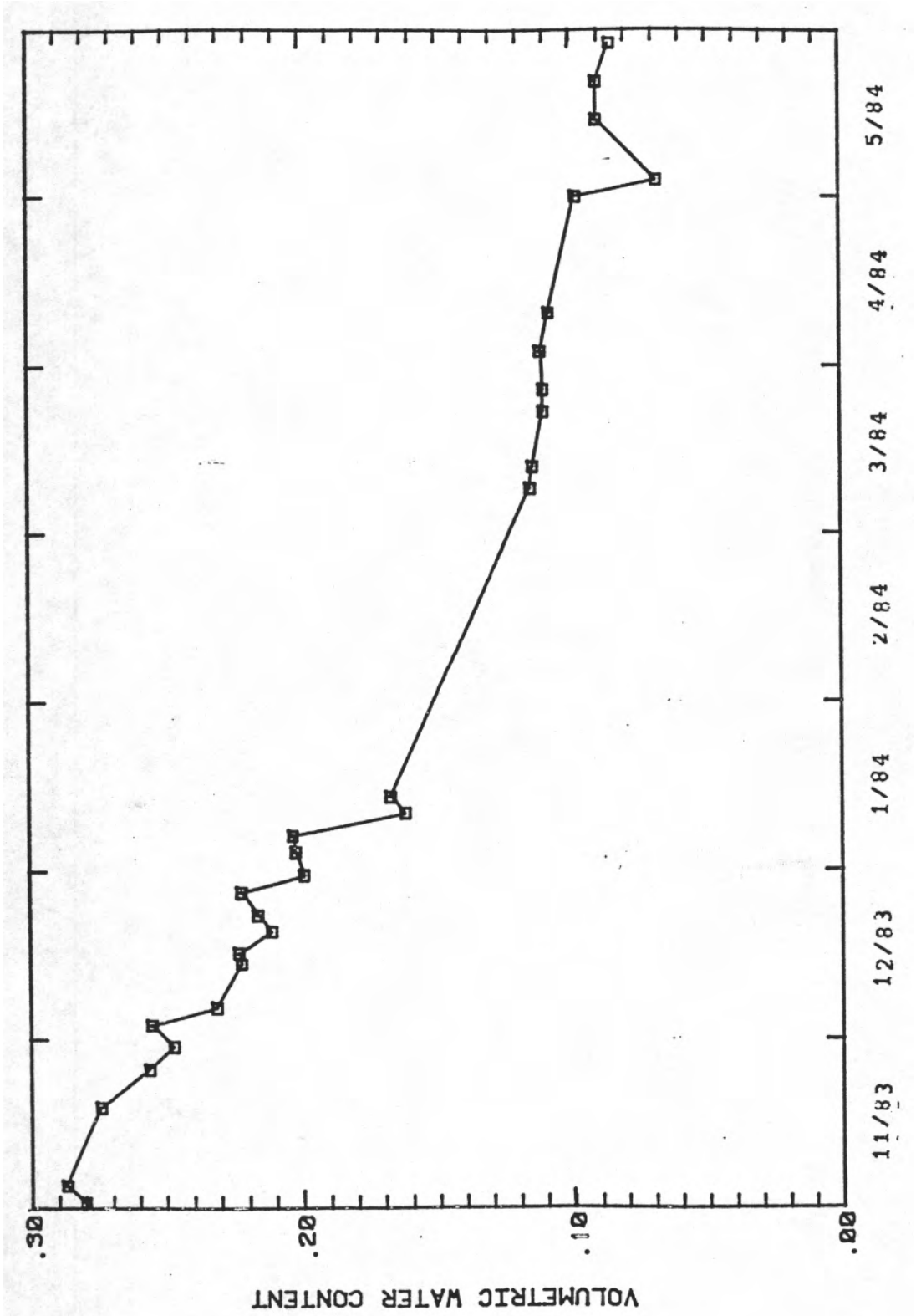

Water Content versus Time for the 549.0cm depth at Soil-moisture Station 1

Total Head versus Time for the 30.5cm depth at

Soil-moisture Station 1

Date	Total Head (cm)
11/12/82	-110.
11/17/82	-71.
11/18/82	-68.
11/19/82	-120.
11/23/82	-137.
11/29/82	-123.
11/30/82	-116.
12/03/82	-67.
12/07/82	-69.
12/09/82	-120.
12/10/82	-85.
12/11/82	-82.
12/12/82	-85.
12/14/82	-65.
12/16/82	-63.
12/22/82	-98.
12/23/82	-73.
12/27/82	-105.
12/28/82	-105.
01/22/83	-67.
01/24/83	-90.
01/31/83	-100.
02/01/83	-87.
02/04/83	-87.
02/05/83	-88.
02/06/83	-94.
02/10/83	-113.
02/12/83	-116.
02/14/83	-119.
02/15/83	-117.
02/22/83	-133.
02/27/83	-102.
02/28/83	-131.
03/04/83	-131.
03/20/83	-69.
03/31/83	-143.
04/11/83	-147.
04/15/83	-117.
04/19/83	-119.
04/22/83	-114.
04/29/83	-129.
05/03/83	-114.
05/07/83	-124.
05/10/83	-133.
05/13/83	-105.
05/18/83	-113.
05/24/83	-139.
05/27/83	-144.
06/01/83	-94.
06/06/83	-79.
06/07/83	-104.
06/14/83	-99.
06/17/83	-93.
06/24/83	-56.
06/28/83	-107.
07/05/83	-87.
07/12/83	-59.
07/15/83	-68.
07/19/83	-94.
07/22/83	-133.
07/26/83	-122.
07/29/83	-122.
08/02/83	-126.
08/04/83	-124.
08/08/83	-91.
08/09/83	-114.
08/10/83	-114.
08/11/83	-117.
08/12/83	-118.
08/16/83	-123.
08/23/83	-134.
08/24/83	-135.
08/25/83	-131.
09/01/83	-133.
09/02/83	-113.
09/06/83	-138.
09/08/83	-142.
09/09/83	-110.
09/13/83	-111.
09/14/83	-115.
09/16/83	-62.
09/20/83	-87.
09/22/83	-86.
09/23/83	-85.
09/24/83	-89.
09/25/83	-70.
09/26/83	-62.
09/27/83	-70.
09/28/83	-83.
09/30/83	-83.
10/03/83	-81.
10/04/83	-85.
10/06/83	-78.
10/07/83	-97.
10/13/83	-85.
10/17/83	-74.
10/18/83	-84.
10/21/83	-91.
10/23/83	-103.
10/25/83	-123.
11/15/83	-82.
11/18/83	-90.
11/22/83	-110.
11/25/83	-91.
11/29/83	-125.
12/03/83	-117.
12/14/83	-93.
12/16/83	-98.
12/20/83	-101.
12/27/83	-69.
01/03/84	-83.
01/06/84	-66.
01/10/84	-69.
01/13/84	-79.
01/17/84	-79.
01/20/84	-82.
01/24/84	-99.
01/27/84	-72.
01/31/84	-71.
02/03/84	-70.
02/07/84	-74.
02/10/84	-85.
02/14/84	-99.
02/17/84	-104.
02/21/84	-78.
02/24/84	-71.
02/28/84	-88.
03/02/84	-84.
03/06/84	-89.
03/09/84	-115.
03/13/84	-68.
03/16/84	-82.
03/20/84	-74.
03/23/84	-78.
03/27/84	-87.
03/30/84	-88.
04/03/84	-77.
04/06/84	-69.
04/10/84	-70.
04/13/84	-71.
04/17/84	-93.
04/24/84	-68.
04/26/84	-137.
04/27/84	-76.
04/29/84	-100.
05/01/84	-77.
05/04/84	-52.
05/08/84	-76.
05/11/84	-85.
05/15/84	-126.
05/18/84	-104.
05/22/84	-121.
05/25/84	-92.

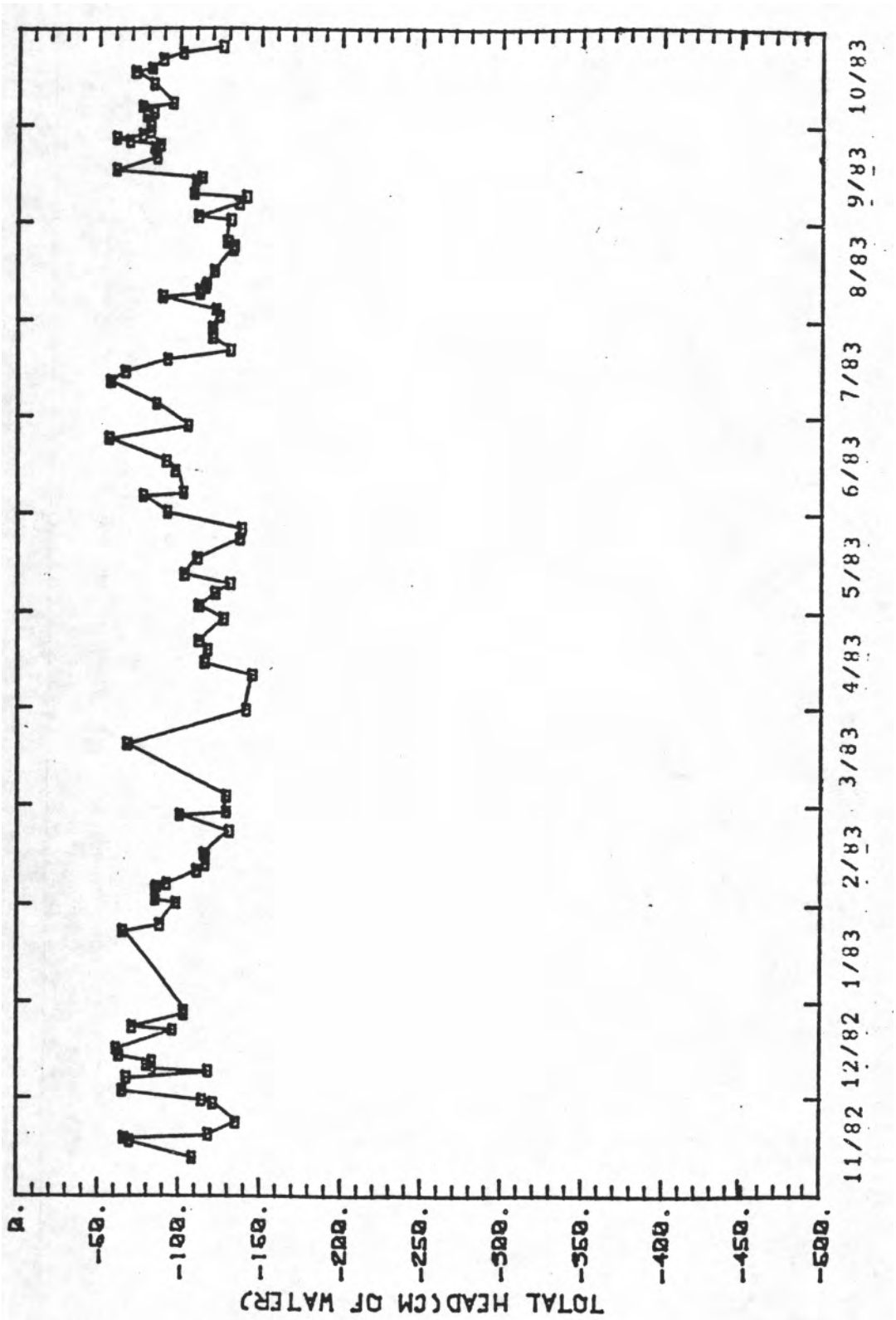

Water Content versus Time for the 30.5cm depth at Soil-moisture Station 1

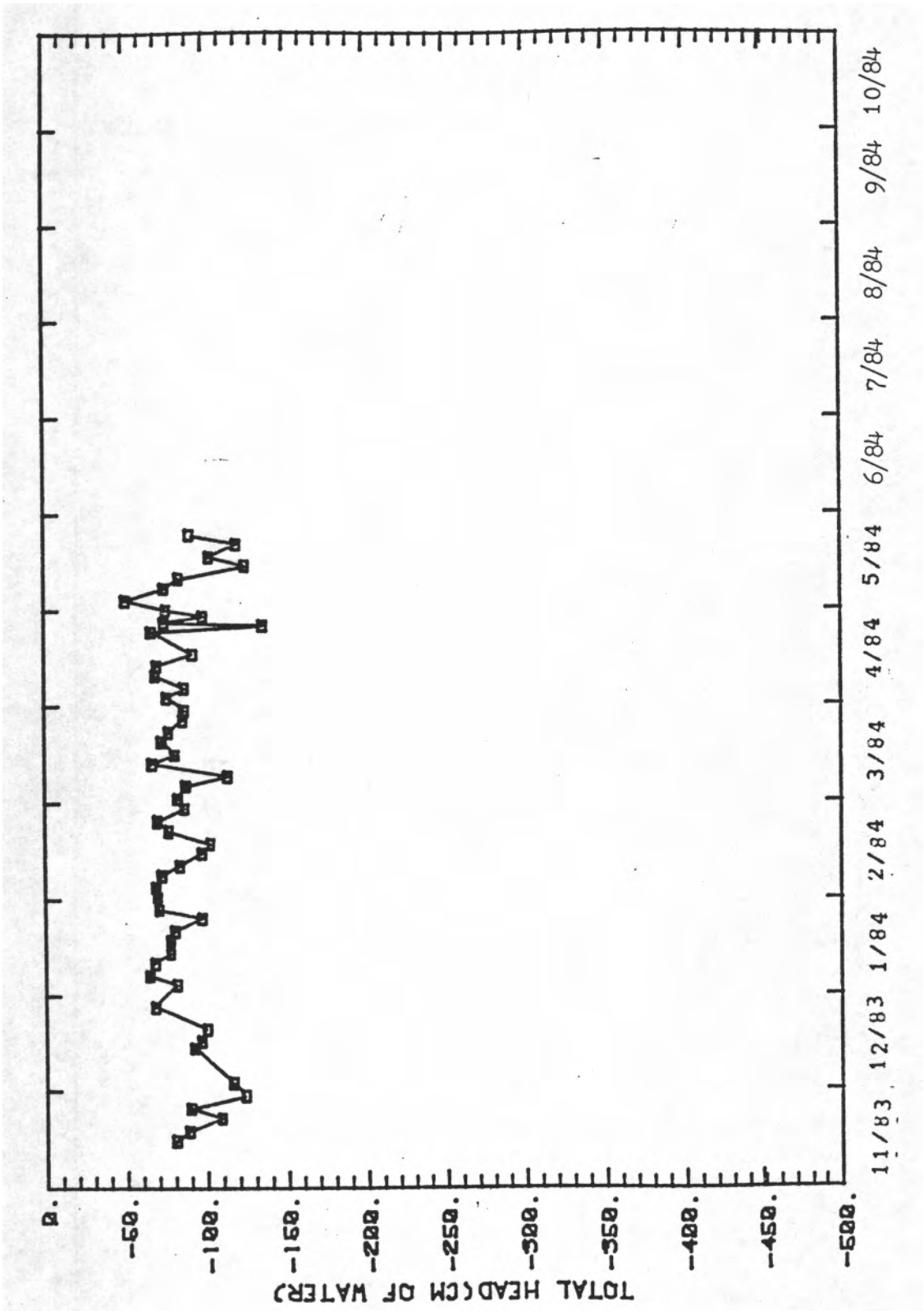

Total Head versus Time for the 30.5cm depth at Soil-moisture Station 1

Total Head versus Time for the 61.0cm depth at

Soil-moisture Station 1

Date	Total Head (cm)
11/12/82	-136.
11/17/82	-143.
11/18/82	-135.
11/19/82	-147.
11/29/82	-181.
11/30/82	-161.
12/03/82	-126.
12/07/82	-116.
12/09/82	-176.
12/11/82	-98.
12/12/82	-143.
12/14/82	-80.
12/16/82	-105.
12/22/82	-119.
12/23/82	-113.
12/27/82	-118.
12/28/82	-114.
12/29/82	-171.
01/21/83	-103.
01/22/83	-104.
01/23/83	-105.
01/24/83	-105.
01/31/83	-121.
02/01/83	-113.
02/04/83	-116.
02/05/83	-118.
02/06/83	-116.
02/10/83	-126.
02/12/83	-126.
02/14/83	-122.
02/15/83	-122.
02/21/83	-134.
02/22/83	-133.
02/27/83	-133.
02/28/83	-143.
03/04/83	-143.
03/20/83	-110.
03/31/83	-150.
04/05/83	-145.
04/08/83	-160.
04/11/83	-143.
04/15/83	-145.
04/19/83	-144.
04/22/83	-142.
04/26/83	-144.
04/29/83	-144.
05/03/83	-144.
05/07/83	-147.
05/10/83	-150.
05/13/83	-150.
05/18/83	-154.
05/24/83	-153.
05/27/83	-168.
06/01/83	-172.
06/06/83	-186.
06/07/83	-164.
06/10/83	-216.
06/14/83	-164.
06/17/83	-152.
07/26/83	-163.
07/29/83	-173.
08/02/83	-172.
08/04/83	-169.
08/08/83	-107.
08/09/83	-139.
08/10/83	-145.
08/11/83	-162.
08/12/83	-147.
09/09/83	-143.
09/13/83	-201.
09/14/83	-121.
09/20/83	-112.
09/22/83	-112.
10/17/83	-111.
10/18/83	-113.
10/21/83	-137.
10/23/83	-119.
10/25/83	-131.
11/15/83	-119.
11/18/83	-119.
11/22/83	-142.
11/25/83	-120.
11/29/83	-158.
12/03/83	-141.
12/14/83	-130.
12/16/83	-147.
12/20/83	-154.
12/27/83	-94.
01/03/84	-109.
01/06/84	-95.
01/10/84	-120.
01/13/84	-120.
01/17/84	-109.
01/20/84	-108.
01/24/84	-122.
01/27/84	-99.
01/31/84	-89.
02/03/84	-86.
02/07/84	-91.
02/10/84	-104.
02/14/84	-116.
02/17/84	-123.
02/21/84	-80.
02/24/84	-111.
02/28/84	-119.
03/02/84	-95.
03/06/84	-99.
03/09/84	-128.
03/13/84	-82.
03/16/84	-94.
03/20/84	-84.
03/23/84	-97.
03/27/84	-96.
03/30/84	-103.
04/03/84	-87.
04/06/84	-99.
04/10/84	-82.
04/13/84	-79.
04/17/84	-109.
04/24/84	-83.
04/26/84	-162.
04/27/84	-92.
04/29/84	-117.
05/01/84	-81.
05/04/84	-73.
05/08/84	-89.
05/11/84	-100.
05/15/84	-141.
05/18/84	-138.
05/22/84	-144.
05/25/84	-126.

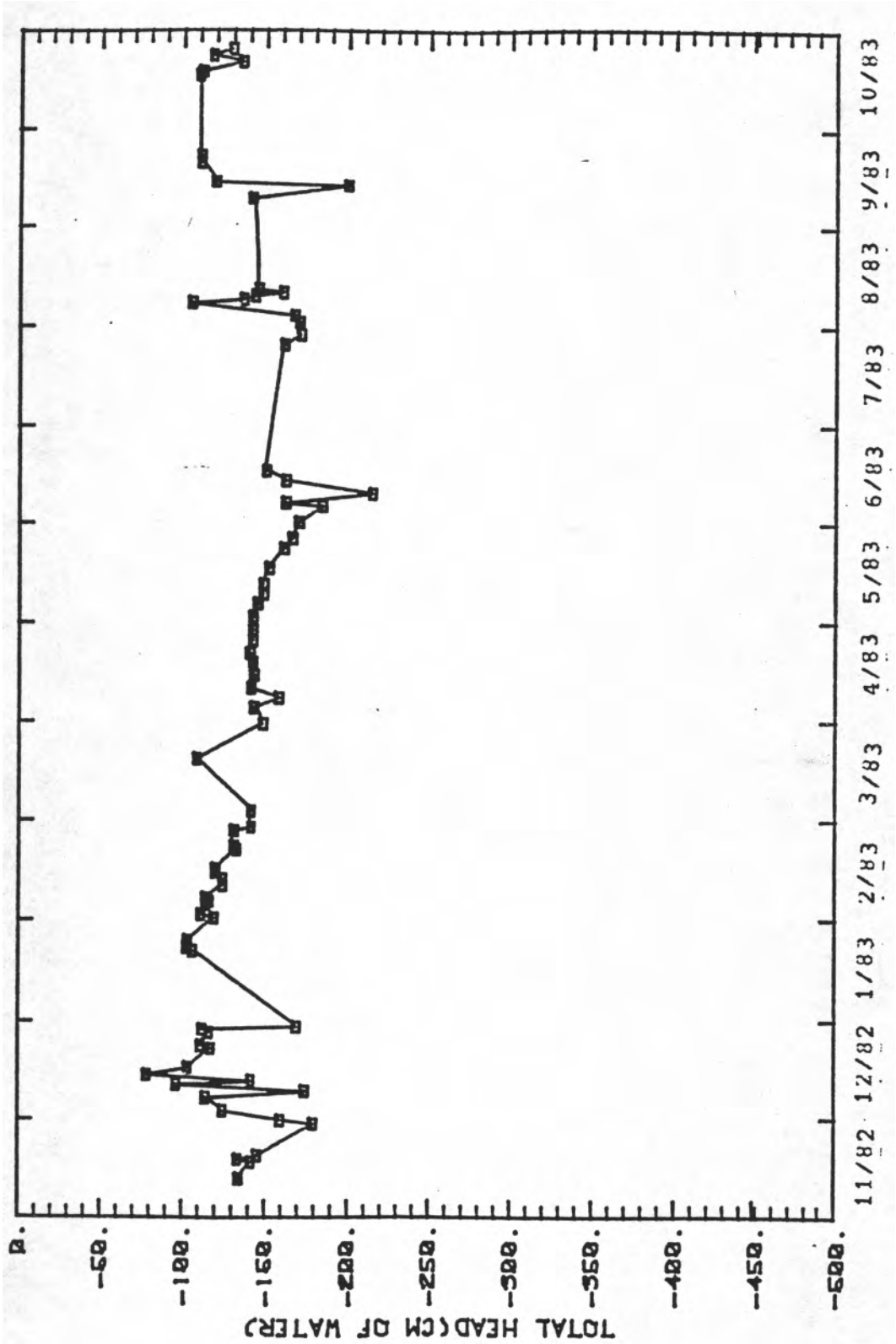

Total Head versus Time for the 61.0cm deptn at Soil-moisture Station 1

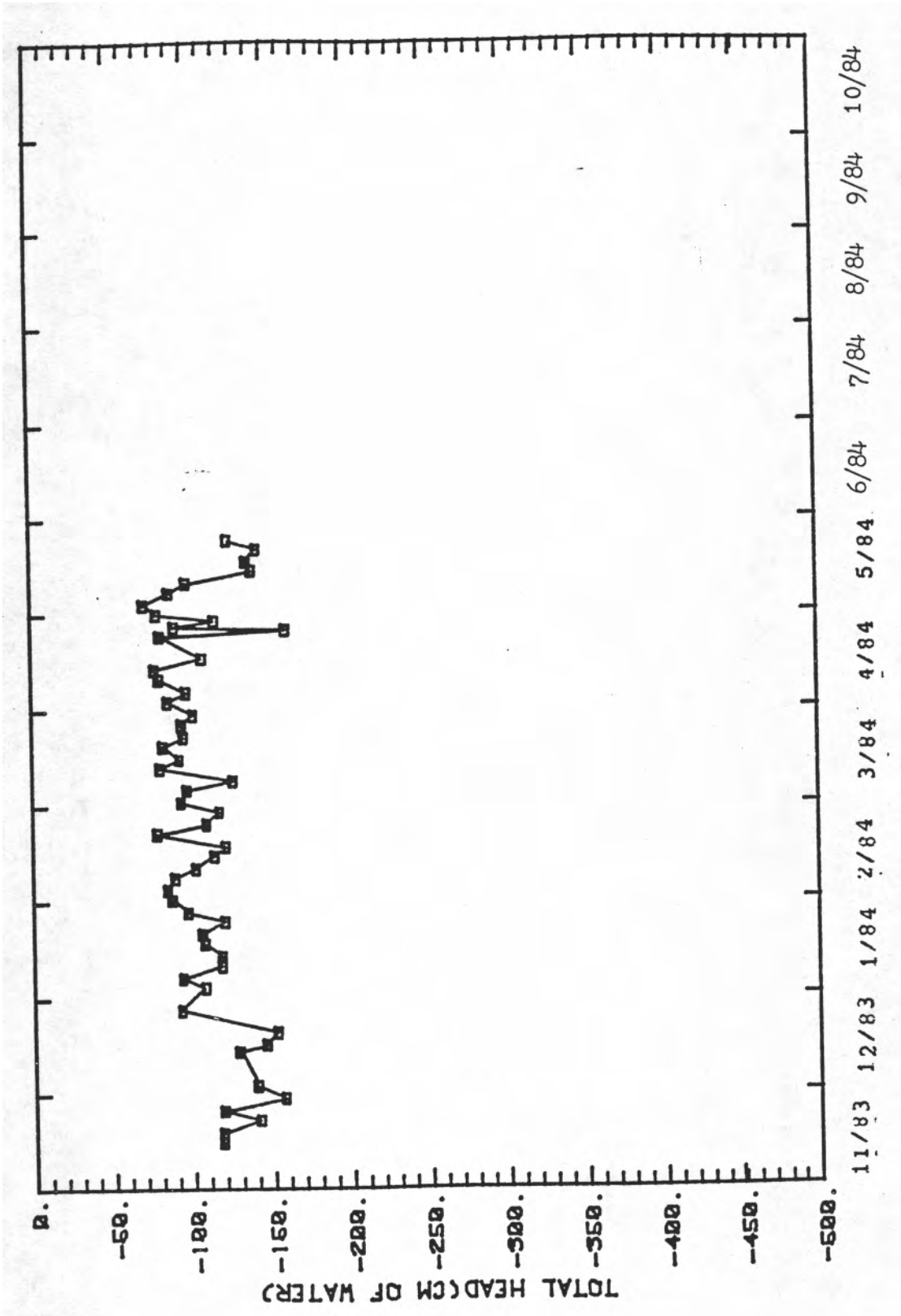

Total Head versus Time for the 61.0cm depth at Soil-moisture Station 1

Total Head versus Time for the 91.5cm depth at Soil-moisture Station 1

Date	Total Head (cm)	Date	Total Head (cm)	Date	Total Head (cm)
12/23/82	-136.	08/09/83	-187.	01/03/84	-148.
12/27/82	-139.	08/10/83	-188.	01/06/84	-134.
12/28/82	-140.	08/11/83	-191.	01/10/84	-154.
01/13/83	-142.	08/12/83	-185.	01/13/84	-156.
01/18/83	-142.	08/16/83	-191.	01/17/84	-149.
01/21/83	-147.	08/23/83	-176.	01/20/84	-146.
01/22/83	-143.	08/24/83	-198.	01/24/84	-157.
01/23/83	-138.	08/25/83	-212.	01/27/84	-130.
01/24/83	-134.	09/01/83	-265.	01/31/84	-124.
01/31/83	-146.	09/02/83	-183.	02/03/84	-123.
02/01/83	-144.	09/06/83	-224.	02/07/84	-130.
02/04/83	-144.	09/08/83	-247.	02/10/84	-135.
02/05/83	-144.	09/09/83	-167.	02/14/84	-153.
02/06/83	-141.	09/13/83	-174.	02/17/84	-158.
02/10/83	-136.	09/14/83	-197.	02/21/84	-202.
02/12/83	-143.	09/16/83	-143.	02/24/84	-128.
02/14/83	-147.	09/20/83	-161.	02/28/84	-143.
02/15/83	-145.	09/22/83	-173.	03/02/84	-129.
02/21/83	-155.	09/23/83	-160.	03/06/84	-133.
02/22/83	-156.	09/24/83	-191.	03/09/84	-157.
02/27/83	-161.	09/25/83	-153.	03/13/84	-118.
02/28/83	-165.	09/27/83	-170.	03/16/84	-129.
03/04/83	-165.	09/28/83	-190.	03/20/84	-123.
03/20/83	-130.	09/30/83	-203.	03/23/84	-129.
03/31/83	-174.	10/03/83	-136.	03/27/84	-134.
04/05/83	-145.	10/04/83	-166.	03/30/84	-133.
04/11/83	-169.	10/06/83	-144.	04/03/84	-127.
04/15/83	-171.	10/07/83	-147.	04/06/84	-127.
04/19/83	-166.	10/11/83	-142.	04/10/84	-120.
04/22/83	-169.	10/13/83	-143.	04/13/84	-117.
04/26/83	-152.	10/18/83	-147.	04/17/84	-137.
04/29/83	-135.	10/21/83	-149.	04/24/84	-117.
05/07/83	-172.	10/23/83	-150.	04/26/84	-164.
05/10/83	-173.	10/25/83	-149.	04/27/84	-122.
05/13/83	-161.	11/18/83	-143.	04/29/84	-145.
05/18/83	-158.	11/22/83	-151.	05/01/84	-115.
06/10/83	-189.	11/25/83	-140.	05/04/84	-110.
07/22/83	-156.	11/29/83	-170.	05/08/84	-119.
07/26/83	-217.	12/03/83	-169.	05/11/84	-133.
07/29/83	-204.	12/14/83	-146.	05/15/84	-163.
08/02/83	-206.	12/16/83	-163.	05/18/84	-159.
08/04/83	-204.	12/20/83	-154.	05/22/84	-167.
08/08/83	-146.	12/27/83	-136.	05/25/84	-152.

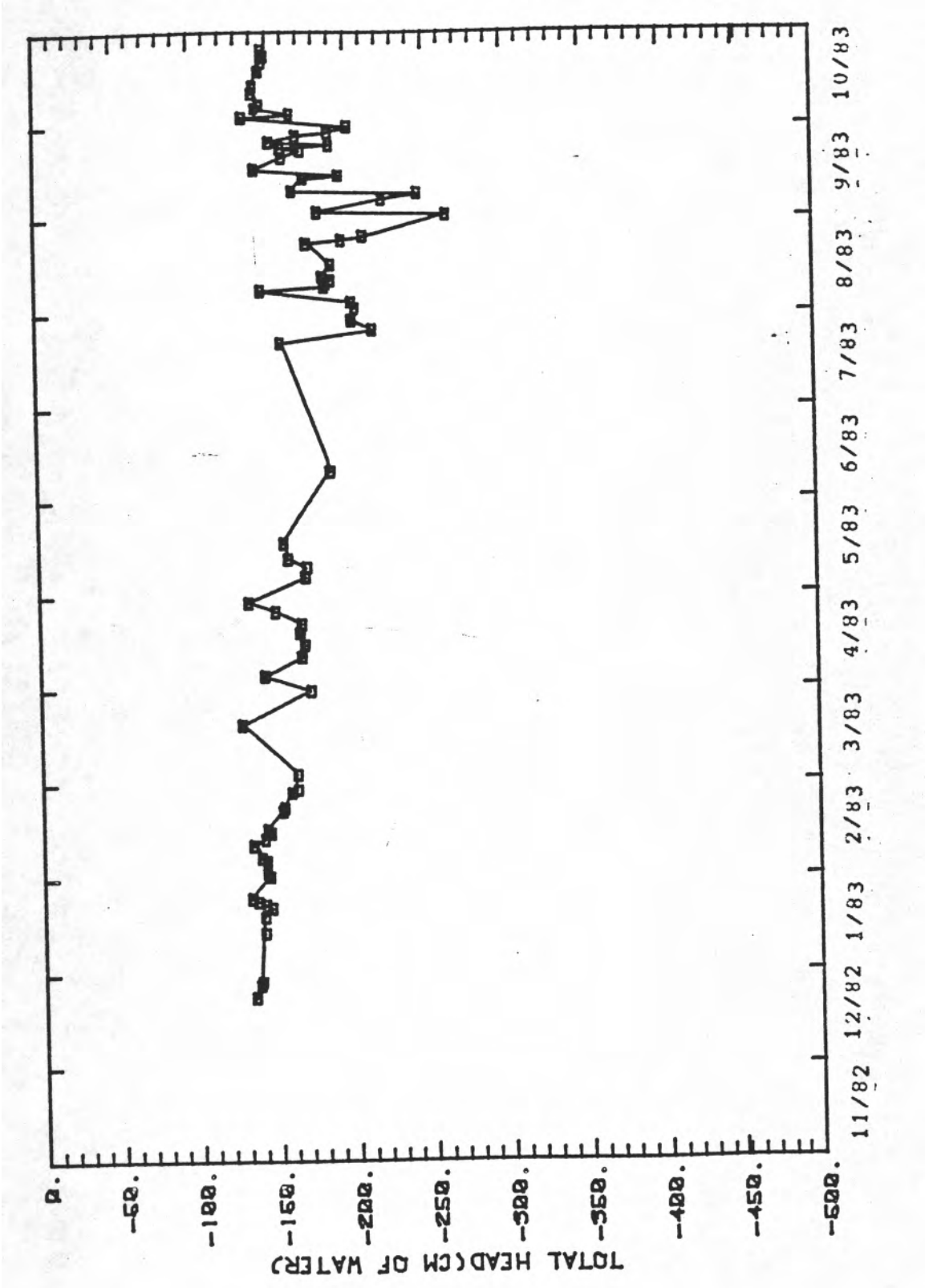

Total Head versus Time for the 91.5cm depth at Soil-moisture Station 1

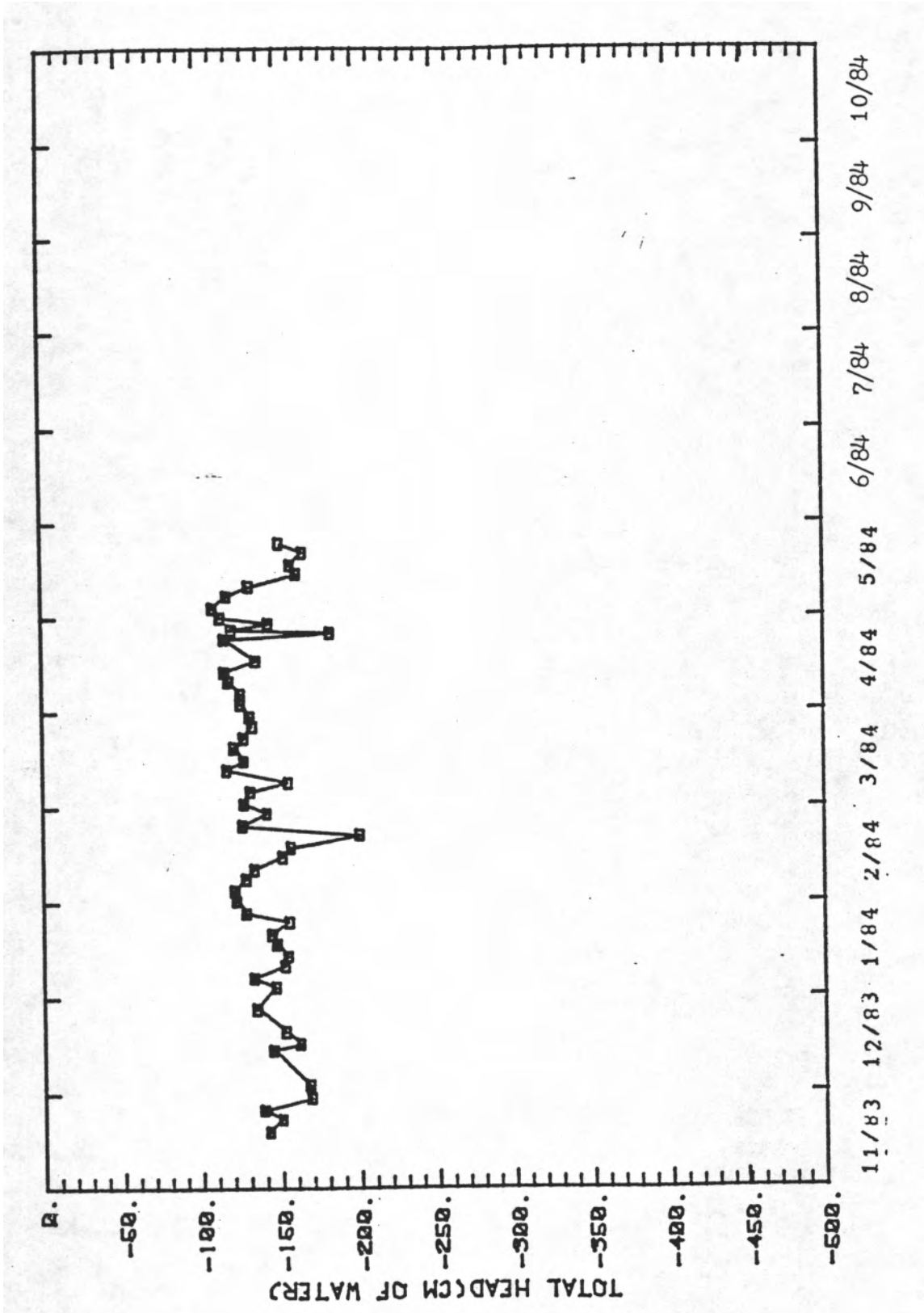

Total Head versus Time for the 91.5cm depth at Soil-moisture Station 1

Water Content versus Time for the 122.0cm depth at Soil-moisture Station 1

Date	Total Head (cm)
11/12/82	-135.
11/17/82	-223.
11/18/82	-194.
11/19/82	-190.
11/23/82	-217.
11/29/82	-216.
11/30/82	-196.
12/03/82	-177.
12/07/82	-163.
12/09/82	-191.
12/10/82	-214.
12/11/82	-184.
12/16/82	-211.
12/22/82	-257.
12/23/82	-170.
12/27/82	-180.
12/28/82	-180.
12/29/82	-214.
01/31/83	-173.
02/01/83	-173.
02/04/83	-172.
02/05/83	-171.
02/06/83	-170.
02/10/83	-169.
02/12/83	-170.
02/14/83	-173.
02/15/83	-172.
02/21/83	-182.
02/22/83	-183.
02/27/83	-182.
02/28/83	-192.
03/04/83	-193.
03/20/83	-164.
03/31/83	-213.
04/05/83	-215.
04/08/83	-215.
04/11/83	-200.
04/15/83	-203.
04/19/83	-203.
04/22/83	-202.
04/26/83	-202.
04/29/83	-201.
05/03/83	-201.
05/07/83	-204.
05/10/83	-207.
05/13/83	-204.
05/18/83	-212.
05/24/83	-223.
05/27/83	-215.
06/01/83	-218.
06/06/83	-222.
06/07/83	-221.
06/10/83	-227.
06/14/83	-237.
06/17/83	-217.
06/21/83	-231.
06/24/83	-238.
06/28/83	-301.
07/05/83	-345.
07/12/83	-269.
07/15/83	-159.
07/19/83	-188.
07/22/83	-204.
07/26/83	-244.
07/29/83	-245.
08/02/83	-245.
08/04/83	-250.
08/08/83	-197.
08/09/83	-235.
08/10/83	-239.
08/11/83	-242.
08/12/83	-245.
08/16/83	-252.
08/23/83	-265.
08/25/83	-230.
09/01/83	-244.
09/02/83	-222.
09/06/83	-262.
09/08/83	-276.
09/09/83	-199.
09/13/83	-213.
09/14/83	-216.
09/16/83	-207.
09/20/83	-192.
09/22/83	-230.
09/23/83	-189.
09/24/83	-241.
09/25/83	-223.
09/26/83	-264.
09/27/83	-273.
09/28/83	-233.
09/30/83	-266.
10/03/83	-246.
10/04/83	-253.
10/06/83	-249.
10/07/83	-235.
10/11/83	-274.
10/13/83	-243.
10/17/83	-294.
10/18/83	-188.
10/21/83	-233.
10/23/83	-267.
10/25/83	-257.

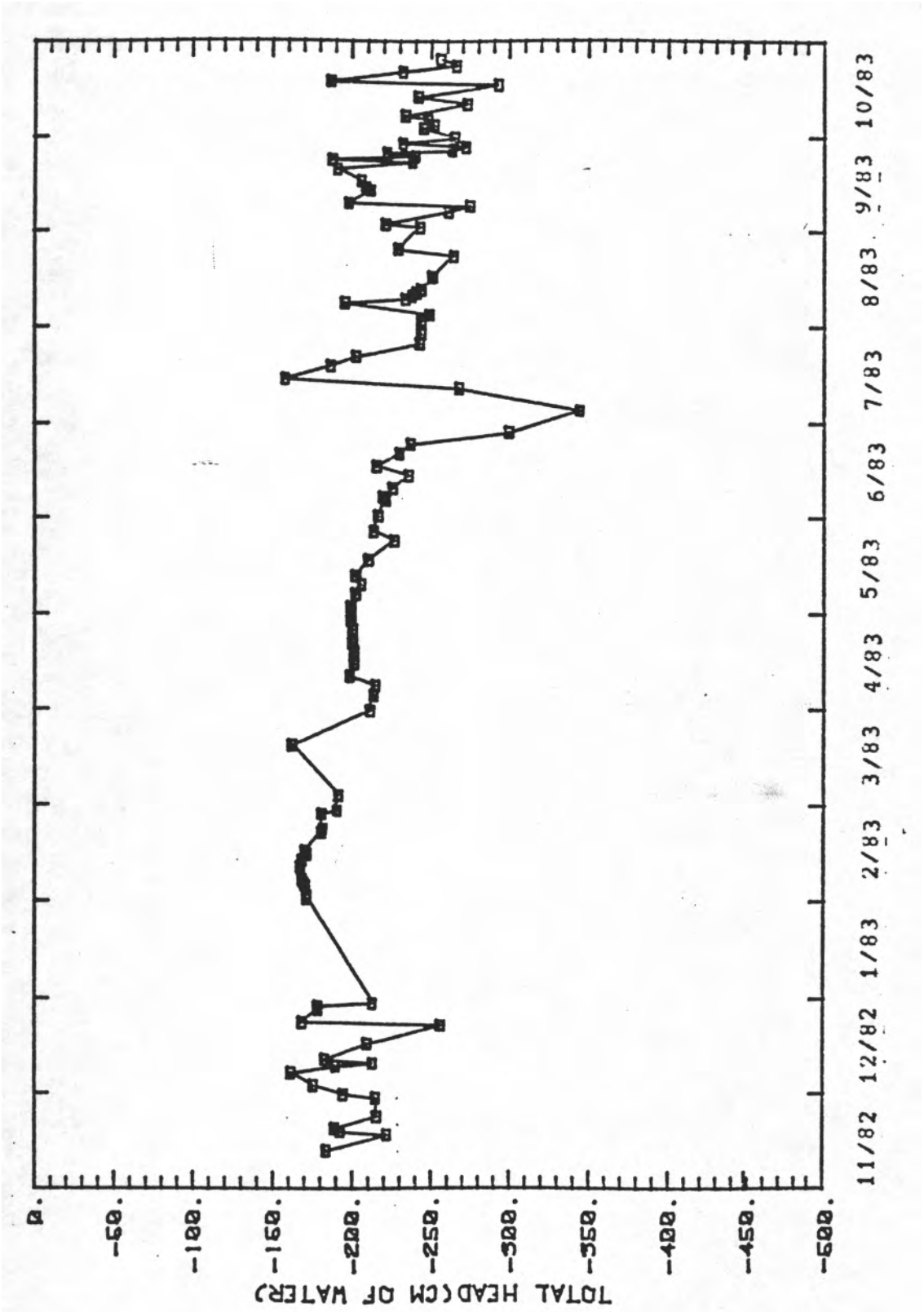

Total Head versus Time for the 122.0cm depth at Soil-moisture Station 1

Water Content versus Time for the 152.5cm depth at Soil-moisture Station 1

Date	Total Head (cm)
11/12/82	-218.
12/23/82	-201.
12/27/82	-241.
12/28/82	-246.
12/29/82	-294.
01/13/83	-201.
01/18/83	-201.
01/21/83	-204.
01/22/83	-206.
01/23/83	-206.
01/24/83	-206.
01/31/83	-201.
02/01/83	-200.
02/04/83	-200.
02/05/83	-199.
02/06/83	-198.
02/10/83	-198.
02/12/83	-197.
02/14/83	-198.
02/15/83	-198.
02/21/83	-205.
02/22/83	-205.
02/27/83	-211.
02/28/83	-214.
03/04/83	-221.
03/20/83	-204.
03/31/83	-227.
04/05/83	-227.
04/08/83	-231.
04/11/83	-219.
04/15/83	-221.
04/19/83	-222.
04/22/83	-221.
04/26/83	-218.
04/29/83	-218.
05/03/83	-221.
05/07/83	-223.
05/10/83	-224.
05/13/83	-223.
05/18/83	-225.
05/24/83	-233.
05/27/83	-223.
06/01/83	-222.
06/06/83	-220.
06/07/83	-190.
06/10/83	-232.
06/14/83	-229.
06/17/83	-219.
06/21/83	-216.
06/24/83	-191.
06/28/83	-176.
07/05/83	-173.
07/12/83	-215.
07/15/83	-224.
07/19/83	-228.
07/22/83	-199.
07/26/83	-247.
07/29/83	-248.
08/02/83	-246.
08/04/83	-246.
08/08/83	-201.
08/09/83	-230.
08/10/83	-236.
08/11/83	-238.
08/12/83	-242.
08/16/83	-246.
08/23/83	-255.
08/24/83	-241.
08/25/83	-246.
09/01/83	-214.
09/02/83	-220.
09/09/83	-215.
09/13/83	-229.
09/14/83	-220.
09/16/83	-225.
09/20/83	-234.
09/22/83	-235.
09/23/83	-241.
09/24/83	-227.
09/25/83	-203.
09/26/83	-216.
09/27/83	-253.
09/28/83	-236.
09/30/83	-262.
10/03/83	-237.
10/04/83	-245.
10/06/83	-217.
10/07/83	-249.
10/11/83	-255.
10/13/83	-249.
10/17/83	-294.
10/18/83	-209.
10/21/83	-226.
10/23/83	-236.
10/25/83	-253.

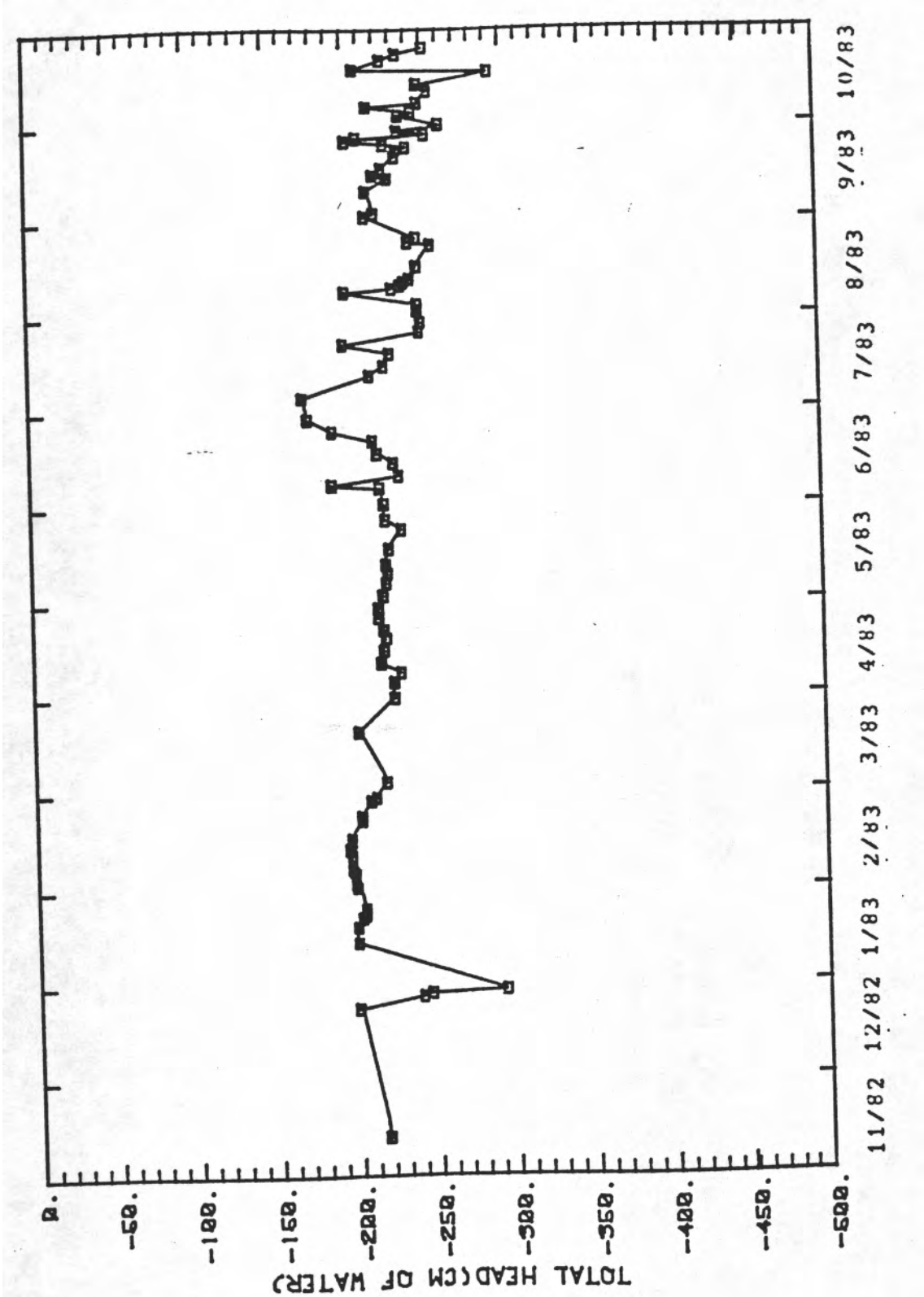

Total Head versus Time for the 152.5cm depth at Soil-moisture Station 1

Total Head versus Time for the 183.0cm depth at Soil-moisture Station 1

Date	Total Head (cm)
11/12/82	-279.
11/17/82	-281.
11/18/82	-284.
11/19/82	-285.
11/23/82	-310.
11/29/82	-316.
11/30/82	-311.
12/03/82	-265.
12/07/82	-234.
12/09/82	-310.
12/10/82	-271.
12/11/82	-257.
12/12/82	-327.
12/14/82	-261.
12/16/82	-237.
12/22/82	-309.
12/23/82	-266.
12/28/82	-332.
12/29/82	-376.
01/13/83	-271.
01/18/83	-285.
01/21/83	-251.
01/22/83	-265.
01/24/83	-242.
01/31/83	-245.
02/01/83	-256.
02/05/83	-272.
02/06/83	-275.
02/10/83	-273.
02/12/83	-235.
02/14/83	-253.
02/15/83	-248.
02/21/83	-241.
02/22/83	-252.
02/27/83	-236.
02/28/83	-265.
03/04/83	-256.
03/20/83	-256.
03/31/83	-261.
04/05/83	-259.
04/08/83	-262.
04/11/83	-231.
04/15/83	-256.
04/19/83	-256.
04/22/83	-255.
04/26/83	-256.
04/29/83	-257.
05/03/83	-260.
05/07/83	-264.
05/10/83	-261.
05/13/83	-262.
05/18/83	-264.
05/24/83	-266.
05/27/83	-267.
06/01/83	-262.
06/06/83	-260.
06/07/83	-264.
06/10/83	-265.
06/14/83	-268.
06/17/83	-266.
06/21/83	-269.
06/24/83	-268.
07/12/83	-268.
07/15/83	-283.
07/19/83	-300.
07/26/83	-264.
07/29/83	-270.
08/02/83	-273.
08/04/83	-273.
08/08/83	-227.
08/09/83	-255.
08/10/83	-258.
08/11/83	-260.
08/12/83	-249.
08/16/83	-265.
08/23/83	-255.
04/06/84	-244.
04/10/84	-232.
04/17/84	-245.
04/24/84	-215.
04/26/84	-309.
04/27/84	-259.
04/29/84	-268.
05/01/84	-215.
05/04/84	-205.
05/08/84	-245.
05/11/84	-229.
05/15/84	-290.
05/18/84	-290.
05/22/84	-279.
05/25/84	-273.

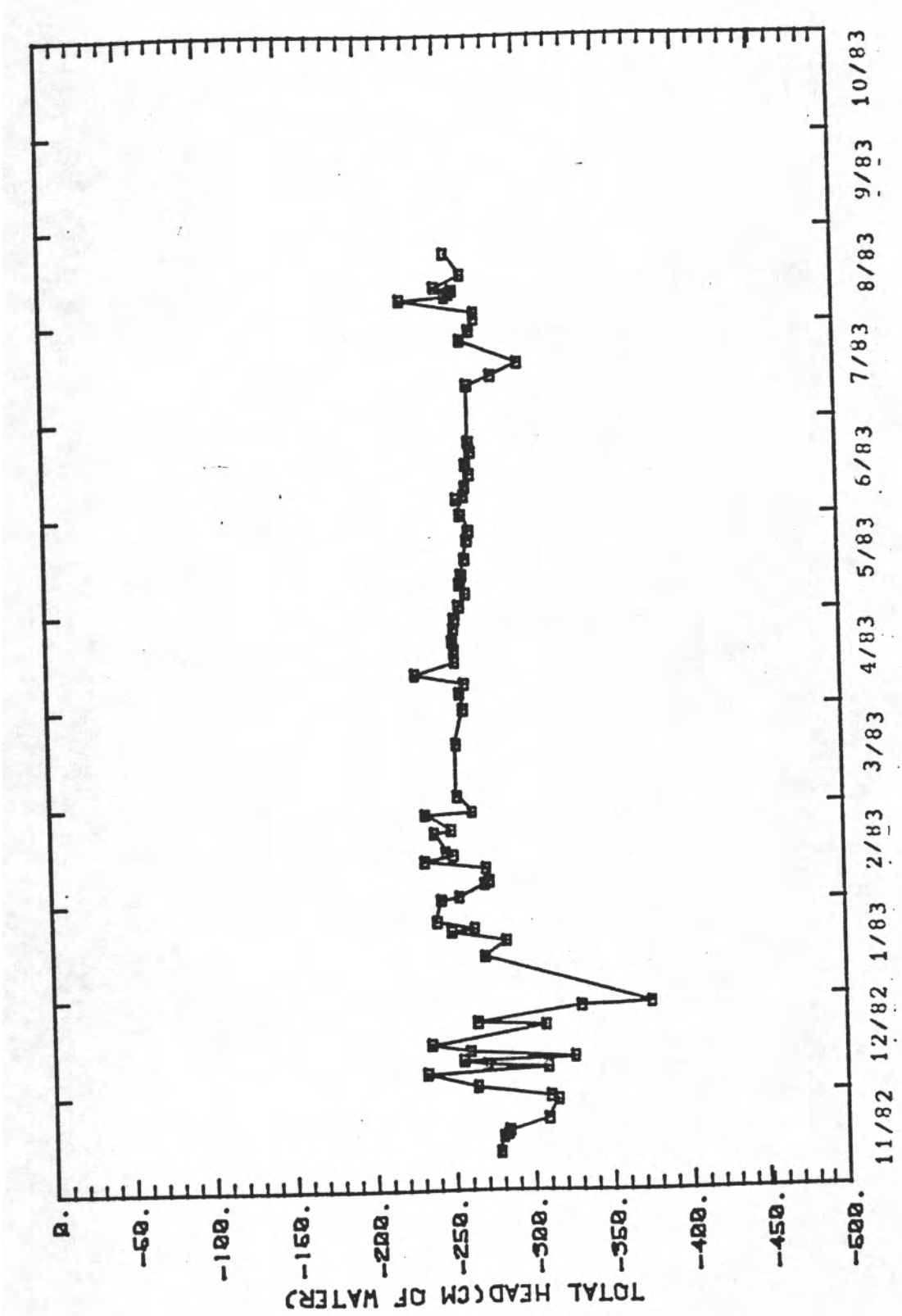

Total Head versus Time for the 183.0cm depth at Soil-moisture Station 1

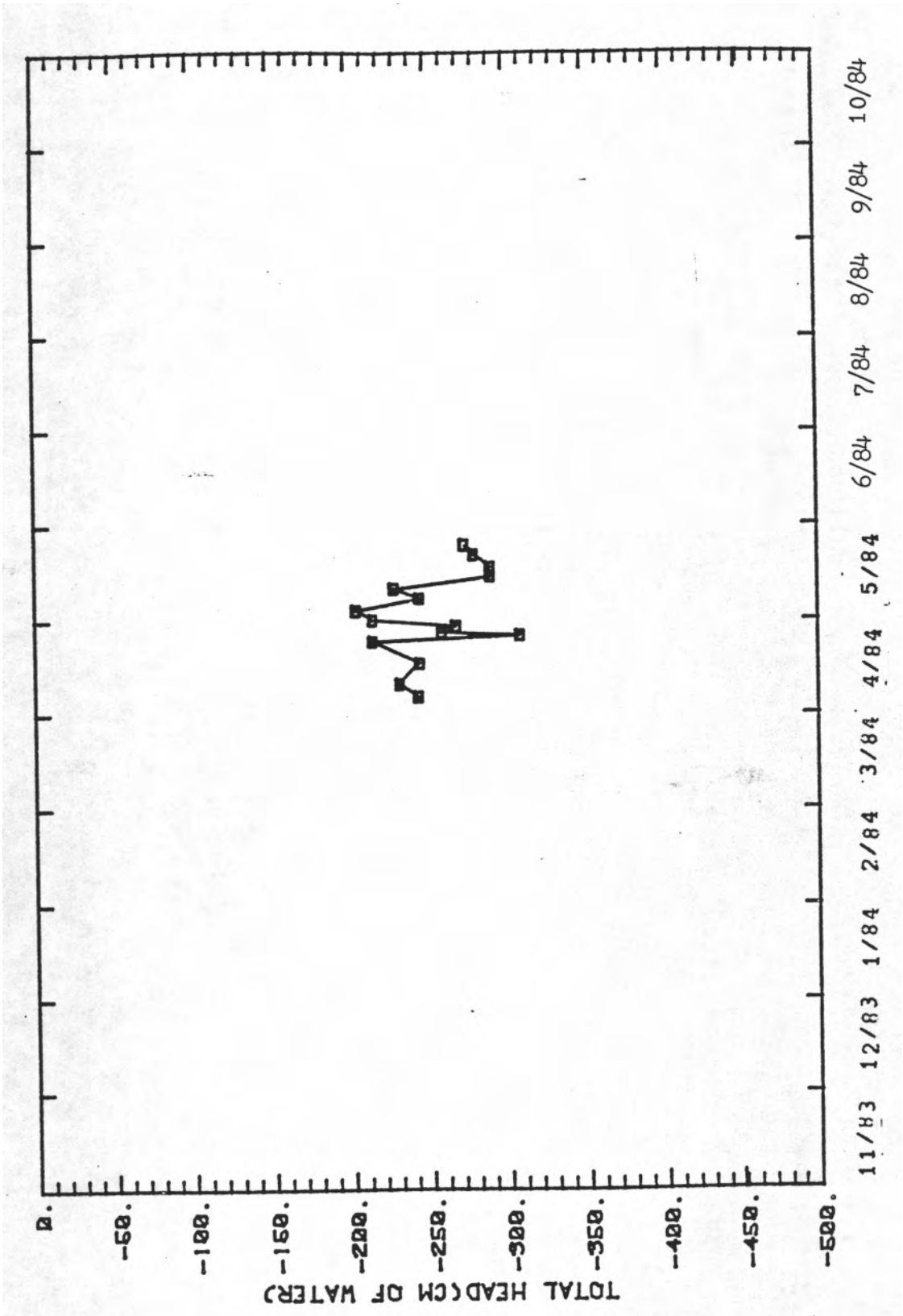

Total Head versus Time for the 183.0cm depth at Soil-moisture Station 1

Total Head versus Time for the 213.5cm depth at Soil-moisture Station 1

Date	Total Head (cm)
08/09/83	-317.
08/11/83	-300.
08/12/83	-302.
08/16/83	-341.
08/23/83	-277.
08/24/83	-273.
09/02/83	-278.
09/09/83	-331.
09/13/83	-304.
09/16/83	-339.
09/20/83	-284.
09/23/83	-305.
09/27/83	-274.
09/28/83	-310.
10/06/83	-327.
11/15/83	-272.
11/18/83	-262.
11/22/83	-285.
12/27/83	-355.
01/03/84	-361.
01/06/84	-363.
01/10/84	-390.
01/13/84	-391.
01/17/84	-383.
01/20/84	-385.
01/24/84	-385.
01/27/84	-364.
01/31/84	-362.
02/03/84	-355.
02/10/84	-333.
02/17/84	-363.
02/21/84	-318.
02/24/84	-323.
02/28/84	-358.
03/02/84	-333.
03/06/84	-355.
03/09/84	-354.
03/13/84	-325.
03/16/84	-341.
03/20/84	-332.
03/23/84	-352.
03/27/84	-357.
03/30/84	-322.
04/03/84	-336.
04/06/84	-333.
04/10/84	-332.
04/13/84	-359.
04/17/84	-339.
04/24/84	-347.
04/26/84	-328.
04/27/84	-312.
04/29/84	-346.
05/01/84	-318.
05/04/84	-328.
05/11/84	-324.
05/15/84	-407.
05/18/84	-431.
05/22/84	-436.
05/25/84	-443.

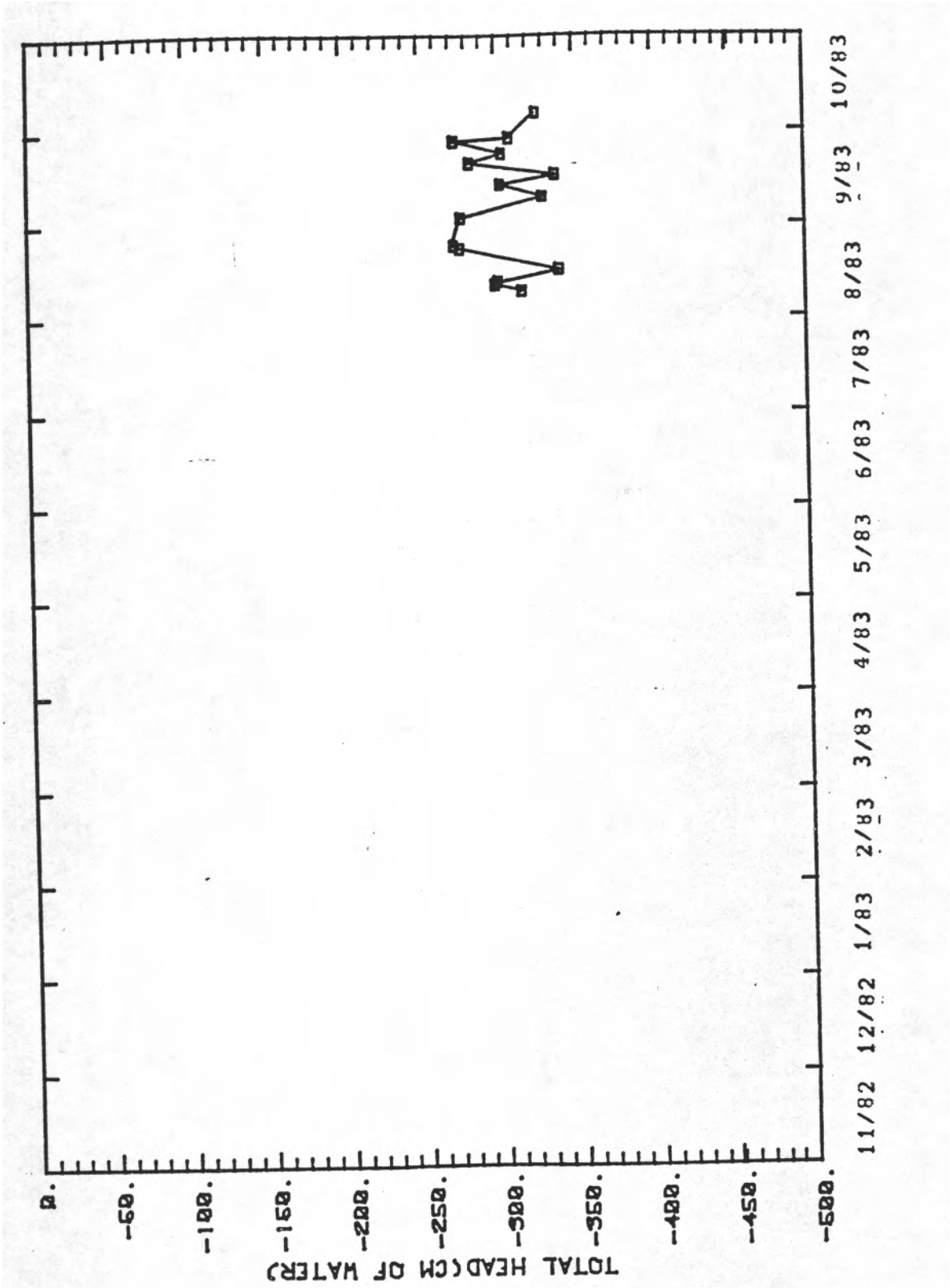

Total Head versus Time for the 213.5cm depth at Soil-moisture Station 1

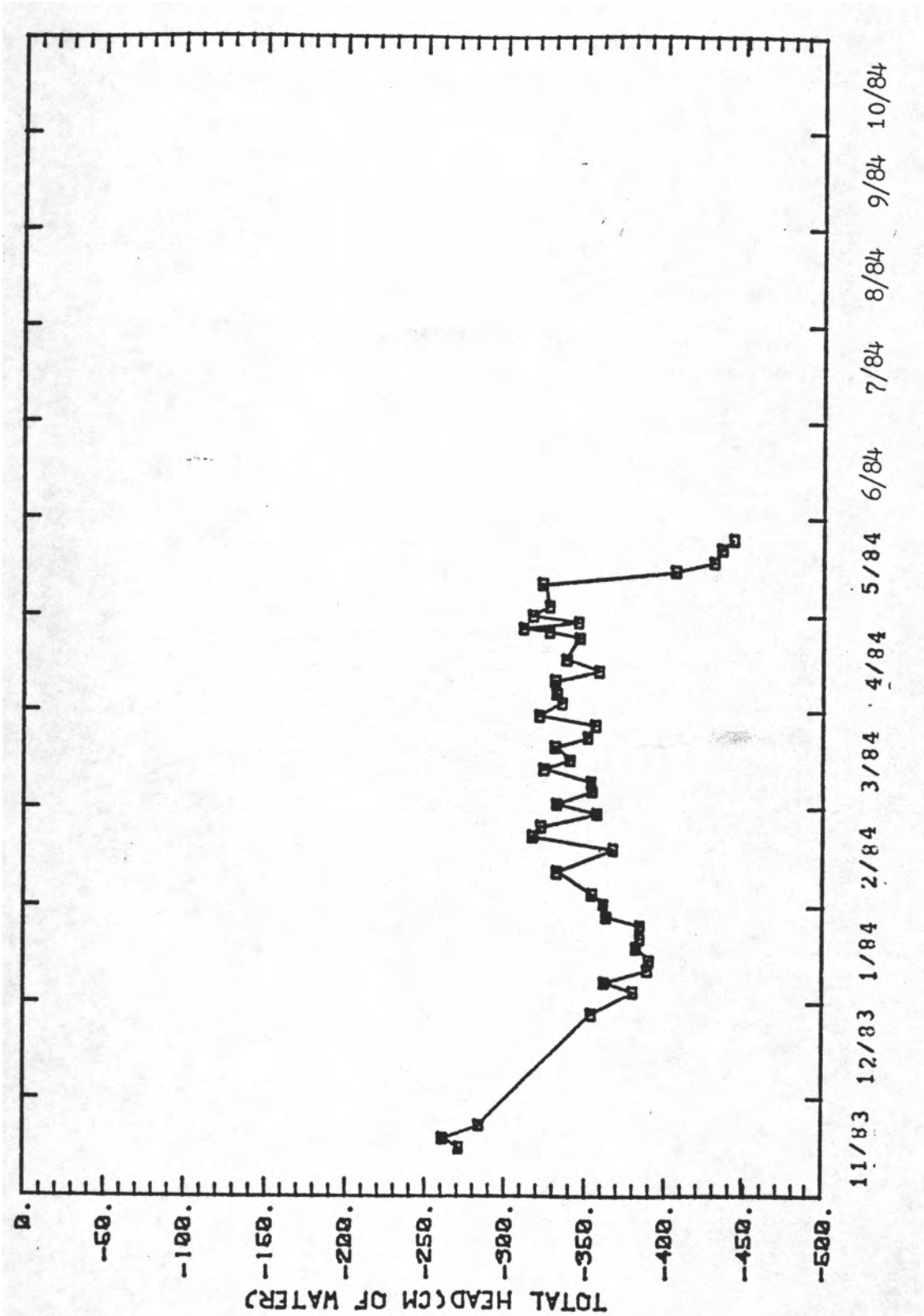

Total Head versus Time for the 213.5cm depth at Soil-moisture Station 1

Total Head versus Time for the 244.0cm depth at Soil-moisture Station 1

Date	Total Head (cm)
08/09/83	-320.
08/10/83	-323.
08/11/83	-327.
08/12/83	-335.
08/16/83	-334.
08/23/83	-320.
08/24/83	-313.
08/25/83	-357.
09/01/83	-373.
09/02/83	-338.
09/06/83	-370.
09/08/83	-389.
09/09/83	-360.
09/13/83	-355.
09/14/83	-359.
09/16/83	-374.
09/20/83	-317.
09/23/83	-314.
09/27/83	-317.
09/28/83	-310.
10/06/83	-328.
10/07/83	-355.
10/11/83	-284.
10/13/83	-268.
10/18/83	-331.
10/21/83	-341.
10/23/83	-348.
10/25/83	-355.

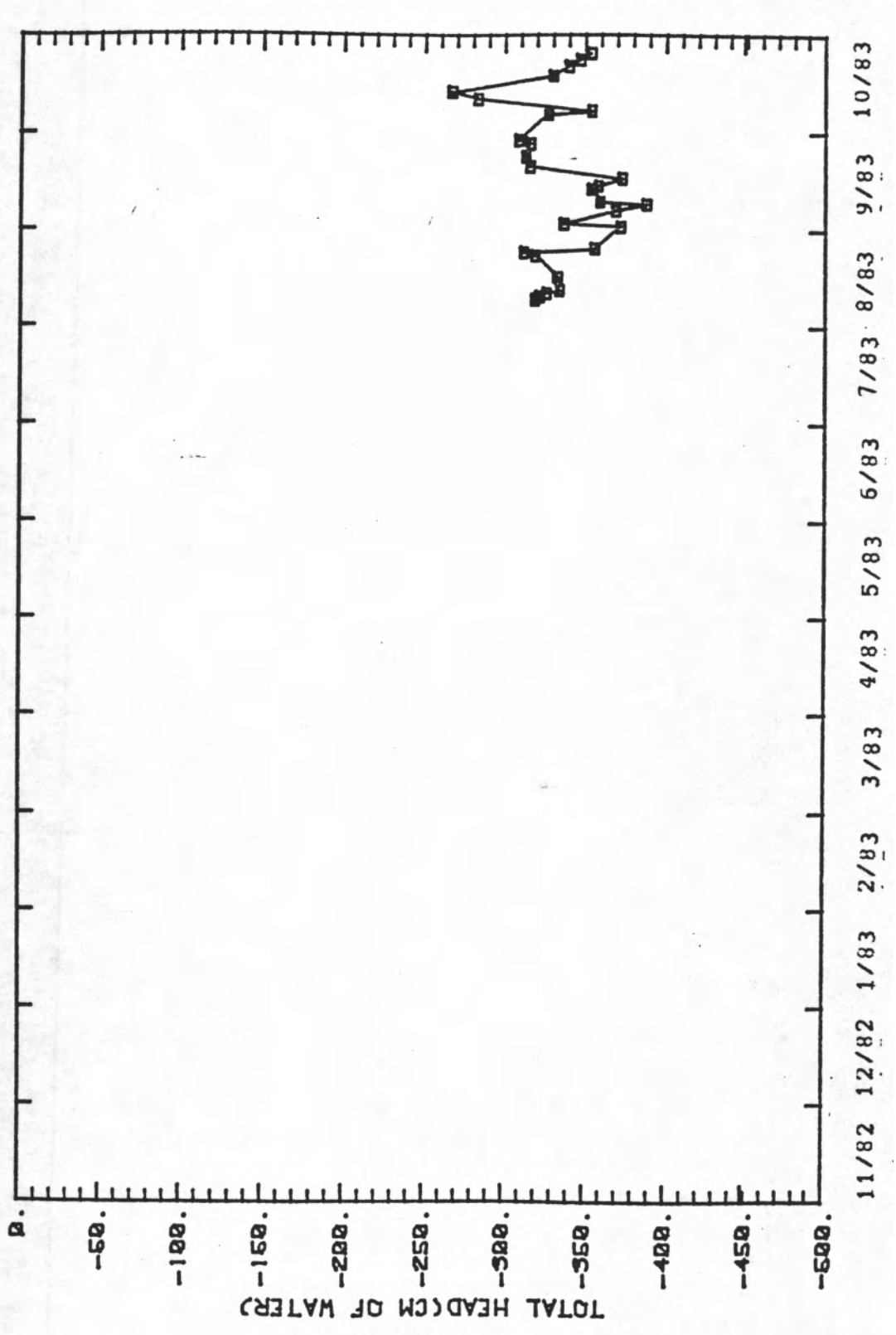

Total Head versus Time for the 244.0cm depth at Soil-moisture Station 1

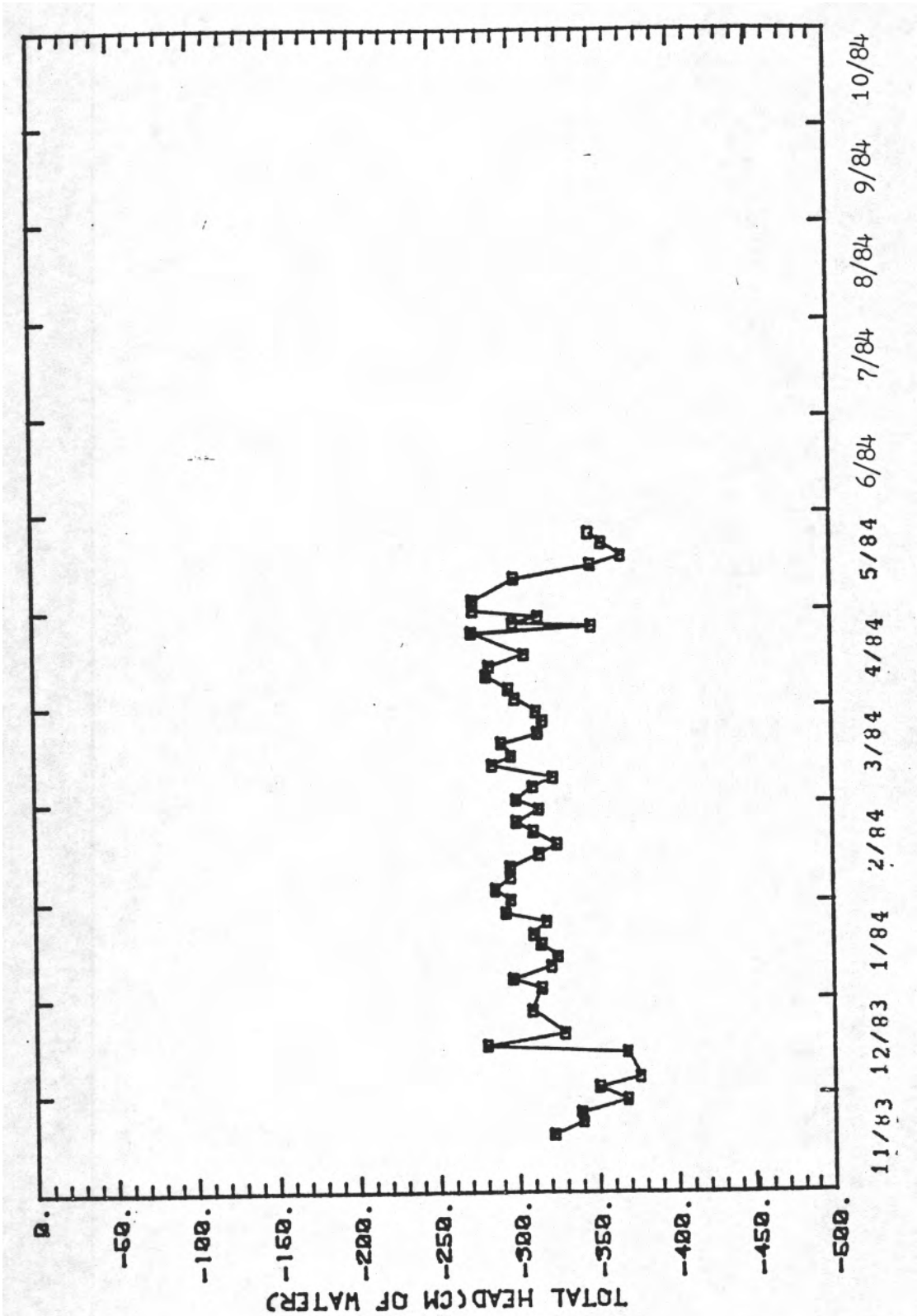

Total Head versus Time for the 244.0cm depth at Soil-moisture Station 1

Total Head versus Time for the 30.5cm depth at Soil-moisture Station 1

Mercury Tensiometer

Date	Total Head (cm)
04/27/84	-127.
04/29/84	-134.
05/15/84	-132.
05/18/84	-73.
05/22/84	-166.
05/25/84	-113.
05/29/84	-68.

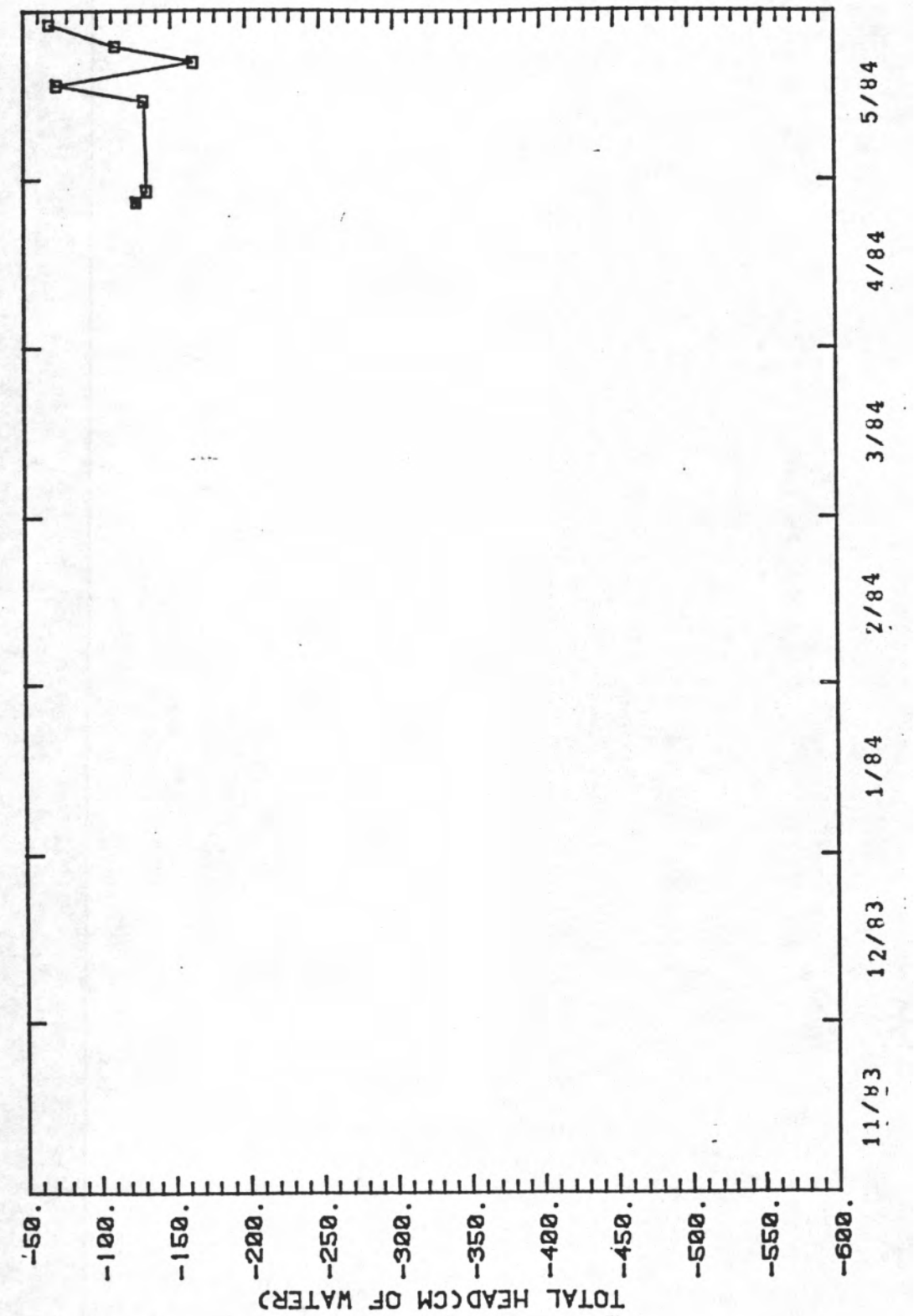

Total Head versus Time for the 30.5 cm depth Mercury Tensiometer at Soil-moisture Station 1.

Total Head versus Time for the 61.0cm deptn at Soil-moisture Station 1

Mercury Tensiometer

Date	Total Head (cm)
04/27/84	-144.
04/29/84	-147.
05/01/84	-137.
05/15/84	-149.
05/18/84	-148.
05/22/84	-155.
05/25/84	-147.
05/29/84	-140.

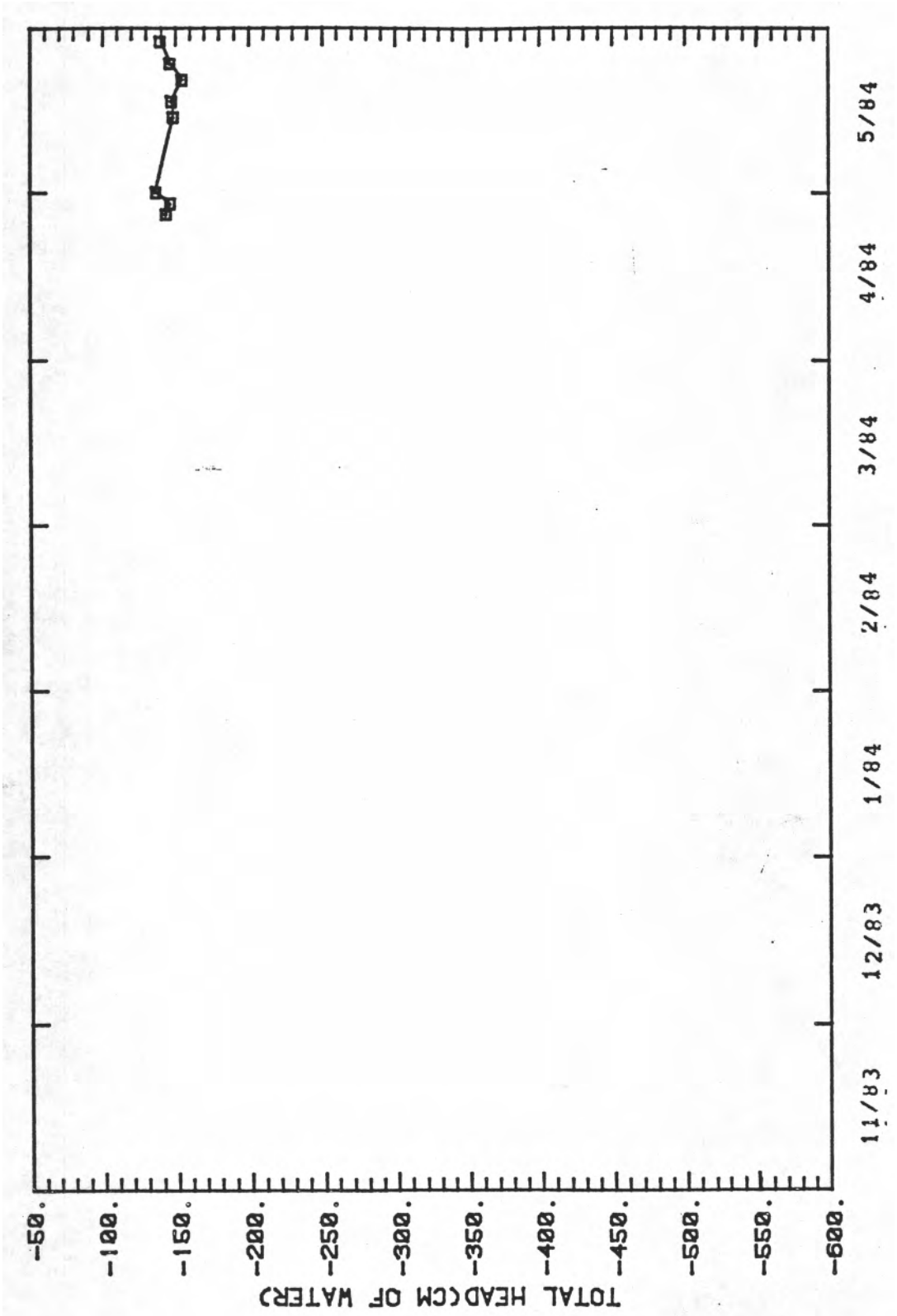

Total Head versus Time for the 61.0 cm depth Mercury Tensiometer at Soil-moisture Station 1.

Total Head versus Time for the 91.5cm deptn at Soil-moisture Station 1

Mercury Tensiometer

Date	Total Head (cm)
04/27/84	-190.
04/29/84	-189.
05/01/84	-94.
05/15/84	-213.
05/18/84	-208.
05/22/84	-214.
05/25/84	-207.
05/29/84	-202.

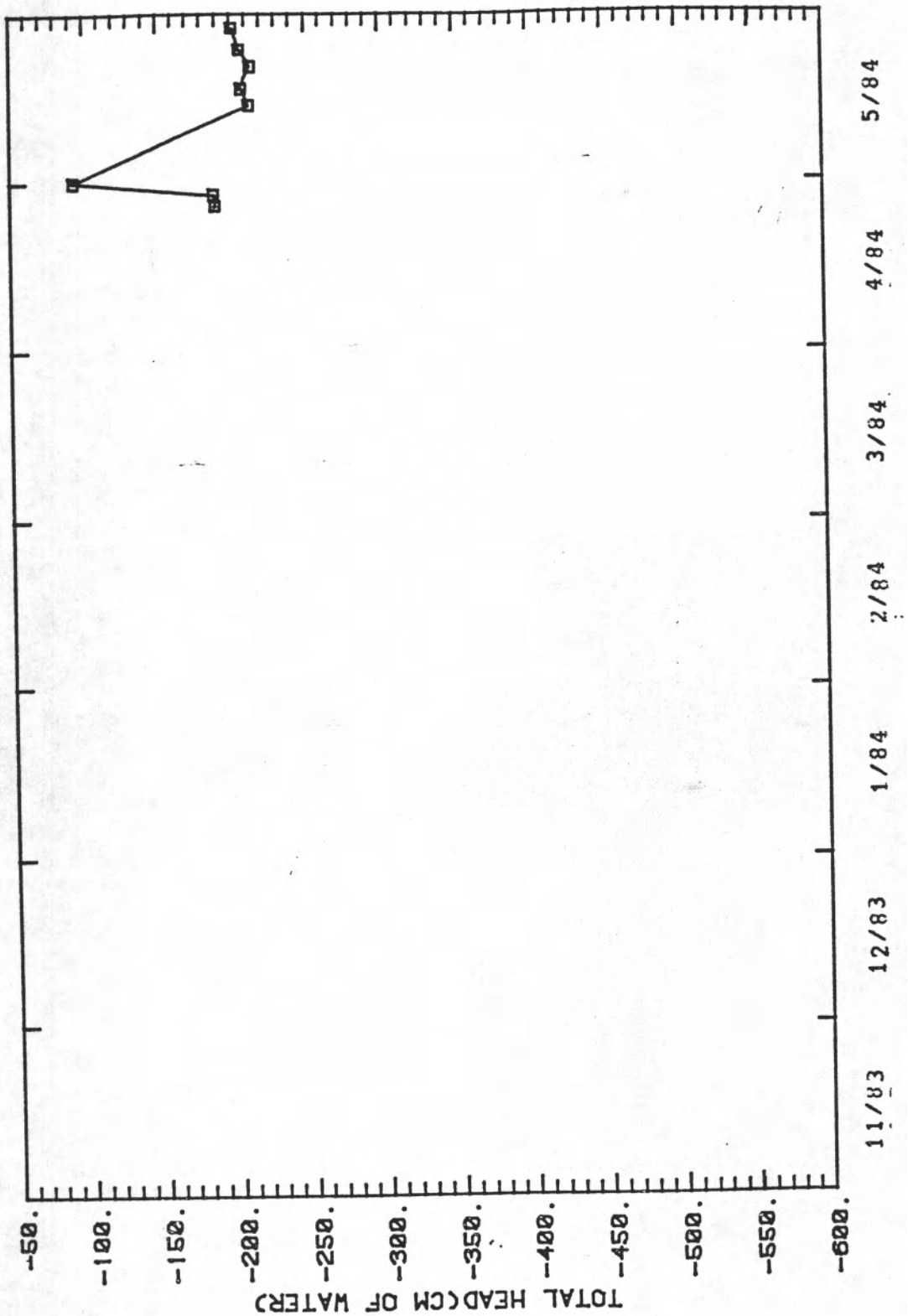

Total Head versus Time for the 91.0 cm depth Mercury Tensiometer at Soil-moisture Station 1.

Total Head versus Time for the 122.0cm depth at Soil-moisture Station 1

Mercury Tensiometer

Date	Total Head (cm)
04/27/84	-117.
04/29/84	-128.
05/15/84	-157.
05/18/84	-174.
05/22/84	-174.
05/25/84	-166.
05/29/84	-178.

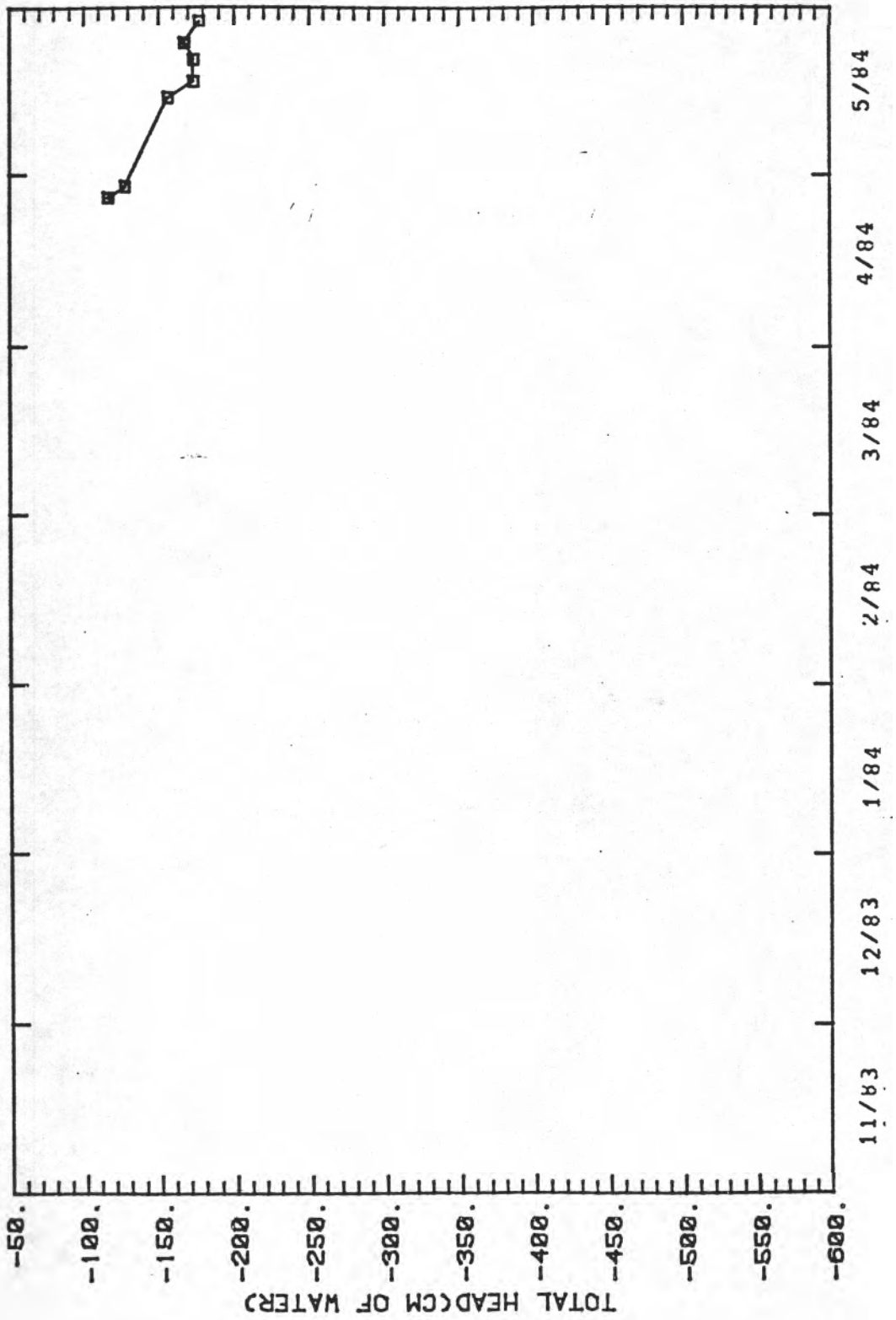

Total Head versus Time for the 122.0 cm depth Mercury Tensiometer at Soil-moisture Station 1.

Water-Table Elevations versus Time for Observation Well Number 1

Date	Elevation Above MSL (ft)
10/03/83	4846.4
10/04/83	4846.5
10/06/83	4846.8
10/07/83	4846.9
10/11/83	4847.1
10/13/83	4847.1
10/18/83	4847.1
10/21/83	4847.0
10/25/83	4846.9
11/01/83	4846.8
11/08/83	4846.8
11/15/83	4846.7
11/22/83	4846.6
11/29/83	4846.5
12/06/83	4846.4
12/13/83	4846.2
12/20/83	4846.1
12/27/83	4846.0
01/03/84	4845.9
01/10/84	4845.8
01/17/84	4845.7
01/24/84	4845.6
01/31/84	4845.5
02/07/84	4845.5
02/14/84	4845.4
02/21/84	4845.4
02/28/84	4845.3
03/06/84	4845.2
03/13/84	4845.1
03/20/84	4845.0
03/27/84	4845.0
04/03/84	4844.9
04/10/84	4844.3
04/17/84	4844.8
04/24/84	4844.7
05/01/84	4844.7
05/08/84	4844.6
05/15/84	4844.5
05/22/84	4844.4
05/29/84	4844.1

Water-Table Elevations versus Time for Observation

Well Number 2

Date	Elevation Above MSL (ft)	Date	Elevation Above MSL (ft)
10/03/83	4848.9	01/10/84	4845.5
10/04/83	4848.8	01/13/84	4845.5
10/06/83	4848.6	01/17/84	4845.4
10/07/83	4848.4	01/20/84	4845.4
10/11/83	4847.9	01/24/84	4845.3
10/13/83	4847.7	01/27/84	4845.3
10/18/83	4847.4	01/31/84	4845.3
10/21/83	4847.2	02/03/84	4845.2
10/25/83	4847.0	02/07/84	4845.2
10/28/83	4846.9	02/10/84	4845.2
11/01/83	4846.8	02/24/84	4845.0
11/04/83	4846.6	03/13/84	4844.8
11/15/83	4846.5	03/16/84	4844.8
11/22/83	4846.4	03/20/84	4844.8
11/25/83	4846.4	03/23/84	4844.7
11/29/83	4846.2	04/03/84	4844.6
12/03/83	4846.1	04/06/84	4844.6
12/06/83	4846.1	04/10/84	4844.5
12/14/83	4845.9	04/13/84	4844.5
12/16/83	4845.9	04/17/84	4844.5
12/20/83	4845.9	04/20/84	4844.4
12/23/83	4845.8	05/04/84	4844.3
12/27/83	4845.7	05/11/84	4844.2
12/30/83	4845.7	05/25/84	4844.0
01/03/84	4845.6	05/29/84	4843.9
01/06/84	4845.6		

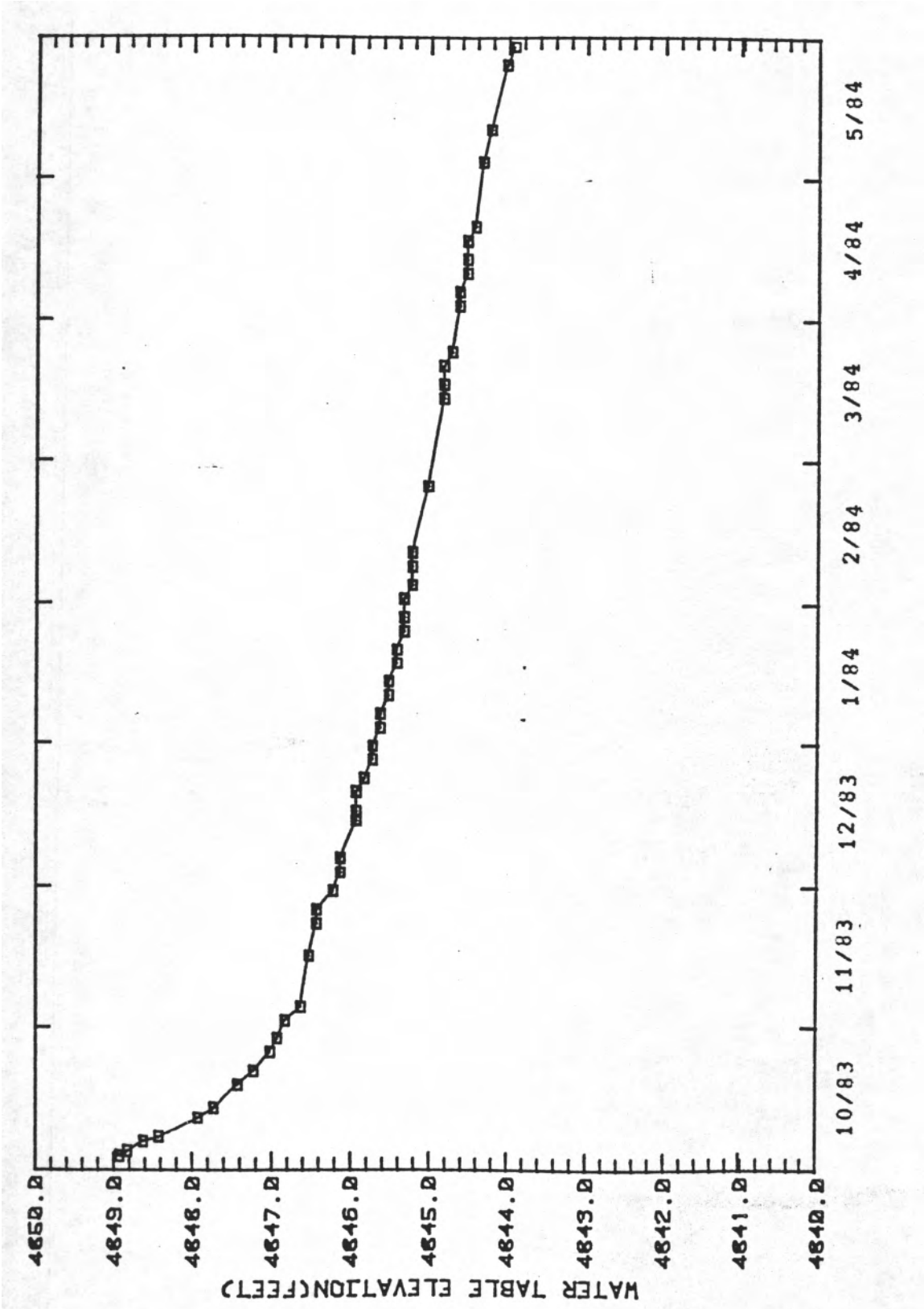

Water-Table Elevations versus Time for Observation Well Number 2

Water-Table Elevations versus Time for Observation Well Number 3

Date	Elevation Above MSL (ft)	Date	Elevation Above MSL (ft)
10/03/83	4845.7	03/06/84	4843.5
10/04/83	4845.9	03/09/84	4843.5
10/11/83	4846.0	03/13/84	4843.5
10/18/83	4845.7	03/16/84	4843.5
10/25/83	4845.5	03/20/84	4843.4
11/01/83	4845.3	03/23/84	4843.4
11/08/83	4845.4	03/27/84	4843.4
11/15/83	4845.1	03/30/84	4843.3
11/22/83	4845.0	04/03/84	4843.3
11/25/83	4845.0	04/06/84	4843.3
11/29/83	4844.9	04/10/84	4843.2
12/06/83	4844.7	04/13/84	4843.2
12/13/83	4844.6	04/17/84	4843.2
12/20/83	4844.5	04/20/84	4843.1
12/27/83	4844.4	04/24/84	4843.1
01/03/84	4844.3	04/27/84	4843.1
01/10/84	4844.2	05/01/84	4843.0
01/17/84	4844.1	05/04/84	4843.0
01/24/84	4844.0	05/08/84	4842.9
01/31/84	4843.9	05/11/84	4842.9
02/07/84	4843.9	05/15/84	4842.8
02/14/84	4843.8	05/18/84	4842.9
02/21/84	4843.7	05/22/84	4842.7
02/28/84	4843.6	05/25/84	4842.6
		05/29/84	4842.5

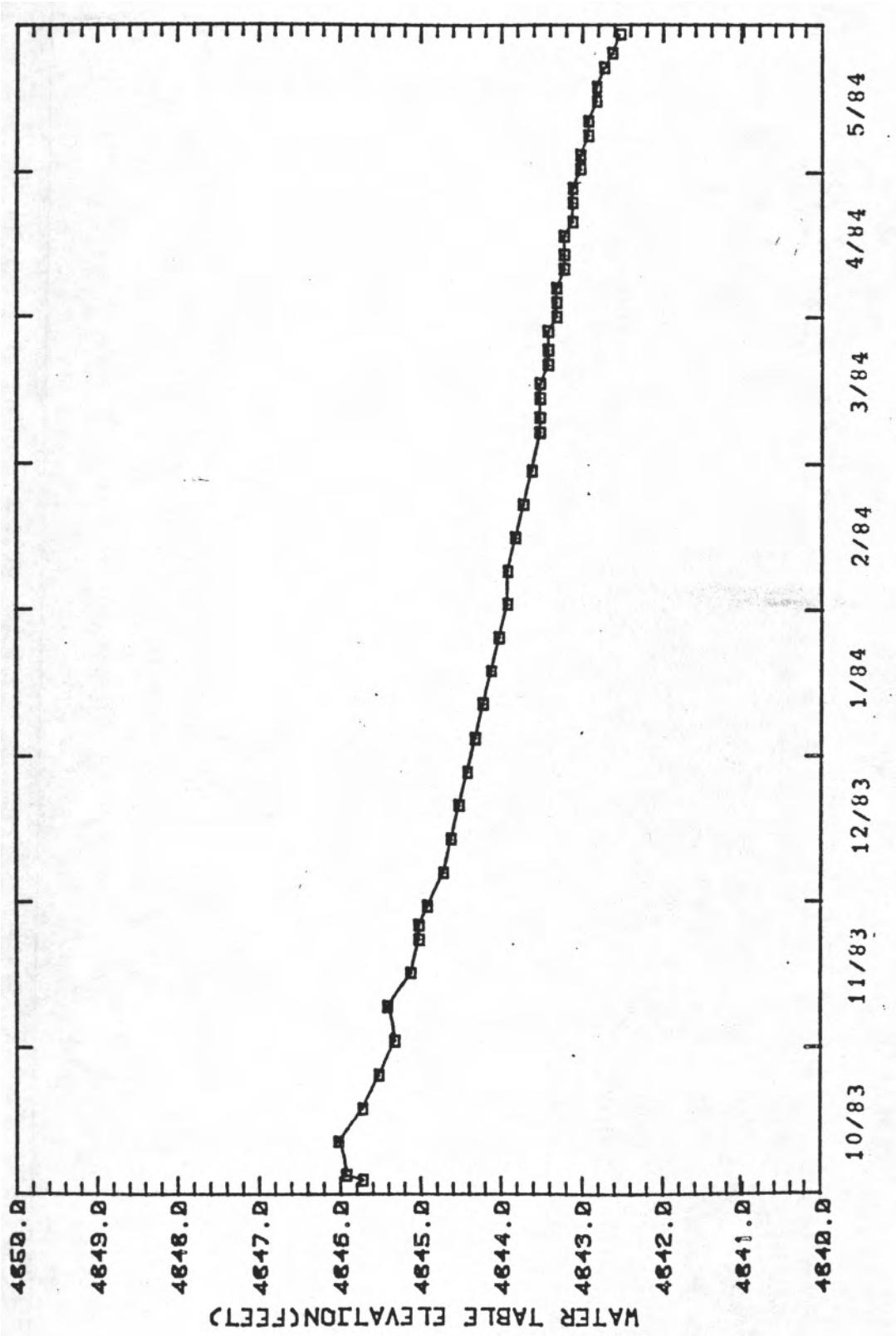

Water-Table Elevations versus Time for Observation Well Number 3

Water-Table Elevations versus Time for Observation Well Number 4

Date	Elevation Above MSL (ft)
10/04/83	4846.0
10/11/83	4846.5
10/18/83	4846.7
10/25/83	4846.6
11/01/83	4846.6
11/08/83	4946.6
11/15/83	4846.5
11/22/83	4846.4
11/29/83	4846.3
12/06/83	4846.2
12/13/83	4846.1
12/20/83	4846.0
12/27/83	4945.9
01/03/84	4845.8
01/10/84	4845.7
01/17/84	4845.6
01/24/84	4845.6
01/31/84	4845.5
02/07/84	4845.4
02/14/84	4845.4
02/21/84	4845.2
02/28/84	4845.2
03/06/84	4845.1
03/13/84	4945.0
03/20/84	4845.0
03/27/84	4844.9
04/03/84	4844.9
04/10/84	4844.8
04/17/84	4844.7
04/24/84	4844.7
05/01/84	4844.6
05/08/84	4844.5
05/15/84	4844.4
05/22/84	4844.4
05/29/84	4844.1

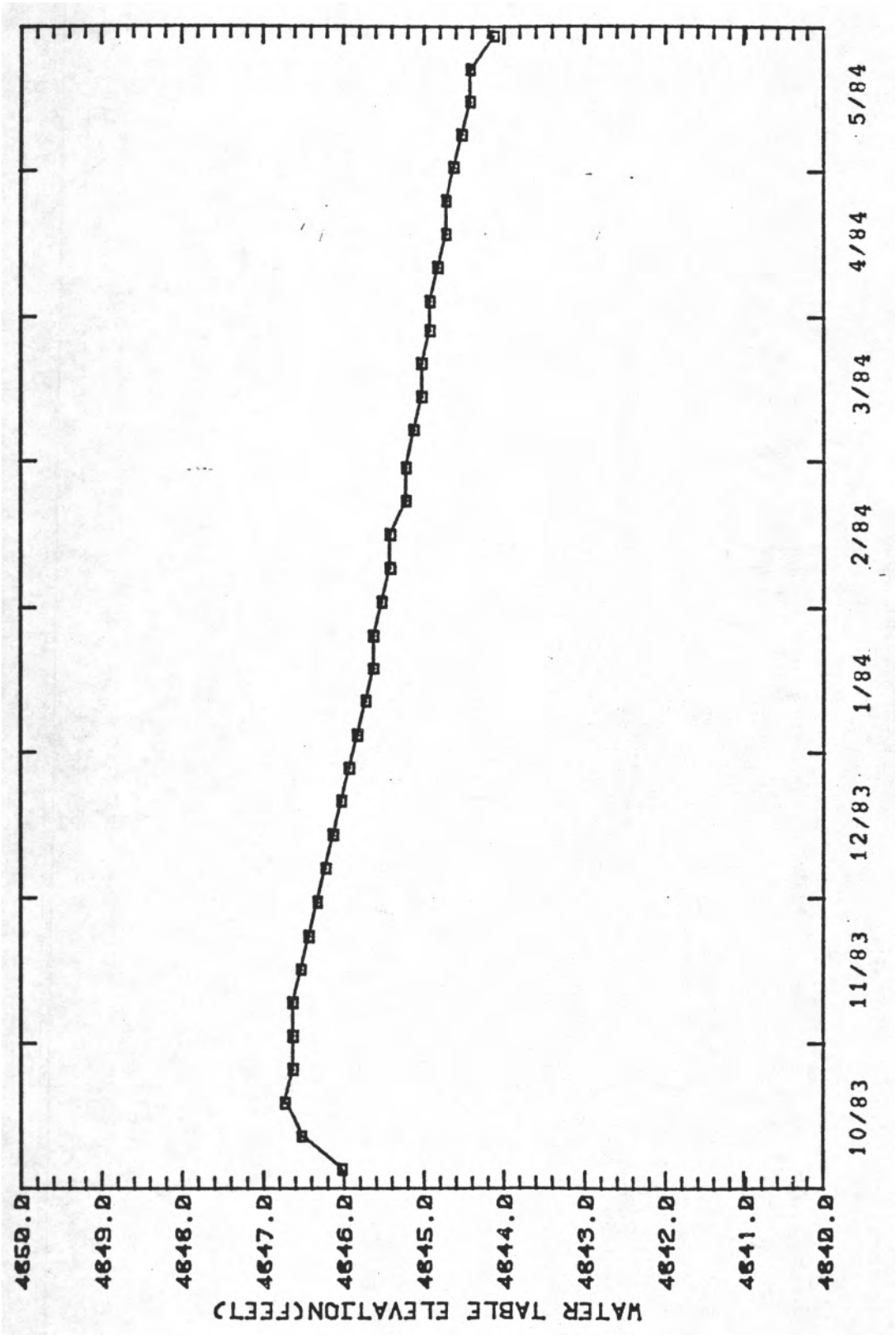

Water-Table Elevations versus Time for Observation Well Number 4

Water-Table Elevations versus Time for Observation Well Number 5

Date	Elevation Above MSL (ft)
01/13/84	4842.2
01/17/84	4843.2
01/20/84	4843.0
01/24/84	4842.9
01/27/84	4842.9
01/31/84	4842.9
02/03/84	4842.8
02/07/84	4842.8
02/10/84	4842.8
02/14/84	4842.7
02/17/84	4842.7
02/21/84	4842.7
02/24/84	4842.6
02/28/84	4842.6
03/02/84	4842.5
03/06/84	4842.5
03/09/84	4842.5
03/13/84	4842.5
03/16/84	4842.4
03/20/84	4842.4
03/23/84	4842.4
03/27/84	4842.3
03/30/84	4842.3
04/03/84	4842.3
04/06/84	4842.2
04/10/84	4842.2
04/13/84	4842.2
04/17/84	4842.2
04/20/84	4842.1
04/24/84	4842.1
04/27/84	4842.1
05/01/84	4842.0
05/04/84	4842.0
05/08/84	4841.9
05/11/84	4841.8
05/15/84	4841.7
05/18/84	4841.8
05/22/84	4841.7
05/25/84	4841.6
05/29/84	4841.6

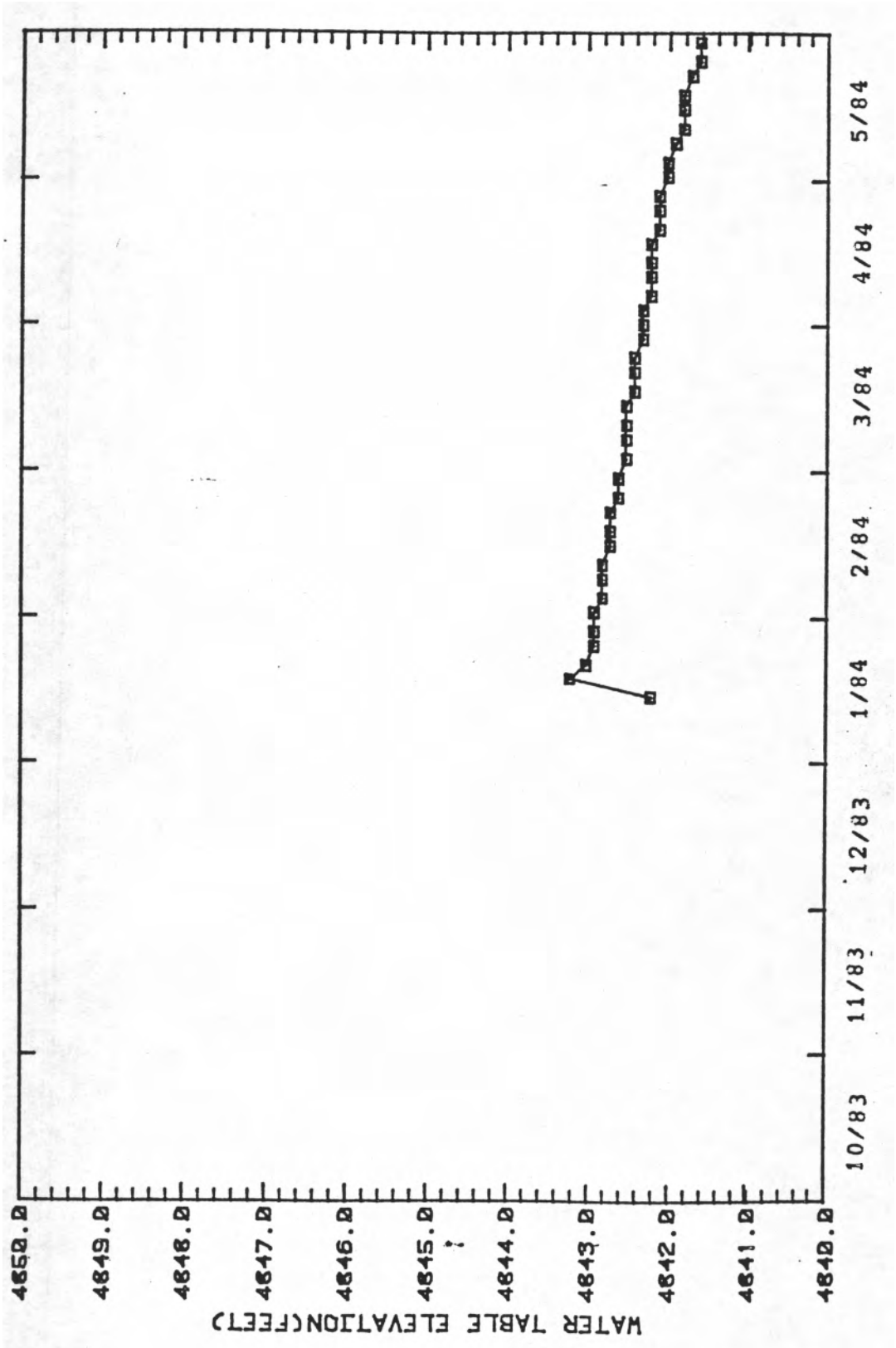

Water-Table Elevations versus Time for Observation Well Number 5

Water-Table Elevations versus Time for Observation Well Number 6

Date	Elevation Above MSL (ft)
01/13/84	4849.2
01/17/84	4849.1
01/20/84	4849.1
01/24/84	4849.1
01/27/84	4849.0
01/31/84	4848.9
02/03/84	4849.9
02/07/84	4848.8
02/10/84	4848.8
02/14/84	4848.8
02/17/84	4848.7
02/21/84	4848.7
02/24/84	4849.6
02/28/84	4848.6
03/02/84	4848.6
03/06/84	4848.5
03/09/84	4848.5
03/13/84	4848.5
03/16/84	4848.4
03/20/84	4848.4
03/23/84	4848.4
03/27/84	4848.3
03/30/84	4848.3
04/03/84	4848.2
04/06/84	4848.2
04/10/84	4848.2
04/13/84	4848.2
04/17/84	4848.1
04/20/84	4848.1
04/24/84	4848.1
04/27/84	4848.0
05/01/84	4848.0
05/04/84	4848.0
05/08/84	4847.9
05/15/84	4847.8
05/18/84	4847.8
05/22/84	4847.7
05/25/84	4847.7
05/29/84	4847.6

Water-Table Elevations versus Time for Observation Well Number 6

Water-Table Elevations versus Time for Observation Well Number 7

Date	Elevation Above MSL (ft)
03/02/84	4845.3
03/06/84	4845.3
03/09/84	4845.3
03/13/84	4845.2
03/16/84	4845.2
03/20/84	4845.2
03/23/84	4845.1
03/27/84	4845.1
03/30/84	4845.1
04/03/84	4845.0
04/06/84	4845.0
04/10/84	4845.0
04/13/84	4845.0
04/17/84	4844.9
04/20/84	4844.9
04/24/84	4844.9
04/27/84	4844.8
05/01/84	4844.8
05/04/84	4844.8
05/08/84	4844.7
05/11/84	4844.7
05/15/84	4844.6
05/18/84	4844.6
05/22/84	4844.5
05/25/84	4844.5
05/29/84	4844.4

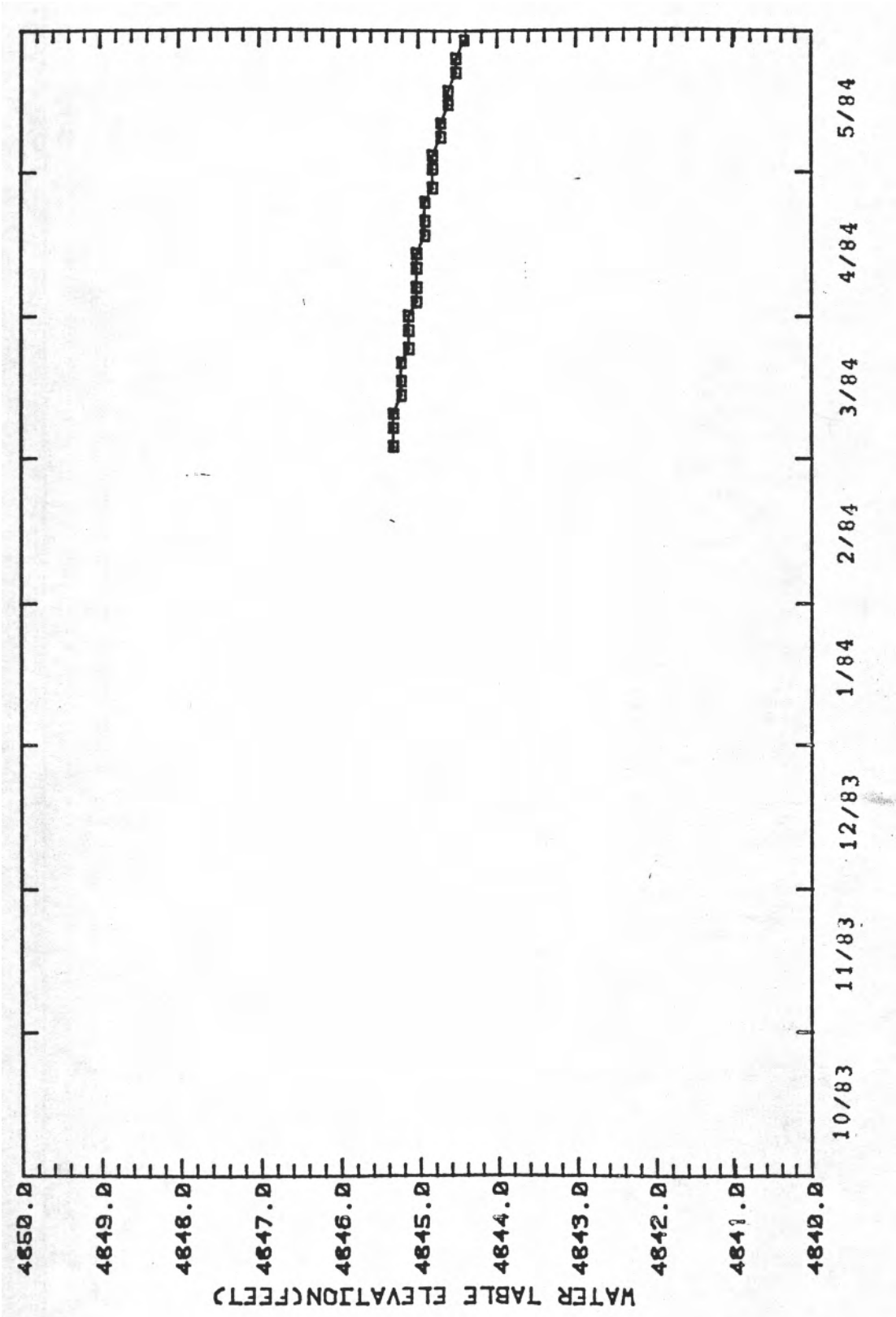

Water-Table Elevations versus Time for Observation Well Number 7

APPENDIX B

CALIBRATION PROCEDURE FOR THE PORTABLE PRESSURE TRANSDUCER

A portable pressure transducer is being used to measure pressure in the tensiometers at the study site. This method makes it easy to measure the tensiometers in a relatively short period of time with a minimum amount of maintenance. A good discussion of the method and the tensiometer construction is given by Marthaler et al. (1983). The pressure transducer setup that is being used on this project is a bit more fragile than the one used by Marthaler et al. (1983), but has essentially the same electronic characteristics.

The pressure transducer is connected to a digital pressure indicator. The voltage output of the transducer is converted into an equivalent pressure head reading in units of centimeters of water. This is not an absolute reading; it must be adjusted with a calibration equation. The actual pressure head and the digital readout have an essentially linear relationship between each other.

A laboratory experiment was set up in which this transducer could be calibrated. A mercury manometer type tensiometer was outfitted with a septum rubber stopper. This facilitated the simultaneous reading of the pressure in a single tensiometer by both the manometer and transducer methods. This tensiometer was then placed in a sealed flask. A vacuum pump was then used to

lower the pressure in the flask incrementally. The tensiometer was allowed to equilibrate and then readings taken. The pressure in the flask was then increased incrementally by allowing some air to enter back into the flask. These procedures produced a good range of pressures from which a calibration equation was estimated.

It turned out that the resulting curve-fits to the data were not the same for increasing vacuum pressure as opposed to decreasing vacuum pressure. This was attributed to the insensitivity of mercury to small changes in pressure. Therefore the mercury manometer was converted to a water manometer. This setup produced better accuracy in determining pressure head readings.

The results of this test were consistent between increasing suction and decreasing suction. Figure B.1 shows the results of this experiment. A linear regression was run on these data with the resulting curve-fit shown in Figure B.1. The regression analysis yielded a coefficient of determination (R^2 value) of 1.00, and the following relation:

$$\psi = 2.2647 + 0.97 \times (PTR + L) \qquad (B.1)$$

where ψ is the actual pressure head in centimeters of water, PTR is the pressure transducer reading (a negative quantity), and L is the length of water in the tensiometer.

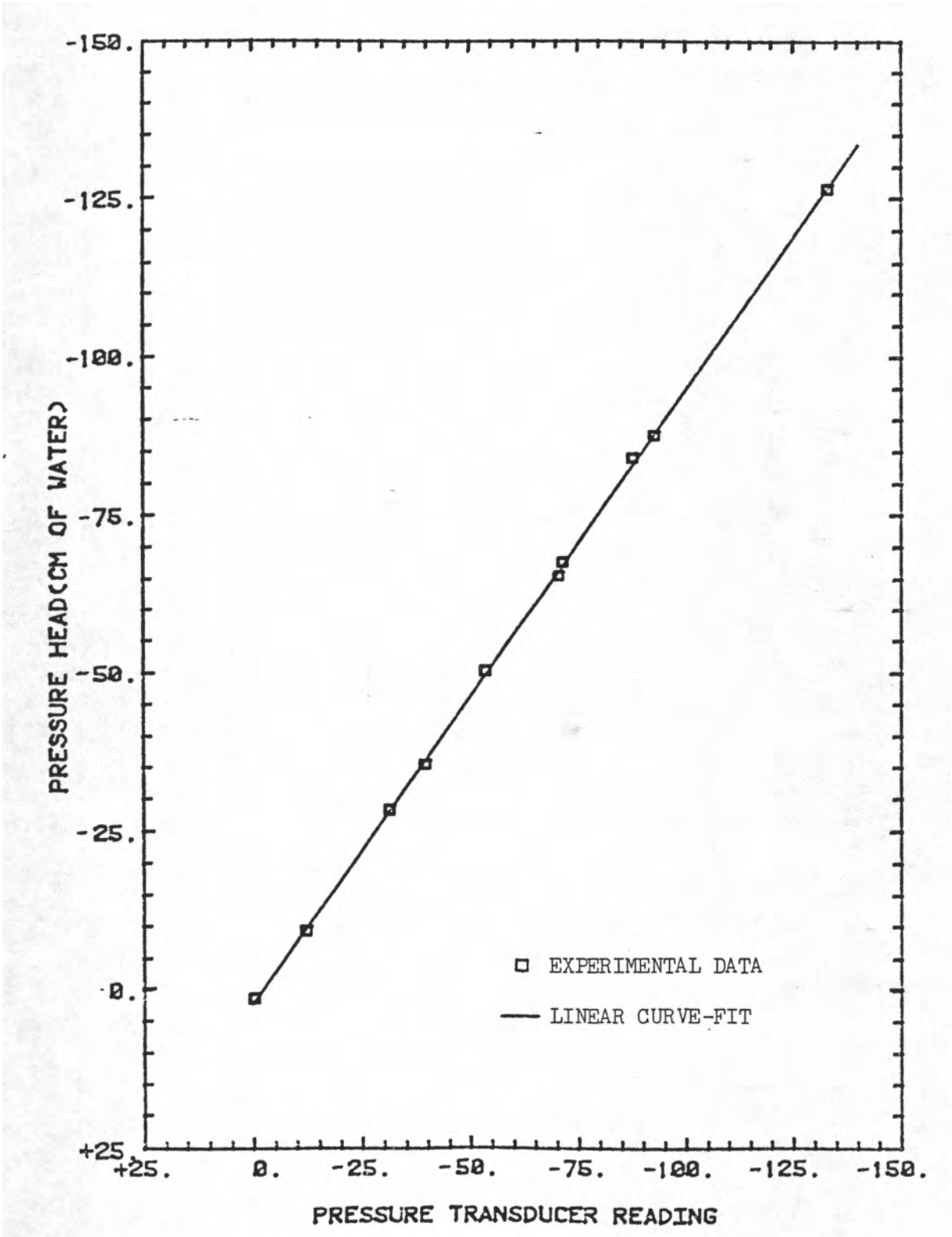

FIGURE B.1 - Actual Pressure Head versus Pressure Transducer Readings from Calibration Experiment, along with Linear Curve-Fit Data

APPENDIX C

CALIBRATION PROCEDURE FOR THE NEUTRON PROBE

The neutron probe currently being used for determining the moisture content within the soil profile is a Campbell Pacific Nuclear, model 503. The probe utilizes a 50 millicurie americium-beryllium source. The unit is calibrated to some known standards of hydrogen density at the factory and this calibration is programmed into the memory of the unit. This calibration, however, does not yield absolute values of moisture content for different soil types. A site specific calibration must be developed for the unit to yield absolute moisture content values.

A field experiment was devised for simultaneously obtaining neutron probe readings and actual water content values. This technique is basically a ponding and vertical infiltration experiment. A neutron access tube was installed to a depth of 2 meters. Special care was taken to ensure that a complete backfill of soil was made in the annular space around the access tube. Next a square-shaped berm was made around the access tube, measuring 2 meters on a side. The site was then ponded with water to a depth of about 5cm for approximately 4 hours. This ponding operation wetted the soil profile to near saturation down to a depth of about 150cm.

Once the ponding had ceased measurements were taken periodically with the neutron probe at various depths. At the same time that each of these measurements was being taken an 'undisturbed' PF ring core was taken at the same depth just outside the radius of influence of the probe, at about 60cm. These cores were capped and taken back to the laboratory for immediate analysis. The cores were weighed, dried overnight at 105 ^{o}C, and weighed again. This data was then used to determine the volumetric water content of each sample. The basic assumption behind this experiment is that there is no spatial variability in water content around the small test area.

The results of these paired values of neutron probe readings and actual water content is shown in Figure C.1. A linear regression was then performed on this data. The resulting curve-fit is also shown in Figure C.1. The coefficient of determination (R^2 value) from this analysis was 0.97. The resultant calibration equation is given as:

$$\theta = -0.0352 + 0.9069 \times NPR \qquad (C.1)$$

where θ is the actual volumetric water content and NPR is the neutron probe reading in decimal percent (ie: a 6.0% water content reading from the neutron probe is represented as 0.06 in equation C.1).

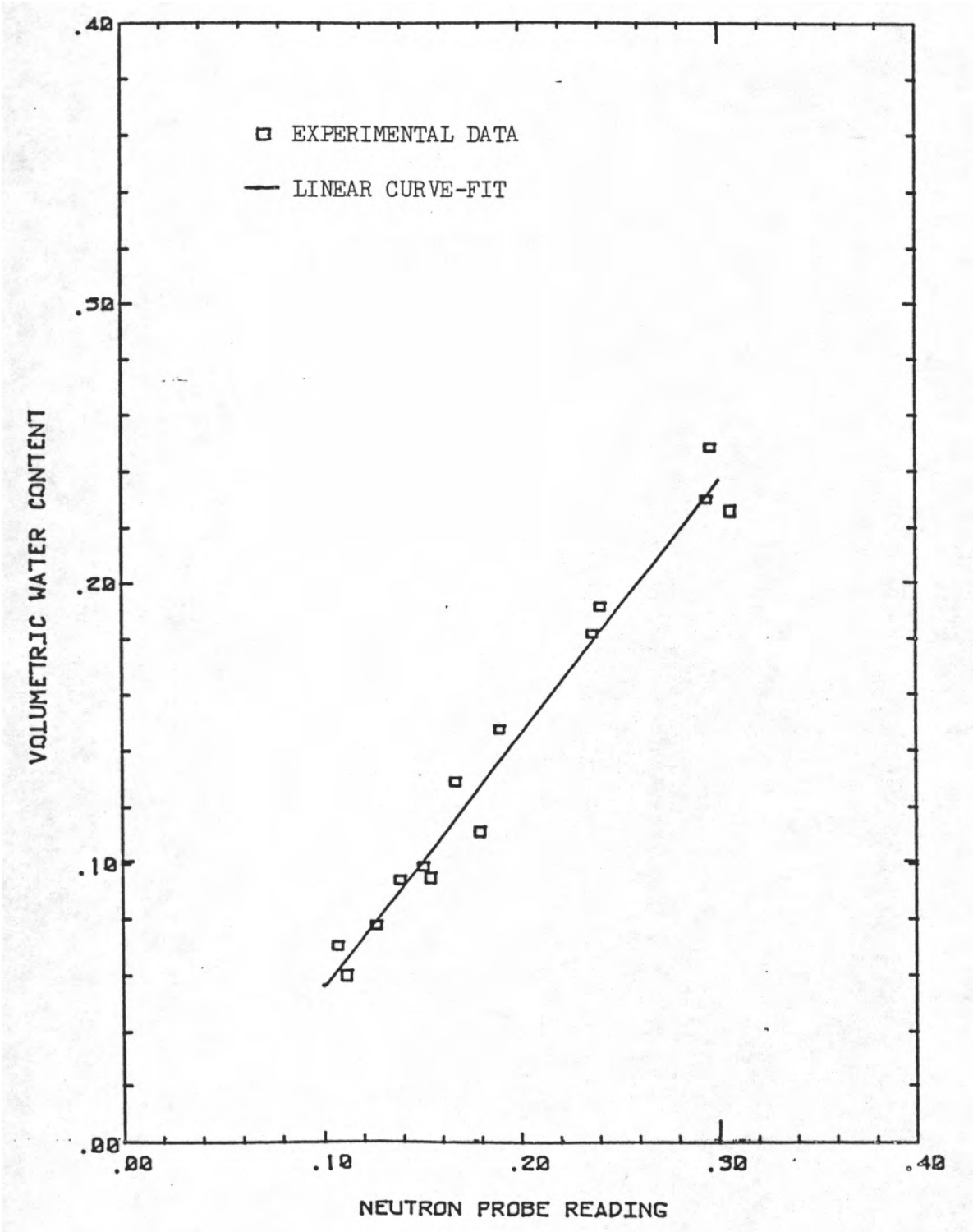

FIGURE C.1 - Actual Water Content versus Neutron Probe Readings from Calibration Experiment, along with Linear Curve-Fit Data

APPENDIX D

ETHYLENE GLYCOL EXPERIMENT

Collecting data throughout the year is important in trying to estimate seasonal changes in watershed hydrology. Tensiometric data is extremely valuable in that it is used in hydraulic calculations and in the pressure head based numerical flow model. The mercury manometer type tensiometers that were used at soil-moisture station 1 during the winter of 1982-1983 had failed numerous times when the distilled water froze in the tubing and cracked it open. A few of the plastic tops on the septum stopper equipped tensiometers also failed during the latter part of 1983. Therefore a new tensiometer fluid was deemed necessary in order to operate these tensiometers throughout the winter months.

McKim et al. (1976) discussed briefly the use of different types of tensiometer fluids in cold climate regions. They expressed a concern for the effects of using ethylene glycol in tensiometers. It was their opinion that not enough was known about the effects of ethylene glycol on surface tension and fluid viscosity. Whether or not ethylene glycol changes these fluid properties to the extent that it alters the pressure in a tensiometer, or the surrounding soil, is not known. A laboratory experiment was devised to observe any differences in measured pressure heads due to different tensiometer fluids. This

experiment was not devised with the intent of quantifying changes in fluid viscosity or surface tension, but rather to just observe any differences in measured pressure that might be caused by differences in tensiometric fluids.

The solution used in this experiment was a mixture of ethylene glycol and distilled water. Using 100% ethylene glycol was deemed unnecessary. The low nightly temperatures during the winter months in this climate are not too extreme and do not warrant a straight solution of ethylene glycol. Also it would not be economical to use this type of solution . Therefore different mixtures were made and placed in a freezer. A 10 and 20 percent mixture of ethylene glycol in distilled water froze at -9oC. The 30, 40, and 50 percent solutions did not freeze. A 40% solution was chosen as the tensiometer fluid. The ethylene glycol appeared to be completely miscible with distilled water, even though it is slightly more dense. The resultant specific gravity of the 40% mixture was calculated to be 1.045.

The experiment was set up to measure pressure heads in tensiometers that are in all facets the same except for the tensiometer fluid. This was accomplished by placing six separate soil columns in a constant head bath, and installing a single tensiometer in each column. The columns were each 30.5cm in height and 10cm in diameter. The bottoms of the columns were screened to contain the soil, and to allow full hydraulic contact

with the constant head bath. This head was kept at 1.8cm above the base of each column. The center of the porous cup of each tensiometer was set at a height of 15.2cm above the water surface. Three of these tensiometers were filled with a 40% solution of de-aired ethylene glycol and distilled water. The other 3 tensiometers were filled with de-aired distilled water. The system was left to equilibrate for one week after initiation of the experiment before taking measurements.

In using this constant head bath it is assumed that steady state conditions exist within the soil columns. It is also assumed that all soil columns are identical. Therefore if all the tensiometers are measuring an average pressure relative to the center of each cup, and each cup is 15.2cm above the constant head source, then each tensiometer should yield a pressure head of -15.2cm of water.

The tensiometers were read periodically for about 44 days. The pressure head in the distilled water filled tensiometers was calculated from the following relation:

$$\psi = 2.2647 + 0.97 \times (PTR + L) \qquad (D.1)$$

where ψ is the actual pressure head, PTR is the pressure transducer reading, and L is the length of water in the tensiometer. The three values of pressure head from this group of tensiometers for each time were averaged together to minimize errors. The three tensiometers that were filled with the 40%

ethylene glycol solution were treated in the same manner, except that the term L in equation D.1 was multiplied by the specific gravity of the fluid, 1.045, to correct for the density difference.

The averaged results from this steady state experiment are shown in Figure D.1. The data show a slight amount of variability. This may be explained by one or more of several different factors. The height of the average pressure measurement along the porous cup of each tensiometer is not truly known. The cups are 5.5cm in length. The measured pressure head could then be anywhere between -12.5 and -18.0cm. A couple of the averaged readings were -18.6cm, which is outside this range of acceptable pressure heads. This may be due to a slight error in setting the height of the tensiometers above the water surface. Other factors that may contribute to the data scatter are human measurement error, and changes in temperature and/or barometric pressure. What influence temperature and barometric pressure have on the pressure transducer and the pressure head readings is not entirely clear at this time. Further research is required into this area.

The averages of all values of pressure head for the entire duration of the experiment were -16.1 and -16.2cm for the distilled water filled tensiometers and the 40% ethylene glycol filled tensiometers, respectively. These values would seem to

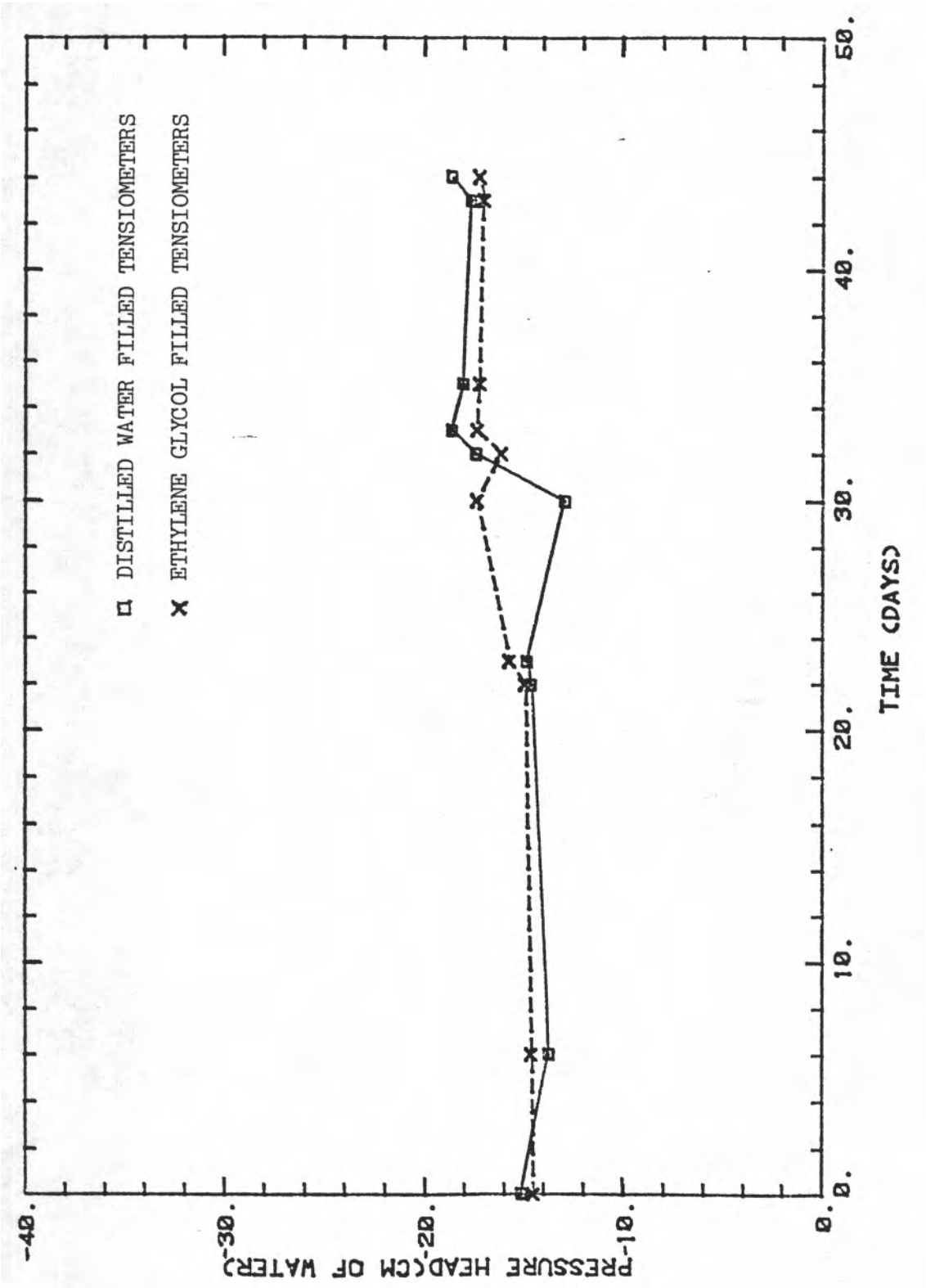

FIGURE D.1 - Pressure Head versus Time for 40% Ethylene Glycol versus Distilled Water filled Tensiometers; Constant Head Experiment

suggest that the ethylene glycol solution has no adverse effects on the measured pressure heads in and around a tensiometer. One major criticism of this particular experiment is that it was run under relatively moist conditions. Under drier soil-water conditions the effects of surface tension and viscosity may become more pronounced when measuring pressure heads in the soil.

With this in mind the water bath experiment was converted into a drainage experiment. The water source was removed from beneath the soil columns and the soil columns were allowed to drain. It was assumed that the effects of evaporation on both ends of each column were identical from column to column. Therefore each column should dry at the same rate and produce the same pressure head around each tensiometer.

Figure D.2 shows the averaged results from this phase of the experiment, where measurements were made for 180 hours of drying time. The results show good agreement between the ethylene glycol tensiometers and the distilled water tensiometers. The ethylene glycol tensiometers yield slightly lower values of pressure head throughout this drainage experiment than do the distilled water tensiometers. The average difference between these readings is 1.0cm. Considering the inaccuracies of the porous cup in measuring pressure heads, as mentioned earlier, and the possibility of human error in setting the heights of these cups, it cannot be established from these results that the

ethylene glycol solution has a detrimental effect on the measured pressure head in a tensiometer. Therefore the assumption was made that if the ethylene glycol mixture does have an effect on the measured pressure head in a tensiometer, then this effect is negligible.

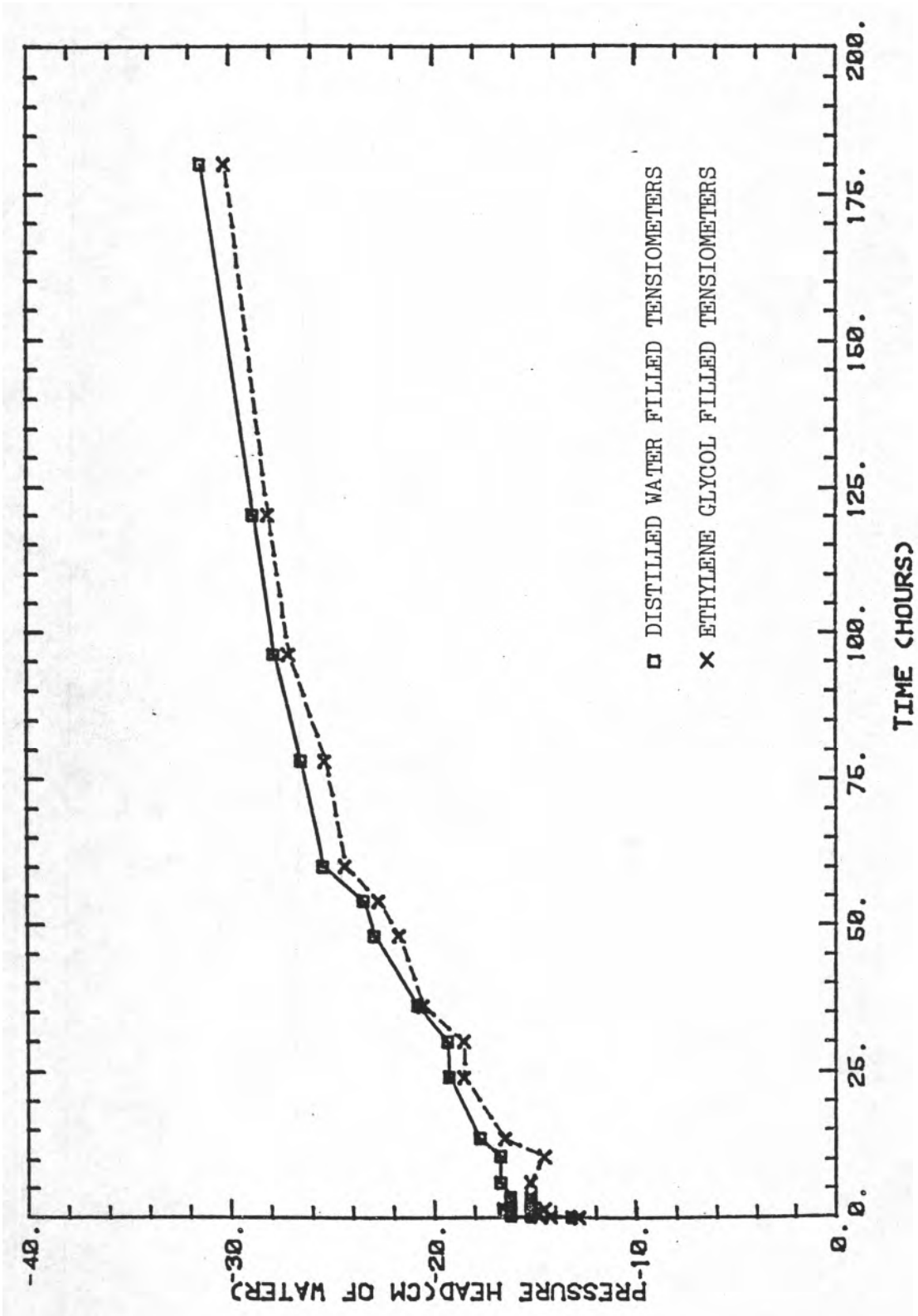

FIGURE D.2 - Pressure Head versus Time for 40% Ethylene Glycol versus Distilled Water filled Tensiometers; Drainage Experiment

APPENDIX E

PROGRAM FOR EVALUATING INSTANTANEOUS PROFILE DATA

The determination of the unsaturated hydraulic conductivity at the Sevilleta research site was accomplished with the instantaneous profile method. The method entails the monitoring of the transient state internal drainage of a soil profile through the use of tensiometers and neutron probe logging. The method is based upon work done by Richards and Weeks (1953), Ogata and Richards (1957), Rose et al. (1965), and Watson (1966). The final procedure developed for field application was devised by Hillel et al. (1972).

The experiment is set up such that tensiometers are installed at various depths throughout a soil profile. A neutron access tube is installed relatively close to the tensiometer setup to obtain simultaneous readings of pressure head and water content with depth and time during drainage. A berm is built around the instrumentation to facilitate the ponding of water over the site to wet up the profile to near saturation. When the profile has been wet to near saturation the ponding is ceased. The surface is then covered with plastic to prevent evaporation and the upward flow of water. The assumption is made that there exists only vertical downward flow during drainage. Measurements of water content and pressure head with time and depth will then allow the solution of the following governing flow equation:

$$\frac{\partial \theta}{\partial t} = \frac{\partial}{\partial z}\left[K(\theta)\frac{\partial H}{\partial z}\right] \qquad \text{(E.1)}$$

where θ is water content, $K(\theta)$ is the unsaturated hydraulic conductivity as a function of water content, t is time, z is depth, and H is total hydraulic head.

Hillel et al. (1972) developed a graphical procedure for solving this governing flow equation. Water content is plotted against time for each depth of measurement in the profile. A slope is then determined graphically from each curve for each time desired for output. This slope is a very critical parameter in the final determination of the unsaturated hydraulic conductivity. The change in moisture with time is then multiplied by the depth increment over which this change has taken place. This quantity represents a flux for that depth increment. The fluxes are then summed for each successively deeper depth. Having obtained this Darcian flux for each depth the next step is to divide by the hydraulic gradient to obtain a value of unsaturated hydraulic conductivity. This is done for all depths at each output time desired. The result is a set of corresponding water content, pressure head, and unsaturated hydraulic conductivity values for each depth.

The method just described generally yields good results. It is, however, a very time consuming procedure which may yield biased results. The calculation of the slope of the water

content versus time plot is done manually by the individual performing the calculations. This is where the bias comes into effect. Two different persons performing these calculations could obtain two different slopes, and therefore different estimates of hydraulic conductivity. In an effort to gain more accuracy into this method, and to cut down on the time involved in processing this data, a computer program was written to do these calculations.

The computer routine follows the same basic formulation as the graphical method just outlined. The major difference is that in place of the graphical procedures the program runs a polynomial regression on the data to obtain a curve-fit to some specified form of an equation. The types of equations available to the user are called linear, logarithmic, exponential, and power curves. These equations have the following general forms:

linear: $Y = A + B1*X + B2*(X^2) + \ldots$ (E.2)

logarithmic: $Y = A + B1*(\ln X) + B2*((\ln X)^2) + \ldots$ (E.3)

exponential: $\ln Y = A + B1*X + B2*(X^2) + \ldots$ (E.4)

power: $\ln Y = A + B1*(\ln X) + B2*((\ln X)^2) + \ldots$ (E.5)

The user then specifies the type of equation to be used in the regression analysis. The maximum degree of the polynomial is also specified. The program then determines the coefficients for each degree of polynomial up to the maximum degree specified. It also calculates the coefficient of determination (R^2 value) for

each polynomial equation and selects the equation with the largest R^2 value for use in determining the unsaturated hydraulic conductivity.

Having fit an equation to the water content versus time data, it is then quite easy to calculate the slope of this curve at any specified time. This is done by taking the derivative of the fitted equation with respect to time. If the curve-fit to the data is good the determination of the slope should be more accurate with this method than with the graphical procedure. Figure E.1 shows a curve-fit to the water content versus time data for the 30.5cm depth. A similar curve-fit is obtained for the pressure head versus time and total hydraulic head versus depth data. For specified output times the program can then output corresponding values of water content, pressure head, and unsaturated hydraulic conductivity. Figure E.2 shows the graphical and computer model results for the 91.5cm depth of pressure head versus water content data. Figure E.3 shows the calculated unsaturated hydraulic conductivity versus pressure head for both the graphical and computer model methods from the 61.0cm depth.

These figures show that there is very good agreement between the graphical and computer model results. The reliability of the computer model results is highly dependent upon the goodness of fit of each polynomial equation. To date the model has only been

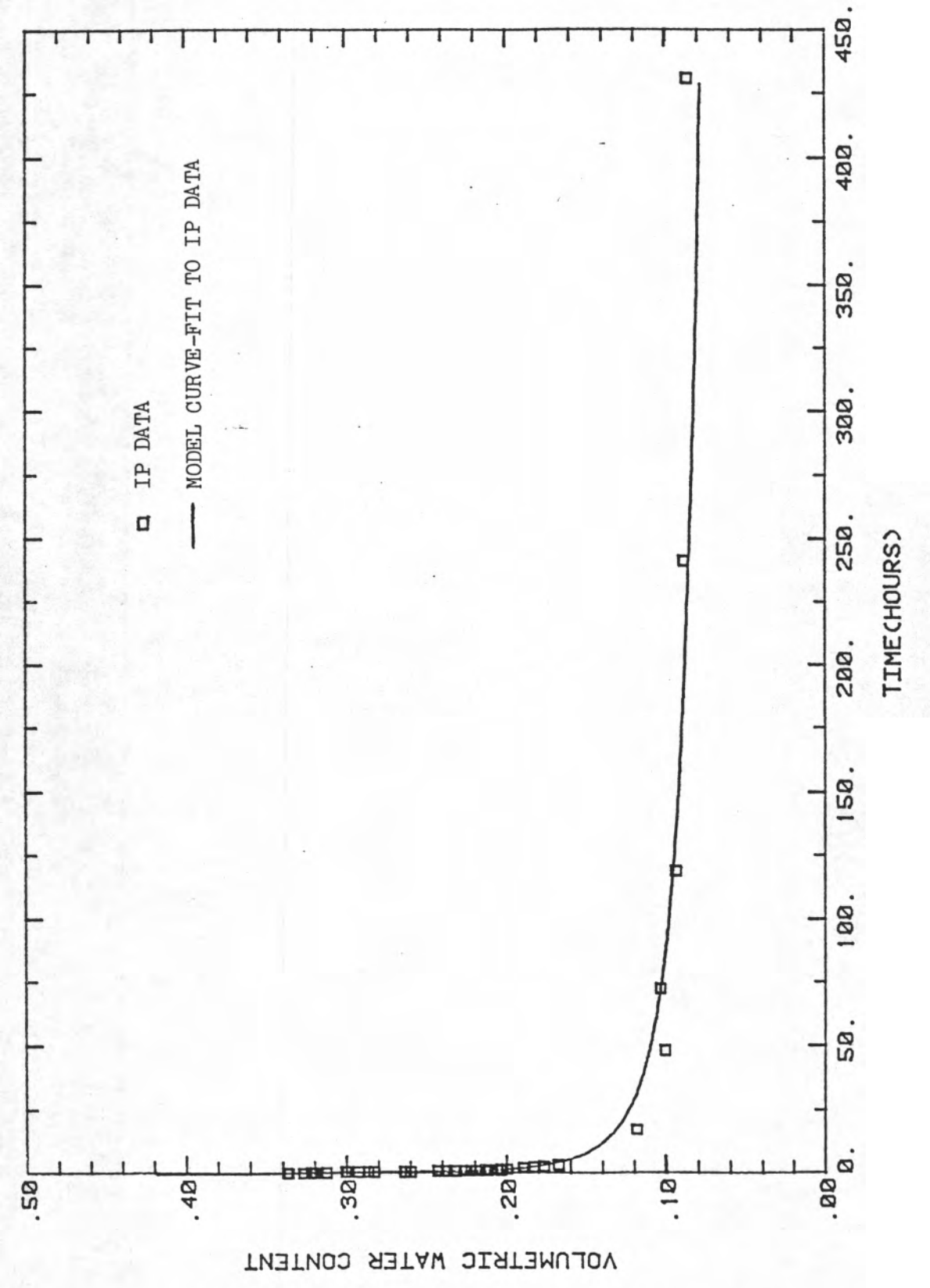

FIGURE E.1 - Water Content versus Time for the 30.5cm Depth from the Instantaneous Profile Test, along with Polynomial Curve-Fit Data

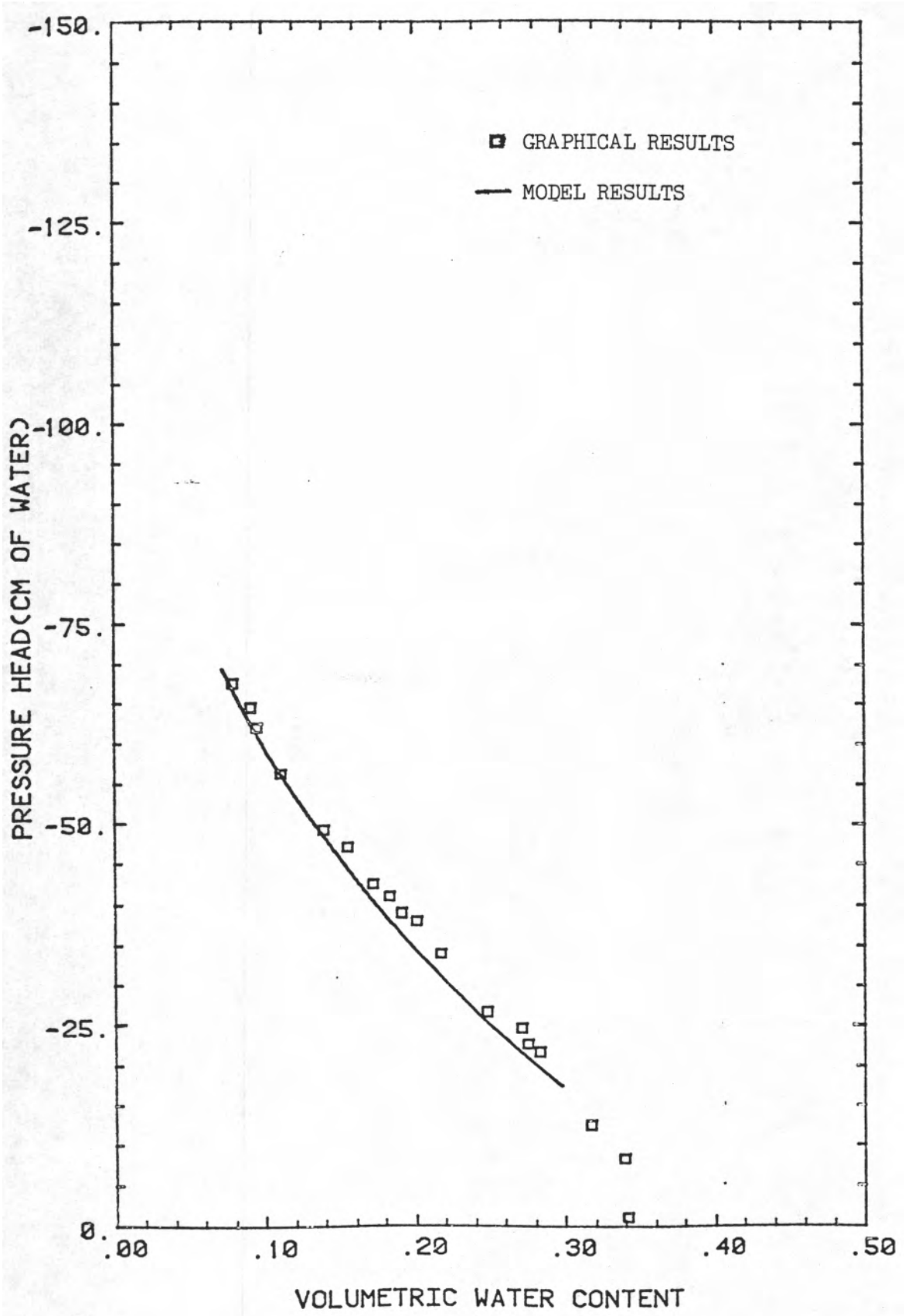

FIGURE E.2 - Pressure Head versus Water Content for the 91.5cm Depth from the Instantaneous Profile Test, Graphical versus Computer Model Results

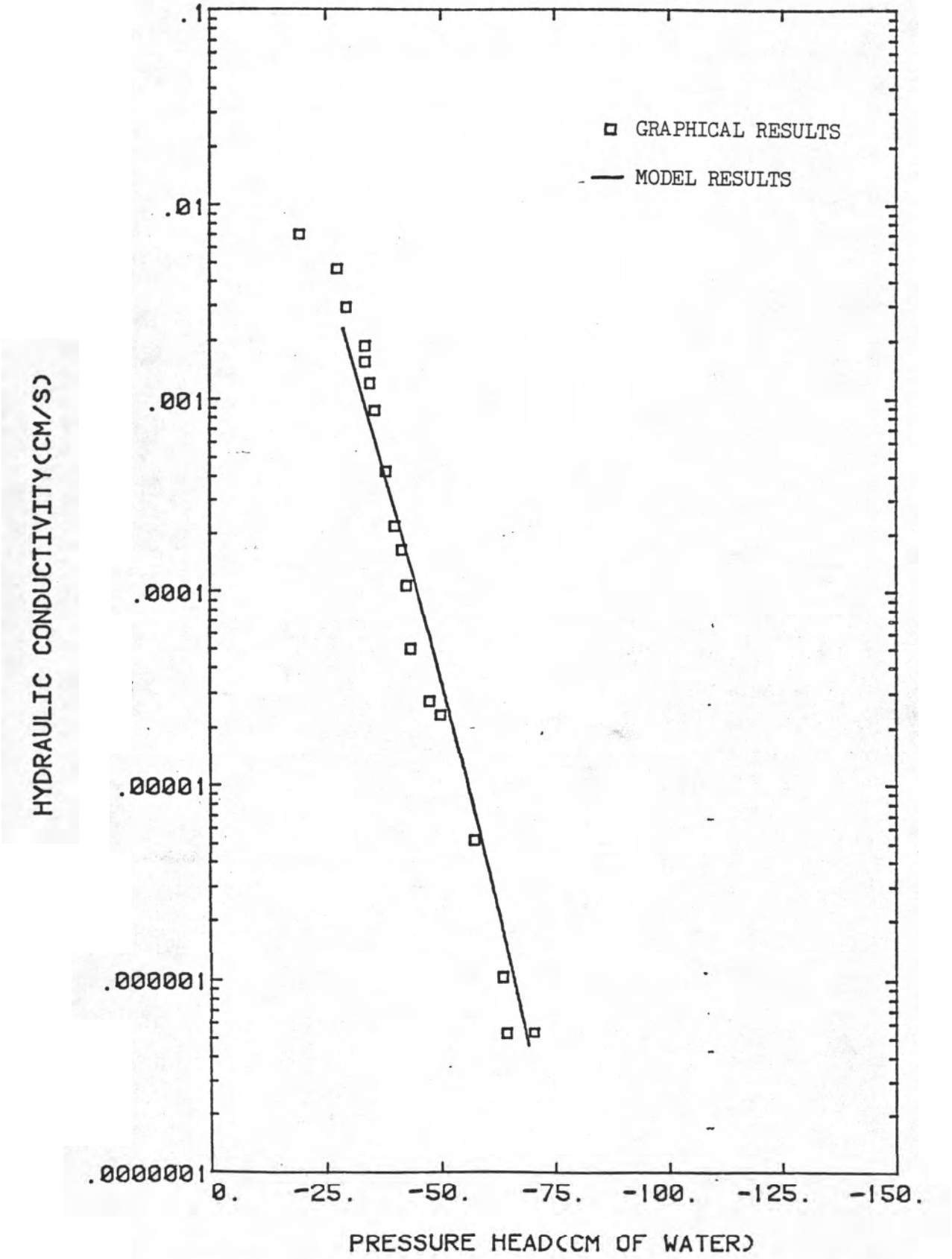

FIGURE 3.3 - K versus Pressure Head for the 61.0cm Depth from the Instantaneous Profile Test, Graphical versus Computer Model Results

checked against one set of instantaneous profile data and should be verified against other data when it becomes available. Flühler et al. (1976) concluded that the instantaneous profile type of method will yield unsaturated hydraulic conductivity values that are within 20 to 30 percent of the true value in a relatively wet profile, and up to a 100% difference in a drier profile. Considering Flühler's results, and the good correlation obtained between the graphical and computer model results, it would seem that this model deserves more attention for future use.

APPENDIX F

LABORATORY DATA

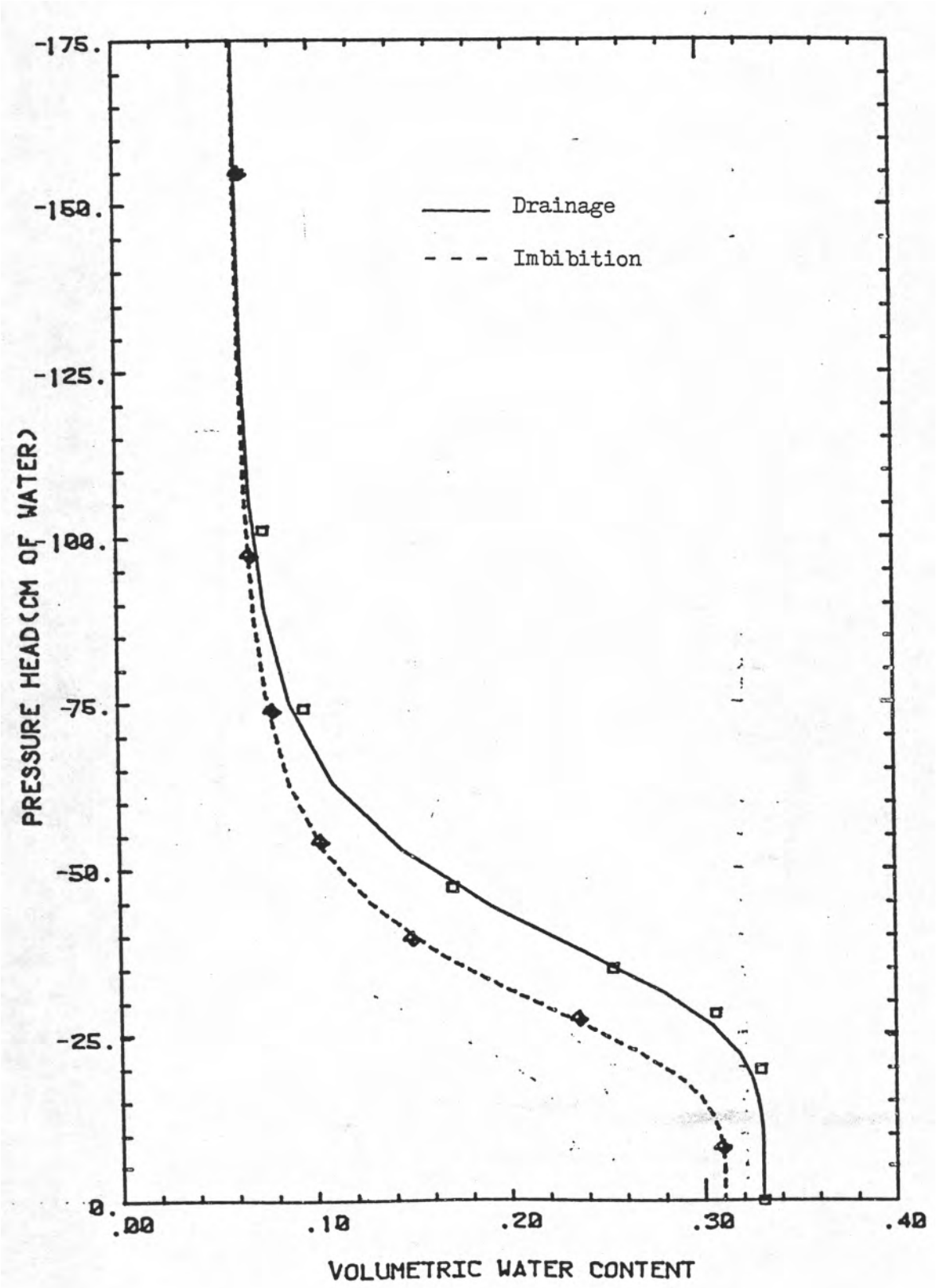

Pressure Head versus Water Content for the 15.0 cm depth near Soil-moisture Station 1. Symbols-laboratory data, lines-Mualem's model results.

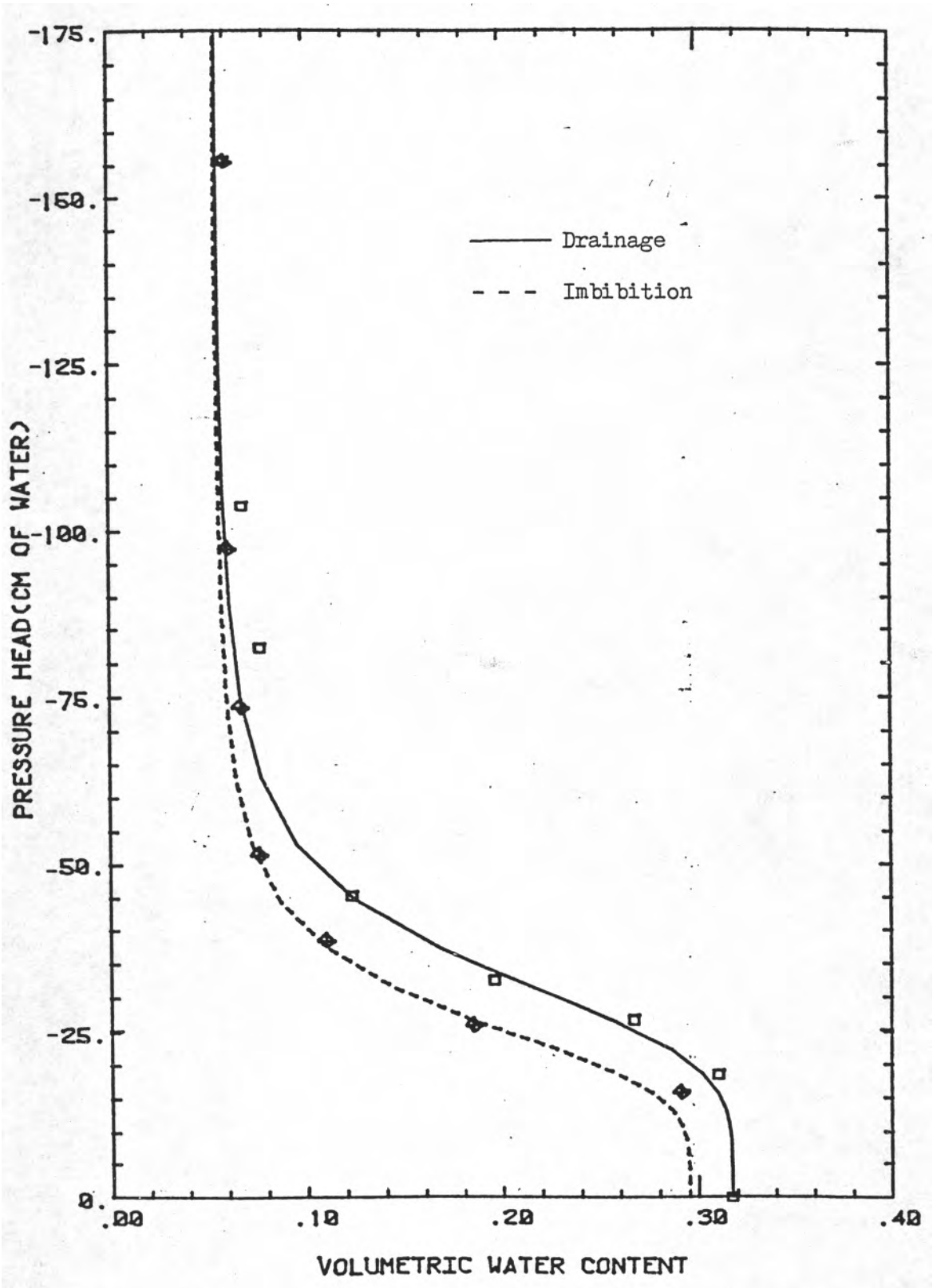

Pressure Head versus Water Content for the 61.0 cm depth near Soil-moisture Station 1. Symbols-laboratory data, lines- Mualem's model data results.

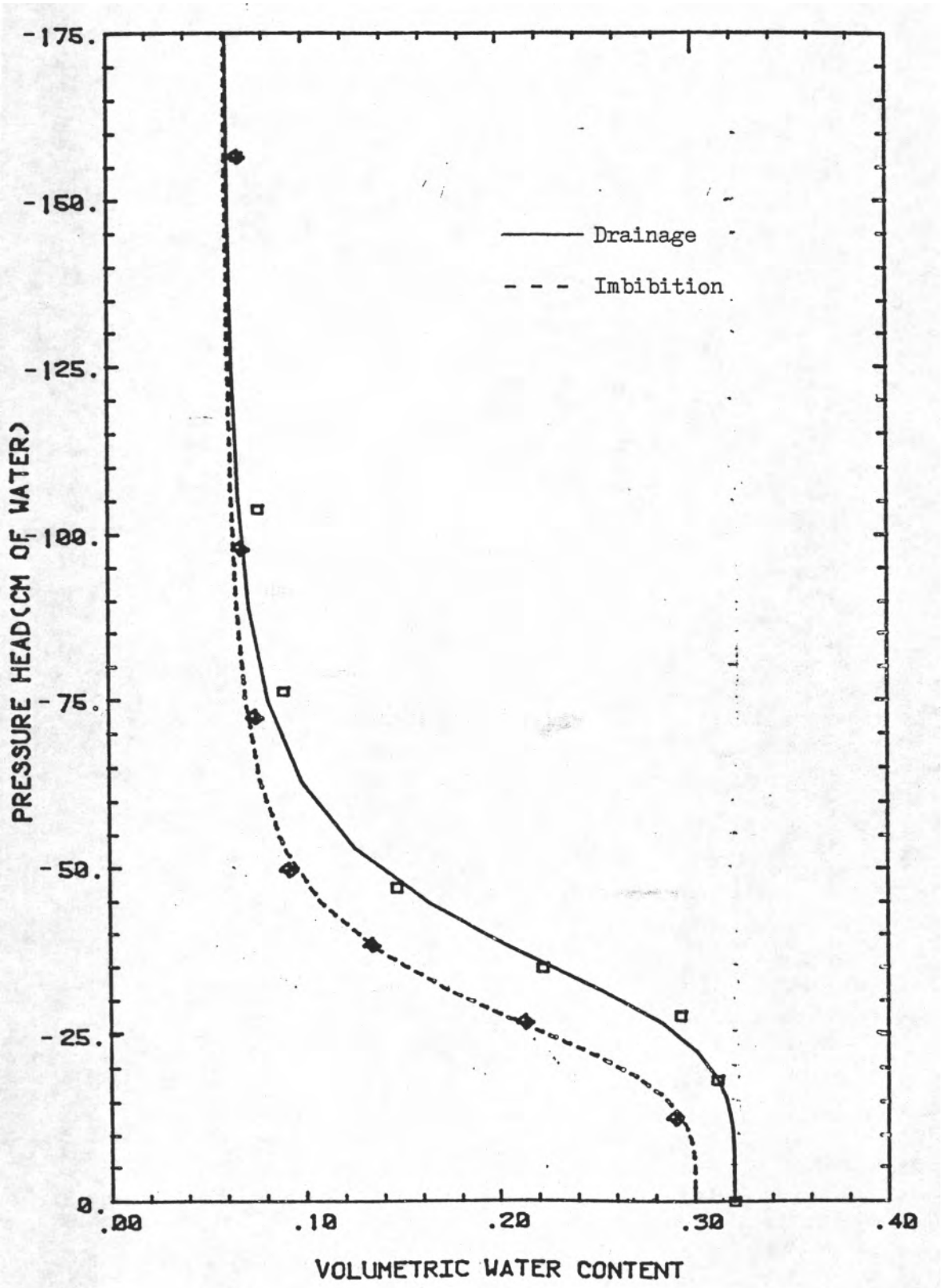

Pressure Head versus Water Content for the 91.5 cm depth near Soil-moisture Station 1. Symbols-laboratory data, lines-Mualem's model results.

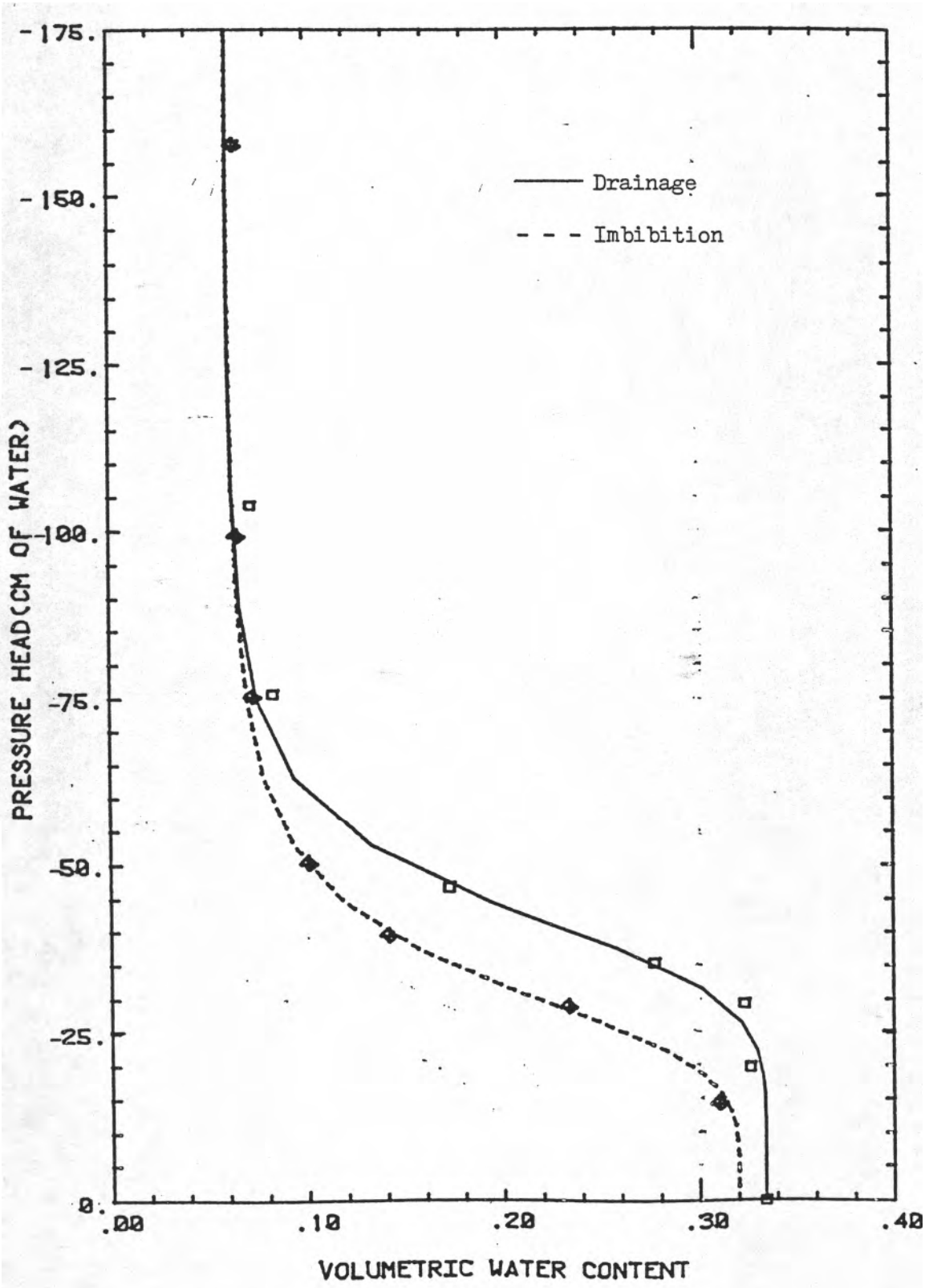

Pressure Head versus Water Content for the 122.0 cm depth near Soil-moisture Station 1. Symbols-laboratory data, lines-Mualem's model results.

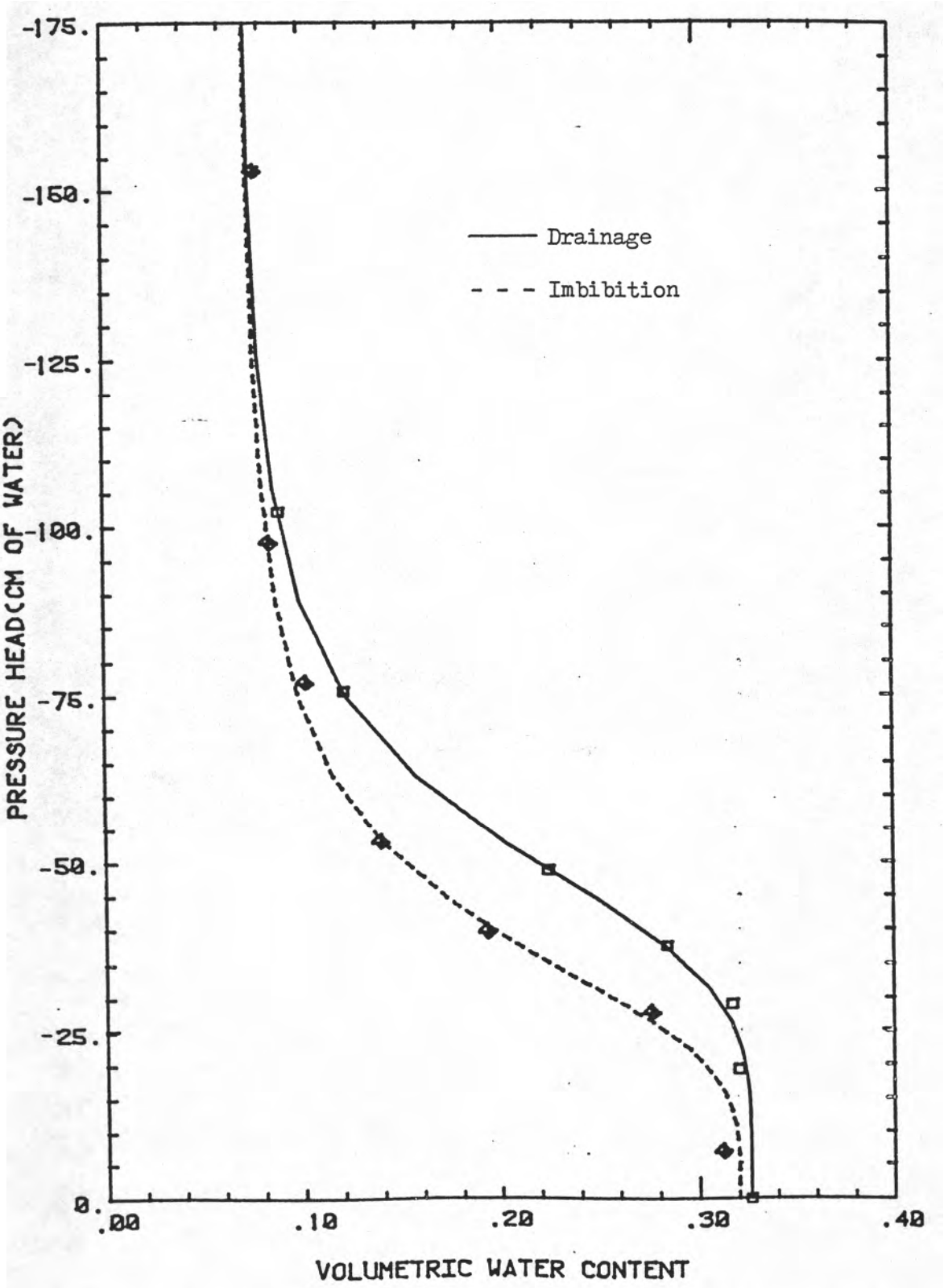

Pressure Head versus Water Content for the 152.5 cm depth near Soil-moisture Station 1. Symbols-laboratory data, lines-Mualem's model results.

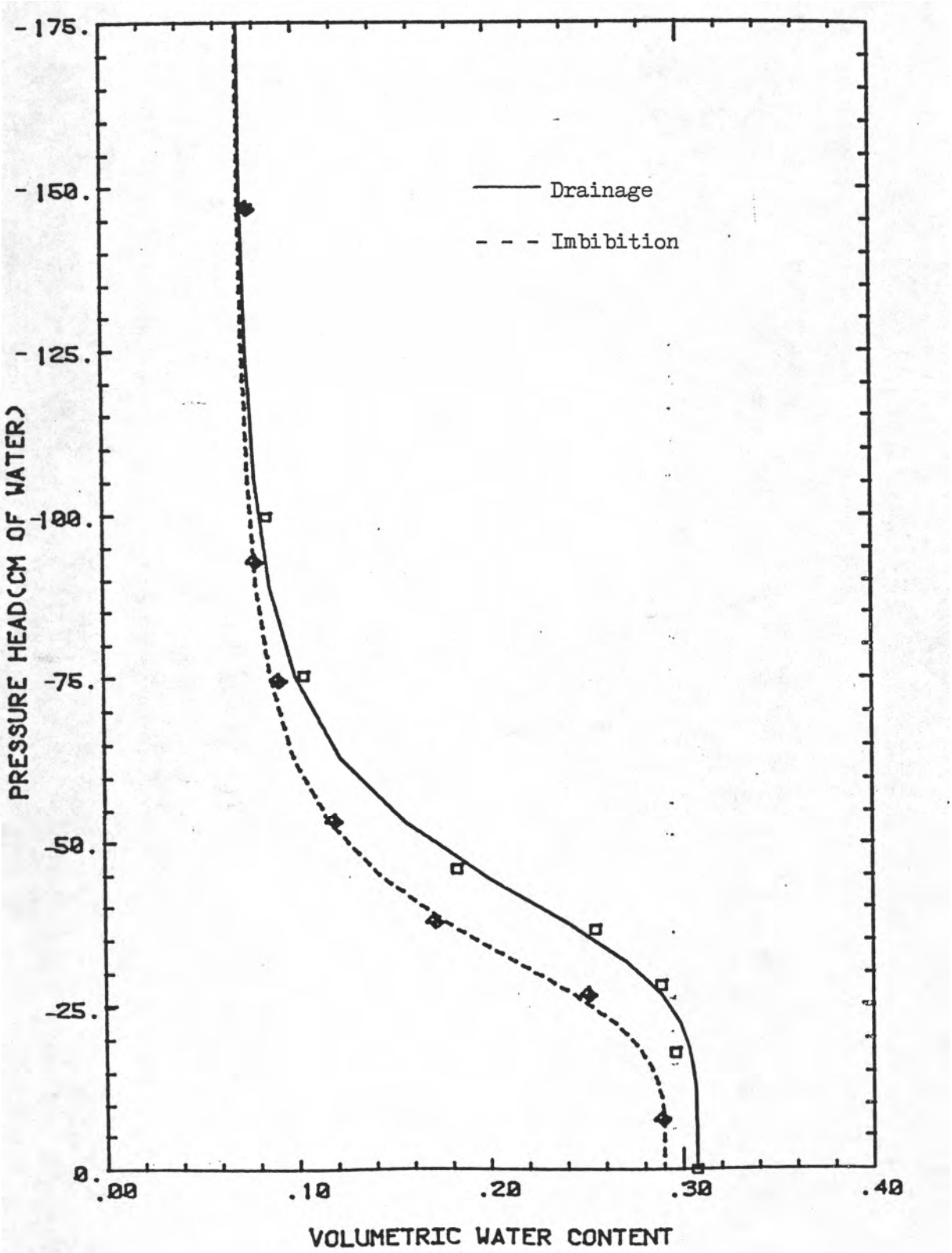

Pressure Head versus Water Content for the 183.0 cm depth near Soil-moisture Station 1. Symbols-laboratory data, lines-Mualem's model results.

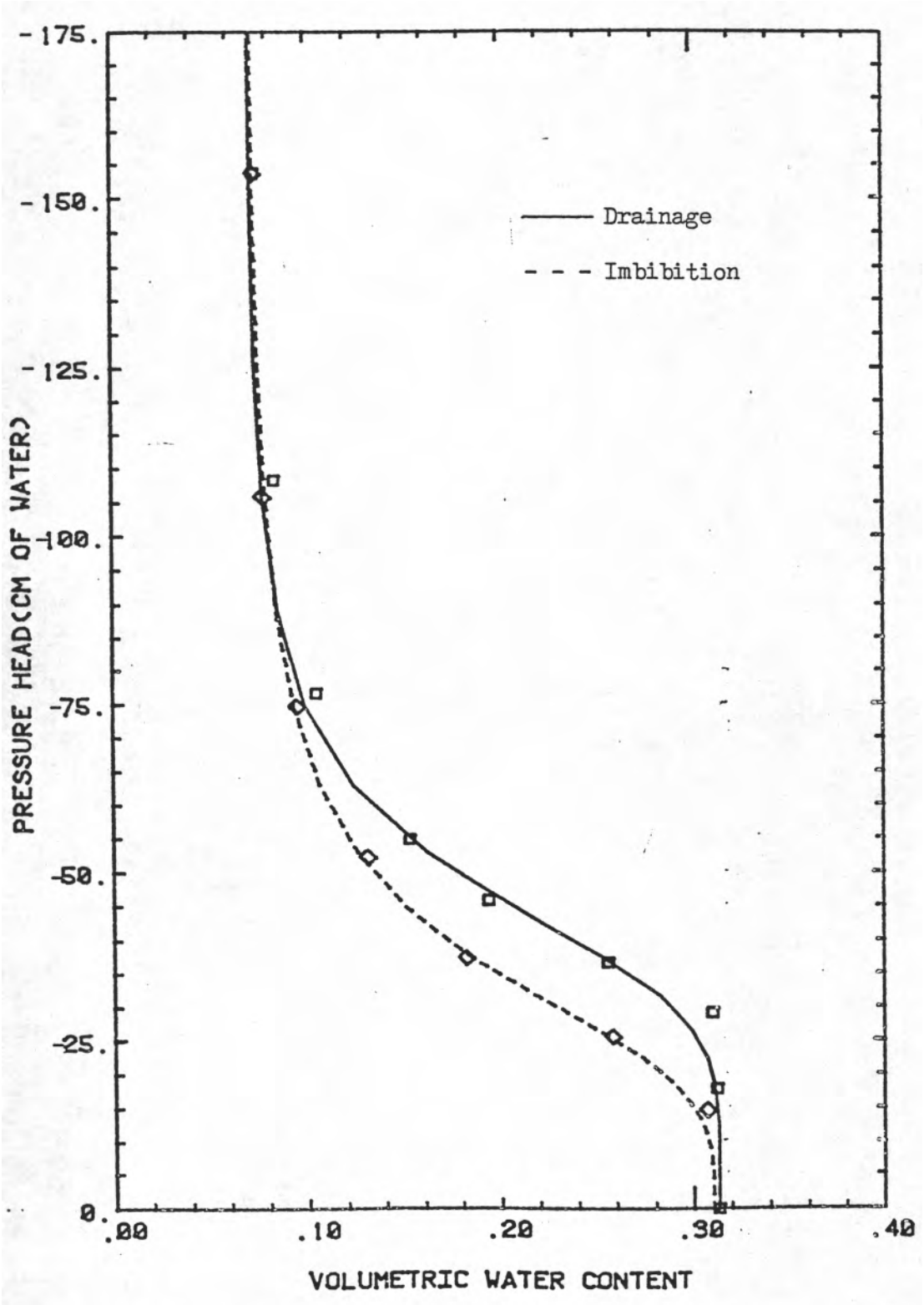

Pressure Head versus Water Content for the 244.0 cm depth near Soil-moisture Station 1. Symbols-laboratory data, lines-Mualem's model results.

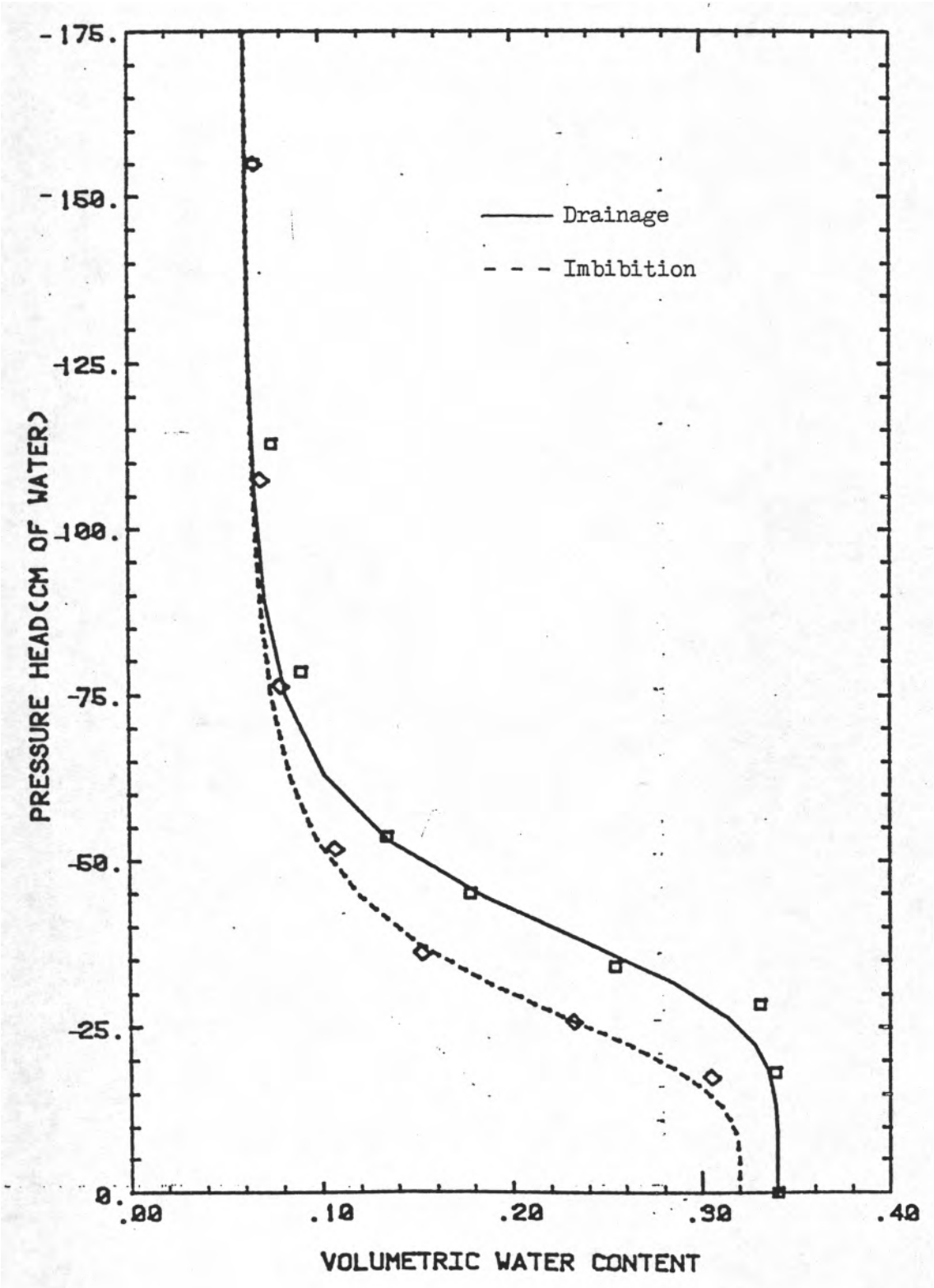

Pressure Head versus Water Content for the 274.0 cm depth near Soil-moisture Station 1. Symbols-laboratory data, lines-Mualem's model results.

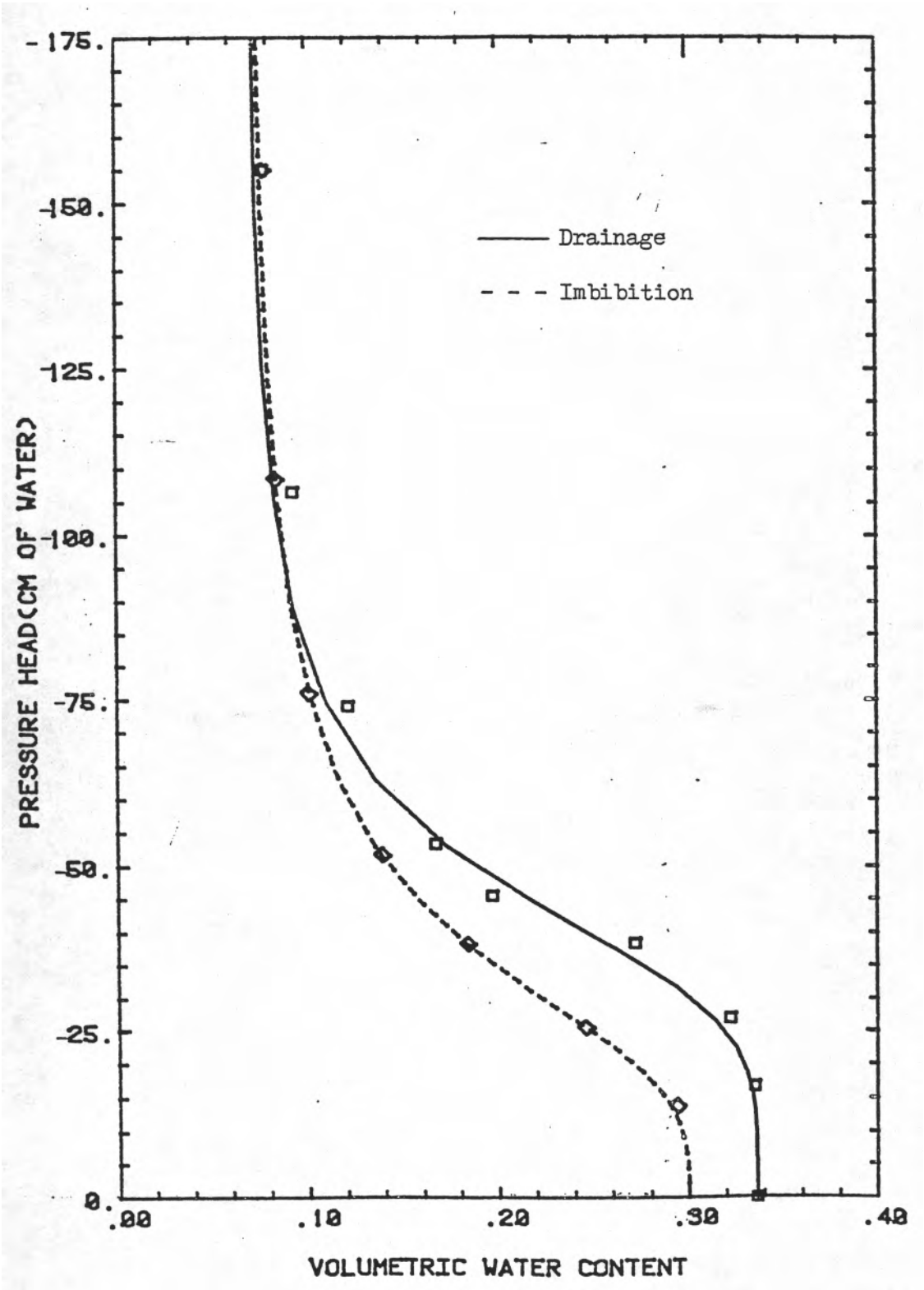

Pressure Head versus Water Content for the 305.0 cm depth near Soil-moisture Station 1. Symbols-laboratory data, lines-Mualem's model results.

Depth versus Saturated Hydraulic Conductivity from Shelby tube Profile adjacent to Soil-moisture Station 1.

Depth (cm)	Hydraulic Conductivity (cm/sec)	Depth (cm)	Hydraulic Conductivity (cm/sec)
-4.8	1.3E-2	-278.1	1.8E-2
-14.8	5.0E-3	-287.1	5.2E-3
-23.0	7.8E-3	-296.1	1.2E-2
-32.0	1.5E-2	-305.1	1.2E-2
-40.9	8.9E-3	-314.1	1.6E-2
-49.9	1.6E-2	-323.6	1.6E-2
-59.7	1.8E-2	-333.1	1.1E-2
-69.3	1.1E-2	-342.1	7.3E-3
-78.2	1.3E-2	-351.1	1.5E-2
-87.1	1.9E-2	-360.1	1.7E-2
-95.9	1.4E-2	-369.1	2.3E-2
-104.8	1.1E-2	-378.7	1.1E-2
-114.1	1.4E-2	-388.2	1.6E-2
-123.6	1.8E-2	-397.1	1.8E-2
-132.6	2.4E-2	-406.1	2.0E-2
-141.6	2.1E-2	-415.1	1.8E-2
-150.6	1.8E-3	-424.1	9.6E-3
-159.7	1.7E-3	-433.1	1.6E-2
-168.5	1.2E-2	-442.0	1.1E-2
-177.2	1.6E-2	-451.0	1.6E-3
-186.2	1.6E-2	-460.0	2.1E-2
-195.2	1.4E-2	-469.0	2.4E-2
-204.2	1.2E-2	-478.0	3.2E-2
-213.3	1.1E-2	-488.4	1.5E-2
-223.3	1.1E-2	-498.6	2.0E-2
-233.3	7.7E-2	-507.3	2.6E-2
-242.1	1.3E-2	-516.0	2.4E-3
-250.8	1.9E-3	-524.6	4.4E-3
-259.4	6.4E-3	-533.4	5.0E-3
-268.6	2.5E-2		

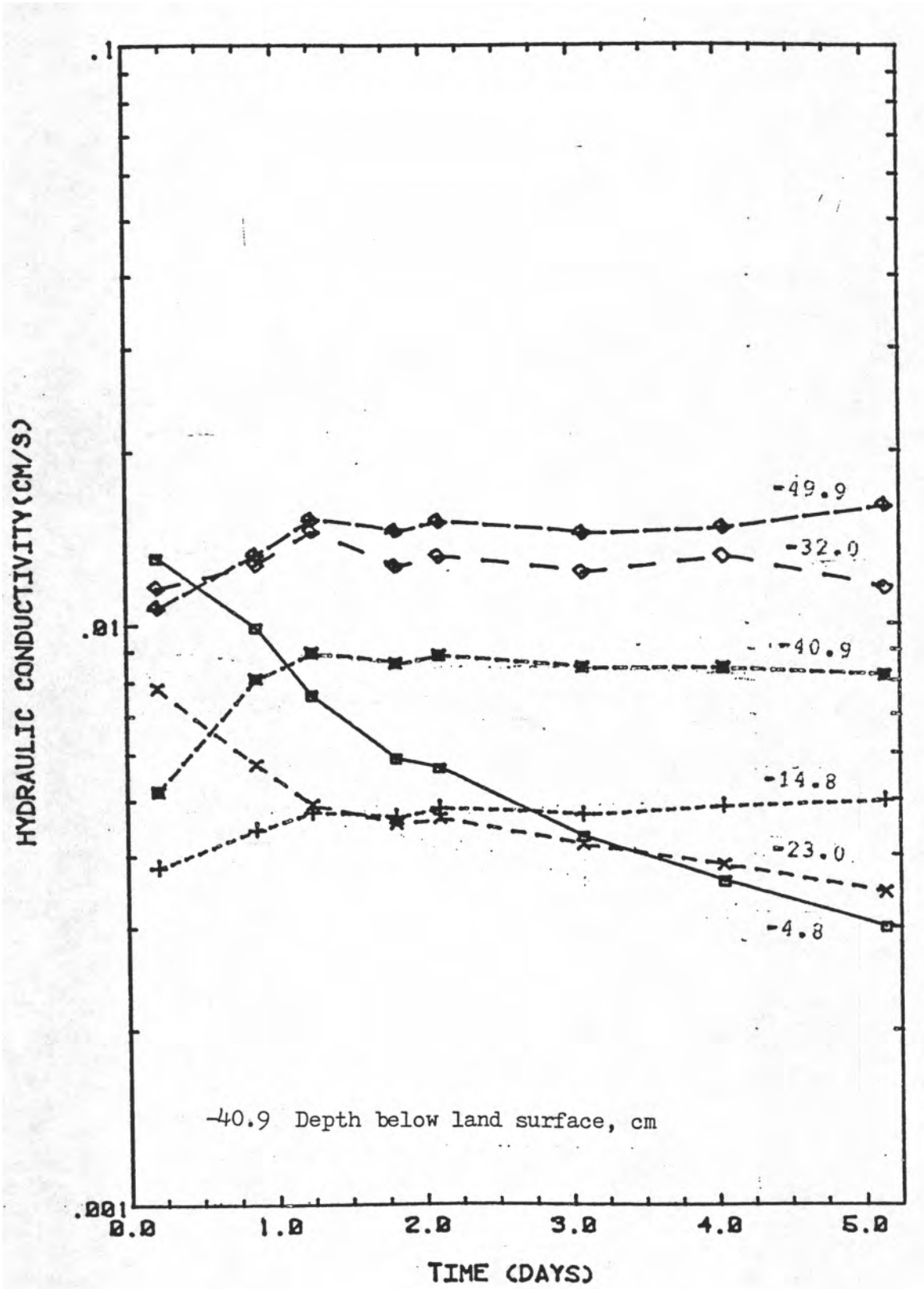

Hydraulic Conductivity versus Time for various depths from Shelby tube number 1, taken near Soil-moisture Station 1.

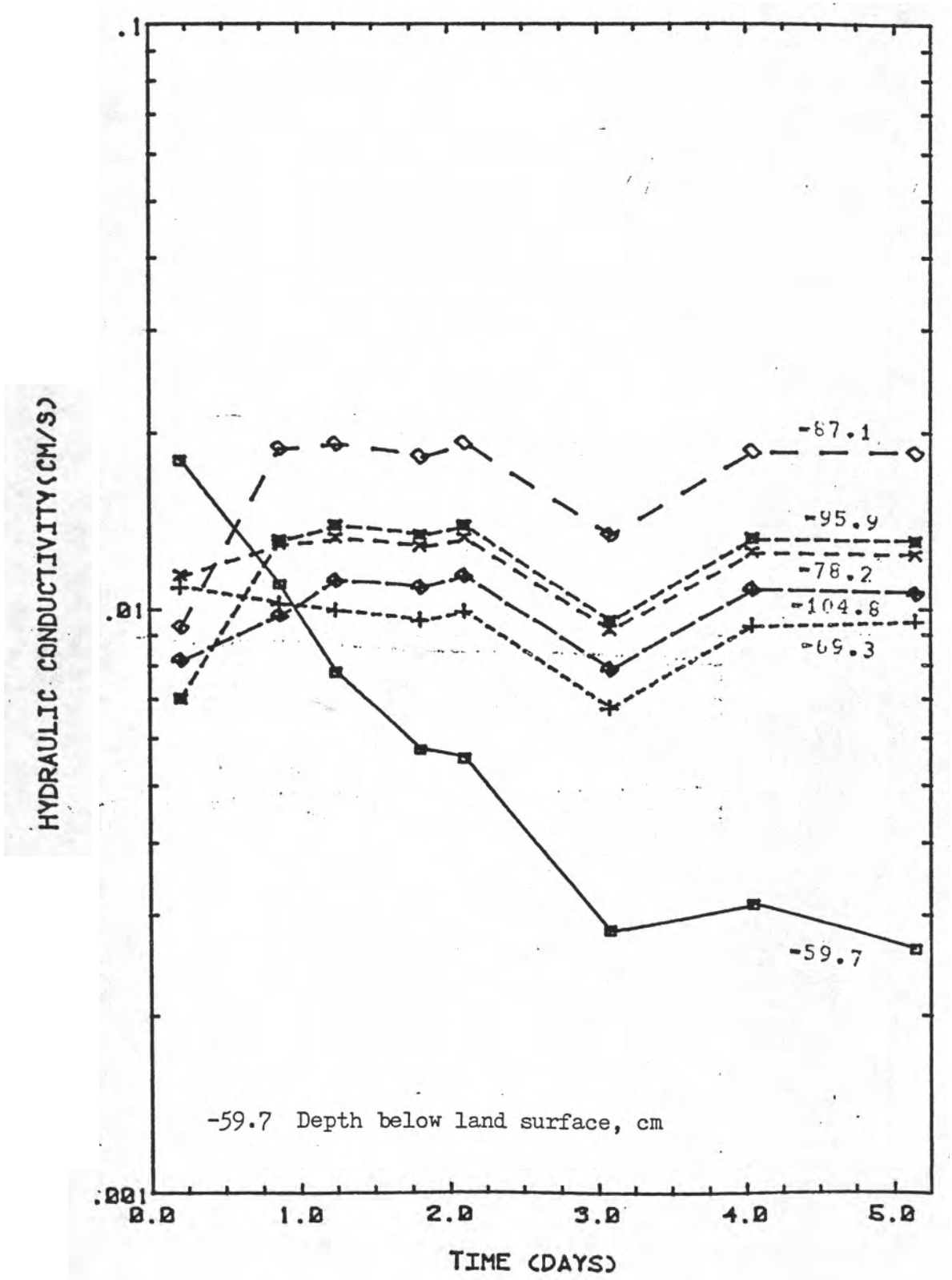

Hydraulic Conductivity versus Time for various depths from Shelby tube number 2, taken near Soil-moisture Station 1.

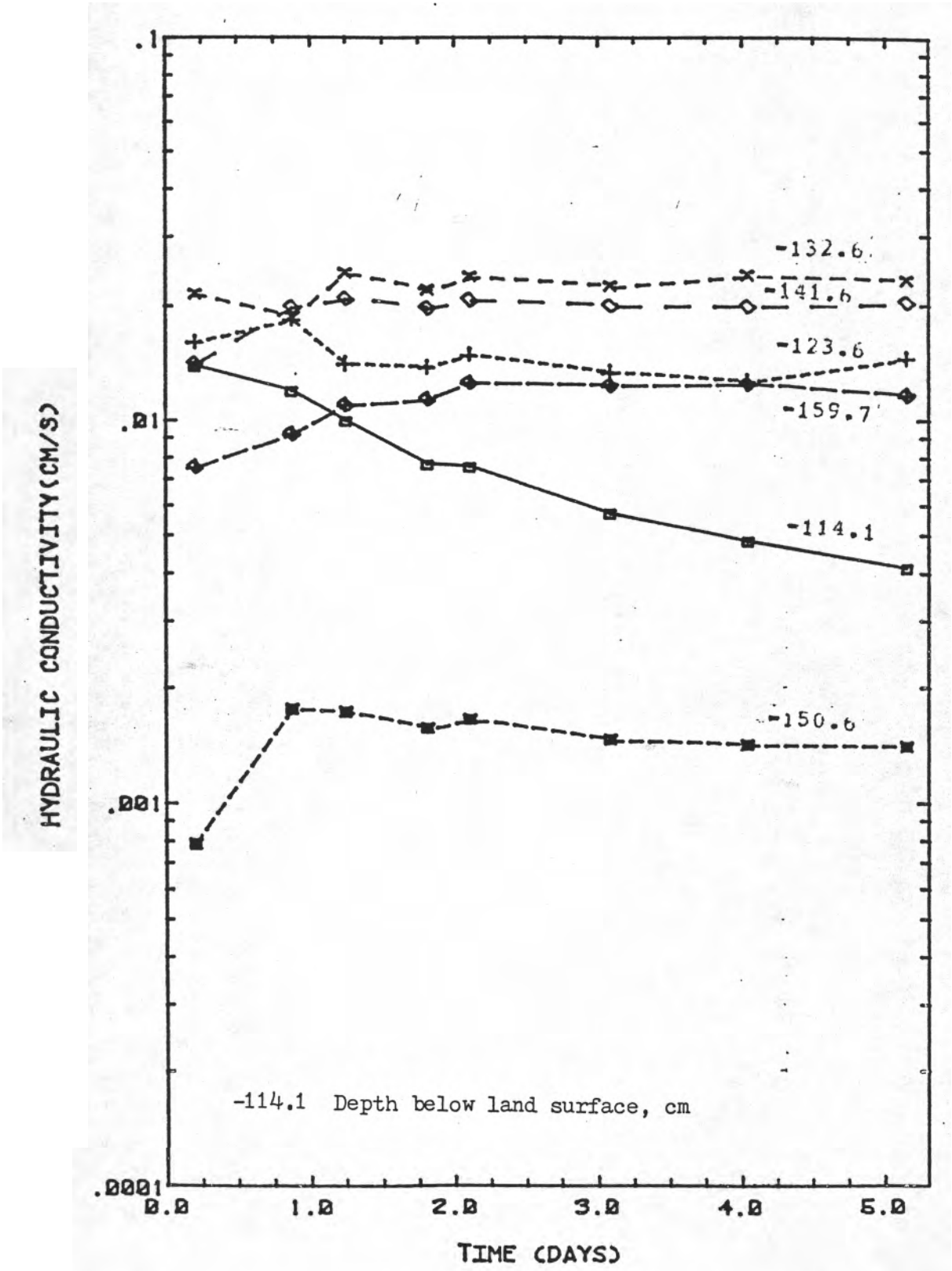

Hydraulic Conductivity versus Time for various depths from Shelby tube number 3, taken near Soil-moisture Station 1.

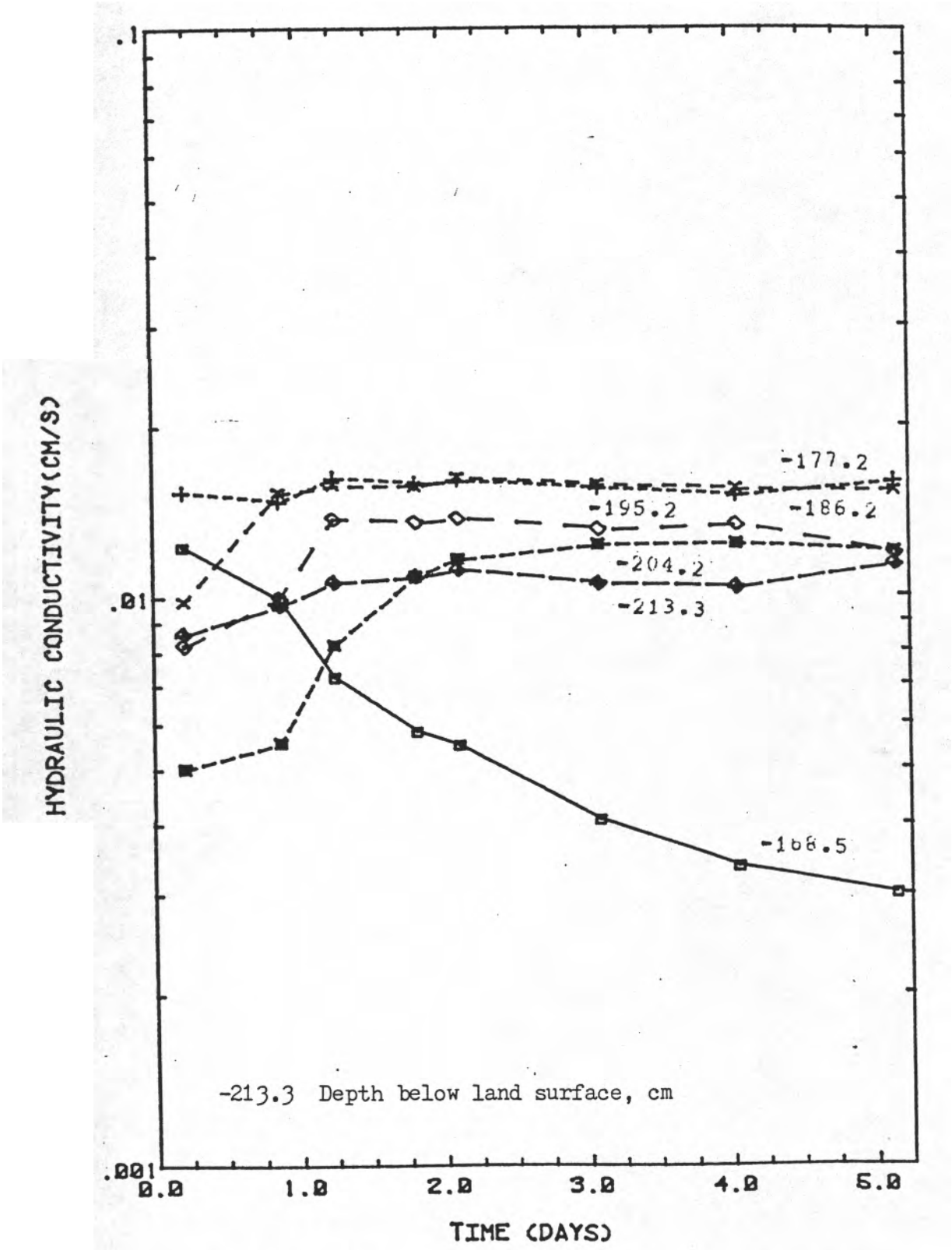

Hydraulic Conductivity versus Time for various depths from Shelby tube number 4, taken near Soil-moisture Station 1.

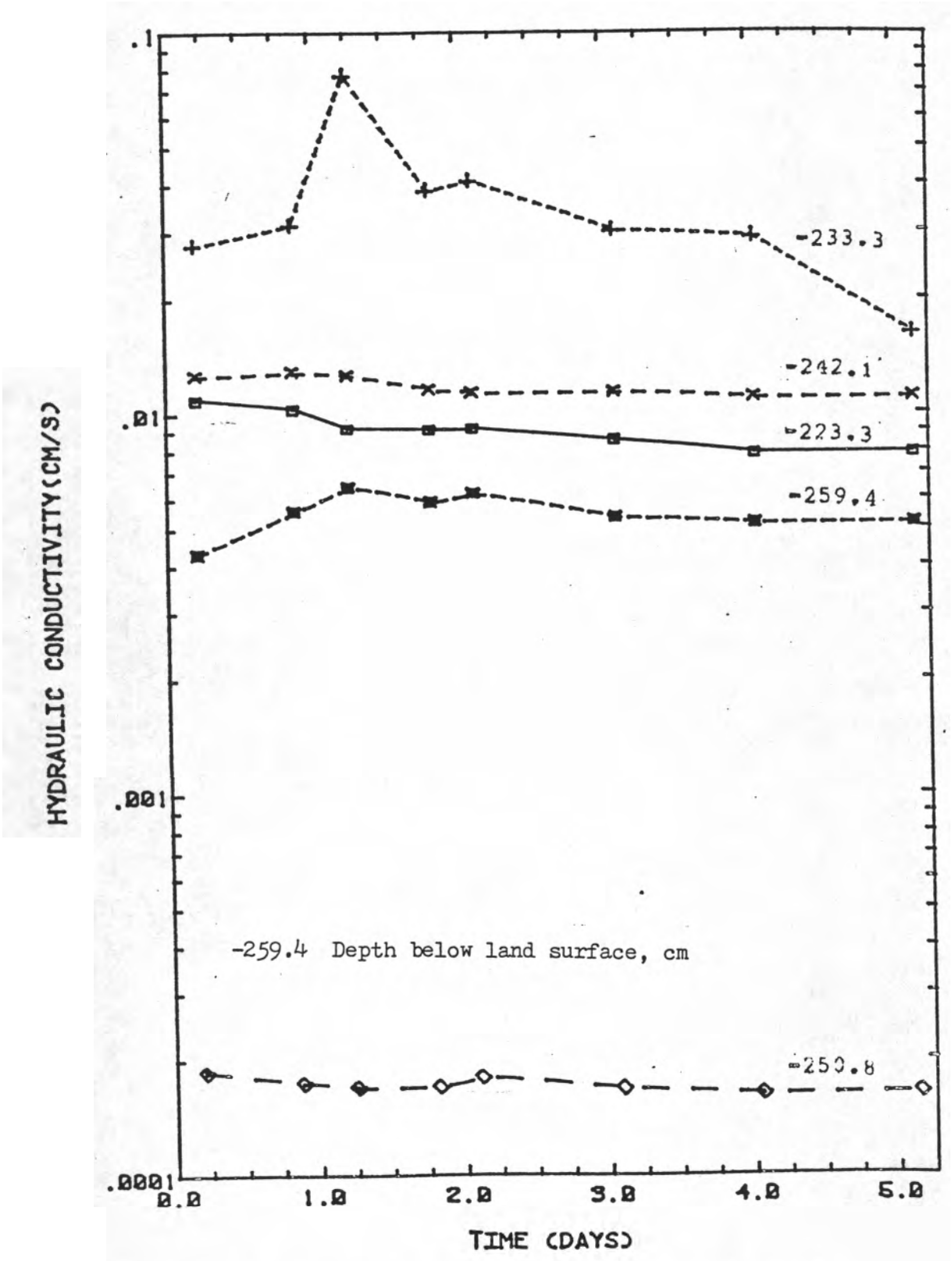

Hydraulic Conductivity versus Time for various depths from Shelby tube number 5, taken near Soil-moisture Station 1.

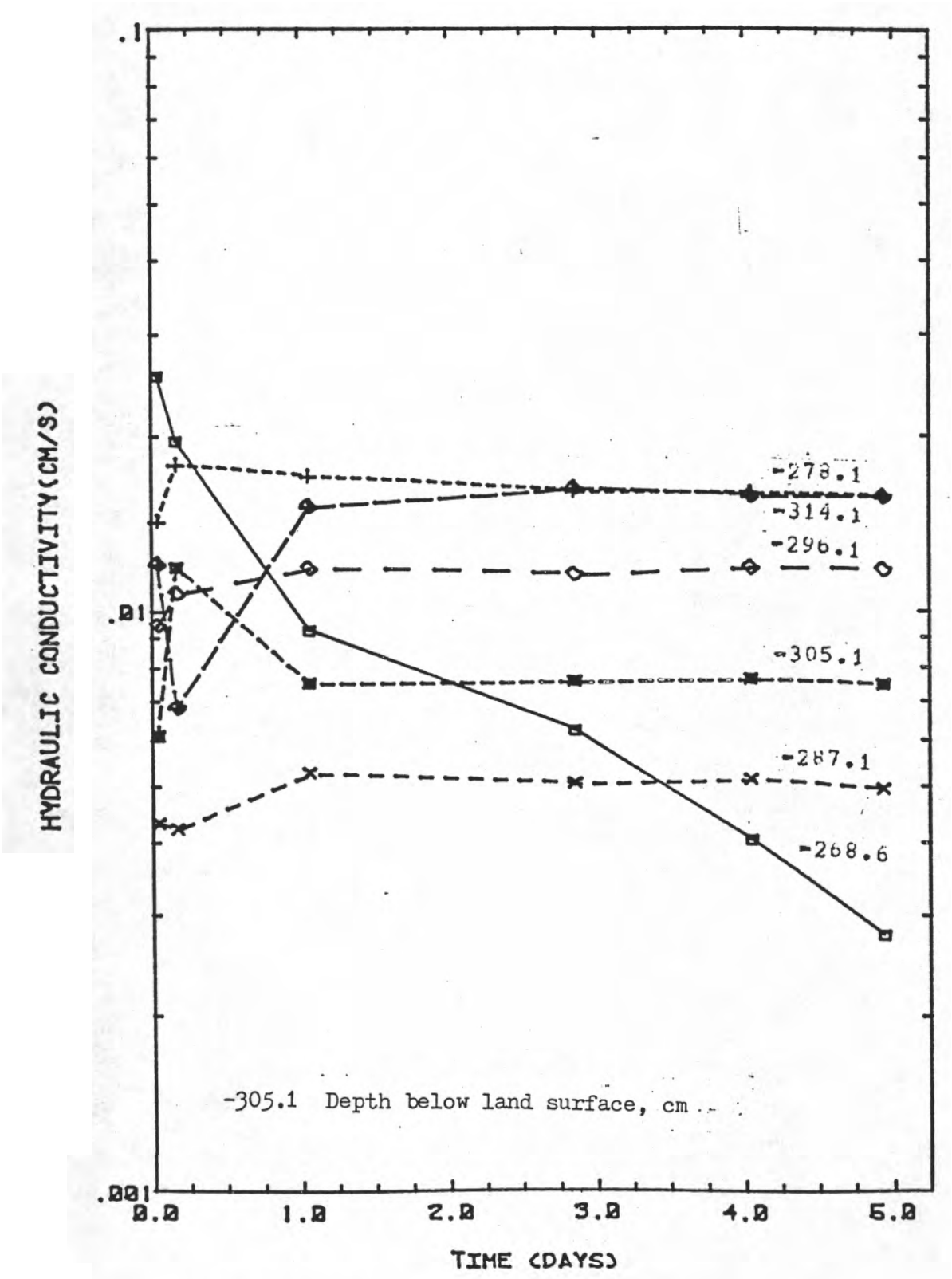

Hydraulic Conductivity versus Time for various depths from Shelby tube number 6, taken near Soil-moisture Station 1.

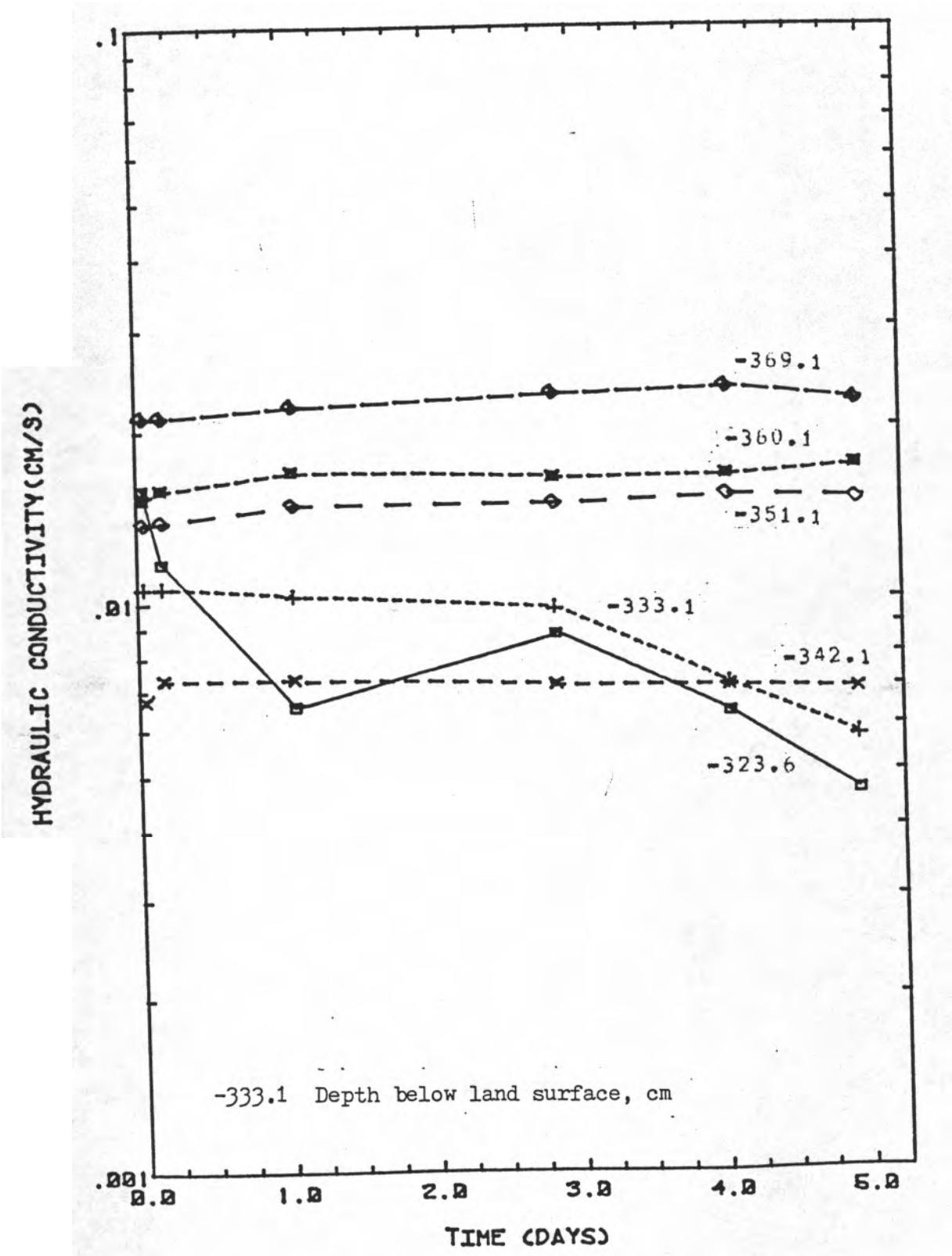

Hydraulic Conductivity versus Time for various depths from Shelby tube number 7, taken near Soil-moisture Station 1.

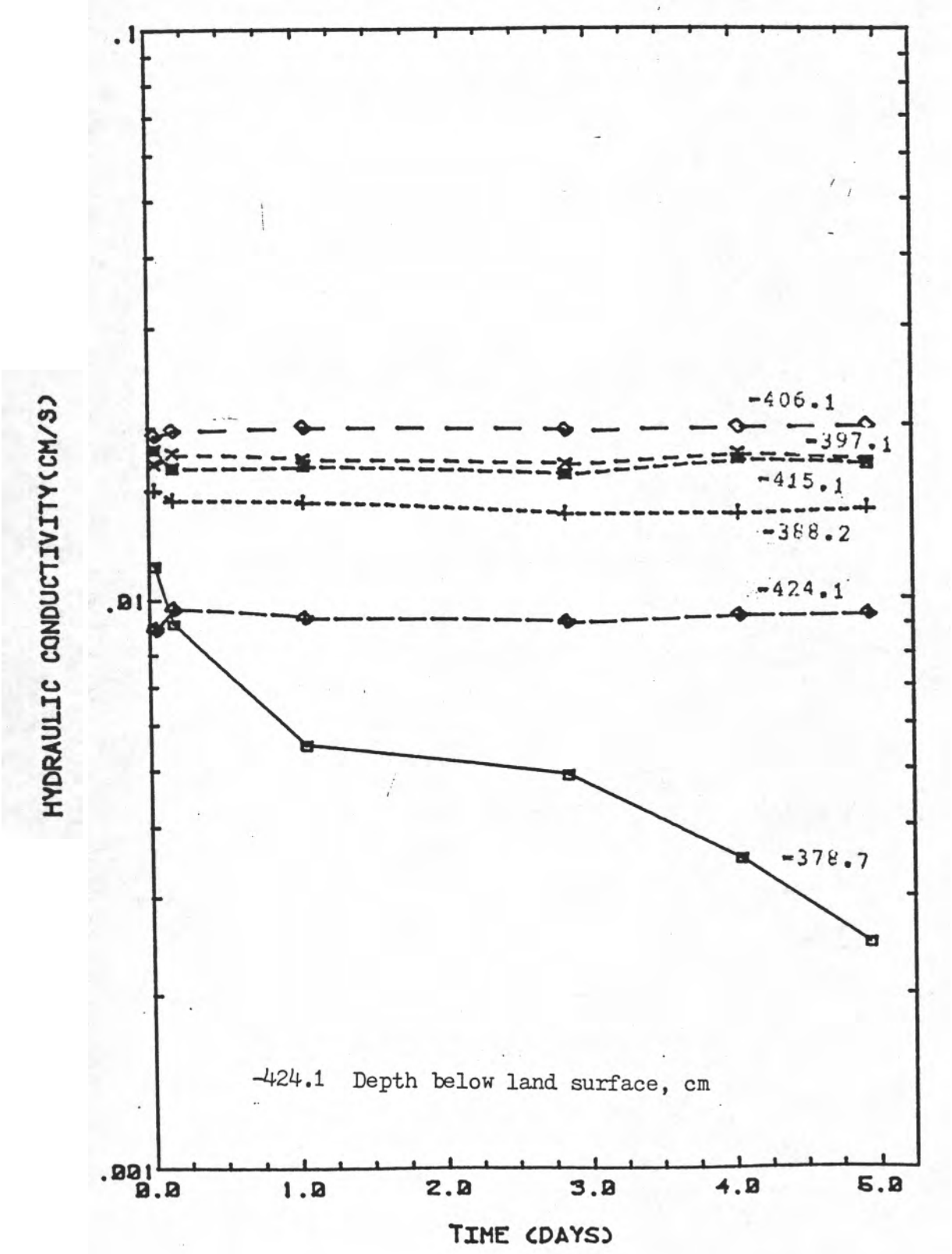

Hydraulic Conductivity versus Time for various depths from Shelby tube number 8, taken near Soil-moisture Station 1.

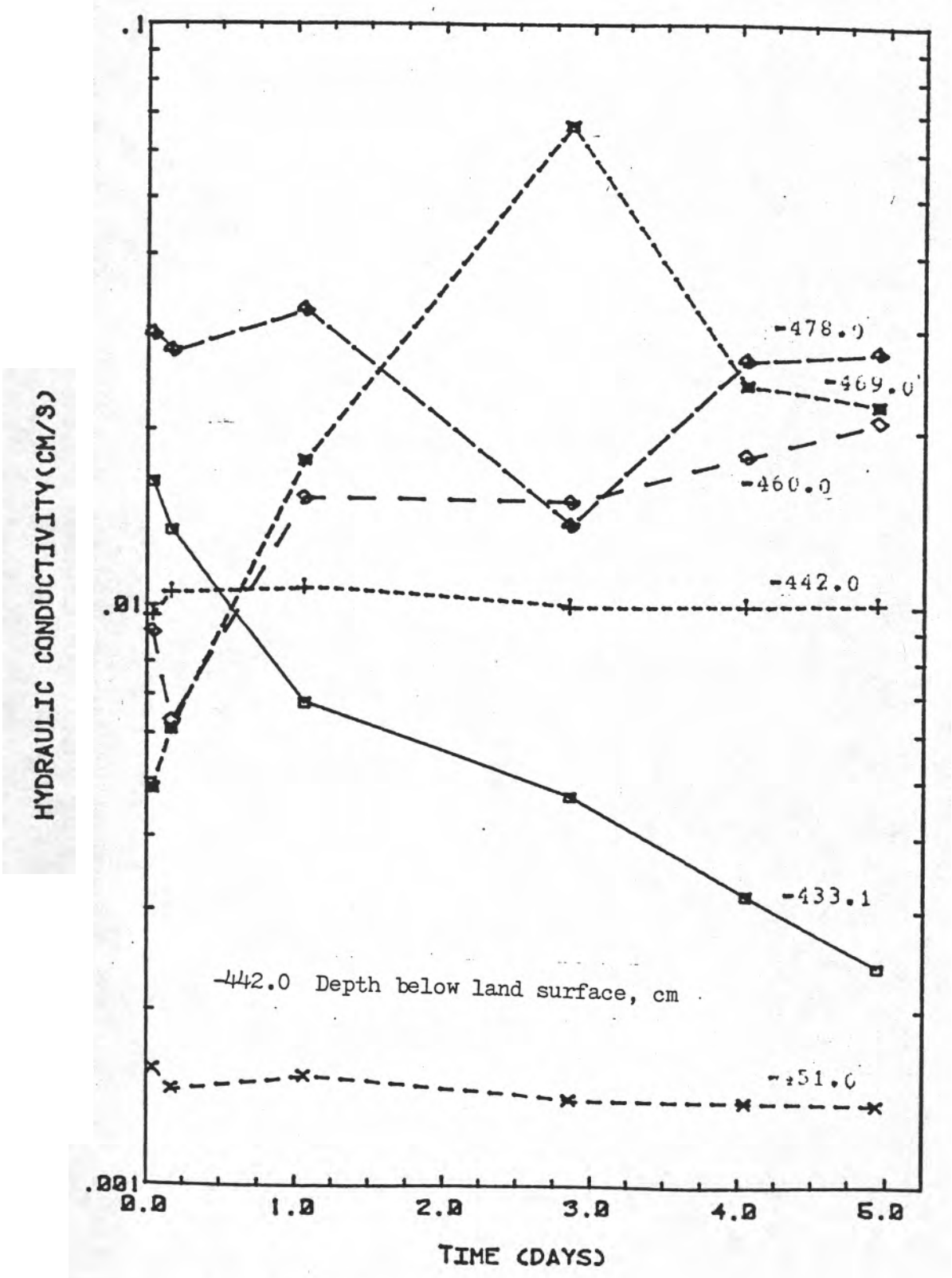

Hydraulic Conductivity versus Time for various depths from Shelby tube number 9, taken near Soil-moisture Station 1.

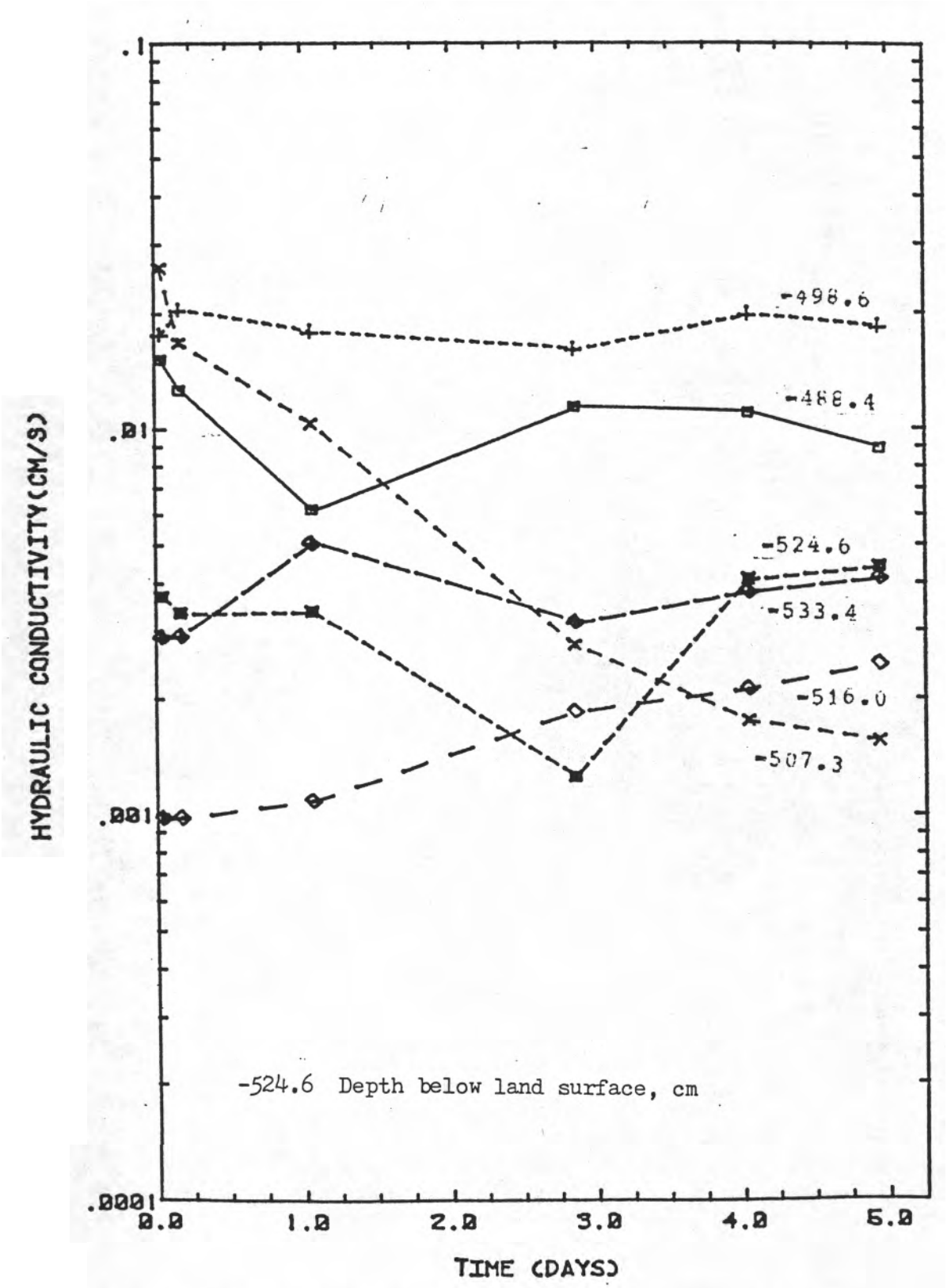

Hydraulic Conductivity versus Time for various depths from Shelby tube number 10, taken near Soil-moisture Station 1.